Federal Agency of Education
Public Educational Institution of High Professional Education
Tomsk Polytechnic University
Institute of Electrical and Electronics Engineers (IEEE)
Electric Devices Society (EDS)

Proceedings of the
16th International Scientific and Practical Conference
of Students, Post-graduates and Young Scientists

MODERN TECHNIQUE
AND TECHNOLOGIES
MTT' 2010

April 12 - 16, 2010
TOMSK, RUSSIA

UDK 62.001.05 (063)
BBK 30. 1L. 0
S568

Russia, Tomsk, April 12 - 16, 2010

The twenty second International Scientific and Practical Conference
of Students, Postgraduates and Young Scientists
"Modern Techniques and Technologies"
(MTT'2010), Tomsk, Tomsk Polytechnic University. –
Tomsk: TPU Press, 2010.- 234 p.

UDK 62.001.5 (63)

CONFERENCE SCIENTIFIC PROGRAM COMMITTEE

V.A. Vlasov	Chairman of Scientific Program Committee, ViceRector on Research, Professor, Tomsk, Russia
L.M. Zolnikova	Academic Secretary of the Conference, TPU, Tomsk, Russia
O.V. Sidorova	Academic Secretary of the Conference, TPU, Tomsk, Russia
A.A. Sivkov	1th Section Chairman, TPU, Tomsk, Russia
V.F. Votyakov	2th Section Chairman, TPU, Tomsk, Russia
B.B. Moyzes	3th Section Chairman, TPU, Tomsk, Russia
O.P. Muravliov	4th Section Chairman, TPU, Tomsk, Russia
G.S. Evtushenko	5th Section Chairman, TPU, Tomsk, Russia
B.S. Zenin	6th Section Chairman, TPU, Tomsk, Russia
A.M. Malyshenko	7th Section Chairman, TPU, Tomsk, Russia
A.P. Potylitsyn	8th Section Chairman, TPU, Tomsk, Russia
V.K. Kuleshov	9th Section Chairman, TPU, Tomsk, Russia
A.S. Zavorin	10th Section Chairman, TPU, Tomsk, Russia
M.S. Kukhta	11th Section Chairman, TPU, Tomsk, Russia
A.A. Gromov	12th Section Chairman, TPU, Tomsk, Russia

Section I

POWER ENGINEERING

MAGNETIC FIELD INFLUENCE ON AN EXPLOSIVE-EMISSIVE PLASMA EXPANSION SPEED

Yulia I. Isakova, G. E. Kholodnaya

Research supervisor: A.I. Pushkarev,

Tomsk Polytechnic University, 634050, Tomsk, Russia

e-mail: principessa-88@mail.ru

I. INTRODUCTION

Modernizing of engineering products is difficult without the application of new progressive technological processes, which allow the increasing of the life and reliability of components and connections under very severe operating conditions. Powerful ion beam irradiation provides heating and cooling of boundary layers of a treated item at a rate of more than 10^7 K/s. This allows compounds and structures to be realized in surface layers, which cannot be made by traditional industrial methods. As a result, the characteristics of materials change: solidity, strength, and wear resistance. While the operational characteristics of items made from these materials improve also. For wide, industrial implementation of the modification methods of boundary layers by high-power ion beams, a reliable and economical powerful ion beam source with long operational life is necessary.

The effective generation of powerful ion beams became possible when two important problems were solved: (i) suppression of the electronic component of diode current and (ii) formation of a solid plasma on the anode surface.

To solve the problem of solid plasma formation on the anode surface, in 1980 Logachev, Remnev and Usov first suggested using the phenomenon of explosive electron emission [1]. In spite of much progress in powerful ion beam generation, many processes in an ion diode with magnetic self-insulation and with an explosive emission anode have not been researched enough. In particular, there is no experimental information about the effect of duration of solid emissive surface formation on anode and plasma extension velocity.

As for the generation of an electron beam, the planar diodes with explosive emission cathodes are widely used. Whenever the micro explosions occur, the plasma forms at the cathode. One of the most important processes accompanying the generation of electron beam in diode with the explosive emission cathode is the expansion of cathode plasma [2]. As soon as the anode-cathode gap is blocked the generation of the electron beam stops. The dynamics investigation of explosive emission plasma expansion represents an interest not only for the developers of high-current electron accelerators. It is also interesting for the study of the behavior of low-temperature plasma with high ionization level as well.

The purpose of this work is to investigate an explosive emission plasma expansion speed in the planar diode, at the point of electron beam formation and during the ion beam generation in a magnetically insulated ion diode.

II. EXPERIMENTAL INSTALLATION

Investigations were conducted at accelerator TEMP-4M (modification of accelerator TEMP-4 [3]. To conduct experiments on the cathode plasma expansion speed in the electron diode, the TEU-500 pulsed electron accelerator was used [4].

To measure the total current consumed by the diode connection, a Rogowski coil with a reverse coil was used. The voltage at the potential electrode was measured by a resistive voltage divider. The recording of the electric signals coming from sensors was performed on a Tektronix 3052B oscilloscope (500 MHz, $5 \cdot 10^9$ measurements per second).

Shown in Fig. 1 is a typical oscilloscope trace of the voltage on the potential electrode and of the load impedance (Accelerator:TEMP-4M).

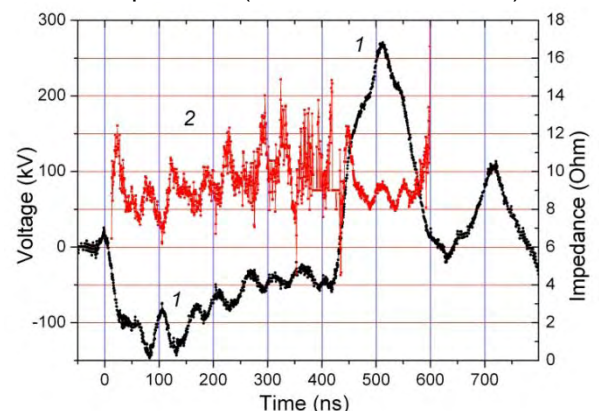*Fig.1. (1) Oscilloscope traces of voltage and (2) calculated values of impedance.*

III. BASIC CALCULATION EQUATIONS

An analysis of plasma behavior in the anode-cathode gap was performed based on the current-voltage characteristics of the diode. The electron and ion current densities flowing through the diode in the mode restricted by volume charge are determined by the following expressions [5]:

electron current

$$J_e = \frac{4\varepsilon_0 \sqrt{2e}}{9\sqrt{m_e}} \cdot \frac{U^{3/2}}{d_0^2} = 2.33 \cdot 10^{-6} \frac{U^{3/2}}{d_0^2} \qquad (1)$$

ion current

$$J_{ion} = \frac{4\varepsilon_0 \sqrt{2z_i}}{9\sqrt{m_i}} \cdot \frac{U^{3/2}}{(d_0)^2} \qquad (2)$$

where U is the voltage applied to the diode; d_0 is the anode-cathode gap, m_e is electron mass; m_i is ionic mass; z_i is ionic charge.

Taking into account the reduction of anode-cathode gap due to expansion of plasma from the emissive surface of the potential electrode, the electron current density is equal to:

$$J_e(t) = 2.33 \cdot 10^{-6} \frac{U^{3/2}}{(d_0 - vt)^2} \qquad (3)$$

where v is plasma expansion velocity.

If the diode operates in the mode of volumetric charge limitation, then from correlation (3), we obtain the cathode plasma expansion speed as:

$$v(t) = \frac{1}{t}\left[d_0 - \sqrt{\frac{2.33 \cdot 10^{-6} \cdot S_0 \cdot U^{3/2}}{I_e}} \right] \qquad (4)$$

where S_0 is the square area of potential electrode (cathode during negative pulsed) of diode. This correlation is used further down in the calculation of plasma expansion speed.

Two modes of diode operation can be pointed out: discrete emission surface mode and space charge limitation mode.

IV. DISCRETE SURFACE EMISSION MODE

Operation of the magnetically self-isolated diode at the first (negative) pulse and during the pause between pulses (see Fig. 1) is analogous to the operating mode of a planar diode with explosive emission cathode at electron beam generation.

Our research shows that in the discrete surface emission mode, the magnetic field influence on plasma dynamics in the A-C gap is insignificant. The duration of plasma solid surface formation on the cathode is proportionate to its area. This is true for the explosive emission cathode in the electron diode (without magnetic field) and in the ion diode with magnetic self-insulation of electrons.

V. SPACE CHARGE LIMITATION MODE

After covering the potential electrode surface with plasma, the total diode current is limited only by the vacuum electron charge in the anode-cathode gap. Figure 2 shows the calculated values of cathode plasma expansion speed according to Eq. 4 for different types of diodes.

Through these experiments, we have found that the magnetically insulated diode expansion rate of graphite plasma (across the A-C gap) is significantly lower than the expansion rate of a plasma in electron diodes with graphite explosive emission cathodes, where it is equal to 2.5±0.5 cm/μs [6,7]. This indicates a significant influence

of magnetic field on the expansion dynamics of explosive-emission plasma within the A-C gap. At PIB generation, the reduction of the expansion of explosive emission plasma is a useful effect, which decreases the possibility of gap bridging by plasma.
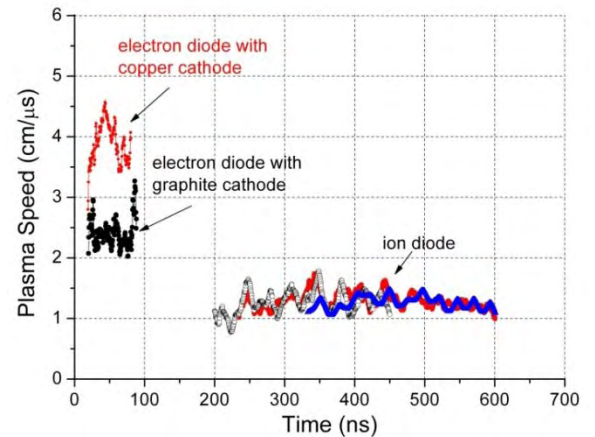

Fig.2. Change of explosive emission plasma speed during mode of volumetric charge limitation in electron diode with graphite and copper cathodes and in ion diode (planar and focusing) with cathode composed of graphite, aluminum and copper.

CONCLUSION

The performed high-time resolution investigations of speed dynamics of explosive emission plasma expansion in the diode showed that after the formation of solid plasma surface on the cathode and prior to the end of pulse the plasma speed does not change and equals 2±0.5 cm/μs for cathode made of graphite and carbon fiber, 4±0.5 cm/μs for copper cathode. The investigations have been performed for various anode-cathode gaps and cathode diameters. Through these experiments, we have found that the magnetically insulated diode expansion rate of cathode plasma (graphite, Al, Cu) across the anode-cathode gap is significantly lower than the expansion rate of plasma in electron diodes with explosive emission cathodes.

REFERENCES

1   E.I. Logachev, G.E. Remnev and Y.P. Usov, *Techn. Phys. Lett.*, vol. 6, no. 22, pp. 1404–1406, Nov. 1980.

2   A.I. Pushkarev and R.V. Sazonov, *IEEE Trans. Plasma Sci.*, vol. 37, no. 10, Part 1, pp. 1901–1907, Oct. 2009.

3   G.E. Remnev, I. F. Isakov, V. M. Matvienko, at all, *Surf. and Coatings Technol.*, vol. 96, pp. 103–109, Feb. 1997.

4   G.E. Remnev, E.G. Furman, A.I. Pushkarev, N.A. Kondratiev, D.V. Goncharov. IEEJ Transactions on fundamentals and materials, 2004, vol. 124, №6, pp. 491-495.

5   Langmuir, *Phys. Rev.*, vol. 2, p. 450, 1913.

6   Pushkarev A.I., Isakova J.I., Saltimakov M.S. and Sazonov R.V. // Phys. of Plasmas 17, 013104 (2010).

7   A.I. Pushkarev, Yu.N. Novoselov. R.V. Sazonov, Techn. Phys., 3, 357 (2008).

PLC TECHNOLOGY AND ITS PROSPECTS FOR RUSSIA'S MARKET

OF BROADBAND SUBSCRIBER ACCESS

Nikolenko K.V.

Scientific adviser: Yrchenko A.V.

Tomsk Polytechnic University, 634050, Russia, Tomsk, Lenina's avenue, 30

E-mail: rubos_saboteur@mail.ru

PLC technology (Power Line Communication) is a commonly known concept, but the real possibilities of technology only a small number of specialists are aware of. This is partially because of manufacturers' information policy and unintelligible marketing, which do not take into account Russia's realities. Besides, the first and second version of the standard did not work properly. This review presents a fresh look at the possibilities of this exciting technology, which is based on standards approved by the UPA in 2006. This standard provides physical data transfer with the rate up to 200 Mbit / sec in half-duplex mode, which corresponds to the maximum actual data transfer rate 80 Mbit / sec in full-duplex mode. Maximum speed is below capacity of FastEthernet because of the costs to the service traffic and data redundancy for error correction protocol.

Domestic market knows PLC technology primarily for "Home network wiring" which is represented by such brands as Zyxel, Dlink, Qlan. Also, the company "Incotex" presents the system for collecting data in the AMR.

Myths and facts about PLC

PLC technology has made a complicated way from handmade devices to solutions for carrier-class. During this way different people had different impressions that underlie some myths [1]. Let's consider some of them:

• PLC technology is slow and unreliable.

• There are some devices that can "lock" the whole network and nothing can be done.

• Deployment of PLC networks may cause harmful interference to radio stations.

• In Russia we have bad power networks, so this technology will never be able to work well.

In fact, a part of the said above does not correspond to reality:

• Early versions of the standards were not very reliable. Third generation devices can boast of high reliability; algorithms and protocols are continuously being improved in a regular software update.

• Devices that have an impact on PLC are well known. These powerful electric motors are used in air conditioners, refrigerators, washing machines with inductive load, as well as cheap small-sized power units made in China without filtering circuits. Ways to fight are well known that is the use of specialized low-cost filters and proper design of PLC network.

• If you transfer, even at a very good power cable, signal attenuates rapidly. As for transmission in the air, such as cottage building, the signal does not have a tangible impact on the technique that works in the village, because the power lines and equipment are at sufficient distance from each other; Low power PLC signal (100 mW) in small portions are 36distributed over a wide range, while high-powered SW radio (1 ... 50 W) is concentrated in a narrow range;

• There are totally different types of power networks. For PLC technology material is important as well as the thickness of wires, its geometry, quality of connections, and number of branches. Russia had a very good school of power supply. In some places, power networks that were built 30 or 40 years ago, now are serving consumers who even increased their consumption by several times – all that thanks due to the Soviet margin. There is little reason to think our power networks are worse than in many countries in Asia or Eastern Europe, which successfully use PLC solutions.

Besides myths, there are definite features caused by the physical characteristics of signal propagation, which greatly narrow the scope of PLC based solutions.

• Some electric meters block PLC signal. There are three possible effects of the counters on PLC work depending on their construction:

- The counter has no effect on a signal. The weakening is about 5 dB;

- Counter weakens PLC signal. The weakening is from 5 up to 40 dB. In this case, you can connect a signal after the counter and to ensure a normal quality of PLC network;

- Counter shunts PLC signal. In this case, most part of a signal is attenuated through the built-in RF shunt; PLC connection does not work before counter, or after the counter. The only possibility of connection is to retreat from the meter on a cable directed toward consumers from 10 meters and above.

• In aluminum wiring attenuation is stronger than in copper, which reduces the communication range of approximately 2-fold.

• In underground cables due to the properties of the ground attenuation is 2 or 3 times more. However, the signal transmission in power network, mainly affects not weakening, but noise level, which is significantly lower in the underground networks.

• Deploying PLC is often cheaper because there is no need to design and lay additional communication networks.

• Routing devices are not more complicated than in LAN-networks.

In real objects the combination of several unfavorable factors may cause the deployment of PLC unprofitable or impossible. Therefore, before network deployment it is always strongly recommended to collect the maximum amount of information, including a plan of power network, the type of cabling, circuit boards and machines, and most importantly, to verify received information with reality.

Technology concept.

The basis of Powerline technology is the use of frequency division of a signal, where high-speed data stream is divided into several relatively low-speed flows; each of them is transmitted on a separate subcarrier frequency, followed by their union into one signal.

When using a frequency-division Multiplexing (FDM), protective intervals (Guard Band) between sub-carriers necessary to prevent mutual interference are quite high, so the available spectrum is not used very effectively.
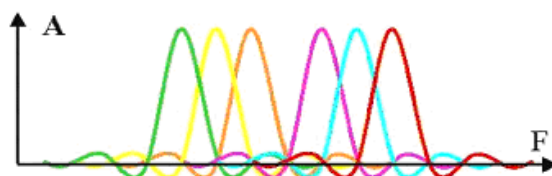

Рис. 1. OFDM

In case of an orthogonal frequency-divided multiplexing (OFDM), subcarrier frequency centers are located in such a way that the peak of each successive signal coincides with a zero value for the previous (Fig. 1). This placement allows more efficient use of available bandwidth.

Before the individual subcarrier is combined into one signal, they undergo a modulation phase, each with its sequence of bits.

After that, they pass through the Power-Packet engine and are collected in a single information package, which is also called OFDM-symbol. Figure 2 shows an example of the relative quadrature phase shift keying (DQPSK - Differential Quadrature Phase Shift Keying) for each 4-subcarrier frequencies in the range of 4.5 MHz.
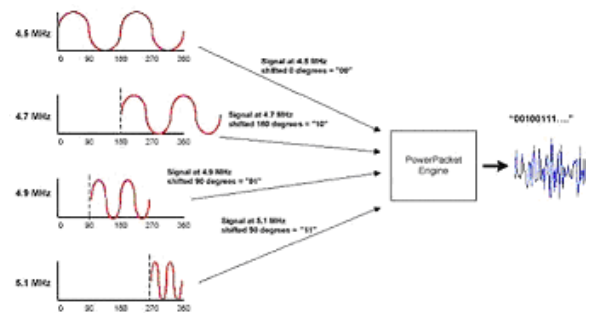

Рис. 2. DQPSK модуляция

The Power-line technology uses 84 sub-carriers in the frequency range 4-21 MHz. The theoretical data transfer rate when using parallel streams with simultaneous phase modulation signals is more than 100 MB / sec.

Adapting to the physical environment, fixing bugs and resolving conflicts are common for 3 generation of PLC.

When you send a signal to domestic power supply network it may experience greater attenuation in the transmission function at certain frequencies, resulting in data loss.

Under laboratory conditions, AMR was built with the use of equipment of the company "Incotex". According to studies, PLC damping is less than expected. Achievement of PLC packages within the same TS was 100%. Thus, PLC technology is most proper for local area networks and data collection.

AMR monitors consumption both from urban power network and from solar energy complex with 240 W. It takes into account generated and consumed electrical energy. Thus, we can assess the effectiveness of energy complex use for lighting.

REFERENCES

1 Свежий взгляд на PLC на примере решений компании Corinex - http://nag.ru/news/16867/

TIME CONSUMPTION OF SIMULATION DEPENDS ON STANDARDS

Paar M., Topolánek D.

Supervised by: Toman P.

Brno University of Technology, Czech Republic, Brno, Technicka 2848/8

E-mail: paar@feec.vutbr.cz, xtopol02@stud.feec.vutbr.cz, toman@feec.vutbr.cz

ABSTRACT

The paper deals with a comparison of penalizations standards simulations from time consumption point of view. Penalization standards are used like one way for evaluation customers' power supply interruption. Two real (Finnish and Portuguese) and three modified standards are tested. The simulation is complex issue which, exclude reliability calculations, contains reconfiguration and optimalization tools for finding minimal costs of outages and power losses. The computation was made on a part of real cable distribution network.

INTRODUCTION

Nowadays many European states use or look for using any types of regulation of market with electrical energy. The liberalization of electrical markets in most European countries cannot delete the fact that market with electrical energy has specific characteristic like impossible or very limited accumulation of electrical energy, necessity of equality consumption and supply energy in every time and natural monopoly of distribution companies and so on. The distribution companies, which own distribution network, are so-called natural monopoly. The regulation of this economical advantage of distribution companies is necessary. The minimal power quality standards are used like one way of this regulation. The monitoring and cost evaluation of continuity electrical energy supply is one part of power quality standards. The electrical energy supply continuity is mostly connected with reliability distribution network and weather influence. The reliability can be affected by high investment to the network, like changing overhead lines by cables that are able to eliminate generally the effect from weather, of course exclude the extreme conditions like floods. The case for middle cost investment can be telemetric switches with remote control but cost-free solutions exits as well. The cheapest solution how to improve reliability of power network is reconfiguration of switches. The aim is to find such a configuration of switches that will lead to maximal reliability of network. Each part of network has own probability of failure and by configuration change the effect of failure to network can be decreased or also raised.

The optimization which is based on reconfiguration carries the problem of network consistency. The ill configuration can lead to disconnection of the several customers or even huge part of network. The disconnection is only one parameter which has to be taken to account. The reconfiguration also changes the power flow in the network that can overload element of it. Therefore the given limits of the elements and output of electrical parameters have to have influence to optimization.

The topological restriction and the others given limits directed the solution to multi-objection optimization. Multiple optimization criteria can be solved easily by one of stochastic methods e.g. by a form of genetic algorithm (GA). The easy extensibility of GA to increase the number of parameters (e.g. special limitation for each supply customers) was another reason why GA was selected.

COMPARED PENALIZATION STANDARDS

The simulation can calculate 5 types of standards, 2 in real use: the Finnish system standard and the Portuguese customers' standard. The other standards are based on Portuguese or Finnish standards.

Finnish continuity standard at system level (FI)

The continuity standards can be divided to system and customer standards according to the penalization acceptor. The standard at system level regulates the power quality without direct payment to customers. This continuity standard is a system standard and it is used by Finnish Energy Market Authority. The penalization payment is a part of complex metrology for setting network tariffs and also to evaluate the efficiency of whole network. [1]

Portuguese customer continuity standard (PT)

Contrary to Finland's standard, the computation uses the Portuguese Single-customer standard [2] excluding system standard. This standard is applied only in case of long interruptions (longer than 3 minutes) and expresses the maximal number of interruptions per year and maximum interruption duration annually. The exact value depends on voltage level (HV, MV and LV) and population density (urban – more than 25 000 customers, suburban – among 2500 to 25 000 and rural customers – up to 2500 customers).

Modified Finnish continuity standards (FT and FL)

Finnish standard contains many items like penalization from unexpected interruption or one

from duration of outages. Modified Finnish standards evaluate oly duration of unexpected outages with two types penalization coefficients for each standard.

Modified Portuguese continuity standard (PS)

This standard is hybrid between Portuguese and Spanish customer standards. In contrary the others standards are not affected by magnitude of customers load before interruption.

SIMULATIONS

The evaluation is base stone of the model and contains steady state analysis and reliability evaluation.

Evaluation of the network parameters

The steady state analysis uses a linear one-line diagram model of power network. Steady state operation is solved taking into account following simplifying considerations. Power consumptions are specified by using electric currents that are independent from voltage applied to their terminals. These simplifications have consequence in a way that calculation suffers from the lower accuracy rate comparing to the power-flow methods, such as the Newton-Raphson but the method is faster and more reliable.

The basement for evaluation penalization standards states on the Monte Carlo method. Before penalization standard is used, the interruptions and duration of interruption are generated. These processes create the artificial history of events in the network. The generation is based on probabilities of events given by historical record of issued distribution network. The artificial history keeps events for 10 thousands years and by this way gives information of possible numbers and duration of failures in future. For each year the standard criteria is applied. The final value for all years, given by mathematic operation, is used for next evaluation processes.

Genetic algorithm and reconfiguration

The whole process of evaluation is cover by optimization system using genetic algorithm. The reconfiguration brought high demands to coding solution for GA and also many parts of them had to be modified as well e.g. initialization system for creating first generation or genetic operators for production followed generation. GA's fitness function for evaluation each solution sum outage costs for selected standard, cost of power losses and value from gamma function. The gamma function evaluates violation of network properties like voltage drop at each node or overload of wires. Transformation GA code to evaluate-able form the graph functions are used like modified DFS (Depth-First Search).

RESULTS

The model was tested on a real MV (medium voltage) cable network based on a two-stage structure. The chosen part of network

circumscribes between two substations (110/22 kV) that serves over 44 818 customers connected to 288 transformation stations.

Testing was done different number of generations with various numbers of members (solutions) in one generation (for general testing was 800 generations and 20 solutions at each) on computers with processor clocking 3 GHz and 1GB RAM.

The *Tab. 1.* shows time consumption of each variant for 4 different sizes of population. The optimization is stochastic process which brings diversity of final times therefore the average value of 10 calculations was used.

Tab. 1. The comparison of consumption times

#	number of generations [pcs.]	number of solutions in generation [pcs.]	standard -	average time consumption [h]
1	800	20	FI	19,5
2	800	20	FL	18
3	800	20	FT	18,5
4	800	20	PS	23
5	800	20	PT	29
6	800	20	only losses	4,5
7	1200	20	PT	40
8	2000	20	PT	66
9	2000	40	FT	94

The Finnish standard (FI, FL and FT) with very simple system of valuation was about 34 % faster than Portuguese (PT) standard with divide calculation to high voltage and low voltage level. Modified Portuguese standard (PS) has very similar system of evaluation with Portuguese without dividing to high and low voltage levels and some simplicity given by not using power consumption of each customer. The simulations using power losses and without them, when some reliability standard was applied, the difference of time consumption was insignificant. From only power losses calculation with before mention can be claimed that optimalization process without evaluation took only 15 % of consumption time at Portuguese standard and 24 % at Finnish standard.

CONCLUSION

The various standards have not only influence to final configuration but also consumption time, depending on complexity of evaluation. Portuguese standard had the higher time consumption for division of calculation to low voltage and high voltage level. The results also show that calculation of power losses take a minor part of whole time consumption. Therefore the calculation of power losses becomes more often part of reliability simulation and in other hand reliability evaluation is not part of simulation where calculation of power losses the primary aim. The results are supported by using on an example of the real cable distribution network which gives time for real size of the network.

REFERENCES

1 K.Kivikko, A. Mäkinen, P. Verho, P. Järventausta, J. Lassila, S. Viljainen, S. Honkapuro, J. Partanen, 2004, "Outage Cost Modelling for Reliability Based Network Planning an Regulation of Distribution Companies ", *IEE Michael Faraday House,*, 607-610.

2 Council of European Energy Regulators, 2008, *3rd Benchmarking Report on Quality of Electricity Supply,* Bruxelles, Belgium, 122-127.

CURRENT TRANSFORMER AND ROGOWSKI COIL ACCURACY CONFRONTATION

Topolánek D.[1)], Paar M.[2)], Toman P.[3)]

Brno University of Technology, Czech Republic, Brno, Technicka 2848/8

[1)] tel: +420 54114 9218, email: xtopol02@stud.feec.vutbr.cz,

[2)] tel: +420 54114 9218, email: paar@ feec.vutbr.cz

[3)] tel : +420 54114 9224, email: toman@feec.vutbr.cz

ABSTRACT

The paper is focused on appreciation of current transformers (CTs) and Rogowski coils (RCs) based on accuracy measuring by the measuring system CPC100. Due to accuracy measuring in the wide range of the current it is possible to compare both current transducers. All CTs and RCs advantages and disadvantages resulting from test are summing up in the paper.

INTRODUCTION

Because currents in the power grid can reach over tens kiloampers, these currents have to be transformed to the values which are measured by protection or measuring systems. This is important for monitoring of power grid current values, evaluation of electric power supply and electric power quality, or for network protection. This transformation is done by induction or electronic current transformers. The conventional induction transformers have few disabilities like saturation, remanence or trouble with open secondary winding. All these disadvantages cut down wide spectrum of CTs utilization in measuring or protecting area. It is one of the reasons for increasing of the current sensors popularity. The operation principle of the current sensor is based on using of non-magnetic core therefore sensor has a linear magnetization characteristic.

ACCURACY OF MEASURING AND PROTECTIVE CURRENT TRANSFORMER

Double-core current transformer support type (TPU) with 80 amps rated primary current was used for measuring of current error and phase displacement. The first secondary winding of the transformer (S1) is designed for measuring purpose and its rated burden is 5VA, accuracy class 0,5 and instrument security factor 10FS. The second secondary winding (S2) is designed for protecting purpose, it has rated burden 10VA and accuracy class 5P. Current error and phase displacement are measured in the range 10A - 800A of the primary current (up to ten times of rated primary current) by primary tester CPC100. The tester generates harmonic current without DC component.

The current error and phase displacement in dependence on ratio of the test primary current and nominal primary current is shown in Figure 1. and 2. There are depicted current error and phase displacement dependences for both winding with burden 5VA (S1 rated burden), 10VA (S2 rated burden) and 15VA.
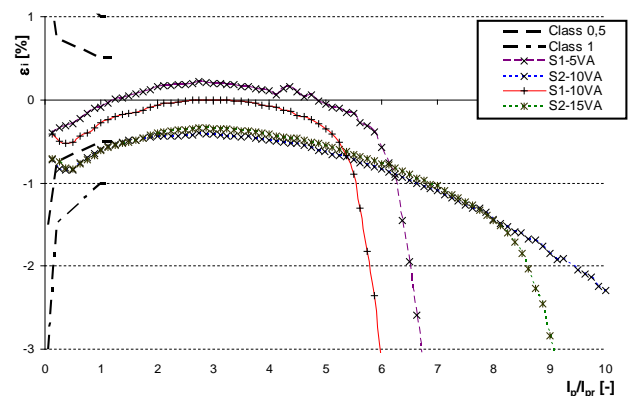

Fig. 1: The current error (ratio error) of the measuring and protective current transformer.
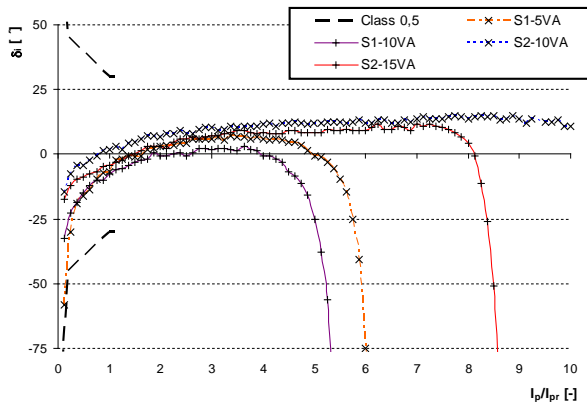
Fig. 2: The phase displacement of the measuring and protective current transformer.

Where I_{pr} and I_p are rated primary current and primary current.

ACCURACY OF ROGOWSKI COIL

Combi-sensor KEVCD 12AE3 was used for accuracy measuring. This sensor has rated secondary output 150mV, rated primary current 80A and accuracy class 3 without calibration factor, accuracy class 1 with calibration factor. Calibration factor 0,9955 was established at routine test report. Figure 3 and 4 show current error and phase displacement of the sensor in the range 10A - 800A of the primary current (up to ten times of rated primary current). The sensor passed accuracy class 0,5 without calibration factor in the test.
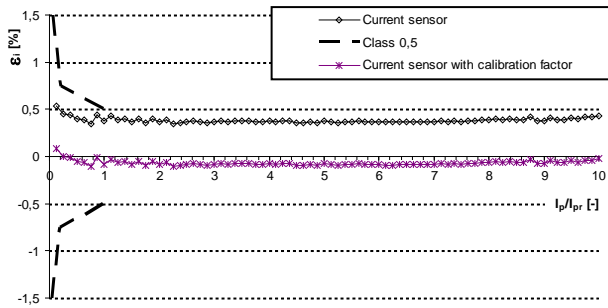

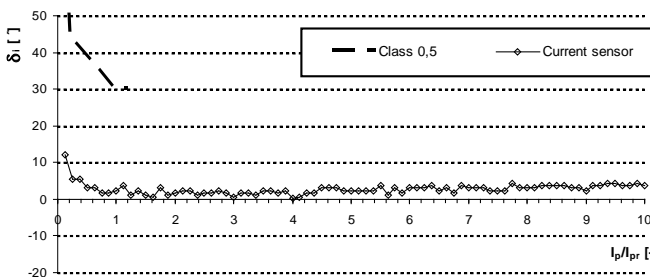*Fig. 3: The current error (ratio error) of the current sensor.*

Fig. 4: The phase displacement of the current sensor.

FINAL CONFRONTATION OF RCS AND CTS

The current transformer and current sensor final confrontation of the current error and phase displacement is shown in Figure 5 and 6. The current sensor transformed tested primary current

with very high accuracy. The current error and phase displacement of the current sensor with used calibration factor is better than in measure current transformer (winding S1) in all tested range - up to ten times the rated primary current.
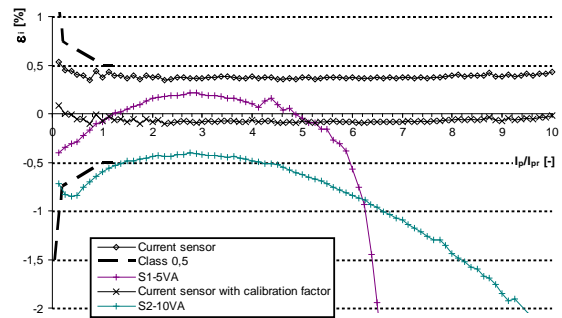

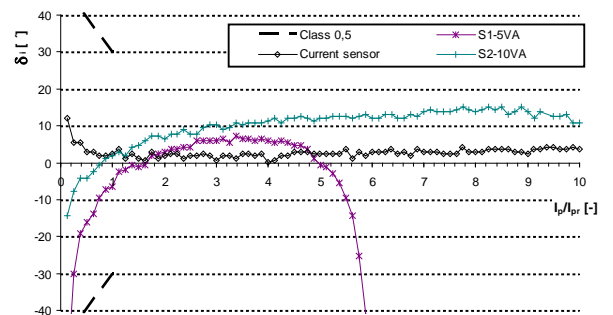*Fig. 5: CT and RC current error confrontation.*

Fig. 6: CT and RC phase displacement confrontation.

The next advantage of the sensors is its compactness. The absence of iron core makes it possible to be a smaller sensor construction than it is with CTs. When only one sensor for measuring and protection is used it can save up its precious size in a distribution point too. The more suitable way is to use a combi-sensor which has the same size as a similar current transformer, but containing a voltage and a current sensor.

Fig. 7: Current transformer, combi-sensor and current sensor.

CONCLUSION

Possibilities of usage, flowing from different construction of instrument current transformer and sensor, were confirmed by testing of their accuracy. Thank ferromagnetic core, over current on the primary side of the current transformer may cause its saturation and secondary current is distorted. In contrast to current sensor which

design is in most cases consistent with Rogowski coil. Thank this construction current sensor has no iron core to saturate and sensor is linear even when is subjected to large currents. Disadvantage of RC´s construction is low power output signal and the signal has to be integrated that the output signal was proportional to primary current. Not only core construction but also connected burden has great influence to current transformer accuracy. When rated burden is exceeded, the saturation come with lower primary current and current error and phase displacement is larger than it is with rated burden of transformer. Advantages and disadvantages are obvious in Figures 5 and 6, where the sensor exceed the protective current transformer (S2) by the linearity in all tested range. Constant current error and phase displacement make possible application the calibration factor of the sensor and reduce current error to the minimum. In this case the sensor has better accuracy then the measuring transformer (S1).

REFERENCES

1 KOJOVIC, Lj.A.: Comparative performance characteristics of current transformers and Rogowski coils used for protective relaying purposes. IEEE, 2007

COMPARISON OF AMOUNT OF SOLAR ENERGY
OF THE PHOTOVOLTAIC PANEL IN THE GIVEN AREA

Khisamutdinov N., Ptáček M.

Supervisor: Toman P., Associate Professor

Brno University of Technology, Faculty of Electrical engineering and Communication, Department of Electrical Power Engineering, Technicka 8, 616 00 Brno, Czech Republic, www.feec.vutbr.cz/UEEN

email: xkhisa00@stud.feec.vutbr.cz, xptace10@stud.feec.vutbr.cz

ABSTRACT

This paper evaluates the results of continuous measurement of static photovoltaic panel. There are also quantified the value of solar radiation incident on the photovoltaic panel. These values are compared with amount of solar energy in photovoltaic database of geographical information system. Furthmore, we describe power potential of the location where the photovoltaic system is located and we present the differences between the measured and theoretical values of amount of solar energy.

1   INTRODUCTION

Today's Europe strongly supports the development and expansion of renewable sources, especially photovoltaic power plants. In many countries, this expansion is influenced by supporting legislation. The main advantage of photovoltaic power plants and photovoltaic panels is the ability to directly convert solar energy into electrical energy. A significant disadvantage of silicon photovoltaic panels is a direct proportionality between the produced electrical power and the intensity of solar radiation. The proportionality creates instability of power supply and it can then affect the overall stability of electric networks with photovoltaic sources. We must predict how electrical power can be produced in the location where the power plant will be constructed. The main input data used in the planning process is solar radiation. Same photovoltaic power plants can produce different electrical energy, because each location has different production potential. The Department of Electrical Power Engineering FEEC, Brno University of Technology was established to do the research that deals with the analysis of photovoltaic panels and suitability of production conditions.

2   FACULTY PHOTOVOLTAIC SYSTEM AND PGIS

Installed power of photovoltaic power plant was 39,51MW and 464,58MW in December 2008 and 2009. This represents great development of use of photovoltaic sources in Czech Republic. Increase of installed power is main reason why we are interested in this analysis. Faculty photovoltaic panel 100Wp is subjected to analyse the primary and instrumental variables. Measuring system mainly evaluates air temperature, temperature of photovoltaic panel, instantaneous electrical power and intensity of solar radiation. Measurement of quantities in the time range is from 6 AM to 9 PM. This interval was found to continue the system's ability to produce energy. To ensure meaningful value of

the measured variables the individual values are recorded every 2 minutes. All variables are processed in the form of database files and their analyse is implemented using MatLab program. The results of solar radiation are evaluated in this paper.

In Brno, the intensity of solar radiation is one of the highest in Czech Republic. Amount annual of solar power is between (1050–1100) $kWh \cdot m^{-2}$ in this location. In general, the intensity of solar radiation quickly increases in the early morning. On the other side it quickly decreases in the late afternoon. The intensity is variable throughout the day because it may be reduced by clouds, atmospheric haze or by the angle of the sun to the surface.

Fig. 1 shows A-V characteristics of photovoltaic panel for different intensity of solar radiation.
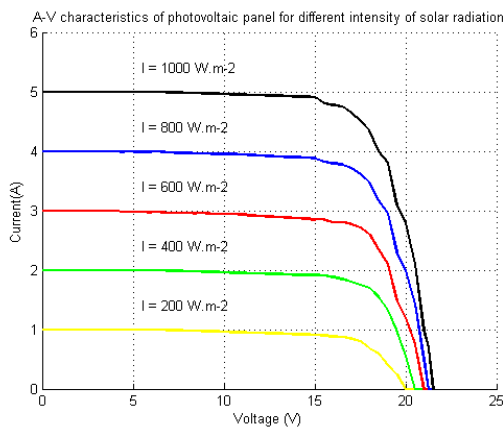

Fig. 1 A-V characteristics of photovoltaic panel for different intensity of solar radiation.

We can observe that the change of intensity leads to a significant change in the current short and slight change in voltage. For each point on the graphs, the voltage and current can be multiplied to calculate power. The intensity of solar radiation is measured by pyranometr which is designed to detect the total intensity of incident direct and diffused solar radiation. The spectral sensitivity of the pyranometer is constant over the whole defined frequency range. The measured intensity corresponds to the intensity of solar radiation in the wavelength range (300–5000) nm.

Our measured values of the intensity of solar radiation must be converted to the amount of solar energy. The relationship between the intensity of solar radiation and solar energy is given by the equation (1.1) below.

$$E = \int_{t_0}^{t_1} I(t) \cdot dt \approx \sum_i I(t_i) \cdot \Delta t_i \qquad (1.1)$$

where E is solar energy per unit area
I is intensity of solar radiation per unit area
Δt_i is time interval

Amounts of solar energy are compared with the equivalent values in the application Photovoltaic Geographical Information System (PGIS) - Interactive Maps, which is created by the Institute for Energy, Renewable Energy Unit. For a chosen location, application provides monthly and yearly averages of amount of solar radiation at horizontal and inclined surfaces and other climatic and photovoltaic related data.

3   RESULTS OF MEASUREMENTS

In PGIS we need to specify exact coordinates where the photovoltaic system is and its other parameters. Location: 49°11'53" North, 16°35'32" East, Elevation: 245 m a.s.l., Irradiation at chosen angle: 60°

Fig. 2 shows average daily amount of solar energy of photovoltaic panel by months.
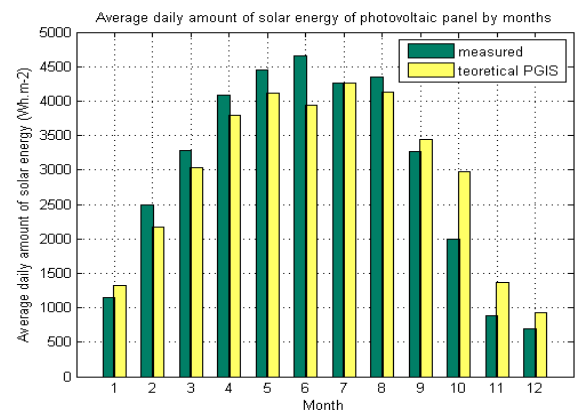
Fig.2 Average daily amount of solar energy of photovoltaic panel by months

Fig. 3 shows the monthly amount of solar energy of photovoltaic panel.
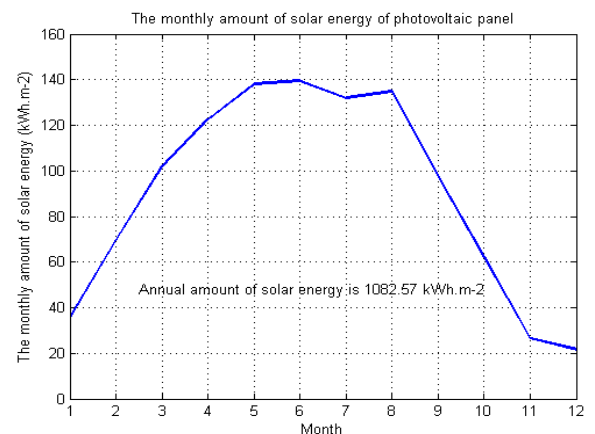
Fig. 3 The monthly amount of solar energy of photovoltaic panel

Graphical distribution of the amount of solar energy confirms the fact that the most appropriate and optimal conditions for the location of the photovoltaic system are in the summer months than winter months. Comparison of measured values with values in the database shows that they are almost identical and the differences are minimal. Significant differences

15

occur in October and November, because the measuring system has been broken for several days in these months.

The database can be considered a very suitable tool for initial design of photovoltaic power plants or for more accurate identification of the potential financial returns. Our measured annual amount of solar energy is 1082,57 $kWh{\cdot}m^2$.

4   CONCLUSIONS

Based on the results, we can state that the main deficiency of photovoltaic power sources seems to be the inability to supply constant electricity independently on a daytime or seasons of a year. A change in the weather has a significant impact on the electrical power of photovoltaic sources, which can be produced from the amount of solar energy.

Installed power of photovoltaic power plants is predicted 1000MW at the end of 2010 in the Czech Republic. In spite of that the electrical power will be a great and variable in summer mounts and sudden change of this electrical power could lead to instability of electrical network. Based on the results we will have to adapt the system of operation of an electricity network.

REFERENCES

[1] Department of Electrical Power Engineering, FEEC BUT, *Laboratory of unconventional energy conversion* [online] Available from URL: http://www.ueen.feec.vutbr.cz/labo-ratory-of-unconventional-energy-conver-sion

[2] Energy Regulatory Office, *Installed power capacity in CR* [online] 2009 Available from URL: http://www.eru.cz/user_data/files/ statistika_elektro/rocni_zprava/2008/index.htm

[3] Energy Regulatory Office, *Installed power capacity in CR* [online] 2010 Available from URL: http://www.eru.cz/user_data/files/ statistika_elektro/mesicni_zpravy/2009/prosinec /page50.htm

[4] European Commission, Joint Research Centre. Institute for Energy. *Photovoltaic Geographical Information System - Interactive Maps*, [online] Available from URL: http:// re.jrc.ec.europa.eu/pvgis/apps3/pvest.php

ECONOMIC ANALYSIS METHOD OF WIND POWER STATION

Suleimenov Ye.K.

Research advisor: Lukutin B.V., doctor of engineering science, professor

Tomsk Polytechnic University, 30 Lenin Avenue, Tomsk, 634050, Russia

E-mail: sulyerzhan@gmail.com

Wind power engineering, like any other branch of energetics, is characterized with such criteria as incremental cost of installed capacity (capital expenses CAPEX) and cost production (which includes operation expenses OPEX). CAPEX of wind-driven power plant comprise costs of purchasing of wind-driven electric plant; transportation expenses; construction expenditure; costs for grid connection; costs for land use and bank loan [1]. The last kind of cost is originated due to huge capital expenses and people (enterprises) have to take a bank loan. According to [2], 1 kWt of installed capacity costs in average around 1 300 – 2 000 $.

In terms of data in [3], capital expenses components of average capacity wind-driven power plant can be represented in next table.

Table 1. Capital expenses components of wind- driven electric plant

Capital expenses components	Share from the overall expenses, %
Wind turbine	74-82
Power connection	2-9
Electrical equipment	1-9
Costing of a foundation	1-6
Financial expenditure	1-5
Costs for road construction	1-5
Land	1-3
Consulting	1-3

It is necessary to note that transportation expenses are included in the costing of wind

turbine, whereas project capital costs are not included. Generally, project capital expenses $(CAPEX_{proj})$ can be identified according to next formula:

$$CAPEX_{proj} = 50 * MRPL,$$

where MRPL – minimum rate of payment for labour, $.

As the Table 1 shows, significant part of CAPEX composes costs for purchasing of wind turbine. However, it is important to take into consideration that costs for electrical equipment and grid connection may rise up to 10%.

The necessity of CAPEX calculation of wind-driven power plant is caused with the possibility to compare it with CAPEX of conventional energy source, thus, to identify economic feasibility and efficiency of wind-driven power plant [4]. It should be noted that for the last 25 years incremental cost of installed capacity decreased from $4000 per kWt to $950 per kWt.

Another significant economic factor is cost production, determined by the volume of produced electric energy. It is interesting to follow that with the growth of wind-driven power plant capacity the cost of 1 kWt⨯hour produced electric energy declines, as the production of electric energy and operation factor of installed capacity increase. In the context of wind power engineering, this operation factor depends on wind velocity, operation and servicing costs, operating life of wind-driven power plant, rate of interest on loan and allowance for depreciation. It must be emphasized that the cost of 1 kWt⨯hour electric energy produced depends on wind velocity to a great degree. For example, it is possible when cost production at larger capital expenditures is lower, than cost production at lesser capital expenses, if wind conditions are better in first case. Also for the last 25 years cost production is also decreased from 30 cents per kWt⨯hour to 4 cents per kWt⨯hour.

Cost production is characterized by next figures: 1) operating factor of installed capacity; 2) operating hours of installed capacity; 3) specific energy generation per square unit of swept area.

Operating factor of installed capacity (F_{OIC}) describes the efficiency of any power station. This factor shows how well maximum possible capacity is used and can be identified by the following formula:

$$F_{OIC} = \frac{W_{actual}}{W_{max}}$$

where W_{actual} - actual annual production, kWt;

W_{max} - maximum annual production, kWt.

In respect to wind power engineering $F_{OIC} = 0,15$ - 0,30. Regarding conventional energy source,

F_{OIC} = 0,4 - 0,8. Overall, this operating factor depends on the following factors:
1) the reliability of power source (how often it is required to carry out repair, inspection);
2) load curve.

Moreover, in terms of wind-driven power plant operating factor of installed capacity depends on wind constancy and wind velocity.

According to the definition, operating hours of installed capacity (T_{OIC}) can be calculated by the following formula:

$$T_{OIC} = F_{OIC} * T = \frac{E_{ann.}}{N_{instal.}}$$

where T - number of hours of consumed electric energy, hours;

$E_{ann.}$ - annual produced electric energy, kWt*h;

$N_{instal.}$ - installed capacity, kWt.

Another typical characteristic of wind-driven power plant is specific energy generation per square unit of swept area [1]. Area of a circle, described with a windwheel, determines amount of potential wind energy which further can be converted into electric energy. As windwheel area of a circle depends on blade diameter of windwheel, thus, with the increase of blade turbine produced power also augments. However, with the increase of blade diameter, wind velocity should be higher in order to rotate wind-driven power plant.

Thanks to three figures of cost production described above preliminary annual volume of produced electric energy (E_{ann}) can be calculated by the following formula:

$$E_{ann} = N_{instal.} ⨯ F_{OIC} ⨯ T,$$

where $N_{instal.}$ – installed capacity, kWt;

T – number of operating hours of wind-driven electric plant, hours.

According to the experts' estimation, in the future cost production drop will be happened due to the following factors:
1) manufacturing optimization of wind driven power plant – 50%;
2) mass reduction of wind turbine – 35%;
3) operating and service costs, expenses for power connection and building of a foundation – 10 %;
4) more efficient conversion of electric energy- 5 %.

One of the most important factors of feasibility and efficiency for building of wind power plant is capital cost repayment period (T_{rep}), which can be identified according to the next formula:

$$T_{rep} = \frac{CAPEX}{I - OPEX}$$

where $CAPEX$ - overall capital expenses, \$;

I - income, \$;

$OPEX$ - operation expenses, \$.

Overall capital expenses ($CAPEX$) should be calculated by the following formula:

$$CAPEX = CAPEX_{spec} \Box N_{instal}$$

where $CAPEX_{spec}$ - specific capital cost for wind driven power plant, \$/kWt;

N_{instal} - installed capacity of wind driven power plant, kWt.

Operation expenses (OPEX) can be calculated by the next formula:

$$OPEX = n \Box CAPEX = n \Box CAPEX_{spec} \Box N_{instal}$$

where n – share of capital expenses for operating expenses (n=20-25%).

Income (I) should be determined by means of fuel costs calculation. In this case it can be calculated by the following formula:

$$I = N_{instal} \Box T_{OIC} \Box q \Box C_{rate} \Box P_{fuel}$$

where T_{OIC} - operating hours of installed capacity, hours;

q – specific fuel consumption in thermal power plants, ton equivalent of fuel/kWt $\Box$ h;

C_{rate} - rate coefficient;

P_{fuel} - fuel price for conventional energy source, \$.

Electric energy price (P_{EE}), produced by renewable energy:

$$P_{EE} = \frac{CAPEX + OPEX \bullet T_{life}}{E_{prod} \Box T_{life}}$$

where T_{life} - life time, years;

E_{prod} - annual produced electric energy for a year, kWt $\Box$ h/year

Economic benefit of wind-driven electric plant use is a price of electric energy, produced with a wind installation after capital cost repayment period.

Thereby, economic benefit (EB) due to the use of wind-driven power plant is identified with the following formula:

$$EB = (T_{life} - T_{rep}) \Box (E_{prod} \Box P_{fuel} - OPEX) \quad (1)$$

As it seen from the formula (1), economic benefit due to the use of wind-driven electric plant is determined with the fuel price for conventional energy sources. It follows that the use of wind driven power plant will have maximum effect at high fuel prices. As a rule, such areas are decentralized areas of power supply [1].

REFERENCES
1 P.P. Bezrukikh The usage of wind energy. - Moscow, Kolos. 2008. – 196 pages.

2 Lukutin B.V.,Surzhikova O.A., Shandarova E.B.: The renewable energetics in decentralized energy power supply. - Moskva: Energoatomizdat, 2008. 231 pages.

3 Renewable Energy World, July-August, 2004, Volume 7, Issue 4.

4 P. P. Bezrukikh, G. A. Borisov, V. I. Vissarionov etal. Energy Resources and the Efficiency of Using Renewable Energy Sources in Russia. – St. Petersburg, Nauka. 2002. – 314 pages.

Section II

INSTRUMENT MAKING

THE MODULUS OF A GYROSCOPIC ACTUATING DEVICE

Kamkin O.U.

The supervisor of studies: Golikov A.N., the higher teacher

The teacher of studies: Ursula., the higher teacher

Tomsk polytechnic university, 634050, Russia, c. Tomsk, Lenina st, 30

E-mail: ILuckyI@mail.ru

In existing down-hole devices for turn the body of down-hole device, which is had a body with a sensing transducers or tools, devices of anchoress up of the one part down-holling are applied, and another part should turn by the electric drive. The disadvantage of such devices is the necessity of their rigid fixing with down-hole walls; knots of such anchoress up of the mechanism in the conditions of a drilling fluid, high temperatures and pressures are elements of low operational reability.

In [1,2,3] is offered to apply gyroscopic executive device for manipulate the geophysic device state in the borehole. The building of such device allows to avoid the usage of mechanisms, operating in the drilling fluid, i.e. without the usage of the fixing devices by walls of the borehole.

Gyroscopic actuation devices (GAD) are applied to form the control moment, which is turned the object around its axis, to quiet or build the oscillations. A basis of such control moments is the gyroscopic moment.

One of the properties of the gyroscope is its precession formed by applied action of the external forces moment. It means to form the required control moment is enough to act by moment by an axis of a two-sedate gyroscope precession, we should apply the rotating moment, which will turn the device around the axis with a required angular speed.

In the picture 1a) the main view of a geophysical complex is presented, which consist of the gyroscopic actuating device 1 (GAD), the juncture device 2, the geophysical device 3, the attitude control system 4 and the geophysical cable 5.

The device's kinematical scheme for a turn down-hole device was compounded by the materials [2] and introduced in the picture 1b. The turn of the device around its longitudinal axis CC is created by the gyroscopic moments, which is form by two controllable gyroscopes. This dual controllable gyroscopes consist of gyromotors 1 with the frame 2, which is kinematical linked among itself by the antiparallelogramm 3. The control of frames rotation with gyromotors is applied by means of electromagnets 4.

The kinetic moments H_1 and H_2 of gyromotors is opposite directed and in start position is perpendicular to the axes of frames rotation $B_1 B_1$

and $B_2 B_2$ and longitudinal axes CC of the down-hole device. The gyroscopes will turn in opposite directions around of its internal axes $B_1 B_1$ and $B_2 B_2$ with angular speed, when one of magnets 4 will be actuated. It allows creating the doubled gyroscopic moment Mg around the longitudinal axis CC. The jet moments around the internal axes $B_1 B_1$ and $B_2 B_2$ compensates, which provides a work of device without of oscillations around of the cross-section axis.

After putting of electromagnets the movement of the actuating device will be stopped.

The next cycle of the further turn of the down-hole device is possible after set up of the axis of a rotation of the gyromotor in a start position. Returning of the frame with a rotation in a start position is by action of the spring linking frame with the gyroscopic actuation devices

a)   b)
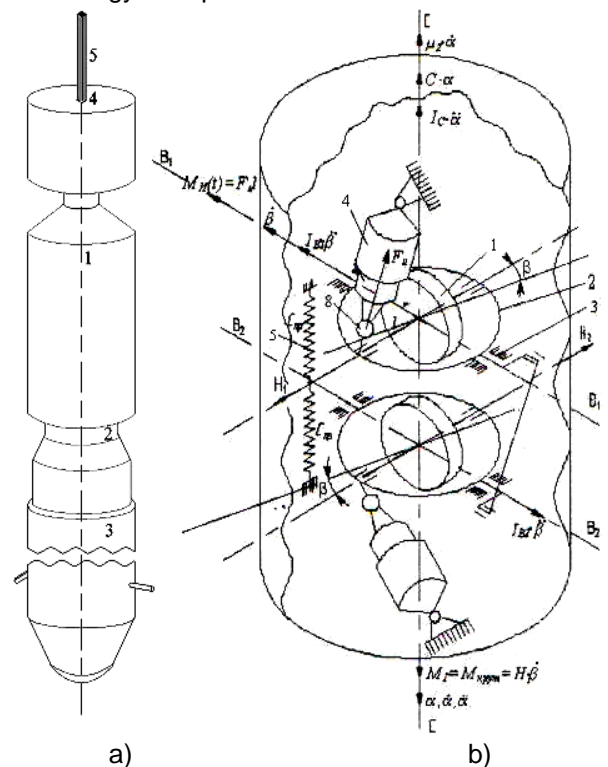
Picture 1. a) The geophysical complex;
b) The gyroscopic device for a turn of a down-hole device:

1 - the gyroscopic actuating device (GAD);
2 - the juncture device;
3 - the geophysical device (The perforator, PC-112);
4 - the attitude control system;
5 - the geophysical cable.

The equation presenting dynamic of gyroscopic actuating device will look like the following:

$$\begin{cases} I_c\ddot{\beta} + H\dot{a} + C_{s.r.}\beta_2 + \mu_1\dot{\beta} = M(t) \\ I_c\ddot{a} + H\dot{\beta} + C_k a + \mu_2\dot{a} = M_{fr} \end{cases}$$

Where: $H = H_1 + H_2$ - (Kinetic moment of dual gyroscopic motors);

I_e - The aggregate inertia moments of two gyromotors concerning an its interior fulcrum of an axes;

I_c - Inertia moment of the geophysical complex concerning an exterior fulcrum of an axes;

$a, \beta, \dot{a}, \dot{\beta}, \ddot{a}, \ddot{\beta}$ - Co-ordinates, angular velocities and rotary accelerations of rotational displacements of gyroscopes;

$C_{s.r.}$ – straight of the spring;

C_k - The conventional rigidity of the borehole cable;

μ_1 - Coefficient of friction in the inside of down-hole device (a friction in knots of bearing boxes and etc.);

μ_2 - Coefficient of a viscous friction of the down-hole device in a drill fluid;

$M(t)$ - The moment of the driving forces affixed on an interior axis

$M(fr)$ - Friction torque by walls of down-hole device

The research of this system dynamics of equations requires of the application of the up-to-date software such as Mathcad and Mathlab.

The influence analysis of affecting factors to geophysics complex by exploitation allowed to form the main engineering problems at realization of the gyroscopic actuating device, which consists of:

1. The device have to work in down-holes of a small diameter, no more than 240 mm, in the depth of 3000 metres and more, as so in surrounded, and as in not surrounded.

Therefore, the diameter of the device have to be smaller value, for example, in the work with the wimbling perforator of the type PC-112 - no more than 112 mm. In this case, it is necessary to use a desksize gyroscopes with a sufficient kinetic moment for the building of required gyroscopic moment.

2. The chisel fluid is a water, or a drill fluid in the drill-hole with oil components form the hydrostatic pressure and enough excited environment. For using devices in this factors is necessary to change of a straight and a protect-corrosion material for device of protective casing.

3. The temperature in a hole can be more than 120°C. In process of dipping in the hole the temperature of all elements of the giroscopic actuation devices is increasing by the ambient temperature, and by the heat releases of working electroelements of the device: the gyromotors, control electronics and others.

Usually the using of lubricants at heats leaks and evaporates, leaving thus an unwanted sediment. Therefore is necessary to search or create of thermally sound electromechanical elements and applying of high-temperature accessories and materials.

4. In process of using the gyroscopic actuating device can be influenced by considerable mechanical actions: vibration , shocks by a tool joints of well casings at a descent-lifting in the hole, jolting in transit. Almost all gyromotors of aerospace assigning are not intended for work in such influence. It is necessary to researches and improve the elements of constructions of gyromotors.

5. The construction is a product of exact electromecanics and demands hi-tech manufacture, which, probablly, may to increase in the cost price.

6. In the conditions of reorientation, i.e. an acclinal or horizontal position the dynamics and view of moving of the device changes and therefore a complementary research of the difficult mechanical system in these requirements is necessary.

7. At engineering of electromagnets there is a problem about an effective disposition of transit conductors. It should take place through electromagnets which is charger for the perforator, dual mechanical giromotors and one more electromagnet in the limited volume. At such position of the device there is a probability "Returning to a starting position" of gyroscopic actuating device on the interior surface of the hole that is invalid for correct manipulation of the device.

The solution of enumerated problems to creation of construction will be makes with use of programs such as Autocad, T-flex, Solidworks, Ansys, Compas. These software products will allow to construct devices and to provide the strength analysis, thermoanalysis of members and a device construction as a whole, that considerably will speed up a projection problem solving, , which is considerably simplifies a decisions problem for creating of elements of the gyroscopic executive modulus.

The important problems at the creation of gyroscopic actuating device is improvement of productivity and quality of work of the device, reduction mass-gabarits characteristics, creation of strong knots of a design and improvement of

its functionality possibitiles. For this purpose is necessary to correct compact placing of all elements down-hole device.

LITERATURE

1 The patent №211287 Russian Federations. The geophysical complex.

2 The patent №2184228 Russian Federations. The gyroscopic device for a turn of a down-hole device.

3 The patent №2184229 Russian Federations, MKI E21B 47/02. The gyroscopic device for a turn of a down-hole device. L.N. Belyanin, A.N. Golikov, V.M. Martemianov - №2000119073; Published by 27.06.2002.

ISSUES OF MEASURING CAPACITANCE-VOLTAGE CHARACTERISTICS OF POWER SEMICONDUCTOR DEVICES BY FREQUENCY METHOD

Glebochkin V. P., Bespalov N. N.

Scientific adviser: Bespalov N. N., candidate of technical science

Ogarev Mordovian State University, faculty of electronic engineering,

430005, Russia, Saransk, B. Khmelnitskogo, 39

E-mail: bnn48@mail.ru

The parameters that determine the quality of manufacturing and reliability of power semiconductor devices (PSD) are their parameters and characteristics in a low conductivity state. Maximum accuracy of measuring the parameters of current-voltage characteristic of PSDs in a low conductivity state is achieved in a static state. Data of the limit parameters of the current-voltage characteristic in manuals are given for a static state in which only active component of current through the PSD is measured. The usage of constant test signals causes rapid overheating of the semiconductor structure, so by [1] the measurement of limit parameters of PSD occurs when it was exposed to a 50 Hz half-sine test signals.

In [2] it was shown that when applying a pulse of half-sine voltage $u_{D(R)}$ to the p-n junction active $i_{D(R)A}$ and capacitive $i_{D(R)C}$ components of the total current $i_{D(R)_{\Sigma}}$ flow through it (1):

$$i_{D(R)_{\Sigma}} = i_{D(R)A} + i_{D(R)C} \qquad (1)$$

The total current $i_{D(R)_{\Sigma}}$ is usually measured during the tests.

The capacitive current $i_{D(R)C}$ is caused by the capacity of PSDs, which depends on the applied reverse voltage. Therefore, for a more precise measurement of the reverse branch of current-voltage characteristic by the method proposed in [2], first it is necessary to measure the capacity-voltage characteristic (C-V characteristic). Knowledge of C-V characteristic helps to determine the values of the barrier capacitance C_b of p-n junction for different values of reverse DC voltage U_R.

Knowledge of C-V characteristic can also estimate the critical rate of rise of voltage on the thyristor dU/dt_{crit}. Functions $C_b = f(U_R)$ of real devices can be used in mathematical models, for example, during scientific research of turn-on and turn-off transient state of several PSDs in parallel connection.

There are several methods for measuring of the C-V characteristics of semiconductor devices, but the range of the test voltage signal in them rarely exceeds 100 V, i.e., they are not suitable for PSDs.

The proposed frequency method and a functional circuit of a device for determining C-V characteristics of PSDs are presented in [3], where C_b is included into an oscillatory circuit as a frequency-master element. C_b is to be found from a period of oscillation, which changes while applying U_R to the p-n junction. Let us consider the problems of measuring of C-V characteristics by frequency method.

One of the main difficulties of measuring of C-V characteristics of PSDs is a large range of C_b: from fractions nF to several uF. This occurs due to the relatively large range of values of the area of semiconductor wafers. Therefore, the influence of various errors during measuring procedure in different regions of the range of the measured capacitance will be different.

Estimation of C-V characteristics of PSDs with different diameters of semiconductor wafers is shown in Fig. 1 and calculated for an abrupt p-n junction by formula (2), which is given in [4]:
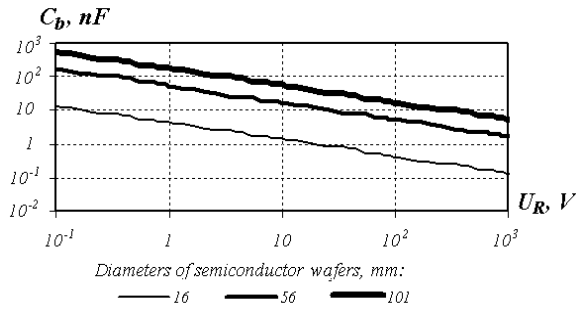
C_b, nF

Diameters of semiconductor wafers, mm:
——— 16 ——— 56 ——— 101

Fig. 1. C-V characteristics *of PSDs with different diameters of semiconductor wafers*

$$C_\delta = \frac{\varepsilon \varepsilon_0 \pi d^2}{2,08 \cdot \sqrt{\rho \cdot U_R}}, \qquad (2)$$

ε — permittivity of silicium; ε_0 — permittivity of free space; d — diameter of semiconductor wafer; ρ — base resistivity; U_R — reverse DC voltage.

Fig. 2. shows the functional diagram of the measuring part of the C-V measurement device containing oscillatory circuit with the measuring
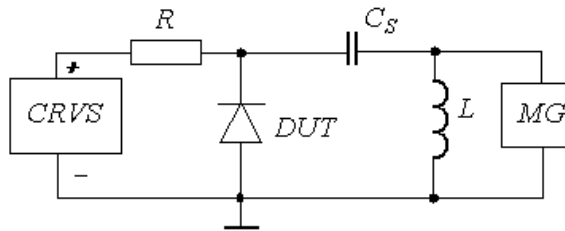

Fig. 2. *Functional diagram of the measuring part of the C-V measurement device*

generator (MG) and the device under test (DUT).

In [3] it is shown that the period of oscillation of the measuring circuit of the generator is given by:

$$T = 2\pi\sqrt{C_\Sigma L}, \qquad (3)$$

L — coil inductance; $C_\Sigma = \frac{(C_S \cdot C_b)}{(C_S + C_b)}$, C_b — measured capacitance of *p-n* junction; C_S — separating capacitance.

From the expression (3) C_b is found as

$$C_b = \frac{C_S \cdot T^2}{4\pi^2 C_S L - T^2}. \qquad (4)$$

To the difficulties of measuring of C-V characteristic should also include the provision of the controlled reverse voltage supply (CRVS) with high frequency isolation. For this purpose separating capacitor C_S is connected in series

with the DUT. However, C_S affects the oscillation period of the generator and makes the error.

In [3] it is shown that the influence of the C_S is most affected when measuring C_b of PSDs with a large wafers. For instance, for the devices with a diameter of the semiconductor wafer of 56 mm it is recommended to use the value of C_S not less than 100 uF to provide errors in determining C_b less than 0,5%. For devices with a diameter of 56 mm the value of C_S will make 300 uF.

The influence of parasitic capacitance, however, will be manifested most strongly in measuring C-V characteristics of the devices with small semiconductor wafers. This makes it difficult to measure PSDs with C_b of less than 1 nF. To solve this problem, we can measure the parasitic capacitance of the circuit. For this purpose, the precision capacitor C_m with a capacity which is equal to the maximum measured PSD capacitance is connected to the circuit instead of the DUT, and then frequency f_1 is measured. Then, it is necessary to disconnect the precision capacitor and measure the frequency f_2 without him. Then parasitic capacitance C_p can be found by (5):

$$C_p = \frac{C_m \cdot f_1^2}{f_2^2 - f_1^2} \qquad (5)$$

Active parasitic resistances also present in the oscillator circuit and affect the oscillation period of the measuring system. However, in [3] it is shown that their effect is small and they can be neglected.

The essential problem of measuring C-V characteristics of PSDs on a small U_R is the influence of the variable component, which arises on the side of the oscillation circuit and which is applied to the DUT. Thus, it modulates U_R and, accordingly, changes C_b.

According to [5], the U_R accuracy should be not lower than 1,5-2%. In [3] it is shown that for compliance with this condition at 1 V amplitude of AC signal of MG capacitance measurement can be performed only after $U_R = 10$ V. Thus, to determine the value of capacitance at lower U_R it is necessary to reduce the amplitude of the AC signal, which leads to noise immunity and frequency instability of MG. Also in [6] it is recommended to choose a step change of U_R at least 10 times larger than the amplitude of the AC signal of MG.

The issues of measuring of C-V characteristics of PSDs, which are considered in this report, are solved. The limits of applications of the frequency method are

23

defined. Currently, the work is underway to design and develop the device for measuring C-V characteristics.

LIST OF ACRONYMS:

C-V characteristic — capacity-voltage characteristic;
CRVS — controlled reverse voltage supply;
DUT — devise under test;
MG — measuring generator;
PSD — power semiconductor device.

BIBLIOGRAPHY CITED:

1   GOST 24461–80. Power semiconductor devices. Methods of measuring and testing. – M. : Publishing Standards, 1981. – 56 p.
2   Bespalov, N. N. Device for measuring of capacity-voltage characteristic of power semiconductor diods / N. N. Bespalov, V. P. Glebochkin. // Proceedings of the XIII Scientific Conference of young scientists, postgraduates and students of Mordovian State University. / Mordovian University, – 2008. – Part 2. – P. 258–264.
3   Bespalov N. N., Glebochkin V. P. On the error of measuring the capacity-voltage characteristics of power semiconductor devices // Electronics and information technology. — 2009 special edition (6) — 2009. — (http://fetmag.mrsu.ru/2009-2/pdf/CV_measurement_%20error.pdf). — 0420900067/0019
4   Calculation of power semiconductor devices / P. G. Dermenzhi [and others] – M. : Energy, 1980. – 184 c.
5   Semiconductor diodes. Parameters, measurement methods / ed. N. N. Gorunov and J. R. Nosov. – M. : Soviet Radio, 1968. – 303 p.
6   Pedersen, M. Measurements of C-V characteristics of different components: a capacitor, a p-n junction, and a MOS circuit. Comparison of different methods of measurements. // Bac. Polyt. Thesis for University of Southern Denmark (SDU), Odense. – 2002. – P. 65.

Section III

TECHNOLOGY, EQUIPMENT AND MACHINE-BUILDING PRODUCTION AUTOMATION

OPTIMIZATION OF THE DESIGN-TECHNOLOGICAL CYCLE TIME

OF THE MANUFACTURING PARTS USING CAD/CAM/CAE SYSTEM

FOR EXAMPLE CHAIN SPOCKET

Artyom S. Babaev, Dmitry Yu. Pyzhik.

Scientific Supervisor: Pavel Yu. Proskuryakov, Senior Lecturer

Linguistic advisor: Lecturer Olga S. Glushakova

Tomsk Polytechnic University, Russia, Tomsk, Lenin str., 30, 634050

E-mail: temkams@mail.ru

To begin with it should be stated that there are constant complication of mechanisms and construction machinery, as the requirements for their performance characteristics increase constantly; high competition on machine-building market makes the need for a substantial reduction in the duration of the cycle of production and technical products obvious. Besides, modern business uses colossal potential of computers, their adaptable graphics modules, and large amounts of memory for the automation of design and direct production tasks - from design concept to technical implementation. That is why to ensure the above requirements one applies CAD (computer aided design), which includes the following modules: CAD (computer-aided design) which is the technology to use computer systems to facilitate the creation, modification, analysis and optimization projects; CAM (computer-aided manufacturing) which uses the computer systems for planning, monitoring and management of manufacturing operations, CAE (computer-aided engineering) which is used to analyze the geometry of the CAD, modeling and studying the behavior of virtual products. In should be taken into account that the systems of this type are used extensively in machine tools, agricultural machinery, roads [1]. Thus, the research paper deals with the optimization and automatization processes of making stars of the roller chain transmission description.

Generally, the researchers deal with regulating and optimization the phase of design and manufacturing process of cycle star roller chain transmission. One must be aware that chain transmission are simple and economical. On the one hand in comparison with gears, they are less sensitive to inaccuracies in the location of shafts, shock loads, allow virtually unlimited spacing on centers, and provide a simpler layout. On the other hand in comparison with belt drive, they are characterized by the following advantages as the absence of slip and the constancy of the average gear ratio. Sprockets are made by running in the special gear hobbing machines [2]. However, it should be emphasized that a significant drawback of this method lies in the fact, that the manufacturing of metal special cutting tool - hob for the production of each new part, which increases the prime cost of the product [3]. Consequently, this approach is acceptable in the single-piece production. From the standpoint of reducing the financial expenditures and increase production to offer cost-effective replacement for a more progressive method of machining, which also will be used and less expensive price of the instrument is required. Thus, the design in this case can be completely streamline and automate with the application of CAD and CAE systems, by this reducing time for designing products and efforts of constructor that allows to expand the range of products at the expense of saving time on geometric calculations and manual formation of a single solid-state model. Foregoing requirements are fulfilled with rules and regulations of common regulatory codes on USDD, USTD and USTPP.

Before us is tasked with regulating the phase of design and technological cycle of manufacturing chain spocket from the moment the assignment of geometric parameters, the accuracy and ending its manufacturing. During the research the application for CAD: KOMPAS-3D V11 which is produced by Company Askon (Russia) and FeatureCAM firm's Delcam (Great Britain), which occurred in the main successive steps of designing and manufacturing products was taken.

So, for the given performance characteristics sprocket chain gear has a number of teeth $Z_{pinion}=22$, driven sprocket – $Z_{driven\ spocket}=44$, (driven sprocket is not considered in this work, but it has a significant influence on the performance of geometric calculations of the model). Profile of the tooth and with a displacement of the arc basins according to GOST 591-69, accuracy according to GOST 591-69 stars of the given group A - high accuracy. Driving roller chain, which is engaged with a sprocket, is designated as OL-19.05-3180 and the length is 1500mm. For the given parameters

in the design and calculation module KOMPAS-3D Shaft-2d is an automated geometrical calculation. The data are stored in a separate block of memory system KOMPAS. Calculation with the required accuracy determines the geometric parameters that are sufficient in the sequel to create a computer-aided three-dimensional model. The resulting design calculations diameter circle protrusions of teeth are D_a=142,63mm, chain's width B=11,66mm. Then one should select the type of stars, in the specific example - single-flat (fig. 1). Generating solid model stars in the KOMPAS-3D system consists of the construction of the periphery of the disc with extrusion, resulting in the previous part of the previous calculation, the profile of teeth. It should be noted that after the formation of the model designer has an opportunity to add or correct the resulting product. One more important issue is that a computer model is needed primarily to identify the geometry and shape of the product surface, and further it defines a toolpath.
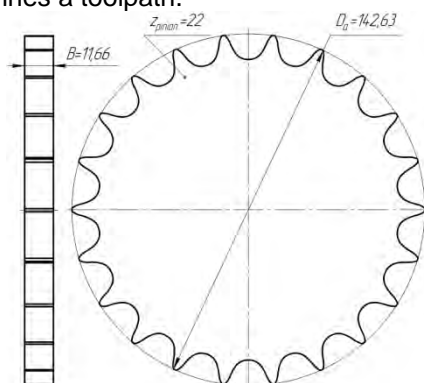

Fig. 1 Sketch star chain transmission

3D - prototype of the part is made and now one must precede the drafting of the route of machining and automated creation of control program which is the final phase of processing of the workpiece on CNC milling machine. For the transfer the model from KOMPAS-3D to applied FeatureCam format *.sat is used. It's recognized by CAM-systems as the standard ACIS-text [4]. FeatureCam generates automatically according to set parameters of the material and shape of the workpiece, form the final product and the type of metal-control program in the form of NC code (numerate control code). If necessary, the strategy process is changed by the engineer-programmer and as a consequence the received code is changed. Nevertheless, the following step is importing the file to the FeatureCam, which later would form the basis for creating the control program. Before you beginning of the work, choose the type of the processing which is defined on the basis of technological considerations and available equipment in machine tools. On default, the system has the
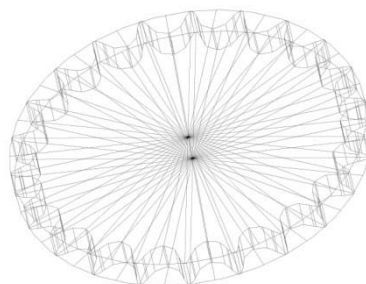
ability to work in metric or inch units.

Fig. 2 Meshwork solid model

For this paper research the metric system was used. The orientation of the parts in space is relative to local coordinate system of programs used in such a way, that the axis OZ passes through the center of researched part, perpendicular to the surface end. The shape of the finished product determines the geometry of the workpiece. Sprocket is made from the disc, which thickness is identical to the thickness of the product (fig. 2).

The diameter of the workpiece drives assigned to the allowance for machining; it is necessary to draw attention to the fact that the axis of the workpiece and the part are on the same line. Material goods determine the cutting tools and modes, which will be processed and, consequently, the time is spent on milling. When specifying the grade of the material FeatureCam automatically calculates and determines optimum cutting tool from the toolbox (also you can create your own set), tool advance and speed of rotation of a tool that on-demand technologies are changing in the process of getting of the NC code. Manufacturing drive chain transfers material steel 5140H, which is selected from the extensive database of materials FeatureCam. Curved surface of the teeth of star form a complex trajectory of the cutting tool. After recognizing solid FeatureCam model, the identification of elements, present a model in the form basic technological elements. FeatureCam degree of automation is high enough, so that for implementing a code generation process must ensure the proposed system versions of processed surfaces, in our case - the front and curved shape of the tooth forming stars. The flexibility of the system in parallel mode allows automatic detection in manual mode. Once the selection is made of material, geometrical parameters of the workpiece, the system laid down by using standard processing techniques from the base of technological elements, tools, and recommended for cutting conditions for the control program and produces two-or three-dimensional visualization processing. It should be pointed out that all parameters processing

technologies can be installed according to preliminary calculations, or can accept the default at any stage of a control program. What is more, the implementation of the visualization allows checking on the occurrence of collisions, in collisions of nodes of the machine or instrument to the profile of the workpiece. The resulting control program in the format encoding Fanuc transferred to the machine, where the final debugging and preliminary simulation of the process. The resulting control program in the format encoding Fanuc transferred to the machine, where the simulation is occurred with the purpose to verify the NC code in a particular system of CNC, if necessary, NC code, adjustment of the machine and processing [5].

As a result of the work chain spocket was designed with the integrated application of CAD system, manufactured and produced an imitation processing studied detail - the drive chain of transmission. Geometric figures parts after milling on the lathe EMCO Concept Mill 155 are installed within tolerances. Sequential control of the technological cycle of manufacturing has allowed stars to obtain the following results:

• Using Modules CAD / CAM / CAE minimizes the cost of temporary registration in accordance with the standard documentation as the design (building products), and the development of a single process;

• Application of CAD has allowed a production of stars by using a universal cutting tool - end mill. From an economic point of view, a departure from the special tool in the factory will create a significant reduction in the cost of parts due to the fact that the hob requires preliminary design and construction for the studied stars in the individual production;

• Implementation of electronic document in the project process cycle a product is organizing an effective synchronous design and technology in enterprises, thereby enhancing the culture of production.

References.

1 *Ли Кунву.* Основы САПР. - СПб.: Питер, 2004.-560 с.: ил.
2 *Маталин А. А.* Технология машиностроения: Учебник.– Л.: Машиностроение, Ленингр. отд-ние, 1985. – 496 с., ил.
3 *Кожевников Д. В., Кирсанов С. В.* Металлорежущие инструменты: Учебник. – Томск: Изд-во Том. К58 ун-та, 2003. – 392 с., ил.
4 САПР технологических процессов: учебник для студ. высш. учеб. заведений/А. И. Кондаков. – 2-е изд., стер. – М.: Издательский центр «Академия», 2008. – 272 с.
5 *Zeid Ibrahim* CAD/CAM Theory and Practice,- Tribune, 2006.

DEPENDENCE OF CHEMICAL COMPOSITION OF WELD METAL OF GL-E36 STEEL JOINT WELDS ON WELDING CONDITIONS

Dr. Chinakhov D.A.

Yurga technological institute (branch) of Tomsk polytechnic university

652055, Leningradskaya st., 26, Yurga, Kemerovskaya oblast, Russia

tel. +7(384-51) 6-53-95, fax. +7(384-51) 6-26-83,

zver73@rambler.ru

One of the important problems of modern production is improvement of technical and economic parameters of weld-fabricated constructions on the ground of reducing their specific metal consumption, increasing service reliability, strength balance and service life. The improvement of production technology allowed to increase the level of secondary characteristics of low-alloyed and alloyed rolled steels, primarily, their resistance to cold cracks formation. These steels provide operation reliability of large-sized constructions, bridge conduits, ship hulls and main pipelines. Herewith it is desirable joint welds to possess required service and technological characteristics without additional thermal treatment [1-4].

One more factor which complicates production of full strength welds of high quality is subjection of alloyed steels to development of brittleness resulted from hydrogenation of weld metal and formation of high-temperature chemical microheterogeneity in joint weld area, that can cause crack formation and lead to destruction of weld-fabricated construction under high internal stress or cyclic external forces [3, 4].

A number of factorial experiments was carried out in order to determine the dependencies of chemical composition of weld metal in GL-E36 steel joint welds on controlled parameters of welding conditions.Mechanized multilayer welding of GL-E36 steel plates 150x300 in size and 18 mm in thickness with slot grooving (pic. 1) using welding wire Union K 52 (tabl. 1) 1,2 mm in diameter in mixture of gases Ar 82% + CO_2 18% was completed with fixed arc with two-spool gas shielding without preheat cycle and post thermal treatment [5, 6].
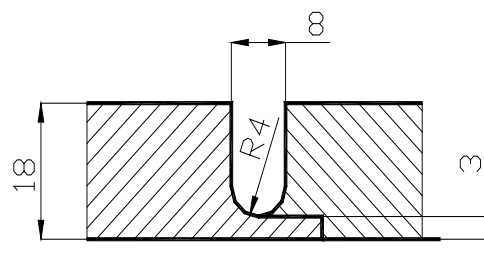
Pic. 1. Slot grooving with U-form

Full factorial experiments were carried out to plan and estimate the results of research [7]. The controlled parameters were varied on two levels: current strength I_{w1} = 170A and I_{w2} = 210A, arc voltage U_{a1} = 25V и U_{a2} = 27V, speed of welding V_{w1} = 25 cm/min и V_{w1} = 30cm/min. Consumption of shielding gas Q = 12 L/min.

Table 1. Chemical composition of GL-E36 steel and welding wire Union K52 according to the steel classifier

Grade	C	Si	Mn	P	S	Cr	Al	Cu	Nb	V	Mo	Ni
GL-E36	<=0,18	<=0,5	0,9-1,6	<=0,04	<=0,04	<=0,2	>=0,02	<=0,35	0,02-0,05	0,05-0,1	<=0,08	<=0,4
Union K52	0,08	0,85	1,5	0,025	0,025							

A matrix for planning of full factorial experiment was worked out to carry out experiments (tabl. 2).

Table 2. A matrix for planning of full factorial experiment

Controlled parameter	number of experiment							
	1	2	3	4	5	6	7	8
1. Welding current strength I_w, A ($\pm$ 3)	170	210	170	210	170	210	170	210
2. Voltage on the arc U_a, B ($\pm$ 1)	25	25	27	27	25	25	27	27
3. Speed of welding V_w, cm/min ($\pm$ 1)	25	25	25	25	30	30	30	30

Chemical composition of weld metal content was tested on obtained welding samples (tabl. 3).

Table 3. Chemical composition of weld metal content of GL-E36 steel welding samples

Number of experiment	C	Si	Mn	P	S	Cr	Cu	Mo	Ni
1	0,103	0,552	1,13	0,0138	0,0238	0,0565	0,0847	0,0127	0,0387
2	0,099	0,572	1,16	0,0143	0,0256	0,053	0,0806	0,0122	0,0351
3	0,101	0,497	1,05	0,0146	0,0231	0,0578	0,0771	0,0137	0,037
4	0,111	0,521	1,11	0,0149	0,0309	0,0609	0,0774	0,0156	0,0396
5	0,095	0,59	1,12	0,0136	0,0249	0,0512	0,0847	0,0122	0,0349
6	0,103	0,617	1,17	0,0136	0,0272	0,0513	0,0832	0,0123	0,0345
7	0,104	0,525	1,02	0,0139	0,0251	0,0545	0,0791	0,0137	0,0359
8	0,124	0,563	1,15	0,0137	0,0254	0,0575	0,0767	0,0133	0,036

The experiments resulted in dependencies of main chemical elements (carbon, silicon, manganese) in added metal of multi-pass joint welds upon controlled parameters of welding conditions (I_w, U_a, V_w). In dependencies the controlled parameters are expressed in terms of non-dimensional units (x_1 – I_w, x_2 – U_a, x_3 – V_w), varying from –1 to +1:

1. Carbon content dependency (%) upon controlled parameters.

Full factorial experiment determined that carbon content (%) in weld metal of GL-E36 steel multi-pass joint welds (in this experiment) doesn't

depend on controlled parameters of welding conditions (I_w, U_a, V_w).

2. Silicon content dependency (%) upon controlled parameters.

$$Si(GL-E36) = 0,533 + 0,012 \cdot x_1 - 0,03 \cdot x_2 +$$
$$+0,017 \cdot x_3 - -0,0003 \cdot x_1 \cdot x_2 + +0,0006 \cdot x_1 \cdot x_3 - \quad (1)$$
$$-0,0037 \cdot x_2 \cdot x_3 - 0,0015 \cdot x_1 \cdot x_2 \cdot x_3$$

3. Manganese content dependency (%) upon controlled parameters.

$$Mn(GL-E36) = 1,112 + 0,028 \cdot x_1 - 0,037 \cdot x_2 -$$
$$-0,002 \cdot x_3 + 0,009 \cdot x_1 \cdot x_2 + 0,007 \cdot x_1 \cdot x_3 - \quad (2)$$
$$-0,003 \cdot x_2 \cdot x_3 + 0,003 \cdot x_1 \cdot x_2 \cdot x_3$$

The dependencies above show the influence of the controlled parameters on percentages of silicon and manganese content in weld metal of GL-E36 steel multi-pass joint welds (in this experiment) and allow to estimate this influence in terms of quantity. However, practical application of these dependences is difficult because numerical values of selected controlled parameters must be converted to non-dimensional units for each new calculation. Besides the models have a number of parameters that don't influence on silicon and manganese percentage in weld metal of multi-pass joint welds. To ease the work the dependences (1) and (2) were transformed into mathematical linear models (3) and (4) which include only influencing factors and allow to use real values of controlled parameters for calculations. Error of values calculated according to the dependencies is not more than 8% in comparison with the values calculated according to the dependencies (1) and (2):

1. Silicon content linear regression dependency (%) upon controlled parameters. Relative error is no more than 8%.

$$Si(GL-E36) = 1,313 - K_U \cdot U_a \quad (3)$$

$K_U = 0,03\ \%/B.$

2. Manganese content linear dependency (%) upon controlled parameters. Relative error is no more than 4 %.

$$Mn(GL-E36) = 1,808 + K3_I \cdot I_w - K3_U \cdot U_a \quad (4)$$

$K3_I = 0,0014\ \%/A,\ K3_U = 0,037\ \%/B.$

The obtained data show the great influence of arc voltage U_a on chemical composition of joint weld and are similar to the results obtained by the authors of the article [8].

The obtained dependencies show that carbon content (%) in weld metal of multi-pass GL-E36 steel joint welds (in this experiment) doesn't depend on controlled parameters of welding conditions (I_w, U_a, V_w), silicon and manganese percentage in weld metal of multi-pass GL-E36 steel joint welds is influenced by the arc voltage U_a, its increasing causes reducing of percentage. Manganese percentage is highly influenced by the welding current strength I_w, its increasing in selected operational range causes increasing of manganese content.

REFERENCES

1 Welding and welded materials: in 3 v. V.1. Weldability of materials. Reference book.//Edited by E.L. Makarov. – M.: Metallurgy, 1991, p. 528.

2 K.V. Frolov Machinebuilding. Encyclopedia. M.: Machinebuilding 2006. – 768p.; pic.

3 L.I. Michoduy, A.K. Gonchar. Welding of thick sheet structures of low-alloy high-strength steels // Automatic Welding. 1990. №10. P. 41-45.

4 U.N. Gotalskiy. About welding of high-strength steels // Automatic welding. 1984. № 6. P.36-40.

5 D.A. Chinakhov, V.T Fedko, U.N. Saraev. Alloyed steels welding in grooving without thermal treatment // Technology of metals. 2005. № 10. P. 27-29.

6 D.A. Chinakhov, V.T Fedko, U.N. Saraev. Welding practice: Device patent № 2233211 (RF). Priority 27.05.2003. 7 B 23 K 9/173//B 23 K 103:04. Publish. 27.07.2004. Bul. № 21.

7 Statistic methods in engineering investigations (Laboratory course): Student's book/ Borodyuk V.P., Votshinin A.P. A.S. Ivanov // Edit. by G.K. Krug. – M.: High school. 1983. 216p.

8 V.G. Grebenchuk, M.V. Karasev, D.N. Rabotinskiy, S.M. Karaseva, R. Rosert. Influence of mechanized welding with metal-particle wire Power Bridge 60M upon melted metal characteristics in bridge construction welding // Welding and troubleshooting. 2009. №1. P. 19-24.

Section IV

ELECTRO MECHANICS

FLYWHEEL ENERGY STORAGE SYSTEM

A.A. Konovalova

Scientific adviser: T.G. Kostyuchenko., associate professor, U.A. Alarushkina

Tomsk Polytechnic University , 634050, Russia, Tomsk, Lenina avenue, 30

E-mail: anastasiya_konovalova@yahoo.com

Today scientists of all over the world try in vain to create cheep, light, compact and high-capacity storage. Whereas such an energy storage already exists.

This is mechanical energy storage based on flywheel. Mechanical devices are inferior to machines with electro motors and electronic circuits. However the future will be more mechanical. Energy storage systems have been increased their capacity in the last ten years. And only they will be used in majority devices instead of conventional electrochemical accumulators [1].

At the present five principal types of flywheels exist. They are:

Pic.1. The wheel with an opening

Pic. 2.The ring with spokes

Pic.3. The equal strength wheel

Pic.4.Circular flywheel

Pic.5.Super flywheel

Each of them has their own advantages and disadvantages and it would be reasonable to compare them.

It is well known that the energy of every kilogram of flywheel depends on its shape and strength. Comparing flywheel types mentioned above, the wheel with an opening (pic. 1) is dismissed as the most inefficient. As a rule, inefficiency is caused by low strength of material the wheel is made of. As usual these materials are steel forged pieces or ingots. But even heavy forged pieces and ingots are not durable enough. It is impossible to avoid the smallest damages in such products. What leads to reducing the whole flywheel strength. The stronger casted or forged flywheel the more dangerous its break and the higher safety factor is needed to avoid the flywheel fracture [2],[3].

Next in energy storage efficiency is the ring with spokes (pic. 2). This flywheel stores 1.5 times more energy in every kilogram of its mass.

Accurate calculating showed it is advantageous to set mass closer to center instead of further from center. Due to this fact flywheels with thin border and heavy center occurred. These are the equal strength wheels (pic. 3).They can store twice more energy than the wheel with an opening with the same mass

The next variant is super flywheel (pic. 5). The simplest example is piece of rope locked in a ring clamp which is set on spindle.

The advantageous of super flywheel is following. If rotate spindle with a pilot spin inside the rope stores kinetic energy as a conventional flywheel does. At the same time rope particles moving inertially stretch the rope trying to fracture it. The heaviest load falls on a center of rope. Due to over-increasing of speed the rope breaks, but it breaks partially, one by one wire and these thin wires are unable to break through a light protective cover, so it means super flywheel fracture flows safe

Because the rope strength (steel string) is 5 times higher than the strength of monolithic steel piece, the super flywheel with string stores 5 times more energy than conventional flywheel with the same mass.

Owing to higher safety, super flywheel does not need too big safety factor and it should be reduce approximately twice in comparison with flywheel. Consequently, super flywheel with rope

is able to store 10 times more energy in every kilogram of mass than conventional steel flywheel.

The circular super flywheels promise big prospects (pic. 4). The flywheel is the ring coiled from high-strength fiber and placed in vacuum camera with a torus shape. As far as circular flywheel does not have a center, strength properties of fibers are fulfilled themselves.

Circular flywheel is held suspended in camera by means of magnetic bearings circumferentially spaced in some places. The wheel itself acts as motor – generator rotor and the places with magnets coils are stator. It simplifies energy collection procedure and flywheel charging.

If compare circular super flywheel with flywheel made of steel with highest strength, the energy density of circular flywheel is 2-3 times higher and comes up to 0.5 mega joule by kilogram of mass. Energy losses of this flywheel 50-100 times less than losses of steel flywheel because the worst losses are bearing friction ones.

However, the circular flywheels possess certain shortcomings such as suspension system complexity and high cost of manufacturing.

Energy density of flywheel is estimated by specific strength that is strength to material specific weight ratio.

The relation between flywheel linear speed and ultimate stress and density of material is shown in the table 1. As for super flywheels, their mass implies decisive importance apart from their strength and sizes. It is ironic that the lighter super flywheel the better as it is shown in table 1.

Table 1. The relation between flywheel linear speed and ultimate stress and density of material

Material	Ultimate stress, (N/m^2)	Density, (kg/m^3)	Linear speed, (m/s)
Steel wire	$3,1*10^9$	$7,8*10^3$	632
Glass fibre	$2,1*10^9$	$2,1*10^3$	1000
Carbon fiber	$1,2*10^9$	$1,1*10^3$	1049
Boron fiber	$5,9*10^9$	$2,0*10^3$	1673

Flywheel storages development is still an embryo in Russia, extensively used manufacturing flywheel storage samples have not been created yet to be more precise.

A great deal of work in this area is done by Nurbej Vladimirovich Gulia doctor of technical science [2]. He has been promoting energy accumulation in flywheels for several years already.

In case of successful usage of flywheel storages, the number of competitors increase and, consequently, prices decrease. And it would be certain to talk about extensive application of flywheels owing to their cheapness and reliability.

REFERENCES:

1 Гулиа Н.В. В поисках энергетической капсулы: научно-художественная литература, М.: Дет. Лит.,1986.
2 Николай Корзинов. Диски высокой энергии: Маховичный накопитель: Журнал «Популярная механика», вып. 2, декабрь 2008.
3 Вращающаяся армия бережет 60 герц стабильного электричества [электронный ресурс]. - режим доступа: http://market.elec.ru/nomer/4/army-60hz/

THE NONPARAMETRIC ESTIMATION OF CHARACTERISTICS

OF RELIABILITY OF ELECTRIC MACHINES ON THE SAMPLE

OF OPERATING TIME

Shevchuk V.P.

Tomsk Polytechnic University, 634050, Russia, Tomsk, Lenin Avenue, 30

E-mail: SheVP@rambler.ru

The qualitative analysis of data on refusals becomes a necessary element of system of maintenance of reliability of electric machines (EM) under operating conditions. In the majority of the scientific literature at a choice of various hypotheses about the type of distribution of

refusals of electric machines the basic emphasis becomes on the studying of physics of refusals. This way is essentially true, though in some cases it is practically unreal. Therefore the problem of finding the function of distribution of refusals of electric machines is one of the main problems. This problem gets a special urgency at the management of operational reliability of electric machines.

The basic elements which are the most often refusing in electric motors, are bearings and windings. In some cases from physical reasons for bearings distribution of Weibull, for a winding – sometimes the exponential law is proved. At the analysis of reliability of electric machines the definition of the law of distribution of refusals of the electric motor as a whole under operating conditions is necessary. In practice refusals of electric motors are defined in a wide spectrum of standard distributions from exponential to lognormal laws of distribution. Actually electric motor refusals are influenced by much bigger number of the reasons connected with a level of production, quality of materials, qualification of the personnel, a condition of park of machine tools etc. Therefore in practice the statistical methods allowing on samples to do reliable enough conclusions about the type of distributions, products describing refusals have a great value.

In process of growth of reliability of electric machines there are situations when the certain part of maintained mechanisms has not given up during supervision, and the other part has given up. In such situations there is a necessity of carrying out the statistical analysis of reliability on the basis of specific samples which basic feature is the absence of data at the moment of refusals of a part of controllable machines. The operating time of the objects which have not given up for the same period is the additional and rather valuable information on reliability of all set of objects. These operating times are called censored. The samples of numbers of operating times of electric machines in which there are available both operating time to the full, and operating time to a casual suspension of supervision, are called casually-censored samples [1].

Now the nonparametric methods of estimation become a special object of research. The feature of nonparametric methods unlike classical methods of mathematical statistics is that the nonparametric methods of indicators of reliability of censored samples (CS) are applied when the kind of the theoretical law of distribution of an operating time to is fully unknown. Such methods allow to receive objective estimations of indicators of reliability without bias to the law of distribution of an operating time to the full.

In the basic size giving the exhaustive description of reliability, the probability of non-failure operation P (t) or share electric machines, fulfilled time t without refusals. It is referred that P (t) is the function of distribution of a random variable t (time of non-failure operation of installation) and within the limits of the probability the theory gives an exhaustive description of reliability [2].

The algorithms are used for the calculation of P (t) in reliability theory based on a hypothesis of the independence of refusals during the next moments of time. The calculations on these algorithms are reduced to the multiplication of probabilities of non-failure operation during these moments of time, therefore the given algorithm is called multiplying:

$$\hat{P}(T_k) = \left(1 - \frac{\delta_1}{N_1}\right)\left(1 - \frac{\delta_2}{N_2}\right) \ldots \left(1 - \frac{\delta_j}{N(T_{j-1})}\right), (1)$$

where $\hat{P}(T_k)$ – an estimation of size P (t) in the end of an interval $[T_{k-1}, T_k]$; δ_j - number of full operating time in an interval $[T_{j-1}, T_j]$; $N(T_{j-1})$ - number of serviceable products in the interval beginning $[T_{j-1}, T_j]$.

As it is known, the empirical function of distribution (EFD) $\hat{F}(t)$ is an estimation of theoretical function of distribution F (t) of a random variable t. The full sample of volume will register as:

$$N_{yj} = N - \sum_{i=0}^{j-1}(r_i + n_i), \qquad (2)$$

Where N_{yj} - conditional volume of censored samples (CS) on an interval $[T_{j-1}, T_j]$; N - initial volume of sample; r_i - number of full operating time; n_i - number of incomplete operating time.

From here it follows, that the empirical function of distribution (EFD) $\hat{F}(t)$ on the sample will look like [1]:

$$F(t) = \begin{cases} 0 & npu\ t \leq 0, \\ l/N_{э1} & npu\ 0 \leq t \leq T_1, \quad l = 0,..,r_1, \\ \left. \begin{array}{ll} \hat{F} + i/N_{э2} & npu\ N_{э2} > 0 \\ \overset{\wedge}{F_1} & npu\ N_{э2} \leq 0 \end{array} \right\} & для\ T_1 \leq t \leq T_2;\ i = 0,...,r_2, \\ \cdots \\ \left. \begin{array}{ll} \hat{F}_{m-1} + \dfrac{z}{N_{эm}} & npu\ N_{эm} > 0 \\ \hat{F}_{m-1} & npu\ N_{эm} \leq 0 \end{array} \right\} & для\ T_{m-1} \leq t \leq T_m;\ z = 0,...,r_m^- \end{cases}$$

(3)

where

$$N_{эj} = N_{э\,j-1} - \frac{n_{j-1}}{1 - F_{j-1}}\ ,\ j = 1,...,m,$$

$$N_{ў1} = N_{б1} = N - n_0;\ F_0 = 0;\ N_{ў0} = N_{б0} = N.$$

The size $N_{ўj}$ entering in (3) is the equivalent volume of censored sample (SC) and is the increment of the empirical function of distribution (EFD) ΔF on one refusal for the full sample is equal to 1/N, and in the case of repeatedly censored samples on the right the size of $N_{эj}$ is back to the increment of the empirical function of distribution (EFD) on one refusal on the interval [T_{j-1}, T_j], т.е. $\Delta F_j = 1/N_{эj}$ The physical sense of expression (3) is that on each interval [T_{j-1}, T_j], after the termination of supervision for n_{j-1} not given up electric machines in the end of an interval [T_{j-2}, T_{j-1}] remained not given up electric machines, are considered as the full sample of electric machines, put on tests under the plan of[$N_{уj}\ U\ T_j$] and have an identical probability of refusal on the interval [T_{j-1}, T_j].

For the estimation of parametres on censored sample we will apply a method of the maximum credibility. Unlike others this method allows to find the estimations of the maximum credibility (EMC) parametres on ungrouped, partially grouped and grouped data. The EMC of unknown parametre on partially grouped supervision are called such value of parametre at which the function of credibility looks like [3]:

$$L(\Theta) = \gamma \prod_{(1)} P^{n_i}_i(\Theta) \prod_{(2)} \prod_{j=1}^{n_i} f(x_{ij}, \Theta),$$ (4)

where γ - some constant; $f(x_{ij}, \Theta)$ - function of density of a random variable;

$$P_i(\Theta) = \int_{x_{i-1}}^{x_i} f(x, \Theta)\, dx$$ − probability of hit of supervision in i interval of values, reaches a maximum on the set of possible values of parametre.

It is obvious, that information remaining in censored sample is sufficient for the estimation of parametres of the law which is interesting for us with demanded accuracy. The analysis of methods on nonparametric оцениванию of censored sample shows, that this method of estimation for the definition of the empirical function of distribution (EFD) is full enough for getting of dot and interval estimations of investigated samples (small and large) at the express analysis of reliability of electric machines. Thus, the problem of creation of scientifically-proved techniques of processing of censored samples which would allow to receive well-founded and unbiased estimations of indicators of reliability with high accuracy, is significant and has an important practical value.

LITERATURE

1   RD 50-690-89. The reliability in enginering. Methods of estimation of indicators of reliability on experimental data. - M: The State Committee of standards of the USSR, 1991.

2   Aronov I.Z., Burdasov E.I. The estimation of reliability by the results of the reduced tests. Moscow. Standards Publishing House. 1987. 182 p.

3   Lemeshko B.Yu., Gildebrant S.Ya., Postovalov S.N. To the estimation of the reliability parametres on censored samples. Factory laboratory. Diagnostics of materials. 2001. Volume 67. - № 1. - 52-64 pp.

THE OPTIMIZATION METHOD AT DESIGNING

OF ENERGY EFFICIENT INDUCTION MOTORS

Tyuteva P.V.

Tomsk Polytechnic University, 30 Lenin Avenue, Tomsk, Russia 634050

E-mail: TyutevaPV@tpu.ru

Enumerative techniques allow organizing the search of an optimum variant at designing of energy efficient induction motors. The application of the given method is often justified by virtue of its simplicity of realization, insensibility to the form of objective function or absence of other effective ways of the specific target solution in which it is required to find an element of given properties in finite set. By even more appropriate application of this method that mathematical tool which is created by present time by scientists for enumerative optimization technique. One of enumerative techniques is the full enumeration method, virtually enumeration is a problems solution arising from given, when value of some required parameter is fixed in a variety of ways, and made the choice from the considered values which gives the most suitable solution. The given method possesses a number of conclusive advantages which is sounded above, and also this method can be applied for any type induction motor optimization.

The purpose of the given work is the examination of an optimization method at designing of energy efficient induction motors.

For reception of optimum designed induction motor or the motor which is pass standards of power efficient it is the most appropriate to use a way of induction motor designing without changing of cross-sectional dimension but at change of cores length and numbers of coils in a stator phase winding [1]. For optimum variant search at simultaneous change of cores length of and numbers of coils in a stator phase winding the full enumeration method is used. The given method allows to bypass the certain points of independent variables and on the basis of the carried out calculations choose an optimum variant. The full enumeration method is enough simple in organization and convenient in use, however possesses one lack – calculation does not stop in a point with an optimum variant of induction motors.

At the optimization problem solution at designing of induction motors following data should be set: independent variables X, objective function $f(X)$, and also the boundary conditions which is imposed on calculation results of the objective function.

As independent variables at full enumeration method realization at designing of energy efficient induction motors following parameters are acted: l_δ – - core length of stator and rotor; w_1 – numbers of coils in a stator phase winding. The ranges of independent variables change:

$$x_1 = w_1 \in \left[0,6 \cdot w_{1bas}; 1,0 \cdot w_{1bas}\right],$$

$$x_2 = l_\delta \in \left[1,0 \cdot l_{\delta bas}; 2,5 \cdot l_{\delta bas}\right].$$

Thus $l_{\delta bas}$ – the base value of core length of rotor and stator, and $w_{1баз}$ – the base value of numbers of coils in a stator phase winding. Then a segment of independent variables range changing is broke into parts by division points, and in each calculation point we receive the value of objective function.

The stopping criterion for the given method is achievement of efficiency levels EFF1 and EFF2 under European specification CEMEP. For general purpose induction motors it is the most expedient to use the resulted expenses as objective function. The resulted expenses for the electric machine during manufacture and operation are the summary economic parameter, including the basic economic equivalents of the basic characteristics. By calculation results of objective function $f(x_1, x_2)$ in all points of independent variables changing and by comparison of the received results the optimum variant is determined which turns out at the minimal value of the resulted expenses.

The optimality test (resulted expenses) can be determined under the formula:

$$f(x_1, x_2) = E_r = C_{Cu} \cdot G_{Cu} + C_{Al} \cdot G_{Al} + C_{St} \cdot G_{St1} +$$

$$+ C_{St} \cdot G_{St2} + C_{пр} \cdot T_e \left(P_{э1} + P_{э2} + P_{ст} + P_{2н}\right),$$

where C_{Cu} – the price of winding copper, C_{Al} – the price of aluminum, C_{St} – the price of electrotechnical steel, G_{Cu} – weight of winding copper, G_{Al} – weight of aluminum, G_{st1} – weight of stator core steel, G_{st2} – weight of rotor core steel, $P_{э1}$ – electric losses in a stator winding, $P_{э2}$ – electric losses in a rotor winding, P_{st} – losses in core steel, $P_{2н}$ – rated power of the induction motor, C_a – the electric power price, $T_н$ – the rated payback period.

The mathematical model of an estimation of economic efficiency at designing of induction motors was used for calculations. It covers the basic design stages of induction motors such as

electromagnetic and thermal calculations of the machine. For calculations by full enumeration method the fourpolar general purpose induction motors of a 4A series were used: 4A80A4, 4A80B4, 4A90L4, 4A100S4, 4A100L4, 4A112M4, 4A132S4, 4A132M4, 4A160S4, 4A160M4, with rated power from 1,1 up to 18,5 kW [6].

With increase of cores length we have induction decrease in tooth and yokes of stator and rotor of the induction motors that leads to the overall underexploitation of magnetic system of induction motors, thus for machines of lower-power (approximately up to 3 kW) the cores length makes nearby 125 … 130 % from base cores length, and for machines with greater rated power the core length for a efficiency level EFF2 will make 120 … 115 %, the numbers of coils in a stator phase winding makes about 90 %. Thus for a efficiency level EFF2 the increase in expenses for active materials makes 4…10 % from the energy efficient induction motors price. Modernization cost of the induction motors at change of cores length and numbers of coils in a stator phase winding or in other words the cost of efficiency increase for 1 % makes 4…12 % from induction motors basic cost.

The change to a efficiency level EFF1 can not be recommended as the way of designing of energy efficient induction motors connected with t change of cores length and numbers of coils in a stator phase winding. Because for designing of induction motors with EFF1 level it is necessary to take cores length stator and rotor 160 … 200 % from its basic value, and number of coils 70 … 60 % from its basis value. At core length above 150 % from basic value the slip in rated conditions exceeds 10 … 12 % that leads to unstable operation of induction motors. The increasing of cores length over the specified value sharply increased losses in stator and rotor winding of induction motors due to increase of active resistance stator and rotor windings. The number of coils in a stator phase winding also should not be taken below 70 % from basic value, because with the decreasing of number of coils in a stator phase winding there is a sharp increase in a stator winding current and also induction increase in tooth and yokes of stator and rotor of induction motors that also leads to sharp increase in losses in a stator winding and besides the induction motors operate in saturation range of magnetic system.

On fig. 1 results of payback period calculation are presented at change to various efficiency levels, energy efficient induction motors are received without changing of cross-sectional dimension. Payback period at implementation of induction motors with efficiency level EEF1 appear below in comparison with induction

motors with EFF2 efficiency level due to greater economy of the electric power.
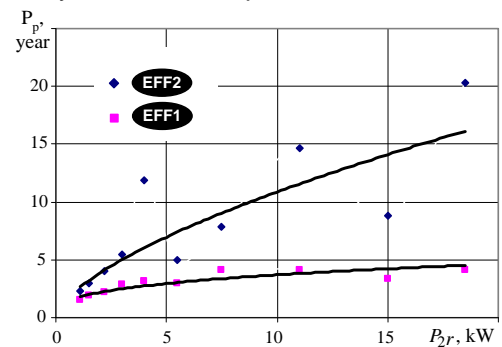

Fig. 1. Payback period at implementation of energy efficient induction motors

Proceeding from the received results, it is possible to formulate the following recommendations for energy efficient induction motors designing at change of cores length and numbers of coils in a stator phase winding:

- For energy efficient induction motors designing are required the simultaneous change of cores length and numbers of coils in a stator phase winding.

- For change to a efficiency level EFF2 the cores length stator and rotor should be equal 120…130 % from basic values, thus great values correspond to the induction motors of lower-power (approximately up to 3 kW). The numbers of coils in a stator phase winding should make about 90 % from basic value.

- For change to a efficiency level EFF1 more serious change of cores length and numbers of coils in a stator phase winding is required, therefore the given way can not be used for energy efficient induction motors designing.

Thus, the realization of the offered full enumeration method of optimum variant search connected with increasing of mass and overall parameters due to change of cores length and numbers of coils in a stator phase winding of the induction motors without changing of cross-sectional dimension, allows to design the machine possessing improved power characteristics. Thus the best power parameters turn out at simultaneous change of length of cores and numbers of coils in a stator phase winding. Cost of efficiency increase for 1 % in energy efficient motor does not exceed 16 % from cost of the basic machine.

Designed induction motors possess power parameters which correspond to efficiency levels according to European specification CEMEP and State Standard R 51677-2000. At realization of a designing way connected with change of cores length and numbers of coils in a stator phase winding without changing of cross-sectional dimension it is possible to reach efficiency level EFF2. For designing of induction motors with a

efficiency level EFF2 it is necessary to take cores length of stator and rotor 120…130 % from basic value, and number of coils 90 % from basic value. Designing of energy efficient induction motors with efficiency level EFF1 without change of cross-section geometry is not obviously possible.

REFERENCES

1 Муравлева О.О., Тютева П.В. Совершенствование асинхронных двигателей для регулируемого электропривода // Известия Томского политехнического университета. – 2007. – Т. 310. – № 2. – С. 177–181.

2 Асинхронные двигатели серии 4А : Справочник / А. Э. Кравчик, М. М. Шлаф, В. И. Афонин, Е. А. Соболенская. — М. : Энергоиздат, 1982. — 504 с.

DEVELOPMENT COMPUTER-AIDED DESIGN SYSTEM OF EXECUTIVE ELEMENTS ON THE BASIS OF FORCE GYROSCOPES WITH A ROTARY FRAMEWORKS DRIVE

Voronova A.S.

Scientific adviser: Kostuchenko T.G., associate professor, Alarushkina U. A., instructor

Tomsk Polytechnic University, 30 Lenin Avenue, Tomsk, Russia 634050

E-mail: nasek19@sibmail.com

The system of stabilization and orientation of a space vehicle (SV) consists of three basic parts: the gauges being sensitive to SV position and specifying its changes; the strengthen - transform device which reacts to changes of parameters perceived by gauges and transforming them to command signals; the executive elements building the command moments[1].

For making the control systems meeting the increased requirements, the specificity of their operation in conditions of absence of atmosphere, weightlessness, small size of the revolting moments, low temperature should be known. It determines specific features for devices and facilities of control systems angular movement of space vehicles, including the executive elements. One of the types of the executive elements building the command moments is the executive element on the basis of a powered gyroscope with a rotary frameworks drive (RFD). It is a complex electromechanical device, multivariate mechanical system.

By the development of the executive elements there are a lot of requirements: according to the linearity of manipulation, the range of the command moments, accuracy, speed, resource, the electric energy demand, dimensions and mass, maximum reliability and rigidity of construction, dynamic qualities[2]. To fulfill effectively these requirements in a system technically is a problem because improvement of one of the parameters leads to the deterioration of others because all parameters of multivariate mechanical systems are simultaneously connected by a direct and inverse relationships. The realization of these requirements gives more perfect qualitative level of all complex of operational characteristics executive elements on the basis of power gyroscopes with a RFD.

Only with the use of the methods of automated designing it is possible to receive the required quality of the developed device on the basis of the great amount of project decisions, therefore the development of computer-aided design system for designing executive elements on the basis of force gyroscopes with RFD is rather an actual problem.

In Russia there are state standards for creating CAD system - GOST 23501.108-85, GOST 23501.101-87. There is also an international standard at the stage of existing period of program production (ISO 12207:1995).

The designing of complex objects is based on the application of ideas and principles stated in some theories and approaches. The most general approach is the system approach which ideas penetrate various techniques of designing of complex systems.

The basic common principle of the system approach consists in the consideration of parts of the investigated phenomenon or the difficult system due to their interaction. The system approach includes the revealing of the structure system, the typification of communications, the definition of attributes, the analysis of the environment influence, the formation of model system, the research of model and probably optimization of its structure and functioning. CAD system belongs to the number of one of the most

difficult artificial systems. Their designing and support are impossible without the system approach[4].

As a rule, CAD system have multimodular structure. In the structure of the developed CAD system there are following subsystems:

• The Graphic kernel. The geometrical kernel realizes the basic operations and procedures of geometrical modeling.

• The Subsystem of bidimentional (2D) graphic, used for obtaining of the drawing documentation.

• The Subsystem of 3D solid-state (volumetric) modeling. In it procedures of constructive geometry with use of base elements of the form are realized.

• The Subsystem of 3D superficial modeling, used for designing details with difficult surfaces (turbines, the case of planes, cars, the ships, etc.).

• The Specialized modules focused on the designing of products of the certain type, for example, of stamps, details from sheet materials, cast products, etc.

• The Subsystem CAM for designing technological processes, synthesis of programs for the equipment with numerical program control, modeling of machining, etc.

• The Database, including archival and help subsystems.

• The Subsystem of the engineering analysis including the programs for modeling of products on micro-and macro levels.

• The Subsystem of import and export (exchange) of data with support of some used graphic formats.

• Subsystem PDM of management of data and design[5].

One of the most effective CAD-systems, covering all design stages is system T-Flex CAD. By means of software package T-Flex it is possible to generate the scheme CAD system of executive elements solving a key problem of automation, which is the increase of efficiency development of executive elements.

On the basis of the above-stated has been designed the scheme CAD system of executive elements on the basis of force gyroscopes with RFD, presented in figure 1.
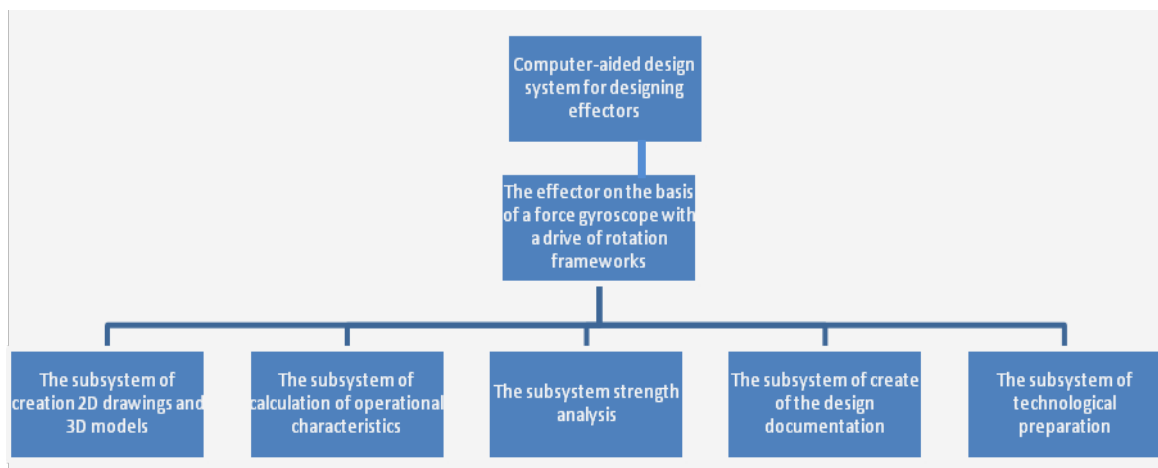

Figure 1 - Block diagram CAD system executive elements

The subsystem of creation 2D drawings and 3D models on the basis of T-Flex CAD 2D is meant for the creation of drawings of details, assembly drawings, specifications; T-Flex CAD 3D it is used for creation of three-dimensional details, assembly designs and automatic receiving of the exact drawings on three-dimensional models.

The subsystem of calculation of operational characteristics is based on module T-Flex CAD 2D/3D. The subsystem allows to count necessary operational characteristics, such as weight, the moments of inertia, the kinetic moment, angular speed and others.

The subsystem of strength analysis is based on module T-Flex Analysis. T-Flex Analysis is the integrated CAE-environment of certainly-element

calculations[3]. Using T-Flex Analysis, it is possible to investigate the developed design on durability, having applied necessary loadings; to calculate resonant frequencies, to lead the analysis of stability and the thermal analysis.

The subsystem of producing of the design documentation is based on module T-Flex 2D/3D. In the subsystem of releasing of the design documentation on the basis of 3D assembly received in the subsystem of creation 2D drawings and 3D models, there is an opportunity to receive both assembly drawings and specifications, and drawings of separate details. Complete set design documentation is formed. Then there is a transfer of drawings and 3D models details for technological preparation

and for machining on machine tools with numerical program control[6].

The subsystem of technological preparation consists of two modules T-Flex TehnoPro and T-Flex numerical program control. In module T-Flex TehnoPro on the basis of 2D drawings and 3D models of details it is made the technological process of machining of details, technological process assembly operations, routing and operational cards are created. In module T-Flex numerical program control on the basis of 2D drawings and 3D models of details operating programs of machining of a detail on machine tools with numerical program control are automatically generated.

REFERENCES

1   Alekseev K.B., Bebenin G.G. « Management of space flying devices »., Mechanical engineering, 1974 - 340 p.

2   Gladyshev A.N., Dmitriev A.S., Kopytov V.I., « The Control system of space vehicles ». Tomsk: TPU, 2000 – 207p.

3   T-FLEX CAD Help. The User's guide. - joint-stock company «Top Systems », Moscow.

4   CAD system technological processes (an electronic resource) www.elib.ispu.ru <http://www.elib.ispu.ru>

5   Bases CAD system (an electronic resource) www.bigor.bmstu.ru<http: //www.bigor.bmstu.ru>

6   Petrov P., Experience of development CAD system of technological process of punching with application T-FLEX CAD. // CAD system and the graphics. - 2003. - № 12. - p. 7-11

Section V

THE USE OF MODERN TECHNICAL AND INFORMATION MEANS IN HEALTH SERVICES

DETECTING UNIT BASED ON GaAs DETECTORS FOR LOW DOSE

MEDICAL EQUIPMENT

Abzalilova L.R., Nam I.F.

Scientific supervisor: Nam I.F.

Tomsk polytechnic university, 634050, 30 Lenin av., Tomsk , Russia

E-mail: lily343@sibmail.com

In this paper the X-rays registration unit on the basis of GaAs detectors is being developed. Let's see it on the example of fluoroscopy apparatus. Fluorography makes it possible to detect the disease is still in embryo, in the absence of symptoms. Thus, in the early stages of such diseases as tuberculosis, which almost flowing without symptoms, only fluorography easily help to find the source of infection. It is believed that mycobacterium of tuberculosis infected about 2/3 of the population of the planet. However, the majority of those infected never develop tuberculosis itself. This occurs only in people with weakened immune systems (especially HIV-infected), when the bacillus overcomes all the protective barriers of the organism, multiplies and causes the current of active disease. Annually ill with active tuberculosis about 8 million people, about 3 million die sick. Fluorography apparent advantage over other methods is the ability to identify documented in preclinical phase of not only tuberculosis, but also tumors of the lungs, pleura chest wall and many inflammatory diseases.[1]

However, the most common type of X-ray examination is chest diagnostic imaging. The number of X-ray chest examinations in the United States, Europe, Japan is approximately 550 000 images every day. Gradually developing, fluorography evolved from uninformative HIGH method for determining gross pathology in high-quality low-dose method for mass research. New technologies have radically changed picture of fluorographic methods for diagnosis. Today we can state with confidence - a more secure and efficient method diagnostic of X - ray than modern digital fluorography simply does not exist.

The main purpose of this work is to develop a digital detecting unit which is capable to get extremely high spatial resolution and contrast of the diagnostic image with a significant dose reduction to the patient. Using digital technology requires lower doses to obtain images with the same quality as film due to the high sensitivity of detectors to the x-rays.

The effectiveness of digital detectors is expressed in quantum detection efficiency (DQE). Irradiation dose depends on the patient drop is equivalent quantum detection efficiency.

The higher quantum detection efficiency, the lower the dose the patient, while image quality remains the same. For most systems, quantum detection efficiency of film about 25%. For digital detectors is much higher.

Digital sensors have demonstrated the highest quantum detection efficiency of about 60% and a low frequency quantum detection efficiency of about 40%.The quantum detection efficiency of screen-film systems reach a maximum of approximately 35% and save only within a small range of exposure, so 25% is average. Digital detectors can register more X-ray quanta, and therefore requires a smaller dose of radiation to produce images comparable to film. [2]

However, to obtain a good image first of all you must have a semiconductor material with high quantum sensitivity to x-rays and low noise of readout electronics.

These requirements are easily achieved using semiconductor detectors based on GaAs, doped with chromium atoms which were developed by the scientists of Tomsk state university.

According to the principle of construction all existing digital detecting systems can be divided into two types. The first type includes two-coordinate (matrix) system. They allow you to get the entire image at once. The second one is scanning systems that form the image line by line due to mechanical movement of the x-ray tube and detecting unit along the object.

Two-coordinate detecting systems have significant disadvantages the main is in registration of the secondary, scattered radiation from the subject and related areas of the detector, which is "veiled" X-ray image of the object. So the background noise appears at the image. As a result diagnostic opportunities of the system become worse. Additionally, they are quite expensive.

Scanning systems have the following advantages:

- high quality of images, due to the lack of "veil" of the scattered radiation;

- significantly lower doses for patients;

-optimal spatial frequency (pixel size) for the set of diagnostic tasks;

- high contrast sensitivity at low doses;

- high-dynamic range (over 500);

- absence of geometric distortion in vertical direction, which makes it possible to examine object under the same "perspective" and makes images easier for the computer diagnostic;

- significantly lower hardware costs (due to decreasing the number of micro detectors and electronics channels as compared with full-size matrix detectors);

- the lower cost of apparatus.

The common disadvantage of all scanning systems are relatively large exposure time (2,5-5,0 sec), so increased load on the X-ray source. That's why it was decided to use a scanning type system. [3]

There are a variety of digital systems. However, in some cases the characteristics of serial fluorographs not satisfy the requirements of modern diagnostics.

a) Indirect registration   **b) Direct registration**

Scintillator CsI(Tl)   GaAs - detectors

Spectral line widening
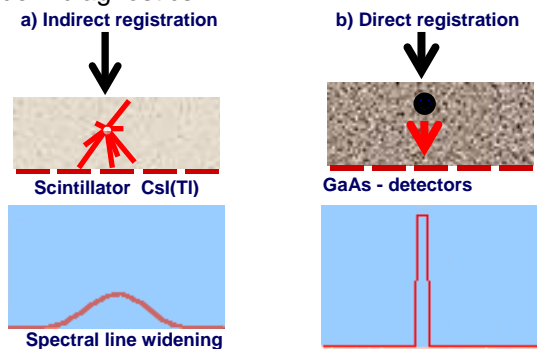
Fig.1. Available (a) and proposed (b) ways of X-ray imaging

It's preferable to use detectors which directly transforming the X-ray radiation into electrical signal. The main advantage of such systems is the high efficiency of registration and getting the images without the intermediate stages of processing. Detectors from Ge, Si, GaAs, CdTe are often used to register the X-ray. But detectors from Ge and Si must be cooled by liquid nitrogen to obtain good spatial resolution. In assessing the parameters of semiconductor detectors for X-ray should also note the radiation hardness and stability. Detecting units that are based on CdTe and CdZnTe, are not enough stable and radiation hardly. Also they are quite expensive.

Among all the semiconductor materials, the most suitable is gallium arsenide (GaAs), It is a material which has a small absorption length of photon and a wide band gap. Similarly to the advantages of this material include:

- high resistivity up to 10 nOm*sm
- high mobility of electrons and holes

- less time drift of charge carriers in the semiconductor, therefore, a high speed of device

- sufficient stability and high radiation hardness.

In Tomsk, the GaAs material with unique technical characteristics were developed due to the basic researches of scientists from TSU in the field of semiconductor materials.

After studding advantages of semiconductor detectors based on gallium arsenide material unit for digital scanning X-ray fluoroscopy were developed.

Experiments on contrast sensitivity (fig. 2) and resolution (fig.3) were performed.

Fig.2. The image of 100 microns of Al on the background of 1.5 mm Al.

From the figure 2 the contrast sensitivity less than 1% can be easily calculated.

We see the wire with the thickness about 50 microns and 60 microns on the figure 3 . It is the result of the high spatial frequency.
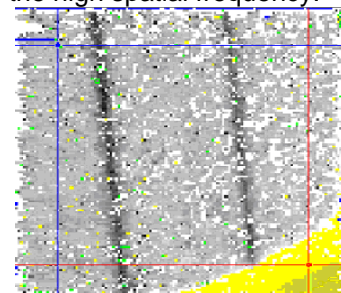
Figure 4. The images of steel wires (Fe) d = 63 and 50 microns correspondently

Thus the results of experiments demonstrate that constructed detecting unit can be used in low-dose medical X-ray systems and provide better technical characteristics with a sensible reduction of the dose at the same time.

References

1   http://tuberkules.ru/publ/1-1-0-25.
2   Digital X-Ray: The Market in Focus
3   Kornev E.A., Lelukhin A.S., Petrushanskii M.G. Digital fluoroscopy system. //Detectors and systems. – 2004.- №6. – p.55 - 58.

REVIEW OF TYPES OF HAND'S ARTIFICIAL LIMB

Kolomeytseva M.O., Kiselyova E.Yu.

Scientific adviser: Kiselyova E.Yu., Ph.D.

Tomsk polytechnic university, 30, Lenin Avenue, Tomsk, 634050, Russia

E-mail: kiseleva_eka@tpu.ru

Representatives of all species, which have extremities, may lose these important parts of the body because of injuries or illnesses. Some animals, for example, tritons, have the ability to recover the lost extremity. People are less fortunate - we have to deal with situations ourselves. Since the twentieth century, disability has become one of the most acute problems of society. Two world and many local wars, car accidents, accidents at work turn to invalids millions people. But people do not agree to tolerate loss of some vital functions of the body and have been trying to synthesize it using improvised materials from ancient time.

An artificial limb is a type of prosthesis that replaces a missing extremity, such as arms or legs. The type of artificial limb used is determined largely by the extent of an amputation or loss and location of the missing extremity. Artificial limbs may be needed for a variety of reasons, including disease, accidents, and congenital defects. A congenital defect can create the need for an artificial limb when a person is born with a missing or damaged limb. Industrial, vehicular, and war related accidents are the leading cause of amputations in developing areas, such as large portions of Africa. In more developed areas, such as North America and Europe, disease is the leading cause of amputations. Cancer, infection and circulatory disease are the leading diseases that may lead to amputation.
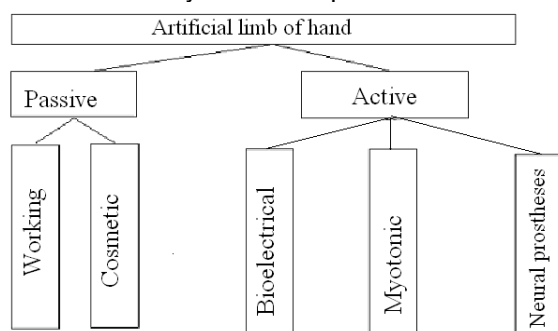
Figure 2 - Classification of artificial limbs of hand

All artificial limbs are divided into two main groups: passive prostheses and active prostheses. Passive prostheses can be working or cosmetic. Cosmetic artificial limbs have the same shape as the natural limb, but they don't have any additional functions. They can be used only to press or hold some objects. Working artificial limbs not look like human's extremity, but they have several special devices – working jet, which can be changed very easily. Each jet can realize one or several certain types of work.

There are three main types of active artificial limbs: bioelectrical, myotonic and neural prostheses. Method of myotonic control is based on changing of muscle volume when it contracts. This change effects on the strain sensor. Sensor generates electric signal, which is used for control of the prosthesis.

In the bioelectrical artificial limbs electrical activity of the muscles is converted into the motion of prosthesis. To determine the type of movement, its characteristics (speed, force) the difference between EMG - signals of antagonistic muscles is used. For example, if the activity of flexor muscle more than extensor muscle activity, the value of the difference between these signals determines the speed (force) of the prosthesis mechanical gripper.

These two types of prostheses have one serious disadvantage. It is the lack of input information. To choose the signal from one specific muscle is very difficult task.

Recently, artificial limbs have improved in their ability to take signals from the human brain and translate those signals into motion of the artificial limb. So more advanced artificial limb is neural prosthesis. [1]

Neuroprosthetics (also called neural prosthetics) is a discipline related to neuroscience and biomedical engineering concerned with developing neural prostheses. Neural prostheses are a series of devices that can substitute a motor, sensory or cognitive modality that might have been damaged as a result of an injury or a disease. In such prosthesis microelectrodes are implanted directly into peripheral nerve. Microelectrodes are able to read the information from motor nerve and to stimulate afferent fibers of peripheral nerve. It gives the opportunity not only to control the prosthesis with the help of nerve impulses, but also to create sensitivity of artificial prosthesis very close to natural sensitivity. The signal which used to control the work of device is the action potential.

Membrane of the neuron has two important levels of membrane potential: the resting potential, which is the value the membrane potential maintains as long as nothing perturbs

the cell, and a higher value called the threshold potential. For typical neuron, the resting potential is around -70 millivolts (mV) and the threshold potential is around -55 mV. Neuron membrane potential in the state of excitation is about +55 mV. Thus, the absolute value of the action potential is about 125 mV. Duration of the neuron action potential is only about 1 ms.

Nerve impulse always has the same characteristics (shape and speed). Each action potential is followed by a refractory period, which can be divided into an absolute refractory period, during which it is impossible to evoke another action potential, and then a relative refractory period, during which a stronger-than-usual stimulus is required.
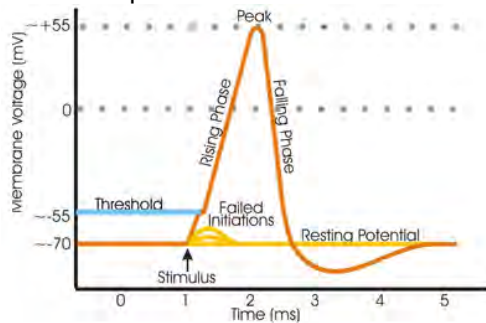
Figure 2 - Neuron action potential

The implantation of arrays of penetrating electrodes in the severed nerves of an amputee could mediate direct neural control of a prosthetic arm in a very natural fashion. The desire to move the arm in a particular trajectory would be recorded as a spatiotemporal firing pattern by specific electrodes. These volitionally evoked firing patterns would be processed and used to control mechanical actuators in the prosthetic arm that bend or extend the elbow, rotate the wrist, or open or close the fingers. The result of the intended movement would be encoded by the network of sensors in the hand and arm, and these signals would modulate electrical currents passed though specific electrodes that target specific sensory nerve fibers. Activation of these fibers would provide feedback to the somatosensory parts of the brain, providing a natural sense of the consequences of the intended movements.

To create a complete system of artificial limb control system signal from the implanted microelectrode array must be strengthened, cleaned from interference and noise, digitized and send to the external control unit. Stimulation of afferent nerve fibers is necessary for the formation of feedback by means of artificially created sensations. In addition, it is necessary to implement the transfer of energy to implanted electronic components.

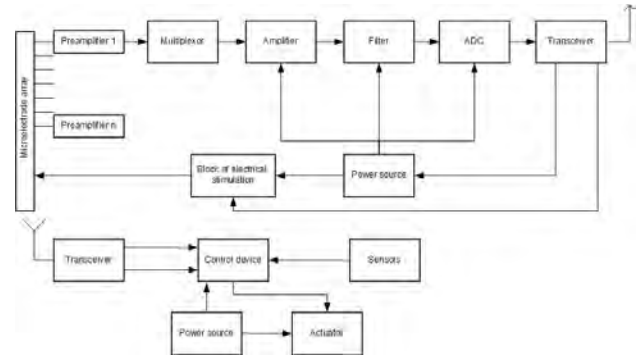Block diagram of the device is shown in figure 2.

Figure 3 - Block diagram of neural prosthesis

With the help of connecting conductors microelectrode array is connected with implanted electronic components (amplifier, filter, ADC) and transceiver, which provides wireless data and energy transmission. The external part of the prosthesis consists of the device which provides sending and receiving of data and energy, control system, actuator and sensor systems (force sensors, position, touch, temperature, etc.).

General requirements to the implanted components are follows:

- minimal size;
- minimal power consumption;
- minimal heating of surrounding tissue;
- tightness and biocompatibility;
- thermal and temporal stability of characteristics.

Requirements to the signal amplifier are practically the same as the general requirements to the amplifiers of biological signals. There are a high input impedance, high ratio of common-mode signal rejection, high gain.

Also implanted components would have to communicate with the outside world wirelessly. Having wires sticking out of the head, hand, etc is not an option. Besides the discomfort and restrictions it would impose on the subject this could lead to infection in the tissue. This bidirectional wireless communication requires a high bandwidth for real-time data transmission; this is a great challenge considering that this data link has to operate through the skin. The minimal size of the implant means no battery can be embedded in the implant, the implant works on wireless power transmission through the skin which is equally challenging as the data transmission. [2]

There are two major challenges in the developing of the artificial limbs. The first problem is creation of the actuator, capable to reproduce all the most important features of replaceable limbs with maximum degree of similarity. The second problem is to select the best way of prosthesis control. Nowadays the first problem is solved quite easily thanks to powerful, economical and small electric motors, light and strong materials, power-consuming and small batteries. The second problem is more difficult than the first one, but a lot of engineers try to

45

solve it. And the great progress will be achieved in this area in the near future.

References

1 Safin D.R., Pil'schikov I.S. Vozmozhnye puti razvitija sovremennyh sistem upravlenija protezami (Possible ways of the development modern control system of prosthetic device) // Zdorov'e – osnova chelovecheskogo potenciala: problemy i puti ih re6enija: materialy konferencii. – Sankt-Peterburg:2007 – s. 144-152

2 Safin D. R., Pil'schikov I. S., Urakseev M. A., Migranova R. M. Voprosy postroenija nejroupravljaemyh protezov (Questions of the construction of neural prosthetic device) // Zhurnal «Medicinskaja tehnika». – 2009. – №4. – c. 16-21.

THE SOFTWARE FOR THE RESPIRATORY MONITORING

AND THE RESPIRATORY PATTERN ANALYSIS

Medyukhina A.A

Scientific adviser: Svetlik M.V.

Siberian State Medical University, 634050, Russia, Tomsk, Moskovsky tract, 2

E-mail: extremal-am@mail.ru

1. Introduction

Breathing is a very important function of a living organizm that supports the delivery of oxygen in tissues and the elimination of carbon dioxide out of the body. Various respiratory diseases or respiratiory pattern disturbances lead to the gas exchange failure that may results in different irreversible changes in tissues.

There are many Pulmonary Function Tests, such as spirometry, pletismography, pneumotachometry, etc. [1], that allow to discover the respiratory failure presence long before the first clinical symptoms appear. They help to specify the failure type, character and severity, to trace the dynamics of the respiratory function alteration due to the disease development and the treatment [2].

However, it is necessary to apply respiratiory monitoring in order to recognize the latent or feebly marked respiratory pattern disturbances. Sleep monitoring systems are more effective then the day monitoring because breathing is controlled constantly and consciously by the individual in the daytime, while it is controlled only by his respiratory center in his sleep. The respiratory monitoring is less widespread than other types of monitoring, such as ECG and EEG monitoring. Nowadays the respiratory monitoring is performed in the context of polysomnography [3], that includes measurement of a great number of parameters, requires the expensive and bulky equipment and is usually performed in special sleep laboratories. The respiratory monitoring problems caused both by the absence of special inexpensive equipment and by the shortage of program-realized algorithms for the respiratory pattern analysis. A great volume of information that is collected during the monitoring requires too much time for manual analysis. That is why it is necessary to create a tool for the automatic analysis of the respiratory pattern that can allow to extract valid information about the respiratory pattern out of the great volume of initial data.

2. The aim

The purpose of this research is to develop the software that includes algorithms for interaction with the monitoring system, data import modules for communication with known similar class equipment, modules with various methods for the respiratory pattern analysis including an opportunity of flexible settings of the processing automation function.

3. Tasks

The research includes the implementation of following tasks:
- to create an interface unit of the respiratory pattern monitoring device;
- to implement algorithms for the respiratory pattern analysis;
- to develop algorithms for recognition of the respiratory pattern disturbances;
- to implement a software interface.

4. Materials and methods

We used the polysomnography records that were made on the Internal Diseases chair of Siberian State Medical University. The recording began at 10 p.m. and lasted continuously during 7-9 hours. Electrocardiography electrodes, an oronasal flow sensor and a thorax movement sensor were used during the recording process.

The oronasal flow was measured by a termoresistor, that was used as the sensor. The sensor work principle is founded on its property

of changing its resistance depending on the temperature value. The temperature rising leads to the resistance increasing, while the temperature fall results in the resistance decreasing. The resistance changes are evaluated with the temperature resistance coefficient that takes both positive and negative values. It's value characterize the sensor sensibility.

Registered signal is gained by an amplifier and sampled by an analog to digital converter. A microcontroller passes the sampled data through RS-232 interface to the computer, where the data is recorded into a file.

The respiratory pattern is saved in a binary file of *.rsp format. Every sample is performed as two 2-byte integer numbers. The first number has got from the oronasal sensor, the second number has got from the thorax movement sensor. This research included only the oronasal flow data analysis.

In order to evaluate breath intervals variety we decided to implement an algorithm of time analysis, which efficiancy was proved in series of researches [4, 5]. Also, algorithms of a fast Fourier transform and a wavelet transform were decided to implement [6].

In order to implement the recognition of the respiratory pattern disturbances an artificial neural network was used. The records with the respiratory pattern of patients with and without disturbances were used as a training set.

We chose the object-oriented programming language C++ [7] and the cross-platform application development environment Qt 4.5 [8] as the most appropriate tools for implementation of the software interface.

5. Results

As a result of the perfomed research a cross-platform software system for the respiratory pattern recording and analysis was created.

The system gives an opportunity to map the respiratory curve directly from the measuring equipment on the computer screen in a real-time mode. This function allows to observe the patient's respiratiory pattern while the mesurement is in process.

The software includes various methods for the respiratiory pattern analysis. The time analysis implies the statistic analysis of breath intervals, inspiratory and expiratory intervals. Because the recognition of the breath interval phases is espacially difficult in the intervals with the respiratory pattern disturbances, we developed a special algorithm that executes this function. It is founded on the differentiation of the respiratiory curve and the control of the amplitude near the point of a presumable extremum.

An opportunity to indicate a target interval for the further analysis is also implemented. The respiratiory pattern can be processed with various mathematical methods, such as Fourier and wavelet analysis, and the results of this analysis can be exported into a text file.

The artificial neural network recognizes the respiratory curve intervals with the respiratory pattern disturbances or the absence of breathing. While working in the real-time mode, the system searches continuously for such intervals and communicate with a biofeedback device in case of their presence. While working with the imported data, there is also an opportunity to recognize the respiratory pattern disturbances and to get the conclusion about the respiratiory pattern of the patient. The conclusion includes information about the patient (name, sex, age, clinical diagnosis), information about the record (date and time of the begining, duration) and results of all methods that have been applied while processing the respiratiory pattern. If the disturbances is found, the information about their type, time of appearance and duration is included in the conclusion. The conclusion includes the descriptive characteristics of breath intervals and inspiratory and expiratory intervals. The Fourier analysis implies information about main frequences of the respiratiory pattern, that allow either to evaluate average respiratiory rate or to specify, what frequency components are contained in the respiratiory pattern. The wavelet analysis allow to describe signals with frequency spectrum that is variable in time. It's results imply the information about different frequency components presence depending on the time interval.

6. Conclusion

The given software may be useful for diagnostics of the latent respiratory pattern disturbances, that requires the application of the sleep monitoring. It allows to use simple sencors to perform the respiratiory monitoring independently from polysomnography, which requires the complex and expensive equipment. Also such software may be convenient for the performance of the further researches, concerned with the respiratiory pattern analysis.

References:

1. Айсанов, З. Р. Исследование респираторной функции и функциональный диагноз в пульмонологии / З. Р. Айсанов, Е. Н. Калманова // Русский медицинский журнал – 2000. – Т. 8, № 12.
2. Гребнев, А. Л. Пропедевтика внутренних болезней: Учебник / А. Л. Гребнев, В. Х. Василенко. – 5-е изд., перераб. и доп. – М.: Медицина, 2001. – 592 с.
3. Spriggs, W. H. Essentials of Polysomnography / W.H. Spriggs, 2008 – p. 615.
4. Кудий, Л. И. Особенности дыхательного ритма в условиях дозированных нагрузок у спортсменов с различной направленностью

тренировочного процесса / Л. И. Кудий, С. Н. Хоменко, А. В. Калениченко // Педагогика, психология и медико-биологические проблемы физического воспитания и спорта – 2007. –№8.– с.70-73.

5. Frey, U. Irregularities and power law distributions in the breathing pattern in preterm and term infants / U. Frey, M. Silverman etc. // Journal of Applied Physiology – 1998 – pp. 789-797.

6. Ifeachor, E. C. Digital signal processing: a practical approach / second edition / E. C. Ifeachor – 2004.

7. Фридман, А. Л. Язык программирования Си++. Курс лекций. Учебное пособие / Издание второе, исправленное / Фридман А. Л. – М.: ИНТУИТ.РУ, 2004. – 264 с.

8. Земсков, Ю. В. Qt 4 на примерах / Ю. В. Земсков Спб.: БХВ-Петербург, 2008. – 608 с.

THE RESEARCH OF SCATTERING PROPERTIES OF DROPLET OF BLOOD SAMPLES.

Rafalskiy A.. S., Aristov A. A, Zhoglo E. V.

Scientific advisor: Aristov A. A, PhD, associate professor

National Research Tomsk Polytechnic University, 634050, Russia, Tomsk, Lenina av., 30

E-mail: rafalskiy_andrey@sibmail.com

Abstract. This paper presents the results of research of the different types effect of red blood cell aggregation on the scattering properties of samples of human blood, formed in the form of sessile drop. We present the scattering droplet samples and the samples contained in a flat, horizontal cuvette, with different levels of hematocrit and antibody titer. The advantage of droplet samples, to research influence of biophysical processes in the optical properties of blood.

Course of various biophysical processes in blood assays leads to change of its physical properties. Such processes as aggregation of the erythrocytes, assays leading to structural changes, find the reflectance in change of optical properties of the explored sample. We had been offered procedure of investigation of the given processes by means of an assessment of scattering properties of samples of the blood generated in the form of the lying drop. The given examinations have allowed to gain the information which can be useful at building of new procedures of diagnostic research.

If to take for object a drop of integral blood its optical properties will vary depending on many parents. We will give the cores:

– Processes of aggregation of cellular and molecular builders, chemical transformations change immersing and scattering properties.

– Initial chemical composition, processes of adsorption of molecules on boundary surface a drop-air result in to interfacial tension change, that is the drop shape, and, hence, and a thickness of an appeared through stratum varies. It result ins to change of the luminous flux transiting through a drop, and on scattering properties of the dropwise sample (scattering indicatrix).

– Processes of subsidence of cells and aggregates are accompanied by redistribution of builders on assay volume. Hence, change of optical properties of various subsamples characterises these processes.

– The top clear stratum of a fluid phase in a drop after the terminal of process of sedimentation of cages carries out a role of a focusing lens. And, hence, influences the light flux going through a drop..

We had been developed the device allowing more full to investigate dispersing properties of the drop samples [1] and to obtain the data about intensity of a scattered radiation under different angles (scatterings indicatrix).

The dropwise sample as object for dispersion examination has a series of essential advantages, before samples prisoners in a cuvette. Because of a natural spherical free surface of a drop (at its small diameter) in the dropwise sample radiation transits almost identical distance from a point of introduction of radiation in a sample (centre of the basis of a drop) to any point of its surface. In our examinations diameter of a drop made 3,5 mm. The height of the dropwise sample measured under the image of a drop gained by means of videocamera, made about 1.7-1.8 mm. On escaping of the dropwise sample there are any additional refracting devices.

Research have shown dependence of scattering indicatrixes both on quantity of a hematocrit of the sample, and on a view of aggregation of cells.

Results of examination have initially been gained in terrain clearance quantities that impeded carrying out of the comparative analysis of indicatrixes, because of the considerable change of level of a signal during examination

and quantity of a hematocrit. Therefore, for an estimate of change of intensity of a scattered radiation, the norming of the data has been yielded for each indicatrix, concerning the peak value of intensity in it, directly past radiation observed at detection (an angle 0 °).

On fig. 1 the indicatrixes gained by us for samples of a blood with a different hematocrit registered at once after formation of drops (fig. 1, a) and in 2 minutes (fig. 1, b) are presented.

Prior to the beginning of aggregation (the initial moment after formation of drops) the considerable influence on character of dispersion renders hematocrit level. At high level of a hematocrit, owing to presence of a great number of separate cellular devices the considerable dispersion of radiation on major angles (50 °-60 °) is observed. At the subsequent aggregation of cells (in 2 minutes) qualitative differences of indicatrixes are reduced to a minimum.

Research of scattering properties of samples of a blood in which have been conducted various views of aggregation proceeded and, accordingly, aggregates of various structure were formed. In blood samples in which anticoagulant is added only, natural spontaneous aggregation of erythrocytes (fig. 2, a) proceeds. At the given view of aggregation the aggregates having structure of monetary columns are formed. At addition in serum blood sample (used a blood of III group and standard serum of II group antibody-containing to III blood type.), there is a specific hemagglutination at which there is a formation of cellular conglomerates not having accurate structure (fig. 2, b).

In diagrammes presented on fig. 3, for blood samples with an identical hematocrit, but different views of aggregation the greatest difference in the form of indicatrixes is observed after the lapse of some time. It is possible to explain the given fact to that the formed units have different geometrical parametres that in turn affects scattering properties of medium.

Results of the spent research have shown that optical properties of the dropwise samples influences not only quantity of particles, but also character of their aggregation. The further studying of scattering properties of samples will allow to develop mathematical model of dispersion of optical radiation by the dropwise sample of a blood that in the future, will allow to develop new procedures of diagnostic research.
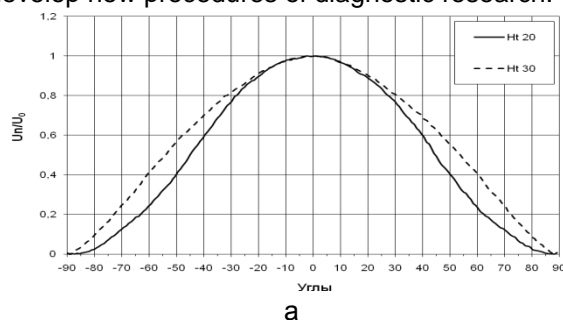

a

b
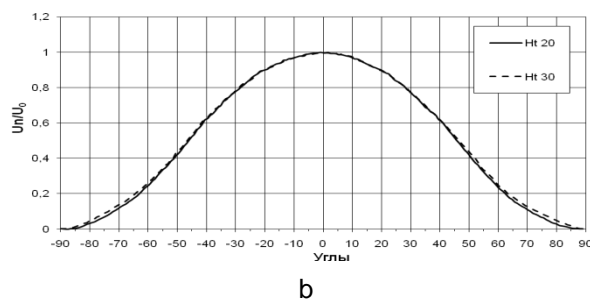
Fig. 1. Scattering indicatrixes of optical radiation by the dropwise samples of a blood with a hematocrit 20 and 30, prior to the beginning of aggregation (a) and after aggregation (b).

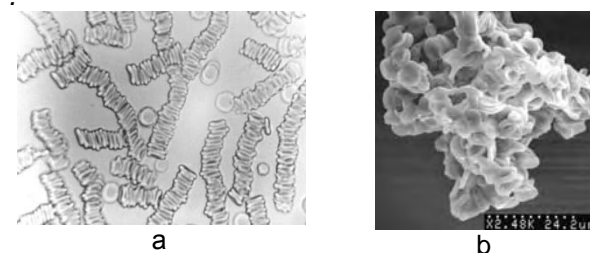.

a   b

Fig. 2. Aggregates in the form of the monetary columns, formed at natural spontaneous aggregation (a) (a photo of authors), and a cellular conglomerate formed during a specific hemagglutination (b) [2].
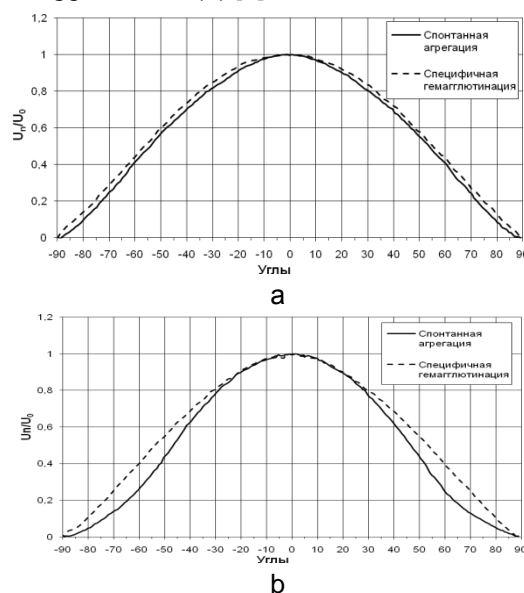

a

b

Fig. 3. Indicatrixes dispersion of optical radiation by the dropwise samples of a blood (Ht-30) with spontaneous aggregation and a specific hemagglutination. Prior to the beginning of aggregation (a) and after aggregation (b).

References:

1 Aristov A.A., Evtushenko G. S, Rafalsky A.S. Biotechnical system for photometric examination of the dropwise assays of biofluids.//the Photonics, 2009. - №6. P.32-35.

2 Nishi K., Rand S., Nakagawa T., Yamamoto A., Yamasaki S., Yamamoto Y. et.al.. ABO Blood Typing from Forensic Materials -

Merits and demerits of detection methods utilized in our laboratories, and biological significance of the

3 antigens. Режим доступа: http://www.geradts.com/anil/ij/vol_006_no_002/papers/paper001.html.

THE MONITORING SYSTEM OF THE MOTHER AND FETUS WITH THE TRANSFER OF DATA OVER THE RADIO CHANNEL

Soloshenko I.S., Tolmachev I.V., Kiselyova E.Yu.

Scientific adviser: Kiselyova E.Yu., PhD

Tomsk polytechnic university, 30, Lenin Avenue, Tomsk, 634050, Russia

E-mail: kiseleva_eka@tpu.ru

Modern medical care to pregnant women is far from ideal. The meaning of medical monitoring during pregnancy is in consultations and diagnostics, which allow to identify the risks for mother and child, as well as the appointment of timely measures to overcome these risks. A good diagnosis when assessing the risk during pregnancy significantly reduces the risk during childbirth, so pregnant women should be observed in well-equipped diagnostic centers, where specialists are working well.

Diagnosis of fetal pathology with subsequent correction of his condition became critical component of obstetric care and forms the direction of perinatal medicine, which treats the fetus as a full-fledged patient. Fetus - a patient the fetal period in which the processes proceed on its own, peculiar only to this period of life laws. Before birth, many of the diseases of the fetus remains unrecognized. Currently, there are various methods of diagnosing pregnancy. The most famous of them:

Auscultation. Auscultation is the technical term for listening to the internal sounds of the body, usually using a stethoscope; based on the Latin verb *auscultare* "to listen". Auscultation is performed for the purposes of examining the circulatory system and respiratory system (heart sounds and breath sounds), as well as the gastrointestinal system (bowel sounds). When auscultating the heart, doctors listen for abnormal sounds including heart murmurs, gallops, and other extra sounds coinciding with heartbeats. Heart rate is also noted.

Cardiotocography. Cardiotocography is one of modern high-informative methods of fetal condition diagnostics during pregnancy with usage of monitoring device. Estimation of condition is carried out basing on fetal cardiac rate analysis and its moving activity. Such investigation is especially important during delivery. Doctors receive 2 diagrams: one shows fetal cardiac rate, other - its moving activity. Uterine contractions are registered at the same time. This research is carried out in the third trimester of pregnancy since 32 weeks.

Phonocardiography. The method of phonocardiography used in cardiotocography first generations. It is based on recording sound effects working heart using a microphone, placed on the abdomen of women. The disadvantage of this method of recording cardiac activity was a large number of artifacts. Any stirring of the fetus, the movement of women, uterine contractions produced their background noise, prevented the registration of are heartbeats.

Fetal Magnetocardiography. Fetal magnetocardiography involves the acquisition and interpretation of the magnetic field near the maternal abdomen due to the electrical activity of the fetal heart. A fetal magnetocardiogram (MCG) can be recorded reliably from the 20th week of gestation onward. Fetal magnetocardiography is a truly non-invasive technique in which the body is not even touched. At FMCG shows typical wave and segments, characteristic of the adult ECG (P-wave, QRS-complex and T-wave). It can be used to classify arrhythmias and to diagnose certain congenital heart defects. Hence, it may help to provide optimum care for the patient. However, until now, fetal MCGs have mainly been measured in research laboratories. Apparently, the application of fetal magnetocardiography in a clinical setting is hampered by the fact that the measuring instrument and its exploitation are still rather expensive and skilled personnel is needed to carry out the measurements.

Echocardiography. Echocardiography - a method of research and diagnosis of the morphology and mechanical activity of the heart. This method is based on recording reflected from moving structures of the heart of ultrasonic signals. For echocardiography used echocardiograph, which contains a generator of ultrasound (frequency of 1 to 10 MHz). The ultrasonic beam is directed through the chest wall to the various departments of the heart. Then the

sensor perceives the reflected ultrasonic signals, converts the perceived ultrasonic waves into electromagnetic waves and amplifies them. Recorder allows imaging of the structures of the heart - echocardiography.

Invasive Electrocardiograph. Internal cardiography provides a quality and reliable signal from the fetal heart. In this method uses two types of electrodes: an active and indifferent. Indifferent electrode attached to the inner surface of the thigh women. Active electrode is superimposed on the set before the head of the fetus. Weak signals are captured, amplified and enhanced electrocardiogram then fed to the amplifier pulse. This technology is detachably fetal electrocardiogram provides its high quality, but can only be used during childbirth.

But, unfortunately, all these methods can not provide long-term monitoring of mother and fetus. Employees of the Department of Medical Cybernetics SSMU developed device for monitoring the status of the mother and fetus to assess the distribution of cardiac rate. This device has many advantages: the possibility of long term monitoring, mobility, ease of applying electrodes to the patient is safe, accurate and reliable information on the status of the mother and fetus, ease of use.
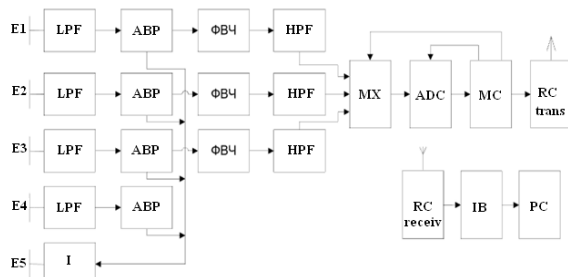
Fig.1 Circuit diagram of the device.

The development of this variant of the device have a problem of choice of technology of data transmission.

Because the medical hardware systems can not guarantee connection in the line of sight, the issue of wireless data focuses on radio wave range. We also recommend using a standardized form of data transmission. This facilitates the use of existing radios that operate the Transmission protocols with error correction, and which may be resistant to interference.

Another advantage of standardized technologies for data transmission is that the various modules are incompatible with each other. Thus, for different application may be fitted with the sensor wireless interface. In cases where monitors are used as personal computers, laptops or PDA, this standard interface can be already integrated. In the process of selection of technology should also be borne in mind that the monitor should be visualized than one device.

One of the radio standards, which is used in medical institutions, is Wireless LAN. Wireless LAN, mainly used in cases where the premises is necessary to build a fixed wireless communication networks with large frequency bands and the distance of 30-100 m. Because of the high carrier frequency and high bandwidth power consumption is very high, which makes the Wireless LAN unacceptable for use in wireless medical sensors.

Zigbee technology is especially suitable for the use of sensors for monitoring and control in everyday life. Since Zigbee technology is quite economical in terms of energy consumption, there is a possibility of its application in medical developments. However, a development, in the field of standardization has not yet reached a level where we can say that there are already solutions for the creation of modules of the primary analysis.

Bluetooth is widely used in many fields.

In medicine, it is also necessary to link with these devices has been free from errors. Studies of this problem showed that transmission errors occurring at the level of the radio channel, fully corrected, so that at the user level, they do not arise. As a transceiver module using a ready channel XTR-CYP-2.4 produced by Aurel, which works at a frequency of 2.4 GHz.
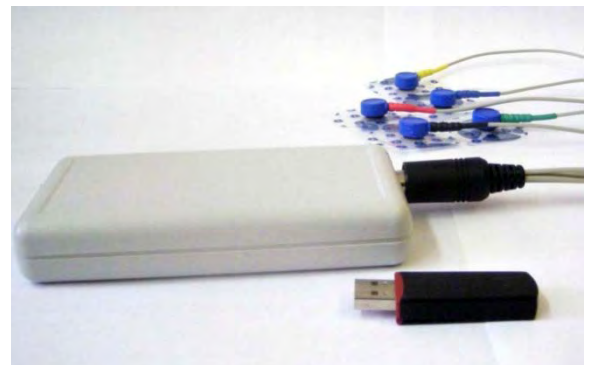
Appearance of the device shown in Figure 2.

Figure 2 - The appearance of portable devices for non-invasive and passive assessment of mother and fetus, with the transfer of data over the radio channel.

Currently, there are various instruments for monitoring pregnant women: stationary, i.e. with a wired connection device and the patient, the device with the accumulation of data on flash media. In the developed device, which is described above, may unification properties of existing devices.

REFERENCES

1 Nikolajchuk O.N. Peredacha dannyh po razlichnym kanalam svjazi (Data communication on different channels of communication) (http://ixbt.com./peripheral)
2 Bray J., Sturman Ch. Bluetooth: connect without cables. – New Jersey: Prentice-Hall, 2001. – 495 p.

Section VI

MATERIAL SCIENCE

WAYS OF INCREASING THE RELIABILITY OF GAS TURBINE BLADES

Barkhatov A.F.

Scientific advisor associate professor N.V.Chuhareva, associate professor R.N.Abramova

Tomsk polytechnic university, 634050, Russia, Tomsk, Lenin av., 30

E-mail: barhatov@sibmail.com

High level of force and temperature impact of the gas stream from the combustion chamber on the operating and distributing blades [1].

Major factors influencing blades during their operation: demands specific require – ments in blade design.

Temperature – force factors due to flame environment degrade metal structure and form not only internal pressure, but also static pressure from centrifugal forces and thermocyclic pressure. Above – mentioned consequences result in such defects as micro – cracks and micro – pores. Vacancy defect and dislocation density increases, line slips and twinnings occur, which, in its turn, results in the allocation of σ – phases and carbides as well as, dissolution, coagulation, etc. This leads to the marginal state and further distruction. Blades are subjected to abrasion, corrosion and therma – fatigue deterioration [2], [3].

Due to severe conditions and operation, regimes the first step blades, under of the turbine high pressure are special details in of gas turbine engines, therefore increasing their durability and reliability is an actual problem in modern technology.

Basic defects. Cracks in the top blade wings are the main defects, including thermal – fatigue characteristics and connected with the temperature change cycle on the blade wing during its operation. Their occurrence is the efficiency infringement equistentn crosspieces δ_C, δ_K (Fig. 1). Fabricated shells are potential sources of more serious defects, such as cracks. Micropores in heat – resistant isolations could result in high – gas temperature corrosion of blades and their gas – erosion deterioration, further reducing its operation life [2].
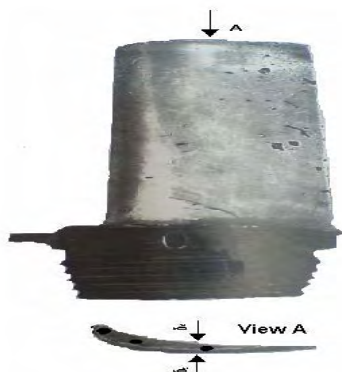
Fig. 1 External view of 1ststep blade of high – pressure turbine

Methods of increasing durability:

1) Reduction of microroughness height leads to the reduction of stress concentrators on the surface. In this case the electrolytic – plasma polishing (EPP) method is used. This method is the following - blades are placed in a NaCl solution at $80 – 85^0$ C. The tank becomes an anode, as it is connected to negative potential. As the blades are emerged into the NaCl solution, a rapid current furms at the surface, where emerging of bubbles temporary plasma discharges occur on the micro – roughness to smooth them out [4].

2) Strength characteristics are increased through the development of modern high heat – resistant alloys. Such alloys increase the gas temperature before the turbine, as well as, new technological turbine designs.

To provide high heat resistant properties during blade productions the technology of high - gradient directional crystallization is used producing of monocrystal structures with set crystallography orientation set. It increases structure, quality provides its uniformity, reduces dendrite liquation , porosity.

Specific characteristic of this process is that the temperature gradient increase decreases the liguid – solid zone height within the temperature ranges TS (solidus) – TL (liquidus) where the dendrite structure forms [5].

Besides, there is a number of other methods, to increase the operation life of turbine blades. Based on the analysis of references resources and data, the following design and technological results were established (Table 1).

Different alloy – types were applied in the production of blades, for example: nickel alloy ChS70 – VI by moulding in a vaccum. The alloy has optimum structure: 0,09 % C, 15,9 % Cr, 10,5 % Co, 2,0 % Mo, 5,3 % W, 4,6 % Ti, 2,8 % Al, 0,2 % Nb, Ni - basis. Alloy IN 738 with optimum chemical alloy composition of: 16 % Cr, 8,5 % Co, 2,6 % W, 1,75 % Mo, 3,4 % Al, 3,4 % Ti, 0,9 % Nb, 1,75 % Ta, 0,17 % C, 0,01 % B, 0,1 % Zr [2], [6].

Principal coatings. Heat resistant combined coatings with two layers. The internal one consists of a solid solution of Cr, Al, Y in cobalt (light phase) and intermetallide Co, Al (dark phase). The intermediate layer - 1,5 microns is

Table 1 Basic design and technological results

Design				Technological results	
Basic attachment methods	Construction application	Material	Coatings	Operation - life	Restoration methods
X – mas - shaped groove T-shaped groove	*Blades:* regulating step *RS*, intermediate step of high pressure (HP), average pressure step in low pressure (LP)	C,Cr,Co, M,W,Ti,A l,Nb,Ni.	Heat resistant coating Ceramic coating	X-ray-spectral analysis Quantitative metallographic analysis	Thermal treatment New coatings

a layer alloy of cobalt and carbides. The external - dioxide zirconium ZrO_2 with impregnations of pure zirconium (light phase). The ceramic coating includes SiC, BN, AlN, Al_2O_3 [2].

Methods of operation – life determination: 1) X – ray spectral analysis based on radiation of a substance through electrode flow or high energy photons. 2) Quantitative metallographic analysis is based on the distribution of the temperature along the turbine blades in dangerous cross – sections. The calculations are based on temperature dependences of element diffusion characteristics on the coating [3].

Restoration methods**.** Thermal processing – hardening at 1100^0 C, exposure time – 2 hours, cooling at air temperature, age hardening at 850^0 C during 24 hours, further cooling at air temperature new coatings of ZrO_2 by gas – plasma method, affer a preliminary cohesive coating [6].

Conclusion:

Based on above – mentioned analysis and revealing the effective methods of increasing blade reliability and operation – life, following ones have been considered: new methods coved increase reliability and decrease expenses.

References

1. Baikin S.S., Rudachenko A.V., Chuhareva N.V. Gazoturbinie ustanovki: - Tomsk: Izdatelstvo Tomskogo polytechnicheskogo universiteta, 2008. - 139 s.

2. Krivina L.A., Sorokin V. A, Tarasenko JU.P. Postexplyatatcionnoe sostoanie lopatok pervoi stypeni TVD// Gasoturbine teechonologii. - 2005 - № 8.

3. Mozhajskaja N.V., Getsov L.B.. Novie metod opredelenia ostatochnogo resursa lopatok GTU s pokritiem // Gasoturbine teechonologii. - 2007 - № 9.

4. Smyslov A.M., Sedov V.V., Pavlinich S.P., Ivanov V. JU. Yprochnenie lopatok gazoturbinih privodov// Gasoturbine teechonologii. - 2006 - № 6.

5. Demonis I.M., Bondarenko J.A., Cablov E.N. Visokogradientnai napravlennai cristallizatcia lopatok GTD s monocristallicheskoi strycturoi// Gasoturbine teechonologii. - 2007 - № 3.

6. Chegolev I.L., Tarasenko J.P., Sorokin V. A, Crivina L.A. Mechanicheckie svoistva i structura materiala rabochih lopatok TVD posle expluatatcii i regeniratcii // Gasoturbine teechonologii. - 2005 - № 1.

ON THE METHODS FOR STUDYING POROSITY OF SHS MATERIALS

Maznoy A.S.

Scientific adviser: Kirdyashkin A.I., PhD

Tomsk state university, 634050, Russia, Tomsk, Lenin avenue, 36

E-mail: maznoy_a@mail.ru

Introduction. One of the advanced methods of production of porous penetrable materials is the method of self propagating high temperature synthesis (SHS). Porous metalloceramic SHS-

materials possess a unique combination of high strength, thermal conduction, chemical stability, stability of operating parameters, and other properties [1]. The features of porosity morphology of SHS materials are poorly understood and are not presented in the literature. It is shown in [2] that the experimental magnitude of pore size is the function of the method for their definition and that the volumetering and continuous-streaming methods are sensitive to pore configuration. Therefore automatic image analyzers for metallographic analysis have become widely spread. However, the analyzers cannot process statistical data on porous morphology using the methods of stereometric metallography. The stereometric metallography calculations allow us to receive the characteristics of a material for 3-dimensional space, while the conventional analyzers give only 2-dimensional characteristics of the objects under study. Therefore the development of such computational procedures is very important. These techniques will allow us to reveal specific features of porous SHS-material morphology and to determine the most important quantitative parameters of the materials. In this paper, several stereometric techniques for porosity analysis are developed.

Investigation techniques. Stereometric procedures are based on the analysis of metallographic section images of the studied materials. There are three classes of porous structure topology [3]: «closed pores», «through pores» and «blind pores» (Figure 1). To consider all plausible cases in porosity analysis it is necessary to take into account not only characteristics of the «cross-sections of pores» but also characteristics of the «cross-sections of porous-material framework elements» in calculations.

Figure 1: Closed, blind and through pores

For exploration of the porosity parameters of functional materials one should know the area of the region S_0 (a region in the picture of metallographic section where we examine pores or elements of framework) and define the following parameters of each object of interest (pores or elements of the framework): 1) equivalent diameter, 2) quantity of inclusions, 3) area of the object of interest, without the area of inclusions, 4) perimeter of the object of interest, 5) area of inclusions, 6) net area of the object of interest.

Let us assume that the images of pores without inclusions are cross-sections of closed pores forming porosity of the framework. Consequently, the images of pores having inclusions are «through porosity» cross-sections.

The calculation of such functional parameters of porous materials as the average diameter of the framework cross-section elements D_{El}, the surface area of «through porosity» S_{Surf}, and the diameter of porous channel D_{Can}, is undoubtedly important owing to possibility of allowance for framework-element geometry by stereometric techniques.

The diameter of porous channel D_{Can} is found on the assumption that the sum of areas of all «through pores» is restricted by the right-angled region with the small leg equal D_{Can}. If the quantity of the framework- element cross-sections per 1 mm^2 of the area of region is N and the coefficient of filling of the region by the framework elements (we allow for pores situated inside the framework elements) is Kz, we have:

$$D_{El} = 2\sqrt{\frac{Kz}{N \cdot \pi}} \qquad S_{Surf} = \frac{\sum_j P_j}{S_0} \cdot 10^3$$

$$D_{Can} = \frac{1}{4}\left[\sum_i P_i + \sum_j P_j - \Delta - \left(\left[\sum_i P_i + \sum_j P_j - \Delta\right]^2 - 16 \cdot \sum_i S_i\right)^{0.5}\right]$$

$$\Delta = P_i^{max} \cdot \left(\frac{Kz}{Kz + 1.75}\right)$$

P_i is the perimeter of i-th pore with inclusions; P_j is the perimeter of j-th framework element; «i», «j» are the quantity of pores with inclusions and quantity of framework elements, respectively; S_i is the area of i-th pore with inclusions; P_i^{max} is the perimeter of a pore with inclusions having a maximum area in the sample.

Definition of the number of spherical particles in the volume of studied material and the particle size distribution parameters in terms of geometric series. There are «the array» and «the framework» structures of porosity which are in turn classified into «regular» and «nonregular» [4]. It is obvious that porous SHS materials refer to the nonregular structures. The nonregular structures can be both isotropic and anisotropic. The special class among the nonregular heterophase systems is the so-called statistically isotropic mixtures in which all phases are presented by equal building blocks. In real porous SHS-materials, the statistically isotropic mixtures are the material of framework where framework porosity is formed by "closed pores". In this case, the characteristic geometrical parameters of the nonregular building blocks (sizes of pores) become random quantities and undergo some kind of distribution. We modified the method for definition of spherical particle numbers in the volume of materials and the size distribution parameters (diameters) in terms of geometric series (method of Saltykov (MS) [5]).

The modified MS allows us to use any quantity of dimensional groups in reconstruction of pore size distribution and to vary the value of the denominator of geometric series of diameters.

Let i be the number of dimensional groups, n_i – the quantities of cross-sections of respective dimensional groups per 1 mm^2 of metallographic section, D_1 – the maximal diameter of pore section, D_i is the diameter of an «i-th» dimensional group, Z is the denominator of a geometrical progression of a decreasing series, the quantity of pores in the «i-th» dimensional group in the volume of framework material, in this case, N_i is calculated as:

$$N_i = \frac{1}{D_i} \sum_{j=1}^{i} \theta_j \cdot n_{1+i-j} \qquad (1)$$

$$D_i = K_i \cdot D_1; \quad K_i = (10^{-Z})^{i-1}$$

$$\theta_1 = \frac{100}{\alpha_1}, \quad \theta_2 = -\frac{\alpha_2 \cdot \theta_1}{\alpha_1}, \quad i \geq 3 \quad \Rightarrow \quad \theta_i = -\frac{\alpha_i \cdot \theta_1}{\alpha_1} - \sum_{j=3}^{i} \frac{\alpha_{2+i-j} \cdot \theta_{j-1}}{\alpha_1}$$

$$\alpha_i = \left| \sqrt{1 - K_i^2} - \sqrt{1 - K_{i+1}^2} \right| \cdot 100$$

The developed method can also be used for materials whose pores are spheroids in the form but only when the pores are represented as ellipsoids, and their spinning axes are codirectional to a certain direction and the studied plane is oriented perpendicular or parallel to the given direction. If the pore number in the «i-th» dimensional group is negative, it is necessary to stop the calculation and for reconstruction to use the data up to «(i-1)-th» dimensional group inclusive. The method can be applied only to analysis of the images of pore cross-sections without inclusions. The obtained data characterize the pore size distribution in the volume of framework material, the total number of «closed pores» in the volume of framework, and characterize framework porosity of a porous material.

On reproducibility of porosity morphology parameters of real SHS materials. Analysis of reproducibility of characteristics of the SHS porosity structures was made. The Ni-Al and Ti-Si systems were used as model reaction SHS systems. The compositions obtained under various conditions of preparation (selections) were analyzed, based on a few experimental points in each sampling and the variation coefficient (VC) [5] was calculated. If the VC < 0.1, then the variability of the variation series is thought to be insignificant, for the VC between 0.1 and 0.2 it is moderate, and for the VC in the range between 0.2 and 0.33 it is significant, the VC > 0.33 – inhomogeneities of information. It was found that the parameters of porosity of SHS products both from a layer to a layer in one sample and in iso-oriented layers of various samples under identical conditions of preparation, are reproduced in the range from insignificant to moderate variability of the variation series.

However, it should be noted that for calculations, it is necessary to use a representative «volume» – the region of interest should be chosen so that the dispersion of morphology parameters is not increased with its size. It is better to analyze the entire cross section of the sample, since it is impossible to determine the area to be studied in advance.

Conclusion. The procedures for direct measuring various morphology parameters of porous materials by geometry methods of stereometric metallography are developed. It is shown that in calculations, it is necessary to take into account both the parameters of the pores, and the parameters of the porous framework elements. We upgraded the method for definition of the number of spherical pores in the material volume (3D) and size distribution parameters (diameters) on geometric series. The method is based on analysis of the data on cross sections of pores (2D) and allows us to consider any quantity of dimensional groups and to vary the denominator of the progression. The advantages of stereometric procedures are the considerable economy of experimenter resources and simplicity of use of the procedures in computer calculations. The developed procedures are tested on a model porous sample and on porous SHS-materials. The results of testing show that the procedures can be used for analysis of porous materials of various origin and porosity structure.

References

1. Borovinskaya I. P. SHS-ceramics: Synthesis, Technology, Application // Engineer. Technologist. Worker. – 2002. – No. 6 (18). - P.28-35
2. Solonin S. M., Chernyshev L. I. Mesostructural Basis of Properties of Porous Materials. 1. The Features of Analysis of Pore Structure of Porous Materials // Powder metallurgy. – 2008. – No. 9/10. – P. 76–88
3. Akshaya Jena, Krishna Gupta, Characterization of Pore Structure of Filtration Media // Fluid Particle Separation Journal, Vol. 4, No.3, 2002, pp. 227-241
4. V. V. Skorokhod. A Theory of Physical Properties of Porous and Composite Materials and Principles of Controlling Their Microstructure in Technological Process // Powder Metallurgy. – 1995 No.1/2. – P. 53–71.
5. Saltykov S. A. Stereometric Metallography (Stereology of Metal Materials) / S. A. Saltykov. – M. : Metallurgy, 1976. – 272 p.

PROSPECTS FOR RESOURCE-SAVING SYNTHESIS

OF ADVANCED CERAMIC MATERIALS

ON THE BASIS OF TOMSK OBLAST RAW MATERIALS

Maznoy A.S.

Scientific adviser: Kirdyashkin A.I., PhD

Tomsk state university, 634050, Russia, Tomsk, Lenin avenue, 36

E-mail: maznoy_a@mail.ru

A continuing demand of industry for stronger materials, with higher wear resistance, and thermal stability capable of functioning in extreme conditions, the question on development of present permeable porous materials becomes very topical. For example, electric power stations working on powdered fuel experience heavy losses from erosion of burner tip, and factories draining coal need abrasive-resisting materials for filtration systems. Therefore the materials are required which can replace traditional tungsten carbide in many applications. An increase in wear resistance and stability to chemically active media are of principal importance for the development of modern hi-tech porous materials.

Ceramics, in spite of the fact that it exhibits high durability and hardness, is fragile and possesses low impact strength, especially in comparison with metals. The mechanical properties of ceramic materials under stretching are low – because of low plasticity ceramic materials crush on achievement of critical stretching in heterogeneous regions of a microstructure. On the other hand, these are able to sustain very high compressive loading.

Nitrogen-containing minerals are not found in nature. However, it was shown that introduction of nitrogen into ceramic structures facilitates a considerable gain of operational characteristics. Silicon nitrides and SiAlONs are the most functional materials among well-known ceramic materials. Their outstanding properties allow them to compete with other technical ceramic and refractory materials such as zirconium oxide (ZrO2), alumina (Al2O3), and silicon carbide (SiC) in many industrial-scale plants of oil and gas sector, metallurgy, heavy, chemical, automobile, and aerospace industries. In an effort to show a unique set of physical properties of nitrogen-containing materials. Table 1 (at the end of the paper) compares some properties of sialons with a number of competitive advanced ceramic materials such as alumina (Al2O3), reaction bonded silicon nitride (RBSN), mullite and silicon carbide (SiC). (Comparative data are from www.syalons.com and www.msiport.com).

The discovery of an alloy of silicon nitride made independently in the UK by Jack and Wilson, and in Japan by Osama et al revealed the advantages of material based upon silicon nitride, which was sinterable. SiAlONs are ceramic alloys based on elements silicon (Si), aluminium (Al), oxygen (O), and nitrogen (N) which were developed in the 1970s to solve the problem of silicon nitride (Si3N4) being difficult to fabricate. The first patent on the production of sialon materials has published in 1972 by Jack and Wilson.

Similar to alloys of silicon nitride, sialons exist in three basic forms. Each form is iso–structural with one of the two common forms of silicon nitride, beta (β) and alpha (α) and with silicon oxynitride. The relationship between sialon and silicon nitride is similar to that between brass and pure copper. In the latter case, copper atoms are replaced by zinc to give a better and stronger alloy than the mother metal. In the case of sialon, there is substitution of Si for Al with corresponding atomic replacement of N by O, to satisfy valence requirements. The resulting «solution» (sialon) has superior properties as compared to the original pure solvent (silicon nitride). See Fig. 1:
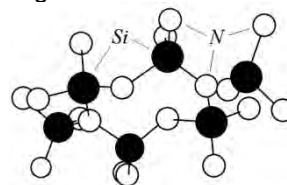

Figure 1. A basic structural unit of silicon nitride

SiN_4 tetrahedron is a basic structural unit of silicon nitride (Si_3N_4). This is analogous to the SiO_4 structural units in silicates. The tetrahedra are linked together into a rigid three dimensional framework by sharing corners. The Si–N bonds are short and very strong. This strong, rigid, compact structure is responsible for many important properties of Si_3N_4.

β–sialon is based upon the atomic arrangement existing in β–Si_3N_4. In this material, Si is substituted for by Al with the corresponding replacement of N by O. In this way, up to two–thirds of silicon in β–Si_3N_4 can be replaced by Al without a change in the structure. The chemical replacement is one of changes of Si–N bonds by Al–O bonds. The bond lengths are about the same for the two cases but the Al–O bond strength is significantly higher than that of Si–N.

In sialon, Al is coordinated as AlO_4 rather than as $AlO6$ in alumina (Al_2O_3). Therefore, in β–sialon the bond strength is 50% stronger than in Al_2O_3. Thus sialon intrinsically has better properties than both Si_3N_4 and Al_2O_3.

α–sialon. The second form of Si_3N_4 with which sialon is iso–structural is α–Si_3N_4. The stacking structure in α–Si_3N_4 is different from β–Si_3N_4 in that the long «channels» which run through the β structure are blocked at intervals. This gives rise to a series of interstitial holes. In α–sialons, Si in the tetrahedral structure is replaced by Al with limited substitution of N for O. Valence requirements are satisfied by modifying cations occupying the interstitial holes. In this way, the cations of yttrium (Y), calcium (Ca), lithium (Li) and neodymium (Nd), for example, can be incorporated into the structure.

Production of ceramic materials demands special technologies. In the so-called «ceramic industries» use is made of ovens with working temperatures up to 1300° C. Using of ovens with higher working temperatures makes the technological process heavier and considerably increases the production cost, therefore they have no wide application. However, for fabrication of silicon nitride and sialon powders such equipment is used. The resource- and energy-saving technologies and equipment for industrial production of **porous** nitride materials are not available. Porousless parts can be formed from synthesized ceramic powders by pressing techniques, however, no industrial technologies of porous materials sintering from these nitride powders are known. Due to the above, the only acceptable way of manufacturing the nitrogen-containing porous ceramics is direct nitriding of porous prematerial by the filtrational wave of self-propagating high-temperature synthesis (SHS).

Self propagating high temperature synthesis is an essentially advanced method of synthesis of inorganic substances. SHS allows us to produce ceramic materials of specified chemical and phase structures without external heating of the initial components, because the synthesis is carried out at the expense of thermal emission of the interaction reaction of initial components. The high thermal effect of the reaction of formation of silicon nitride (750 kJ/mol) allows addition up to 70 wt% of raw component into an initial alloy. However, the problem of production of porous sialon materials or other metalized-hybrid components has not been solved so far.

A Tomsk group of researchers successfully uses the SHS method for producing porous materials with predicted parameters of porosity and forms of parts. In the centre of attention of our studies there are ways of synthesis of porous nitrogen-containing SHS-ceramic materials and products from them on the basis of silica-alumina raw materials. It is supposed to use kaolinite clay produced by the company «TGOK «Il'menit». The kaolinite clay contains 65.7 wt% SiO_2 and 26.7 wt% Al_2O_3, as well as oxides of alkaline metals (about 2 %) and oxides of Ti, V, Cr, Zr, Fe, P, Mg, Mn and Ca. Granulometric analysis shows a bimodal content of disperse phases of particles. The first maximum > 83 % is seen for the particles less than 63 μm and the second peak 12 % for the particles about 100 μm. The kaolinite clay deposit is in the Tomsk oblast.

Thus, on the basis of analysis of synthesis principles of nitrogen-containing ceramic materials it was possible to develop theoretical and technological principles of SH-synthesis of porous composites containing phases of silicon nitride, α - and β-sialons with predicted parameters of porosity and forms for the first time at the Department of structural macrokinetics of Tomsk scientific center of the SB RAS. The developed porous materials can be used:
1. as carriers of catalysts for synthesis of synthetic liquid hydrocarbons and synthesis-gas;
2. for dehydration of hydrometallurgical pulps after floatation;
3. for blowing down inert gases through liquid metals for their hashing;
4. for filtration of liquid black and nonferrous metals for their cleaning from impurities;
5. for scrubbing hot smoke gases from dust, impurities, and harmful gases;
6. for floatation, aeration, ozonization of water systems in small bubbling systems of gas distribution;
7. for pneumatic transport and hashing of powdered and superfine powder materials;
8. other purposes.

The favorable «legal climate» of Tomsk technological-innovation zone and opportunities for education of qualified scientists and engineers on the basis of Tomsk universities and research-educational centers facilitate organization of an industrial cycle of manufacturing porous ceramic materials by the SHS method in Tomsk. Therefore manufacturing of new ceramic materials can improve social and economic situation in the sector of industrial enterprises of the Tomsk oblast.

Table 1 Basic design and technological results

Table 1. The properties of sialons with a number of competitive advanced ceramic materials**Properties:**	Dimensionality:	RBSN	Mullite	Al_2O_3	SiC	α-SiAlON	β-SiAlON
Room temperature modulus of rupture	MPa	*180*	*180*	*350*	*459*	*800*	*945*
Modulus of rupture at 1000 °C	MPa	-	-	*205*	*430*	*750*	*670*
Room temperature hardness	$Hv_{0.3}$ Kg/mm^2	*800*	*1100*	*1400*	*2200*	*2000*	*1500*
Fracture Toughness K¹C	MPam½	*2,5*	*2*	*3,5*	*4,3*	*6,5*	*7,7*
Thermal Shock Resistance	ΔT°C	*300*	*305*	*205*	*180*	*600*	*900*
Room Temperature Thermal Conductivity	W/(mK)	*14*	*6*	*29*	*100*	*20*	*28*

THE INFLUENCE OF TECHNOLOGICAL DEFECTS ON THE STIMULATED RADIATION GENERATION IN ZINC SELENIDE CRYSTALS

Gorina S.G., Vilchinskaya S.S., Lyapunova K.V.

Scientific supervisor: Vilchinskaya S.S., associate professor, candidate of Sc. (Physics and Mathematics)

Tomsk Polytechnic University, 634050, Russia, Tomsk, Lenin Avenue, 30

E-mail: svetlana.gorina@mail.ru

In spite of unique electrophysical, photo-electric and optical properties of semi-conductor crystal materials of group $A^{II}B^{VI}$ the restriction in their use is caused by the big complexity of crystals production with reproducible properties. Therefore the urgent question for today is a development and modernization of semi-conductor materials quality control methods, one of which is the method of the pulsed luminescent analysis with a nanosecond time resolution. This method allows not only to control the grade of purity and imperfection of crystals, but also to receive additional information about luminescence centers from change of kinetic characteristics of luminescence attenuation, to study density effects.

The purpose of the current work is to research technological defects influence on the stimulated radiation generation in ZnSe crystals grown in various technological conditions and having different previous history.

The practical importance of the work is defined by the possibility of threshold processes application for the development of powerful, stable against degradation semiconductor electron-beam-pumped lasers.

Luminescence spectral-kinetic characteristics of high-clean zinc selenide monocrystals are studied in the work. They were produced by flux growth (ZnSe №5) and chemical vapor deposition (ZnSe №1-4, CVD - technology). The samples differed in a deviation from stoichiometry and uncontrolled impurity content.

Absorption spectra of investigated samples have been measured on spectrophotometer SP-256. As can be seen from fig. 1, absorption edge of investigated ZnSe crystals is shifted to long-wave region as compared with fundamental absorption edge of pure ZnSe which position is defined by free exciton FE_{ZnSe} (λ~ 443 nm).
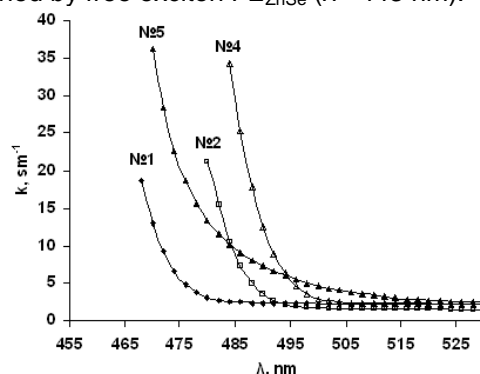
Fig.1. Absorption spectra of ZnSe crystals measured at temperature 300 K.

The samples excitation was carried out by a pulse cathode beam in vacuum at residual gases pressure ~10^{-4} Pa at temperatures 27 K and 300 K for research of pulse cathodoluminescence (PCL) spectra.

The measurement of ZnSe monocrystals PCL spectral-kinetic characteristics was carried out in geometry α = 45^0 at cathode beam energy density 0.02 J/sm^2 (G = 10^{26} sm^{-3}s^{-1}) and temperature 300 K. It is ascertained that the spectra consist of the edge emission fundamental band (fig. 2) which maximum changes in the

range 468 - 489 nm for different ZnSe samples, for the №2 sample two PCL bands are observed at λ=470 nm and λ=483 nm. More long-wave component becomes apparent in №3 and №5 samples PCL spectrum at λ=531 nm (τ~50 ns) and λ=550 nm, respectively. Spectra of №5 sample measured in 100 ns and 2.5 µs have made it possible to separate wide ($\Delta E_{1/2}$ = 0.37 eV) long-wave band at λ=550 nm measured in 50 ns into two components at λ=540 nm and λ=600 nm. The research of kinetic characteristics of №5 sample spectra has made it possible to calculate relaxation time which is≤ 20 ns for the band at λ=468 nm, 50 ns for λ=520 nm, 5 µs and 25 µs for λ=600 nm.

The direct gap semiconductor application as the quantum electronics devices active medium demands to study the processes occurring at high excitation levels. We studied a stimulated radiation line position at electron excitation level G = 10^{27} sm^{-3}s^{-1} (0.2 J/sm^2) and compared it with spontaneous radiation spectra.

At T = 27 K the generation line of №1 and №3 samples is observed at λ=451 nm that corresponds to I_1–2LO. The long-wave region shift of superluminescence band (λ=468 nm) is observed for №4 ZnSe sample having a self-absorption edge shift to long-wave region.

Temperature rise up to room temperature causes the changing to intensification at recombination in electron-hole plasma. Typical PCL spectra of №1-5 ZnSe samples are measured at 300 K at geometry α=90^0 at cathode beam energy density 0.2 J/sm^2 (G=10^{27} sm^{-3}s^{-1}). The luminescence intensification is observed in all investigated crystals except №4 sample (fig. 2). The luminescence changing to an amplification mode is corroborated by sharp increase of luminescence intensity and radiation directivity occurrence. The superluminescence band maximum position is individual for each ZnSe sample: it is located at λ= 476.8 nm for the №1 sample, λ=491.5 nm for №2, λ=475.3 nm for №3 and №5. The bands half-breadth is about 1-3 nm. The luminescence time of №1-5 samples does not exceed the installation time resolution (≤ 20 ns) in a superluminescence mode.
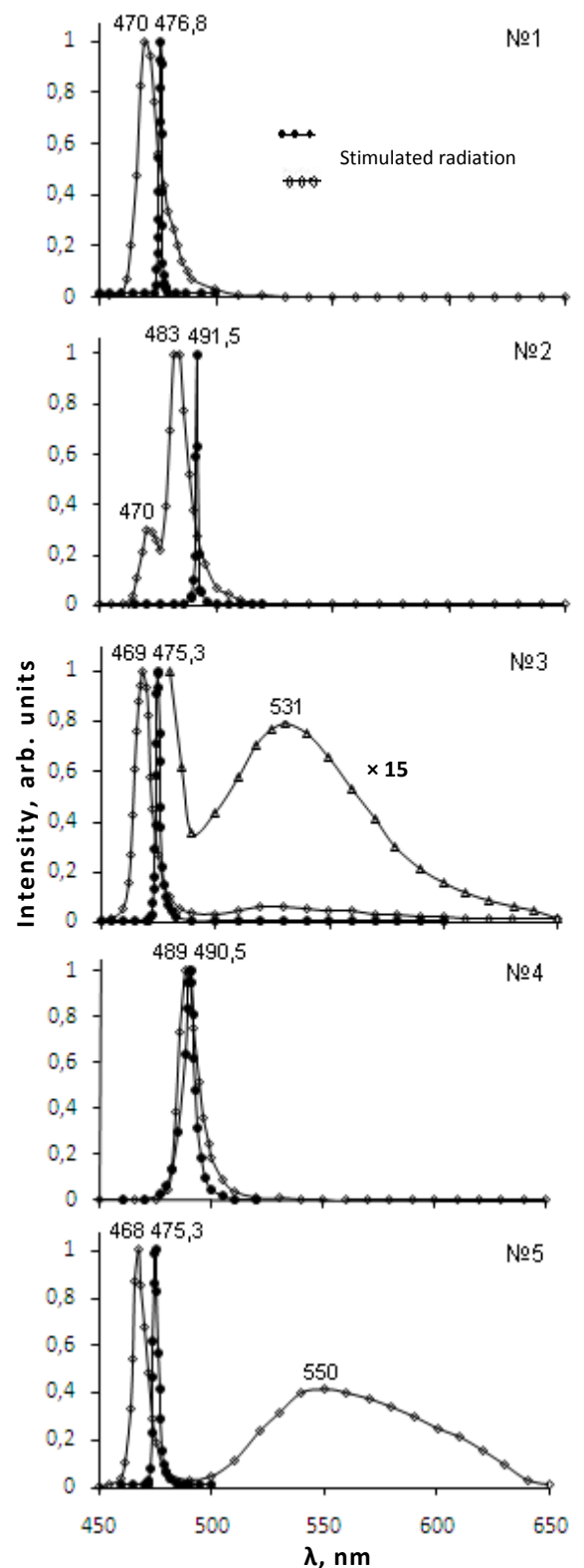
Fig. 2. The PCL ZnSe crystals spectra measured at temperature 300 K.

So far there is no single opinion concerning the luminescence band nature occurring in conditions of high intensity of excitation in science [1]. In work [2] the bands occurring in ZnSe luminescence spectra at high excitation levels are explained by Auger-processes with excitons and charge carriers participation, in [3] –

by charge carriers recombination into an electron-hole liquid.

In real crystals the competition of various mechanisms intensification which depends on crystals quality, excitation level and temperature is observed. To practical purposes, the mechanisms allowing to provide a generation at room and higher temperature are the most interesting. Electron-hole plasma recombination and band-to-impurity recombination satisfy that conditions.

Temperature effect on a generation line shift to long-wave region is explained by self-absorption edge modification, plasmons influence or energy gap width renormalization [4]. An excitation level growth and temperature growth up to room temperature cause changing to generation at electron-hole plasma recombination [5].

Summary:

I. The threshold of generation and the emitting recombination mechanism causing the stimulated radiation in real ZnSe crystals are characterized by the type of defect-impurity complexes and their concentration at cathode beam excitation.

II. The comparative analysis of the spontaneous and stimulated radiation spectra of ZnSe crystals with different previous history shows that the production of effective semiconductor electron-beam-pumped lasers demands to use high-purity crystals with low concentration of deep centers or to apply the alloyed samples with high concentration ($\geq 10^{19}$ sm^{-3}) of shallow acceptor level.

III. The results of research of PCL spectra, excitation threshold level dependences on previous history of samples can be put to the basis for nondestructive method of $A^{II}B^{VI}$ monocrystals cull for devices with electron excitation.

References

1. Gurskii A.L. Electron-Beam-Pumped Lasers Based on A^2B^6 Compounds (Review)// Journal of Applied Spectroscopy. – 1999. – V.66, N 5. – P. 601-618.
2. Saito H., Shionoya S. Luminescence of high density excitons in CdS, CdSe and ZnSe in the 4.2-90 K temperature range// Techn. Reports ISSP. Ser. A. – 1974. – N 631. – P. 1-25.
3. Baltrameyunas R., Kuokshtis E. Electron-hole liquid in ZnSe monocrystals // JETP. – 1980. – V. 79, N 4. – P. 1315-1321.
4. Kempf K., Klingshirn C. Experemental investigation of the electron-hole plasma expansion in CdS // Solid State Commun. – 1984. – V. 49, N 1. – P. 23-26.
5. Gurskii A.L. et al. Electron beam pumped lasing in ZnSe epitaxial layers grown by metalorganic vapour phase epitaxy// J.Appl.Phys. – 1995. – V. 77, N 10. – P. 5394-5397.

SPECTRAL–KINETIC CHARACTERISTICS OF EDGE EMISSION IN CADMIUM SULFIDE MONOCRYSTALS

Lysyk V.V., Oleshko V.I.

Scientific supervisor: Oleshko V.I., associate professor, candidate of Sc. (Physics and Mathematics)

Tomsk Polytechnic University, 634050, Russia, Tomsk, Lenin Avenue, 30

E-mail: lvv1287@mail.ru

Introduction

A^2B^6 semiconducting crystals are supposed to be promising materials for optoelectronics and quantum physics [1,2]. The structural perfection of mono-crystals is determined by process of crystal growth and makes a figure in the creation of optoelectronic devices with specified characteristics. It is known that a variety of properties of A^2B^6 semiconductors is determined by intrinsic point defects and impurities that always can be found in the composition of "pure" unalloyed crystals [3].

The luminescence excited in the crystals of A^2B^6 compounds by different types of energy deposition (cathode-, photo-, electroexcitation) bears information about processes occurring in intrinsic lattice with the participation of defects (intrinsic, impurity and their complexes). The luminescence can be used to control optical characteristics of semiconductor crystals and related technologies for their growth and processing.

Up to the present moment, there is no concurrent view on the nature of spontaneous luminescence bands majority observed in unactivated A^2B^6 crystals. Since information on development of models for luminescence centers about kinetic parameters of radiation of observed

luminescence bands and their dependence on experimental conditions (excitation level, technology for preparation of samples, temperature) is not sufficient [3-8].

The purpose of the work is to present results of investigations of edge emission (EE) spectral-kinetic characteristics in CdS crystals, which are fundamental [2] and observed in A^2B^6 compounds.

Experiment

Excitation of samples was carried out with high-current electron beam with following parameters: average energy of electrons in the beam ~ 0.35 MeV, pulse duration at half maximum ~ 15 ns. The residual gas pressure in experimental chamber was ~ 10.4 Pa, temperature ~ 15 K. High-purity cadmium sulfide monocrystals used in this work was obtained by a vapor-phase method (Davydov-Markov) [9] with a deviation from stoichiometry toward an excess of cadmium. CdS samples were in the form of 2 mm plates and cut from the block perpendicular to the optical c-axis of the crystal. Cut surfaces were subjected to mechanical polishing. The sample was placed at an angle of 45° to the direction of electron flow. The angle between the excited surface of the crystal and optical axis of the system of registration of radiation was 45°. Luminescence of the sample was projected with a lens onto the entrance slit of the monochromator MDR-23 and recorded using photoelectric multiplier PEM-84 and storage oscilloscope Tektronix TDS 2022. Time resolution of recording route was ~ 15 ns, spectral resolution was ~ 0.01 eV [10].

Experimental results

Figure 1 (curves 1-3) shows typical spectra of pulsed cathode luminescence (PCL) measured at various moments after pulse excitation at 15 K. As shown on the figure, the spectrum of not intentionally doped CdS crystal has a pronounced long-wave series of equidistant emission bands with the maximum of zero-phonon luminescence band at λ = 518 nm. The emission lines of long-wave series shifts toward lower energies (see Fig. 1-2). At the same time there is a change in their form. At the initial moment the half-width of zero-phonon line is 33 meV, in length of time it decreases to 16 meV doesn't change thereafter (Fig. 2). The intensity-temperature dependence of the long-wave series was studied. It is founded that with a rise of temperature edge emission experiences heat quenching (Fig. 3). The figure shows that the edge emission almost completely damped at 50 K.
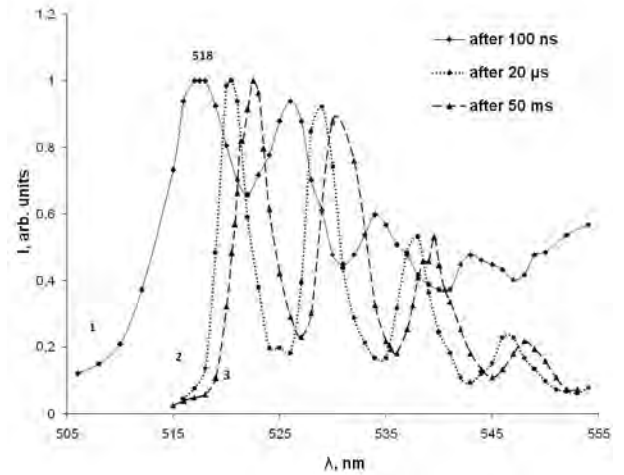
Fig. 1. The fine structure of the spectrum of long-wave series and its change in CdS crystal at 15 K according to the time elapsed after excitation by pulse electron beam.
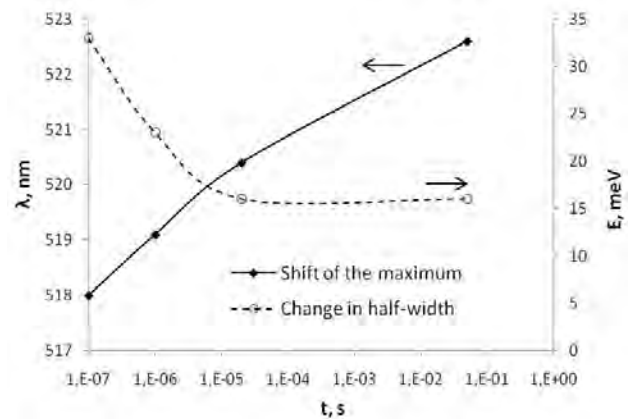
Fig. 2. Variation of half-width of equidistant lines of long-wave series and of zero-phonon line (λ = 518 nm) position in CdS crystal at 15 K according to the time elapsed after excitation by pulsed electron beam.
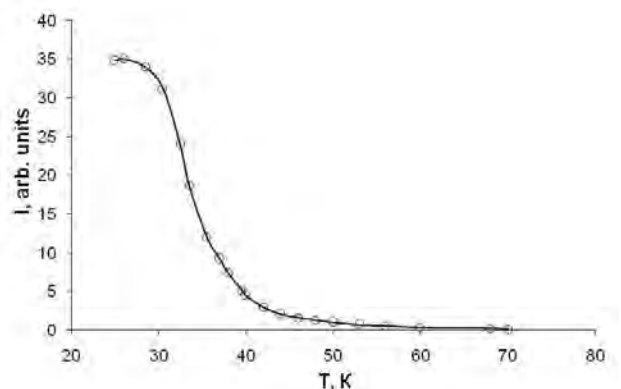
Fig. 3. Heat quenching of edge emission (λ = 518 nm) in not intentionally doped cadmium sulfide in the time of electron excitation.

Discussion

Edge emission was found in zinc selenide by Kroger. In crystals A^2B^6 it is observed in the form of two the most specific series – short-wave (SS) and long-wave (LS) [2, 4]. Both have a structure in the form of equidistant bands of electron-phonon interaction. So far, the mechanism of electron transitions and the nature of defects, which responsible for this emission in A^2B^6 crystals, are discussing [3-8]. Before it, edge emission was associated with interband, exciton and interimpurity transitions in donor-acceptor pairs. At the present time, it is generally accepted representation [3, 5, 8], that LS is dependent on impurity transitions in donor-acceptor pairs (DAP), and SS – transitions from c-zone → acceptors. It is believed that donors are shallow, and acceptors, corresponding to both series, are deep and have a common nature. Results of investigations of spectral-kinetic characteristic of edge emission in CdS monocrystals, obtained in the work, can be explained with donor-acceptor model of luminescence center. Because of the Coulomb attraction oppositely charged donors and acceptors (thay may be impurities and lattice defects) tend to occupy neighboring lattice sites. The wave functions of localized carriers overlap, and give the probability of direct radiative transition of an electron from donor to place of acceptor's hole. The limit distance between donor and acceptor, which is necessary for the tunnel transition of bounded carriers can be estimated as the sum of orbits radia for the localized carriers. Many authors consider DAP with different distances (from 1-3 to 10 lattice parameters and more). Spectral and kinetic properties of DAP with different distances differ essentially. Distance changes the probability of radioactive recombination, effective cross-section capture, activation energy and total number of DAP. These changes lead to change in emission spectrum whilst.

Conclusions

For the first time method of pulsed spectrometry was used to measure spectral and kinetic characteristics of edge emission in cadmium sulfide crystal at a temperature of 15 K in range from 10^{-7} to 10^{-2} s.

The time shift of the spectrum of edge emission was measured. It is shown that the maximum of green band LS shifts from 518 nm to 522.6 nm with time increase after excitation pulse.

It is founded that the half-width of equidistant bands LS reaches 33 meV at the initial moment, and then decreases to 16 meV and gets stable.

The results of research confirm donor-acceptor model of the center, responsible for edge emission in unalloyed CdS crystals, grown by sublimation from gas phase.

Literature

1. Physics of A^2B^6 compounds/ Ed. A.N. Geargobiani, M.K. Sheinkman – M.: Nauka, 1986. – p. 320.

2. V.I Gavrilenko and other. Optical properties of semiconductors. – Kiev: Naukova Dumka, 1987. – p. 607.

3. N.K. Morozova, A.V. Morozov, I.A. Karetnikov, L.D. Nazarova, N.D. Danilevich. Physics and Technics of Semiconductors, **28** (1994) 1699-1713.

4. F.J. Bryant and C.J. Radford. J. Phys. C: Solid St. Phys., **3** (1970) 1264-1274.

5. G.E. Daviduk, N.S. Bogdanuk, A.P. Shavarova. Physics and Technics of Semiconductors, **28** (1994) 2056-2061.

6. I.B. Ermolovich, A.V. Lubchenko, M.K. Sheinkman. Physics and Technics of Semiconductors, **2** (1968) 1639-1643.

7. L.S. Pedrotti. Phys. Rev. **120** (1960) 1664-1669.

8. V.F. Grin, A.V. Lubchenko, E.A. Salkov, M.K. Sheinkman. Physics and Technics of Semiconductors, **9** (1975) 1507-1511.

9. A.A Davydov, E.V. Markov. Izv. USSR. Ser. Neorg. Mater., **11** (1976) 1755-1759.

10. V.M. Lisitsyn, V.I. Korepanov. Spectral measurements with a temporal resolution: a training manual – Tomsk: Izd. TPU, 2007. – p. 94.

SOME PHYSICAL PROPERTIES OF ZN-LI-PHOSPHATE GLASS DOPED WITH RARE EARTH ION

V.M. Lisitsyn, E.F. Polisadova, H. A. Othman

Supervisor: V.M. Lisitsyn, Professor Doctor of physico-mathematical sciences,

Tomsk polytechnic university, 30 Lenin Avenue, Tomsk 634050, Russian Federation

E-mail: elp@tpu.ru

Abstract

P_2O_5-Li_2O-ZnO: xDy_2O_3 glasses were prepared. where x ranging from 0.5 – 5.0 wt % Dy_2O_3 content. The suggested structure of the obtained glass is investigated. IR spectra are discussed the observed peaks assigned to the vibrational modes of the phosphate glass and shows, that the structure of the glasses under study is independent of rare earth ion concentration.

Introduction

Rare earth (RE) -doped glasses are interesting materials for optical devices such as lasers [1], fiber amplifiers [2], ultraviolet (UV) detectors [3] and hole-burning high-density memory [4]. Doping of glasses with europium (Eu), samarium (Sm) or dysprosium (Dy) leads to light emission in the visible range [5], so can be used in many applications. Characterization of the glass and the effect of rare earth doping in the structure of the obtained glass is of significant importance.

Experimental
Glass preparation

P_2O_5-Li_2O-ZnO:xDy_2O_3 glasses were prepared from laboratory reagents grades of Analar phosphorus pentaoxide P_2O_5, lithium Carbonate Li_2CO_3 and Dysprosium oxide Dy_2O_3, using alumina crucible, heated in an electric furnace open to the atmosphere. The weighed quantities of these reagents in appropriate proportions were thoroughly mixed and placed in an electric furnace held at 350°C for one hour. This allows the P_2O_5 to decompose and react with other components before melting would ordinary occur. After this treatment the mixture was placed for one hour in a second furnace held at between 850 – 1050 °C, the highest temperature being applicable to the mixture richest in Dy_2O_3 content. The glass melts were stirred occasionally with an alumina rod to ensure homogenous melts. Each melt was cast into two mild steel split-moulds to from glass disks. After casting, each glass was immediately transferred to an annealing furnace, held at 350°C for one hour. After this time, the furnace was switched off the glasses were allowed to cool (in situ with the furnace door closed) to room temperature, at an initial cooling rate at 3°C per minute.

Infrared spectra

The vibration spectra of various glasses were obtained using KBr pellet technique in the range 400–4000 cm^{-1} on Perkin–Elmer 467 IR spectrometer.

Results
Structure and IR absorption
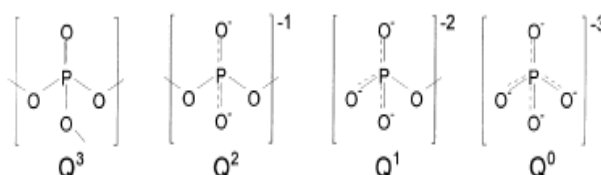
Fig.1. Phosphate tetrahedral sites that can exist in phosphate glasses. After[6].

The basic building blocks of crystalline and amorphous phosphates are the P-tetrahedra that result from the formation of sp^3 hybrid orbitals by the P outer electrons ($3s^23p^3$). The fifth electron is promoted to a 3d orbital where strong π-bonding molecular orbitals are formed with oxygen 2p electrons [7]. These tetrahedra link through covalent bridging oxygens to form various phosphate anions. The tetrahedra are classified using the Q^i terminology [8], where 'i' represents the number of bridging oxygens per tetrahedron. The networks of phosphate glasses also can be classified by the oxygen to phosphorus ratio, which sets the number of tetrahedral linkages, through bridging oxygens, between neighboring P-tetrahedra. With the nominal composition of the studied glass ([O]/[P])=3 which is a meta-phosphate glass. Meta-phosphate glasses have structures that are based on phosphate anions. The average chain-length (n_{av}) of an anion in a polyphosphate glass is given by Van Wazer [9]

$$n_{av} = 2(1-x) / (2x-1). \qquad (1)$$

Note that when x = 0.5 (the meta-phosphate stoichiometry), n is∞. This conclusion assumes that there are no cyclic anions, the presence of which will reduce the average chain length.

For a polyphosphate glass, the average chain length n_{av} can also be computed directly from the glass composition [10] by equating the charge on the metal cations with the charge on the phosphate chains. For the purpose of computing

the total charge contributed by the anions, the glass is envisioned to have only chains of length n_{av}. The total number of phosphate chains is [P]/n_{av} where [P] is the molar concentration of phosphorus in the glass. The charge contributed by these chains is simply the number of chains times their charge or [P](n_{av} + 2)/n_{av}. The total charge contributed by the metal cations is

$$\sum_i [M_i] q_i$$

where [M_i] is the molar concentration of metal i, and q_i is the charge on the metal cation of type i. Equating the charge from the anions and cations gives

$$n_{av} = \frac{2}{\sum_i [M_i] q_i / [P_i] - 1} \quad (2)$$

Using the above equation gives average chain length for the nominal composition of 5 phosphate anions.
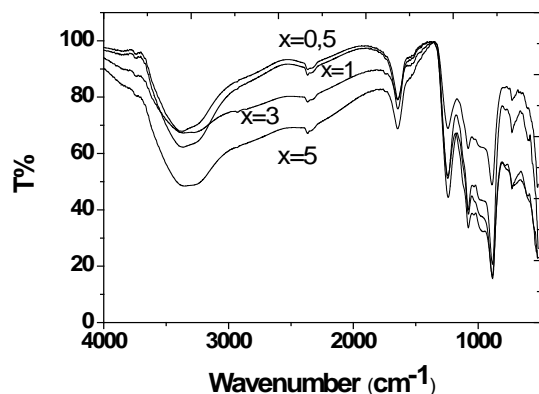
Fig.2. IR transmission of the Li_2O-ZnO:xDy_2O_3 (x=0.5, 1.0, 3 and 5 wt%).

The infrared spectra of these glasses show eight to nine absorption peaks. The peaks are sharp, medium and broad. The broad bands are exhibited in the oxide spectra, most probably due to the combination of high degeneracy of vibrational states, thermal broadening of the lattice dispersion band and mechanical scattering from powder samples.

The position of the absorption bands in both crystalline and glassy phosphates occur between 500 and 1270 cm^{-1}. The majority of the phosphates exhibit a number of strong absorption bands in this region. It has been concluded that these bands are due to the vibration of a PO_4^{3-} tetrahedron. But this mode is triply degenerate However, in the crystalline and glassy state one could expect that interaction between any (PO_4^{3-}) ion and neighboring atoms and ions could remove the degeneracy and cause three bands to appear. The observed strong absorption peak centered at about 1078 cm^{-1} is expected for the symmetric PO_2 stretching on Q^2 tetrahedra. It

was assumed by Higazy and Bridg[11] that when ZnO contents less than 50 mol.% the Zn atoms reside entirely in network forming positions, whilst for oxide contents exceeding 50 mol.%, Zn atoms also start to enter interstitial positions. So we could assume that the structure of the present glass consists of (PO_4)$^{-3}$ groups connected via Zn atoms, while the rare earth ions reside in interstitial positions. With changing the concentration of the rare earth dopant, very small change in the absorption bands may occur that do not account for major structural changes.

Conclusion

It is concluded that the structure of the studied Zn-Li phosphate glass consists of randomly connected (PO_4)$^{-3}$ groups, belongs to the meta-phosphate structure, based mainly on Q^2 anions. The addition of the ZnO to the glass composition increases the rigidity, and decreases the hydroscopicity of the glass, by re-polymerization and connection of the (PO_4)$^{-3}$ groups .And the structure of present glass system is independent of rare earth content.

References

1   R.J. Mears, L. Reekie, S.B. Poole, D.N. Payne Neodymium-doped silica single-mode fiber lasers// Electron. Lett. 21 (17) (1985) 738.

2   R.J. Mears, L. Reekie, I.M. Jauncey, D.N. Payne Low-noise erbium-doped fiber amplifier operating at 1.54 μm // Electron. Lett. 1026 (1987) 23.

3   M. Schem, M. Bredol, The use of glassfibers coated with terbium doped sol–gel films in UV sensors // Opt. Mater. 26 (2004) 137.

4   R.S. Meltzer, W.M. Yen, H. Zheng, S.P. Feofilov, M.J. Dejneka, B.M. Tissue, H.B. Yuan, Evidence for long- range interactions between rare-earth impurity ions in nanocrystals embedded in amorphous matrices with the two-level systems of the matrix // Phys. Rev. B 64 (2001) 100201.

5   G. Blasse, B. Grabmaier Luminescent Materials, Springer, Berlin, 1994.

6   R.K. Brow / Journal of Non-Crystalline Solids 263&264 (2000) 1-28

7   D.W.J. Cruickshank, /J. Chem. Soc. (1961) 5486.

8   F. Liebau, in: M. O'Keefe, A. Novrotsky, //Structure. and Bonding in Crystals II. Academic Press, New York, 1981, p. 197.

9   J.R. Van Wazer, /Phosphorus and its Compounds, vol. 1, Interscience, New York, 1958

10   B.C. Sales et al. / Journal of Non-Crystalline Solids 226 (1998) 287-293.

11   A.A. Higazy, and B. Bridge / J. Material science, 20.No. 7(1985).

THE FLUORINE-BASED PURIFICATION OF SILICON DIOXIDE

Pakhomov D.S., Sobolev V. I,

Advisor: Kraydenko R.I.,Manuylova E.V.

Tomsk Polytechnic University , 634050, Russia, Tomsk, 30 Lenin Avenue

E-mail: tornadoo@sibmail.com

Introduction

Nowadays, the most quickly-developing branch of industry is electronics and energetics. The development of solar energy is closely related with the search for renewable and clean energy sources. Electronics based on semiconductors microchips is one of the most knowledge intensive and highly developed sectors of worldwide economics. The main trouble of silicon-based technologies is high cost of end product purification. Searches for alternative semi-conductors materials are connected with multistage and energy consumption of silicon technology. The reserves of mineral raw materials for production of silicon are practically inexhaustible, so while lowering production costs the development of this branch of industry will occur [1].

The basic method of obtaining silicon is reducing it from its oxide by carbon. This technique is used for obtaining technical silicon for metallurgy.

Mono-, micro-, multi-, polycrystalline and amorphous silicon is used for electronics and energetics because of its semiconductor properties. Quality of semiconductors is defined by the content of metal impurities in the sample. In obtaining of the high-quality end product, technical silicon is additionally purified in gaseous phase and reduced [2].

This paper studies analytical reviews of methods to replace and reduce the number of stages in obtaining final silicon production.

Enrichment and concentration of quartz material allows to organize the production of cheap solar silicon. It is necessary to use chemical methods to obtain cleaner silicon [3].

Chemical methods of purification of silicon and its compounds are widely spread and numerous, whereas silicon is used as a "white soot" (SiO_2) and other important reagents. Modern technologies of production of SiO_2 are outdated, and have the following disadvantages:

– multistage of technological cycle;

– using of liquid inorganic acids and large amount of sewages;

– using of high-temperature modes (1000–1100 °C), requires a lot of energy and special construction materials;

– concentrated acids and toxic gases are very harmful for the environment;

– high cost of end product [4].

Therefore, the existing technology of SiO_2 obtaining is ineffective and dangerous for environment.

The main lack of classical method of SiO_2 purification is – is low purity of the product. So, obtaining of high-quality SiO_2 is a very expensive process , therefore it is very hard to use SiO_2 as a raw material to obtain Si.

The Fluorine-based purification of silicon dioxide

Researches of new, safe and wasteless method of obtaining highly-purified SiO_2 are held in the Tomsk Polytechnic University. It is based on fluoride technology.

Ammonium fluoride is selected as a fluorinating agent, it is a waste of aluminum and plastics processing.

Ammonium fluoride under normal conditions is non-aggressive, solid, crystalline substance. The molten ammonium fluoride – is more effective fluorinating agent, than gaseous hydrogen fluoride.

The advantage of ammonium fluoride is a vigorous interaction of its molten form with a silicon oxide, the result of this interaction are silicon-based compound of NH_4F , for example – $(NH_4)_2SiF_6$, which at normal conditions is a powder, non-aggressive and high-soluble in water. When heated $(NH_4)_2SiF_6$ sublimes without decomposition, while cooling it desublimes – this property is used for purification of quartz concentrate [5].

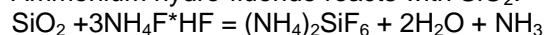### Description of technological operations of high-purity SiO_2 obtaining with ammonium fluoride:

NH_4F or NH_4F*HF is added to the original quartz concentrate, than this mix is heated.

Ammonium fluoride reacts with SiO_2 in the reaction:

$SiO_2 + 6NH_4F = (NH_4)_2SiF_6 + 2H_2O + 4NH_3$
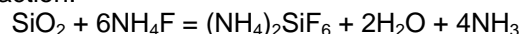
Ammonium hydro-fluoride reacts with SiO_2:

$SiO_2 +3NH_4F*HF = (NH_4)_2SiF_6 + 2H_2O + NH_3$

$(NH_4)_2SiF_6$ is obtained during the reaction passes in gaseous phase when heated. The gaseous $(NH_4)_2SiF_6$ is desublimated, treated with ammonia water with accompanying regeneration of the fluorinating agent. Following reaction describes the process:

$(NH_4)_2SiF_6 + 4NH_4OH = SiO_2 + 6NH_4F + 2H_2O$ [6].
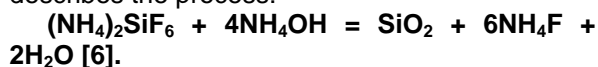
Then the sediment of hydrated silicon dioxide is separated from solution of ammonium fluoride by the filtration. The solution of ammonium fluoride is boiled down and crystallized as a

technical ammonium fluoride with the following composition - 25% NH_4F, 75% NH_4F*HF. As a result of drying and calcinating the precipitate the silicon dioxide obtained in finely separated form [7].

$$SiO_2 + 3NH_4F*HF = (NH_4)_2SiF_6 + 2H_2O + NH_3$$

$$(NH_4)_2SiF_6 + 4NH_4OH = SiO_2 + 6NH_4F + 2H_2O$$
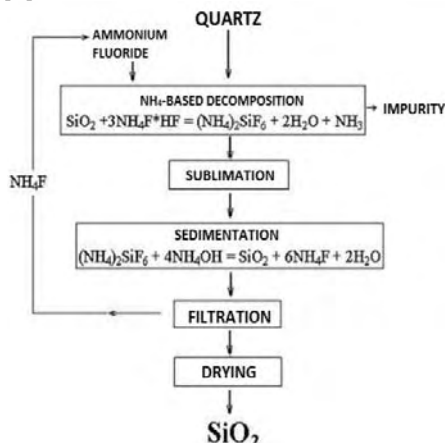
(Figure1. Schematic diagram of the SiO_2 purification)

The regenerated ammonia water (NH_4OH) which is obtained by interaction of original SiO_2 (quartz sand) with the NH_4F is used at the stage of sedimentation of hydrated silicon dioxide. So, the developed NH_4F-based technology of SiO_2 obtaining is almost waste-free, since it uses reagents regenerated during the technological cycle [8].

The modes of obtaining ultrafine powder with silicon dioxide content 99.999% were tested in this research. It should be noted that the described method uses low-temperature processes and it is characterized by almost complete (95%) regeneration of fluorinating agent [9].

Thus, fluoride processing of quartz material allows obtaining of low-cost silicon dioxide with a purity of 99,995-99,999% that allows obtaining silicon purity of at least 99.99% (using a high-quality low-sol carbon) by direct reduction.
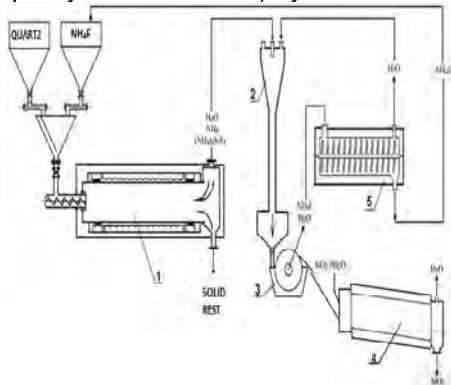
(Figure2. Apparatus scheme of NH_4F-based purification of silicon dioxide:

1) drum-rotary furnace; 2) absorber; 3) filter; 4) calcinations furnace; 5) crystallizer)

Conclusion

Within the framework of this research the review of various methods of SiO_2 obtaining was made.

Instead of using silane and chlorine-silane methods of technical silicon purification it was proposed to use NH_4F-based technique to obtain high-purified SiO_2, because deep cleaning of substances using traditional methods may be done only through the selective gas transport reaction. Refining of raw quartz materials to highly-purified end-product is a highly profitable process. It is a low-temperature process (no more than 370 °C).

Some ecological criteria: purification technology of silicon uses chemically aggressive and toxic gases (chlorine, hydrogen chloride, etc.). In fluoride purification of the SiO_2 ammonium fluoride is used, which at room temperature is crystalline solid that is safe for the environment.

In addition to environmental safety and low energy consumption, economic efficiency, the technology developed for ultra-pure silicon dioxide, primarily associated with a fairly simple and complete regeneration of the fluorinating agent.

References

1. http://www.pcmp.ru/catalogue/show_product/1
2. http://www.sibghk.ru.
3. Фалькевич Э.С., Пульнер Э.О., Червоный И.Ф. и др. Технология полупроводникового кремния – М.: Металлургия, 1992, 408 с., С. 137–146.
4. Ивановский В. И.. Технический углерод. Процессы и аппараты: Учебное пособие. – Омск: ОАО «Техуглерод», 2004.
5. http://ftortechnology.ru/f891.html
6. http://bkk-rgk.ru/product/44373
7. Мельниченко Е.И. Фторидная переработка редкометальных руд Дальнего Востока. Владивосток:Дальнаука, 2002, 268с.
8. Раков Э.Г. Химия и технология неорганических фторидов. – М.: Изд-во МХТИ им. Д.И. Менделеева, 1990. – 162 с.
9. Рысс И.Г. Химия фтора и его неорганических соединений. – М.: Госхимиздат, 1956. – 625 с.

INCREASING WEAR RESISTANCE OF UHMWPE BY ADDING NANOFILLERS AND ION IMPLANTATION

[1]T. Poowadin, [1,2]S.V. Panin, [2]V.P. Sergeev, [2]L.R. Ivanova, [2,3]L.A. Kornienko, [2]A. Sungatulin

[1]Tomsk Polytechnic University, Mechanical Engineering Faculty

[2]Institute of Strength Physics and Materials Sciences SB RAS, svp@ispms.tsc.ru

[3]Russian Materials Science Center, Tomsk, Russia

Abstract

Ultra high molecular weight polyethylene (UHMWPE) composites, filled with 0.5wt% of carbon nanofibers (CNF) and surface modified by aluminum boride (AlB_x) ion implantation, were investigated under dry wearing at "block-on-ring" tests. It was revealed that decreasing of wear rate at the steady stage up to 3 times might be achieved at adding CNF. In case of surface modification, the ion doses were varied from $0.5*10^{17}$ cm^{-2} up to $2*10^{17}$ cm^{-2}. Implantation of the of UHMWPE specimens with dose of $1*10^{17}$ cm^{-2} also ensures pronounced decrease of wear intensity with decreasing of wear rate by approximately 3 times (like at adding CNF).

Keywords: UHMWPE; ion implantation; wear resistance; carbon nanofibers

Introduction

UHMWPE is a subset of the thermoplastic polyethylene. It is a promising polymeric material which may be used to replace metals in tribotechnical applications such as gears, bearings, and seals. It is also widely used in orthopedic surgery for joints replacement in orthopedic application due to its good processability, very low friction coefficient, high impact resistance, high resistant to abrasion (15 times more resistant to abrasion than carbon steel), very low wear, chemical resistance and biocompatibility. It is odorless, tasteless, and nontoxic [1]

However, even though UHMWPE has very low wear compared to other polymers wear is still a major problem in tribotechnical applications. A lot of attention recently has been paid to increasing the strength and wear resistance of composite polymeric materials. Traditionally, strength and wear resistance of polyolefines are increased by the adding of micron size reinforcement particles obtained from inorganic material. Recently, intensive investigations have been carried out to explore the possibility to add nano-sized fillers due to theirs redundant surface energy (they have very high surface energy). The small size of the filler particles can provide a very fine and uniform structure in the UHMWPE specimens [2].

Furthermore, ion implantation is one of the most effective techniques to increase wear resistance of UHMWPE due to its low-temperature processing which make the treatment suitable for low melting materials such as polymers. Besides ion implantation technique seems to be good candidate to modify the surface of polymeric materials. AlB_x ion implantation was employed to improve surface of UHMWPE+CNF specimens with the irradiation dose up to $2*10^{17}$ cm^{-2}, in order to estimate the effect of the ion dose variation onto wear resistance and surface hardness of the modified specimens [3].

Experimental

Materials and specimens preparation

UHMWPE powder with particle size of 50-70 μm (GUR by Ticona, Germany) was used for the specimen preparation. The molecular weight of the UHMWPE powder used makes $2.6×10^6$ g/mol. CNF in the form of multiwall nanotubes with external diameter of 50-60 nm, internal diameter of 10-20 nm and length of 2-3 μm, were blended at volume fraction of 0.5 wt.% using high speed homogenizer in liquid form and then dried at temperature of 80ºC for 3-4 hours. UHMWPE powder was used to prepare test piece specimens by using a compression machine and subsequently, a hot-pressing mould. The compression pressure was 10 MPa and the temperature was maintained at 190ºC for 120 minutes. Specimens were cooled in the mould at a cooling rate of 3-4ºC/min. The specimens have shape of the rectangular prism 45 mm long, 50 mm wide and 5 ÷ 8 mm high. In case of Ion implantation, UHMWPE+CNF specimens were performed by the AlB_x ion implantation under the 60 kV accelerating voltage in vacuum chamber with residual pressure $1*10^{-3}$ Pa by the "DIANA" vacuum-arc impulse ion source at the 50 Hz frequency of current pulses, 250 μs of its duration, while the ion doses varied from $0.5*10^{17}$ cm^{-2} up to $2*10^{17}$ cm^{-2}, the treatment temperature was controlled at the rate of below 70ºC.

Wear and Friction tests

Wear tests were performed using the "SMT-1" friction machine. Tests were run without lubrication according to ASTM G77. Specimen shape was in the form of a rectangular prism 7 mm long, 7 mm wide and 10 mm high, the roller diameter was 62 mm, the revolution rate was 100 rpm, and the applied loading was set to P=160 N, scheme shown in Fig 1. Images of wear track were investigated by shooting micrographs using an optical microscope "Carl Zeiss Stemi 2000–C" and measuring track area with the help of software Rhinoceros, v.3.

Friction coefficient was measured using a pin-on-disk tribometer according to ASTM G99 and DIN 50324, with a fixed steel ball of 3 mm diameter positioned at the indenter tip.
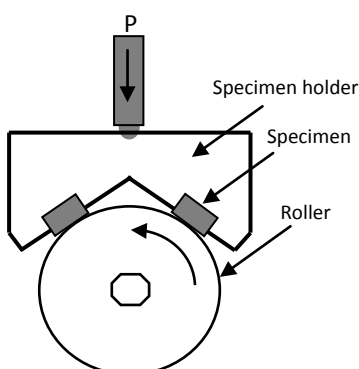
Figure 1. Schematic for block-on-ring wear test

Results and Discussion
Wear resistance property

The wear resistance of UHMWPE specimens is increased when CNF is added to UHMWPE. At the wearing stage the wear resistance of the latter may be estimated as 3 times higher in comparison with UHMWPE specimens without the filler.

In case of surface modification, wear resistance of UHMWPE+CNF specimens is increased after implantation. Wear rate at the wearing stage for implanted specimens is lowest 5.714E-6 mm^2/Nm at ion dose of $1*10^{17}$ cm^{-2} which lower than ones of specimens with the ion dose of $0.5*10^{17}$ cm^{-2} and $2*10^{17}$ cm^{-2} respectively. In term of comparison with UHMWPE specimens, wear resistance of implanted UHMWPE+CNF specimen at ion dose of $1*10^{17}$ cm^{-2} may be estimated as 3 times higher as well as of filled UHMWPE specimen with 0.5 wt% CNF
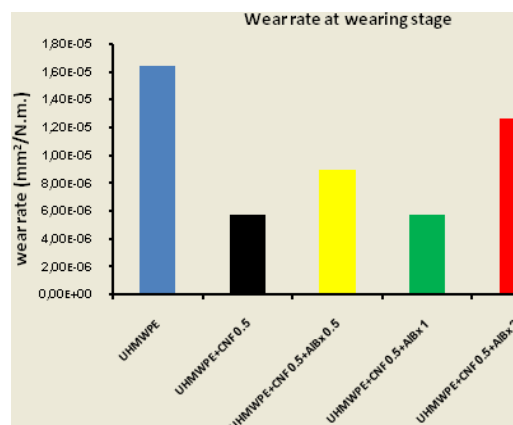
Figure 2. Wear rate of UHMWPE+CNF specimens with different dose of AlB$_x$ ion implantation

Physical and tribological properties

The experiments performed have shown that the adding of the CNF and surface modification by AlB$_x$ ion implantation exerts substantial influences onto physical properties of UHMWPE (see Table 1). It is seen that CNF and the AlB$_x$ ion implantation can significantly increase the surface hardness of the specimens. Shore hardness also increases gradually at increasing of the implantation dose. The highest values of Shore hardness are reached at ion dose of $2*10^{17}$ cm^{-2}. Friction coefficient at initial state UHMWPE is equal to 0.143, and UHMWPE+CNF is equal to 0.153, then it increases to 0.421, 0.281, and 0.304 respectively when the implantation dose increases.

Table 1   Physical and tribological properties

Specimens	Ion dose	Hardness	Friction coefficient
	(x 10^{17} cm^{-2})	(shore A)	(□)
UHMWPE	0	97.94	0.143
UHMWPE+CNF	0	98.13	0.153
UHMWPE+CNF+AlBx0.5	0.5	98.22	0.421
UHMWPE+CNF+AlBx1	1	98.35	0.281
UHMWPE+CNF+AlBx2	2	98.51	0.304

Conclusion

Addition of 0.5 wt% CNF into UHMWPE gives rise to improving physical and tribotechnical properties of UHMWPE. This is in line with literature data on the influence of carbon nanotubes onto tribotechnical behaviour of UHMWPE [4]. Similar to our results they had obtained increase of wear resistance up to 3 times. AlBx ion implantation allows to reduce the wear intensity at the wearing stage. Specifically, the ion dose of $1*10^{17}$ cm^{-2} provides substantial decrease of wear intensity like at adding of 0.5 wt% CNF when the wear rate at wearing stage was decreased by 3 times.

Reference

[1] Kurtz S.M. *The UHMWPE handbook.* Elsevier: California, USA; 2004.

[2] Wannasri S., Panin S.V., Ivanona L.R., Komeinko L.A., Piriyayon S. *Increasing wear resistance of UHMWPE by mechanical activation and chemical modification combined with addition of nanofiber.* Mesomechanics 2009, Oxford, England. 2009.

[3] Poowadin T., Panin S.V., Sergeev V.P., Ivanova L.R., Kornienko L.A. *Modification of UHMWPE by Mechanical Activation and AlBx Ion Implantation.* IFOST 2009, p.47-51.

[4] Zoo Y.S., An J.W., Lim D.P., Lim D.S. *Effect of carbon nanotube addition on tribological behavior of UHMWPE.* Tribology letter vol. 16 no. 4 2004. p. 305-309.

A STUDY ON WEAR RESISTANCE OF ULTRA-HIGH MOLECULAR WEIGHT POLYETHYLENE (UHMWPE) MIXED WITH GRAFTING UHMWPE AND NANOFILLERS.

[1] SOMPONG PIRIYAYON, [1,2] S. V. PANIN, [2] L. R. IVANOVA, [2,3] L .A. KORNIENKO

[1] Tomsk Polytechnic University, Mechanical Engineering Faculty

[2] Institute of Strength Physics and Materials Sciences SB RAS, svp@ispms.tsc.ru

[3] Russian Materials Science Center, Tomsk, Russia

Abstract

UHMWPE (Ultra High Molecular Weight Polyethylene) is one of the high resistance materials but hardly bonding with any substances. One of perspective ways to bond UHMW-PE with filler is its grafting. There is one more interesting approach, when graft UHMWPE is added to UHMW-PE in order to react both with latter and nanofiller. In this paper we attempted to increase the mixture ability of UHMW-graft-SMA for enhancing its wear resistance properties.

We employed UHMWPE powder chemically modified with Styrene Maleic Anhydride. This material denoted UHMWPE-g-Silane. Copolymer and its mixtures with UHMW-PE. Mixture was UHMWPE-g-Silane 3, 5, 10 and 20 wt%. Add 0.5% CNF (Carbon Nano Fiber) and 0.5% Al_2O_3 (nanosize) to the mixture. Specimens were tested by the "Block-on-Roller" technique for the wear resistance.

The results of the wear resistance show that wear resistance of UHMWPEg 10 with 0.5% Al_2O_3 is the highest. The second is UHMWPEg 3 with 0.5% CNF However, in contrast with this result, wear resistances is increased when amount of UHMWPE-g-Silane in the mixture is enlarged.

Key words: UHMWPE-g-Silane, CNF, wear resistance, Al_2O_3.

INTRODUCTION

UHMWPE comes from a family of polymers with a deceptively simple chemical composition, consisting of only hydrogen and carbon. However, the simplicity inherent in its chemical composition belies a more complex hierarchy of organizational structures at the molecular and super molecular length scales. At a molecular level, the carbon backbone of polyethylene can twist, rotate, and fold into ordered crystalline regions. At a supermolecular level, the UHMWPE consists of powder (also known as resin or flake) that must be consolidated at elevated temperatures and pressures to form a bulk material. Further layers of complexity are introduced by chemical changes that arise in UHMWPE due to radiation sterilization and processing.

EXPERIMENTAL

Materials

The UHMWPE-g-silane was supplied by OLENTA group company, Moscow, Russia. UHMWPE-g silane (product code OLENTEN® UHMWPE-g-SMA). UHMWPE was purchased from Ticona Corp., The molecular weight of UHMWPE powder used is 2.6x10^6 **g**/mol

Preparation of UHMWPE-g-silane-mix-UHMWPE

The graft copolymer (UHMWPE-g-silane) and UHMWPE were melt mixed in the mold of hot pressing at the temperature of 190°C, compression pressure 10 MPa. Holding time 120 minute, obtain a plate of 8 mm thickness. The content of UHMWPE -g-silane was set as 0, 3, 5, 10 and 20 wt% to give five materials denoted UHMWPEg 0, UHMWPEg 3, UHMWPEg 5, UHMWPEg 10 and UHMWPEg 20.

Characterization

Wear resistance was tested by machine "SMT-1" run without lubrication according to the "block-

on-roller" according to ASTM G77 Specimen size $8\times8\times10$ mm^3, the roller diameter is 62 mm, revolution rate is 100 rpm, and loading is 160 N. The images of friction track were investigated by shooting photographs between loadings by optical microscope "Carl Zeiss Stemi 2000–C" and measuring friction track area by software "Rhinoceros version 3" testing picture was showed in figure 1 and wear track was showed in figure 2.
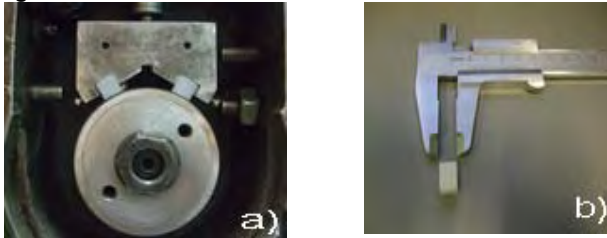

Fig. 1. Block on Roller test a) two specimen during testing with "SMT-1" b) size of specimen for testing.

Figure 2. Wear track from wear resistance testing a) 10 min. b) 60 min. c) 120 min. d) 180 min.

The picture from optical was shown in Fig.2. When the period of time in the Block on Roller test is increase. The area of wear track of mixtures go up. However the area of wear track of UHMWPE g 5 during time 50-180 minute is quite similar. Figure show about 4 time of test are 10, 60, 120 and 180 minute.

RESULTS AND DISSUSSION
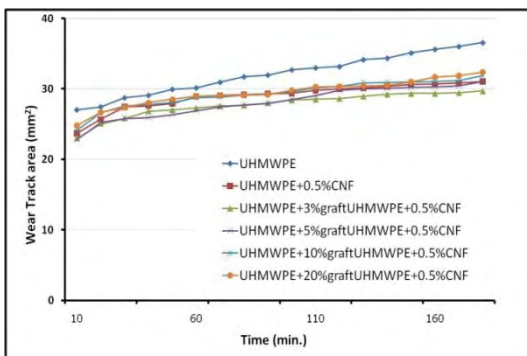
Figure 3. Wear resistance of UHMWPE / UHMWPEg / CNF mixture
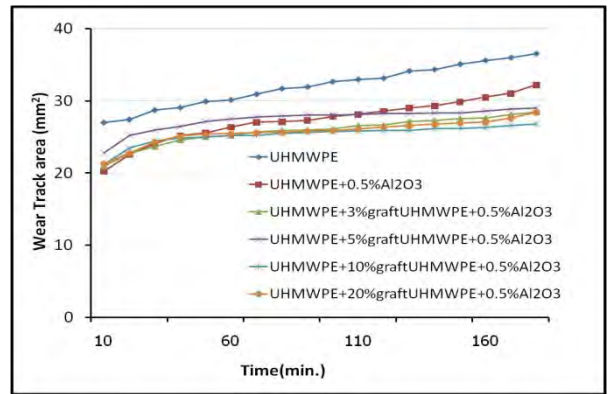
Figure 4. Wear resistance of UHMWPE / UHMWPEg / Al$_2$O$_3$ mixture

UHMWPEg / nanofiller / UHMWPE mixture is formed by hot pressing molding and gets crosslink during process. The wear resistance of mixture decrease when mix UHMWPEg and nanofiller with UHMWPE. UHMWPEg with 0.5%CNF and UHMWPEg with 0.5%Al$_2$O$_3$ get tendency regularly but lower than pure UHMWPE. UHMWPEg 3 with 0.5%CNF gets wear rate up quickly on first stage from 10 minute till 40 minute and increase slowly after second stage from 40 minute till 180 minute. Detail was show at figure 3. UHMWPEg 10 with 0.5%Al$_2$O$_3$ gets wear rate up quickly on first stage from 10 minute till 50 minute and increase slowly after second stage from 50 minute till 180 minute. Detail was show at figure 4.

CONCLUSIONS

Wear resistance of UHMWPEg 10 with 0.5% Al$_2$O$_3$ is the best. The second is UHMWPEg 3 with 0.5% CNF However, in contrast with this result, wear resistances is increased when mix the UHMWPE-g-Silane and nanofiller in the mixture.

ACKNOWLEDEMENT

REFERENCES

1. Steven M. Kurt, The UHMW-PE handbook, Elsevier 2004, p 109.

2. Oklopkova A.A., Popov S.N., Sleptzova S.A., Petrova P.N., Avvakumov E.G. Polymer nanocomposites for tribotechnical applications. Structural chemistry, 45 (supplement), S169-S173: 2004.

EFFECT OF GEOMETRY OF COATING - SUBSTRATE INTERFACE PROFILE ON DEFORMATION AND STRESS FIELDS OF THERMAL BARRIER COATINGS

S.A. Yussif[1], V.E. Panin[1,2], S.V. Panin[1,2],

Scientific supervisor: V.E. Panin, Academician of RAS, professor

[1]Tomsk Polytechnic University, Tomsk, Russia

[2]Institute of Strength Physics and Material Science, Siberian Branch, Tomsk, Russia

E-mail: salah.aleasha@hotmail.com

Abstract Varying geometry of coating – substrate profile influences stress and strain intensities which are responsible for delamination of thermal barrier coatings. In addition to flat coating – substrate interface which is commonly used in TBC, this paper introduces another profile that is saw – toothed interface. Finite element method is used to solve thermo – elasto - plastic equations. Simulation results proves that saw – shaped interface disperses stress and strain intensities in multi regions which causes multi – fragments fractures instead of bulk fracture which occurs in case of flat coating substrate interface.

I. INTRODUCTION

Thermal barrier coatings are used to protect hot sections of gas turbines and jet engines such as blades, burners, transition ducts and nozzles [1], Fig. 1.
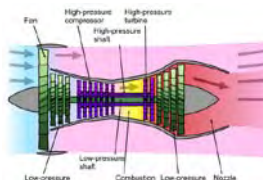
Figure 1. The major components of a jet engine where TBCs are used.
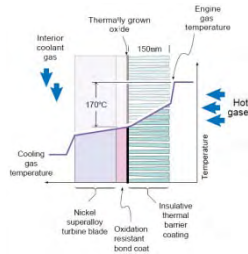
Figure 2. Main components of TBC system.

Figure 2 illustrates main components of TBC. The two main parts of TBC are substrate layer that is the hot section which is to be protected (turbine blade, nozzle … etc.) and coating layer that is thermally insulating layer which protects substrates from high thermal stresses and corrosions.

Flaking off of coating from substrate is considered as one of the major problems of TBC system that should be solved. Experimental data shows that under thermocycling of Si-Al-N coating (dark regions) is delaminated in a chessboard-like pattern [2], Fig. 3.a. When the numbers of thermal cycles are increased up to 55, Fig. 3.b, the copper substrate (bright regions) appears on the surface and pushes the coating layer away from the system. Since the copper substrate appears on the surface in a chessboard–like pattern [3], therefore the topology at coating – substrate interface is changed as well. Consequently, this topological change at the coating – substrate interface will influence the thermal strain and stress distributions at the interface and within coating layer. This paper is devoted to investigating the effect of varying the profile of coating – substrate interface on the developed thermal strain and stress fields. The finite element method is used to solve the thermo-elasto-plastic equations [4,5,6].
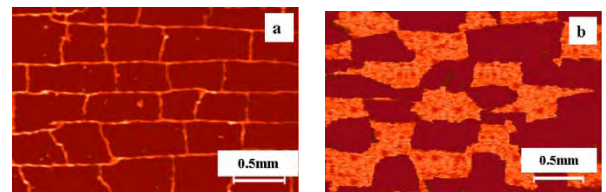

Figure 3. Thermocycling of Si-Al-N coating (dark regions) on a copper substrate (bright regions). Surface layer of substrate was nanostructured by a beam of Cu+ ions before deposition of coating: a – after 34 cycles of thermocycling, b – after 55 cycles

II. METHODOLOGY AND MODEL DESCRIPTION

In order to investigate the effects of varying the shape of coating – substrate interface on strain and stress fields, a two – layer two – dimensional model is used, fig. 4. The model consists of two layers: copper substrate and ceramic coating. Two profiles of coating – substrate interface are used: flat and saw-toothed The dimensions of substrate layer are kept fixed at $120\mu m \times 120 \mu m$, coating thickness is varied from $10 \mu m$ to $70 \mu m$. The top surface of ceramic coating and the bottom surface of copper substrate are assumed to be isothermal surfaces. The first is kept at $1000^{o}C$ and the second at $0^{o}C$. The left and right edges are assumed to be adiabatic surfaces in order to prevent heat leakage to the surroundings from the side edges of the model. Symmetric boundary condition is imposed on the left edge of the model and the right edge is left free. No constrains are applied to the top coating surface. Substrate bottom

surface is constrained to move in vertical direction in order to obtain stable elasto-plastic system. The model is meshed by linear three nodes triangular elements and mechanical and thermal properties of substrate and coating materials are assumed to be temperature – independent functions. Heat transfer problem is solved first to calculate the temperature field of the system. The second step is to use this temperature filed as body loads to system in order to calculate deformations, strains and stresses.
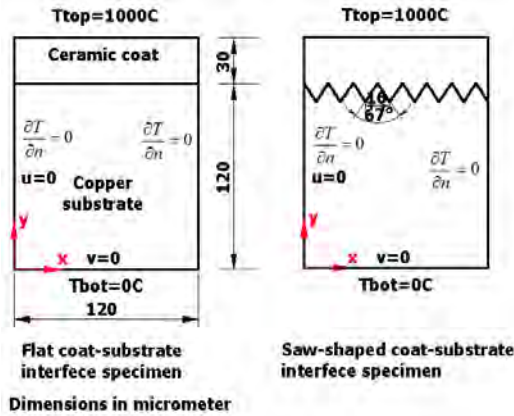
Figure 4 Two - dimensional two-layers TBC model with flat and sinusoidal profile of coating-substrate interface.

III RESULTS, DISCUSION AND CONCLUSION

Temperature, elastic strain intensity, plastic strain intensity and stress intensity fields for $30 \mu m$ in case of flat and saw – toothed profiles of ceramic coating interface were calculated. The average values of elastic, plastic and stress intensity fields are compared while varying coating thickness from $10 \mu m$ to $70 \mu m$, figures 5, 6 and 7.

It is shown that the idea of non – flat interface is to localize stress and strain intensities at coating –substrate interface and therefore the corresponding fracture pattern is fragmental. Saw – shaped profile of the interface realizes this idea. Moreover when stress and strain intensities are average over the interface, saw profile gives minimum average of stress intensity.
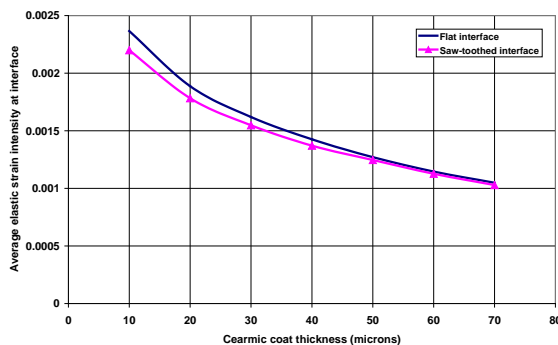
Figure 5. Comparison between average

elastic strain intensity at coating-substrate interface in case of flat and saw –toothed profiles
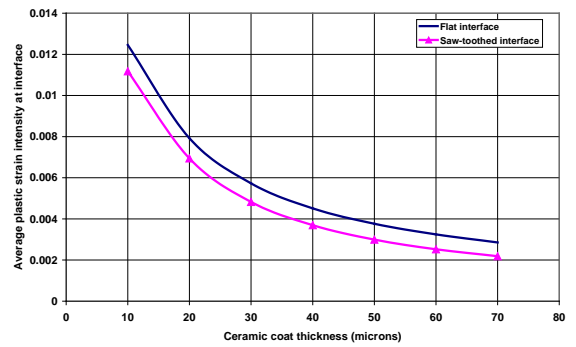
Figure 6. Comparison between average plastic strain intensity at coating-substrate interface in case of flat and saw –toothed profiles
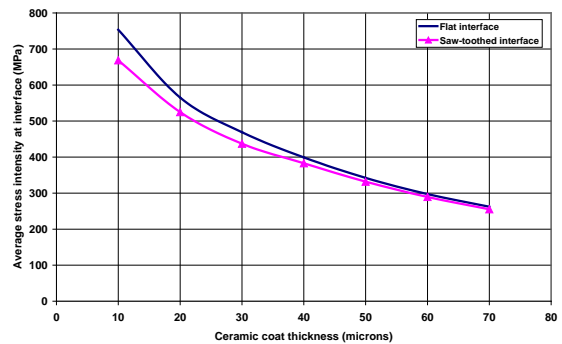
Figure 7. Comparison between average stress intensity at coating-substrate interface in case of flat and saw –toothed profiles

IV. REFRENCES

1. V.E. Panin, et al, Surface layers and interfaces in heterogeneous materials, Russian academy of Sciences, Siberian Branch, ISPMS SB RAS. Novosibirsk, SB RAS Publishing House, 2006, 520 p.

2. V.E. Panin, V.P.Sergeev, A.V.Panin, Yu.I.Pochivalov. Nanostructuring of surface layers and deposition of nanostructured coatings – effective approach for strengthening modern structural and tool materials. FMM, 2007, Vol. 104, Is. 6.

3. V.E. Panin, A.V. Panin, D.D. Moiseenko, Physical mesomechanics of a deformed solid as multilevel as a multilevel system. II. Chessboard – like mesoeffect of the interface in heterogeneous media in external fields, Phys. Mesomech., 10, No. 1 – 2 (2007)5.

4. Eschenauer H., N.Olhoff, W.Schnell. Applied structural mechanics, Springer,1996.

5. Oden. Finite element method in nonlinear mechanics of continuum media, Mir, 1976.

6. Segerlind L.S. Applied Finite Element Analysis, Moscow: Mir, 1979.

DIRECTIONALLY CRYSTALLIZED COMPOSITE OF B_4C-CRB_2 FOR CUTTING TOOLS

E. Zagorodnia, I. Bogomol

Research manager: I. Bogomol, Assistant Professor, teacher

National Technical University of Ukraine "Kyiv Politechnical Institute", Physical Engineering Faculty,

Peremogy Avenue, 37, Kyiv, 03056, Ukraine

E-mail: elina_zv@ukr.net

Refractory compounds, which are based on the light components stated value of running ability: a high chemical durability, small density, high strength, and are the base for creation of ceramic materials of different function.

Great interest present ceramics as a high speed cutting tool material is based primarily on favorable material properties. The cutting tool is considered as an important factor on which the quality and productivity of the cutting manufacturing process depend on. The efficiency of the cutting tool, defined by its serviceability at maximum possible tool life, depends mainly on the material of the tool working part. As a class of materials, ceramics possess high melting points, excellent hardness and good wear resistance. Unlike most metals, hardness levels in ceramics generally remain high at elevated temperatures which mean that cutting tip integrity is relatively unaffected at high cutting speeds. These attributes allow them to be used to machine metals at high cutting speeds and in dry machining conditions because it is not necessary to reduce temperatures on the cutting edges of this tools.

High-melting compounds, which are contained boron, wide use for creation different materials not only for machine metals but for modern techniques too. Complicate terms of use and close-tolerance materials lead to the creation of composite materials with controlled structure and properties. A great interest has the creation of the physicochemical basis for design of cemented materials which are based on the B_4C. This compound presents interest both from the fundamental point of view due to its unusual crystal structure and some its physical properties, and due to its successful application in different technical fields, particularly due to its hardness and neutron absorption ability. Boron carbide exhibits outstanding properties such as high hardness, high elastic modulus, wear resistance, high melting point and low density which make it a suitable material for various industrial applications. But in some cases its application in individual form is limited by very high brittleness, and then the question of creating new

compositions with its participation is very important.

Hot pressing is used for obtaining of such materials but this method is inadequate for achieving of high purity and structure perfection which are crucially important for functional materials. Employing directional crystallization of the boride systems enable one to fabricate high purity self-reinforced composites which consist of ceramic matrix reinforced by ceramic inclusions with advanced mechanical properties when compared to individual borides.

Technical pure powders of B_4C and CrB_2 were taken as initial materials and were mixed in eutectic ration 63% by weight CrB_2 according to the phase diagram (Fig. 1) [1].
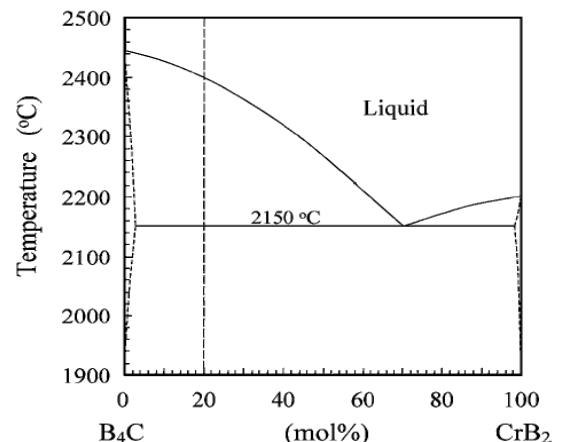

Fig. 1. The phase diagram of the B_4C-CrB_2 system

Directionally solidified eutectic B_4C-CrB_2 composite was prepared by a floating zone method, based on crucibleless zone melting of compacted powders, on the device Crystal 206 in helium gas under pressure 1 atmosphere according to the work [2]. The powder mixture is pressed at room temperature into a pellet. A floating zone method is much easier and faster than the traditional high-pressure high-temperature (HPHT) sintering, but it produces relatively porous pellets. An "impurity solvent" is added to the initial powder mixture; its melting temperature is lower than the melting

temperature of the main component. During the zone melting, the impurity solvent moves along the temperature gradient through the pores in the compacted powder. This diffusion allows to achieve, in one step, both densification of the pellet and its refinement by the zone melting.

Received crystals (Fig. 2) were cut in cross and slit directions and were put to metallographic analysis on the optical microscope Neophot 21 with filing adaptor Imagelab 1.0 and on the electron microscope Selmi РЭМ-106И. The definition of micro-hardness of received composite was carried out on the device PMT-3.

Fig. 2. B_4C-CrB_2 crystal rod.

The investigated alloy of B_4C-CrB_2 was biphasic. While high heat treatment is not accompanied by mutual dissolution [3].

The metallographic analysis of directionally solidified eutectic B_4C-CrB_2 composite (Fig.3) reveals, that composite consists of CrB_2 matrix which includes inclusions of B_4C. Large grains of B_4C are wedge-shaped because B_4C has rhombohedral lattice. It was noticed, the structure of composite B_4C-CrB_2 is complicate regular structure of anomalous eutectic.

a)

b)
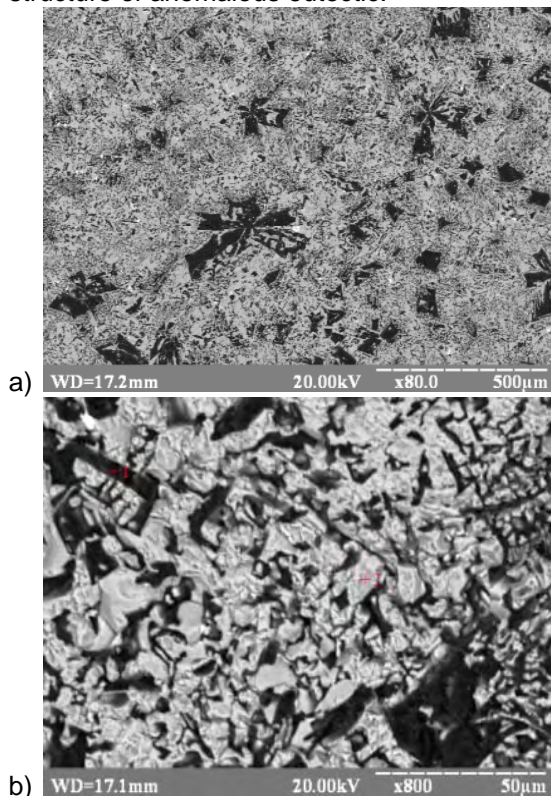
Fig. 3. Metallographic analysis of B_4C-CrB_2 composite.

Was noticed, that when the rate of crystallization increases, dimensions of inclusions B_4C are decrease (Fig. 4). Because this palate-shaped inclusions of B_4C with the increasing of the rate of crystallization are crystallized faster on the top point of the rate of crystallization than on the first point.
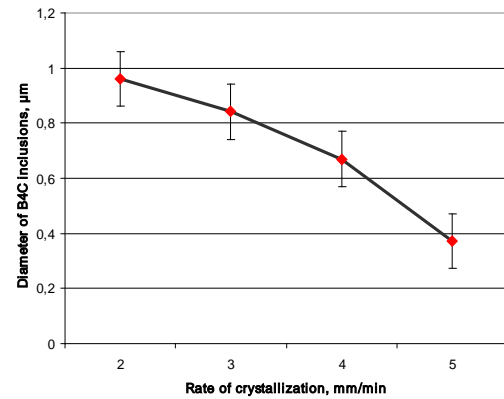
Fig. 4. Dependence the diameter of B_4C inclusions of the rate of crystallization.

The definition of micro-hardness (Fig. 5) shows, that with the increasing of the rate of crystallization, the micro-hardness of composite B_4C-CrB_2 increases and it is approach to additive and it lies between micro hardness of B_4C and CrB_2. The average value of the indentation diagonal was in the range 6,5-8 μm which is much more than the dimensions of eutectic components. The cracks of the pyramid indent on the device PMT-3 and on the optical microscope with zoom in 1000 times of our composite are not noticed. It shows that the fracture toughness of composite B_4C-CrB_2 much higher than in pure B_4C and micro-hardness of composite B_4C-CrB_2 higher than CrB_2.
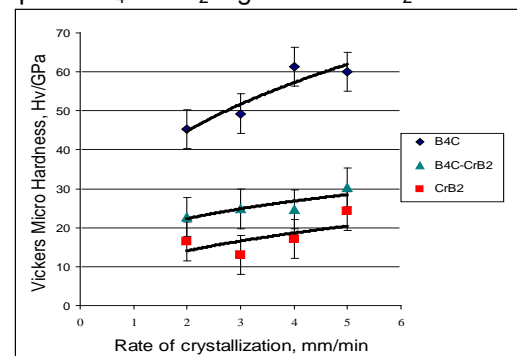

Fig. 5. Micro-hardness dependence of the rate of crystallization.

Thus, directionally crystallized composite of B_4C-CrB_2 has a very high hardness and we can use this material for cutting tools.

References
1. S. Ordanian, A. Dmitriev, Proceedings of the USSR Academy of Sciences 4 (1989) 685-687.

2. P. Loboda, I. Bogomol, M. Sysoev, G. Kysla, Superhard Materials (translation of Rus: Sverkhtverdye Materialy) 28 (5) (2006) 28-32.

3. S. Ordanian, A. Dmitriev, K. Bizev, E. Stepanenko, Powder metallurgy, 10 (1987) 66-69.

STRUCTURE AND MECHANICAL PROPERTIES OF FE-MN-V-TI-0,1C

LOW-CARBON STEEL SUBJECTED TO SEVERE PLASTIC DEFORMATION

Zakharova G.G., Astafurova E.G., Tukeeva M.S.

Supervisor: Astafurova E.G., PhD, assistant professor

Institute of Strength Physics and Materials Science, Siberian Branch of Russian Academy of Sciences,

Tomsk

E-mail: galinazg@yandex.ru

The commercial low-carbon steel Fe-1,12Mn-0,08V-0,07Ti-0,1C (wt.%) in ferritic-pearlitic state (normalization at 950 °C at 30 min.) was subjected to severe plastic deformation by equal channel angular pressing (ECAP) and high pressure torsion (HPT). The ECAP procedure was performed at 200 °C using two channels intersecting at 120°, the samples were processed for four passes by route B_c in which the work piece was rotated 90° along its longitudinal axis after the each pass. HPT was realized at room temperature for 5 revolutions at P=6GPa. The investigation of structure and mechanical properties (microhardness) was carried out at room temperature in initial state, after ECAP, after HPT using transmission electron microscope Philips CM30, scanning electron microscope Quanta 200 3D, diffractometer Shimadzu XRF-6000 with Cu-K_α radiation, microhardness-testing machine Duramin 5 with 200g load.

Figs. 1(a, b) show a structure of lamellar pearlite and coarse-grained ferrite for steel Fe-1,12Mn-0,08V-0,07Ti-0,1C (wt.%) in initial ferritic-pearlitic state. The ferrite grain size is measured as ~ 4,2 μm, the average distance between lamellas of pearlite is 45 nm. The microstructure contains approximately 20 vol.% of pearlite before ECAP [1]. The banded contrast exists on grain boundaries and indicates that structure is balanced. The round shaped carbides of VC, TiC with the average sizes of 15-20 nm is observed both inside grains and on its boundaries.

SPD leads to formation of ultrafine grained structure (UFG) in steel. Figs. 2 (a, b) show that the initial structure of steel is fragmented and distorted by ECAP and HPT. According to TEM dark field analysis, ECAP provides a formation of unequiaxed UFG structure with an average size of (sub-) grain of 260±90nm. The grain boundaries are non-equilibrium; there are many extinction contours inside grains. The selected area electron diffraction (SAED) pattern in Fig. 2(a) shows diffraction spots arranged in quasirings with typical azimuth spreading indicating the presence of boundaries with both high and low angles of misorientation (diffraction was done from the area of 1,4 μm^2). X-ray researches show that ECAP decreases the intensity of X-ray peaks and makes them wider in comparison with the initial state.

For example, the value of microstrain iş $3,0 \times 10^{-4}$ in initial state and gets $1,7 \times 10^{-3}$ after ECAP. These microstructural characteristics of steel investigated indicate that the structure after ECAP is in non-equilibrium state and has high internal stresses. It has been shown that ECAP of ferritic-pearlitic steel leads to fragmentation and partial spheroidization of Fe_3C in pearlite, but a whole solution of cementite does not observed. The analysis of dark field images obtained in reflections of Fe_3C illustrates that plates of cementite are separated into independent segments, which are shifted and misoriented one from another.
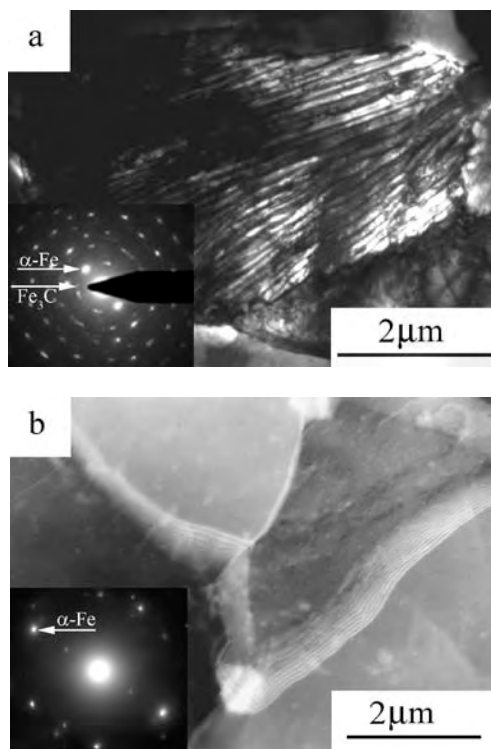
.

Figure 1. TEM micrographs of ferritic-pearlitic steel: a, b –bright field images of initial pearlitic and ferritic structure, respectively.

Figure 2. TEM micrographs of ferritic-pearlitic steel: a, b - bright field images of ferrite after ECAP and HPT, respectively.

The carbides in ferrite are also fragmented by ECAP into smaller ones with irregular shapes. The carbides such as V_8C_7, V_2C, Fe_3C are situated as on dislocations inside of grains as on grain boundaries. It should be noted that ECAP was carried out at 200°C and it can promote the appearance of carbides during deformation. Analysis of steel structure evolution after deformation allows to conclude that ECAP at 200^oC is resulted not only in formation of UFG structure but also promotes the solution, redistribution and extraction of carbides. ECAP causes a formation of non-equilibrium state, decreasing of carbides and provides more homogeneous their distribution as inside grains as on grain boundaries in comparison with initial state. These carbides can be responsible for high hardening, pinning of grain boundaries and the high thermal stability of UFG structure after ECAP.

During HPT of steel the realized strain and pressure are much higher in comparison with ECAP that is why evolution of ferritic-pearlitic steel has some differences. After HPT (Figs. 2 b) steel is highly deformed and fragmented into small structure elements. The structure of steel after HPT is a composition of two types: ma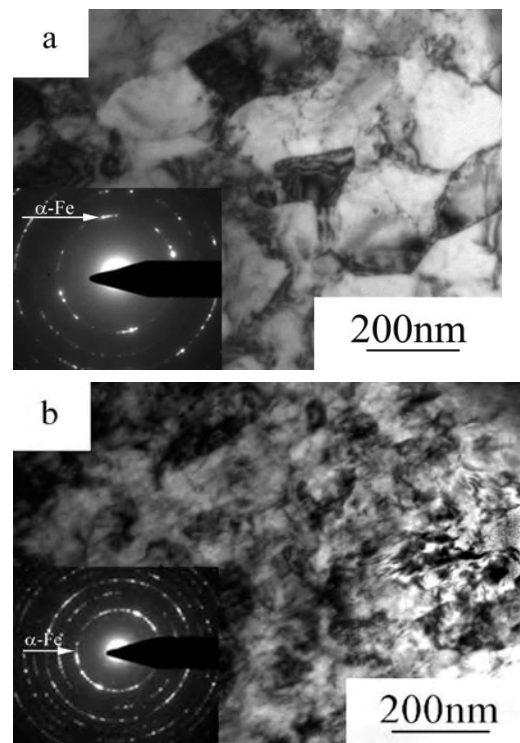inly oriented non-equiaxed ferritic structure with an average (sub-) grain size of 90±50 nm determined by strong localization under deformation and occasionally equiaxed one with grains of 200-300 nm in size [1]. The extinction contours inside grains are clearly visible after HPT, the grain boundaries are distorted and diffused. This confirms that structure formed by HPT is more non-equilibrium, but more homogeneous in comparison with structure after ECAP. Examination of the SAED patterns (from the area of 1,4 μm^2) indicates that formed structure is UFG and grain boundaries have mostly high angle character as the SADP is shaped close to a circle (Fig. 2b). X-ray analysis also identifies the significant difference between X-ray lines of initial and deformed states. X-ray peaks get less intensive and wider after HPT that after ECAP [2]. A variety of small carbides as V_8C_7, V_2C, Fe_3C, $M_{23}C_6$, M_6C were observed in steel structure after HPT. These particles have mainly a spherical form. The plates of Fe_3C were not found after HPT.

Both investigated SPD methods lead to growth in strength properties of steel (Table1). The increase of microhardness up to 2,9GPa after ECAP and up to 6,4GPa after HPT was observed whereas initial value was 1,6 GPa.

Table 1. The influence of SPD on mechanical properties and grain sizes (ferrite) of steel investigated

	H_μ [GPa] (ΔH_μ=0.02 [GPa])	Grain size [nm]
Initial state	1,6	4200±1600
ECAP	2,9	260±90
HPT	6,4	90±50

The differences in strain and pressure realized during ECAP and HPT allow us to analyze structural distinction. Both methods form an UFG structure. The size of structural elements and carbides are smaller after HPT than after ECAP. It is caused by the lower strains and higher deformation temperature of ECAP in comparison with HPT. The high strain, pressure and low deformation temperature are the main reasons for formation a very homogeneous and non-equilibrium structure after HPT, which is evenly deformed through all area of specimen.

Severe plastic deformation of Fe-1,12Mn-0,08V-0,07Ti-0,1C steel in ferritic-pearlitic state by ECAP and HPT leads to strong fragmentation of initial structure. ECAP forms structure with an average size of structural elements of 260±90 nm, and HPT - 90±50 nm. Formation of UFG states causes the increase in mechanical properties after both of SPD methods. HPT produces smaller structural elements and carbides which lead to higher hardening and lower thermal stability in comparison with ECAP. A system of fine carbides formed during ECAP and HPT are of great importance for increasing of mechanical properties of steel investigated.

References:

1. E.G. Astafurova, S.V. Dobatkin and : Mater. Sci. Forum Vol. 584-586 (2008), p. 649-654.
2. E.G. Astafurova, S.V. Dobatkin, E.V. Naydenkin, S.V. Shagalina, G.G. Zakharova, Y.F.Ivanov: Nanotechnologies in Russia Vol. 4, Nos. 1–2, (2009), p.109-120.

Section VII

INFORMATICS AND CONTROL
IN ENGENEERING SYSTEMS

REGULAR EXPRESSION MATCHING

Blech E.I.

Scientific supervisor: Pichugova I.L., senior teacher

Tomsk Polytechnic University, 30, Lenin Avenue, Tomsk, 634050, Russia

E-mail: ketra@avtf.net

By the late 1970s, regular expressions were a key feature of the Unix landscape, in tools such as ed, sed, grep, egrep, awk, and lex. The authors were Thompson and Ritchie.

This paper is concerned with two approaches to regular expression matching. One of them is in widespread use in the standard interpreters for many languages, including Perl. The other is used only in a few places, notably most implementations of awk and grep. The two approaches have significantly different performance characteristics:
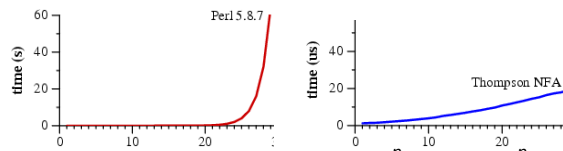
Figure 1. Time to match a^n against a^n.

Notice that Perl requires over sixty seconds to match a 29-character string. The other approach, labeled Thompson NFA for reasons that will be explained later, requires twenty microseconds to match the string. It takes several seconds for the Perl graph to plot, while the Thompson NFA graph needs microseconds to do it: the Thompson NFA implementation is million times faster than Perl when running on a miniscule 29-character string. Looking at the Figure 1, you can see that the Thompson NFA handles a 100-character string within 200 microseconds, while Perl would require over 1015 years [1].

It may be hard to believe the information presented on the graphs. Perhaps you've used Perl, Python, PHP, or Ruby, and it never seemed to you that regular expression matching was particularly slow. In fact, most of the time regular expression matching in Perl is fast enough. As the graph shows, it is possible to write the so-called "pathological" regular expressions that Perl matches very slowly. In contrast, there are no regular expressions that are pathological for the Thompson NFA implementation. Looking through the graphs, the following question arises: "Why doesn't Perl use the Thompson NFA approach?" In general, the rest of this article is devoted to this topic.

So, regular expressions are a notation for describing sets of character strings. When a particular string is in the set described by a regular expression, we often say that the regular expression matches the string.

The syntax described so far is a subset of the traditional Unix egrep regular expression syntax. This subset suffices to describe all regular languages: loosely speaking, a regular language is a set of strings that can be matched in a single pass through the text using only a fixed amount of memory. Newer regular expression facilities (notably Perl and those that have copied it) have added many new operators and escape sequences. These additions make the regular expressions more concise, and sometimes more cryptic, but usually not more powerful, i.e. new regular expressions often have longer equivalents using the traditional syntax.

Let us go closer to the theme. One common regular expression extension that does provide additional power is called backreferences. A backreference like \1 or \2 matches the string which was matched by a previous parenthesized expression, and only that string: (cat|dog)\1 matches catcat and dogdog but neither catdog nor dogcat. As far as the theoretical term is concerned, regular expressions with backreferences are not regular expressions. The power that backreferences add comes at great cost: in the worst case, the best known implementations require exponential search algorithms, like the one Perl uses. Perl (and other languages) could not now remove backreference support, of course, but they could employ much faster algorithms when regular expressions do not have backreferences, like the ones considered above.

Further, when a machine reads an input string one character at a time following the arrows corresponding to the input, it moves from state to state and each possible input letter leads to, maximum, one new state in any state. In that case, the machine is called a deterministic finite automaton (DFA), see Figure 2.
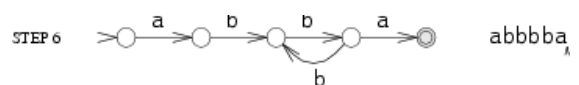

Figure 2. Deterministic finite automation.

The machine in Figure 3 is not deterministic because if it reads a b in state s2, it has

multiple choices for the next state: it can go back to s1 to see another bb, or it can go on to s3 to see the final a.
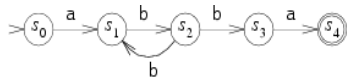

Figure 3. Non-deterministic finite automata.

Therefore the number of states in the final NFA is equal to the length of the original regular expression. It is important, because in an NFA with n nodes, there can only be n reachable states at any step, but there might be 2n paths through the NFA. The backtracking approach thus requires O(2n) time, so it will not scale much beyond n=25.
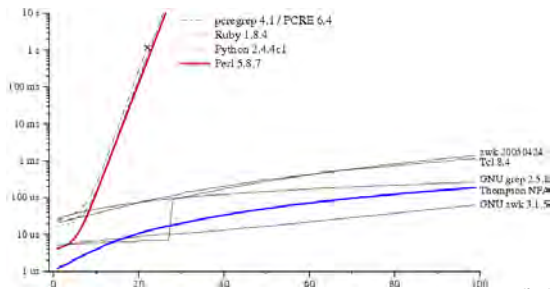
Figure 4. Time required to check whether $a?^n a^n$ matches a^n.

The thick blue line in Figure 4 is the C implementation of Thompson's algorithm given above. Awk, Tcl, GNU grep, and GNU awk apply DFAs or they compute and use the on-the-fly construction. Notice that the graph's y-axis has a logarithmic scale

in order to be able to see a wide variety of times on a single graph.

Considering this problem, the author suggested a way to convert any NFA into an equivalent DFA. Each DFA state corresponds to a list of NFA states.

In a sense, Thompson's NFA simulation is executing the equivalent DFA: each list corresponds to some DFA state, and the step function is computing, given a list and a next character, the next DFA state to enter. To implement the cache, we first introduce a new data type that represents a DFA state:

```
struct DState
{
        List l;
        DState *next[256];
        DState *left;
        DState *right;
};
```

The DState is the cached copy of the list l. The array "next" contains pointers to the next state for each possible input character: if the current state is d and the next input character is c, then d->next[c] is the next state.

If d->next[c] is null, then the next state has not been computed yet. "Next" state computes, records, and returns the next state for a given state and character.

```
Int match(DState *start, char *s)
  {
    int c;
    DState *d, *next;
    d = start;
    for(; *s; s++){
      c = *s & 0xFF;
      if((next=d->next[c])==NULL);
      next = nextstate(d, c);
d = next;
    }
    return ismatch(&d->l);
}
```

The regular expression match follows d->next[c] repeatedly, calling nextstate to compute new states as needed.

Rather than throwing this work away after each step, we could cache the lists in spare memory, avoiding the cost of repeating the computation in the future and essentially computing the equivalent DFA as it is needed.

In conclusion, NFAs derived from regular expressions tend to exhibit good locality: they visit the same states and follow the same transition arrows over and over when running on most texts. This makes the caching worthwhile: the first time an arrow is followed, the next state must be computed as in the NFA simulation, but future traversals of the arrow are just a single memory access. Real DFA-based implementations can make use of additional optimizations to run even faster.

All in all, regular expression matching can be simple and fast, using finite automata-based techniques that have been known for decades. In contrast, Perl, PCRE, Python, Ruby, Java, and many other languages have regular expression implementations based on recursive backtracking that are simple but can be excruciatingly slow. With the exception of backreferences, the features provided by the slow backtracking implementations can be provided by the automata-based implementations at dramatically faster, more consistent speeds [2].

References:

1. Ken Thompson, "Regular expression search algorithm," Communications of the ACM 11(6) (June 1968), pp. 419–422. http://doi.acm.org/10.1145/363347.363387
2. Regular Expression Matching Can Be Simple And Fast. [Electronic resource]. – 2010. – Access mode: http://swtch.com/~rsc/regexp/regexp1.html

TIME CONTROL SOFTWARE DESIGN OF PROCESS PERFORMANCE
FOR SH7201 MICROCONTROLLER MICROKERNEL

Gavrilenko A.V.

Scientific advisors: Ofitserof V.V., Yurova M.V.

National Research University of Resource-Efficient Technologies "TPU"

silkbliss@mail.ru

Introduction

Renesas is the one of the largest microprocessor-based techniques producers. It holds 40% of the market. Products of this company are used everywhere: from household appliances to automobiles. One product of this company is SH7201 microcontroller. It was built with the use of Harvard and RISC architecture. It takes 200MIPS, i.e. 200 million operations per second. Its frequency is 120 MHz. For extra information of this microcontroller you can visit the site of the company.

Embedded software designed for SH7201 microcontroller must operate properly in all running period of intellectual equipment use. That's why for all situations which can cause the bugs (fails) proper diagnostics and handling must be provided.

Exceptions

Situations which can cause bugs (fails) are called exceptions. An exception is an event that you would not expect during the normal device operation. It's unusual and unexpected occurrence [1]. Time and location generally cannot be predicted.

Exception handlers can be triggered by different sources, such as:

▪ Resets – manual and power-on;
▪ CPU address error;
▪ Bus error;
▪ Register bank errors (overflow and underflow);
▪ Instructions (FPU exception, general and slot illegal instructions, integer division exception – division by zero and overflow).

All exceptions have their own priority [2]. Table 1 shows their priorities.

Table 1. Exception priorities

Exception	High
Power-on reset Manual reset CPU address error	
Bus error FPU exception	
Division by zero Overflow Bank underflow Bank overflow Illegal instructions	Low

When several exception handling sources occur at once, they are processed according to their priority [1]. Every exception has its own service routine and before exception handling begins running the exception handling vector table must be set in memory, which stores the start addresses of the exception service routines. For example, for resets this table stores values for 2 registers – PC (program counter) and SP (stack pointer).

Hardware offers methods to react, recover and restart the process [3]. But developer has no information about the occurred error and even about its appearance. And it's a big disadvantage especially during software development process. Thus, software debug monitor was developed as a service for user. It allows to indicate (fix and recognize) and handle exceptions according to the source.

Diagnostics results are fixed into special log-file (or into table), which contains error registration information; for example, exception source and place of occurrence (address error). Given software is designed for software diagnostics and may be used for direct hardware examination (detection of the contacts malfunction, for instance).

Software designed for SH7201 microcontroller is realized with the help of special software product – microkernel, which is an instrument helping the developer to project the developing imbedded software task. Mechanisms, negotiated in microkernel, allow to execute the code of critical areas without prohibitions of the interrupt rise.

Software structure designed with the use of microkernel contains functions of the microkernel, background task, user's directives, the queues of the priority-driven processes and the reserved parts of the interrupts.

▪ **Background task** – the part of program code which is implemented as an endless process. It consists of several calls of user's routines in free order and has the lowest priority of execution.

▪ **Interrupt reserved parts queue –** queue of the program code parts which are executed integrally, interrupts of all sources are available.

▪ **Queue of the priority-given processes** – queue of the user's code implementation processes with the integral execution (with

respect to other priority-given ones) according to the priority with open interrupts.

▪ **User's directives.** Directive is a program code designed with microkernel agreement which is implemented integrally with respect to reserved parts of the interrupts. Directives have higher priority than priority-given processes and background task. Directives and reserved parts of the interrupts have the equal priority.

Reserved parts of the interrupts

Among these elements interrupts have the highest priority, that's why they can stop implementation of the background task, directives, priority-given processes and reserved parts of the other interrupts. According to the microkernel agreement interrupt service routine (ISR) is designed following the certain rule.

According to the designed microkernel ISR is divided into two parts. So, one part of the code is executed as an interrupt service routine (ISR) and the other (reserved) one is executed with open interrupts.

The main property of such decomposition is possibility of the developer to decide singly which part of the ISR must be implemented as a critical area and the other will be a reserved part.

It's very important to avoid cycling of the reserved parts of the interrupts there because then it becomes impossible to implement elements with lower priority (background task and priority-given processes), and the reserved parts of the other interrupts which can abort the execution of this looped process will be placed in queue. That's why it's very important to avoid mistakes in coding of the interrupts reserved parts. Suitable addition was built in developed software. It allows to fix implementation time of the reserved part of the interrupt and in case this time becomes greater than the user specified value, cycling process integrally is deleted.

It's realized with the help of PDB fields monitoring (Process Descriptor Block) – special structure for every reserved part of the interrupt. At the same time the user is given information about the amount of reserved parts of the interrupts implementation of which was stopped, time taken to handler for code implementation, etc.

Priority-given processes

Background task consists of several logical calls of user functions. There is a necessity for execution of several functions on the level of priority-given processes. As a result microkernel developers realized the system directive which put priority-given processes in implementation queue. Queue of the priority-given processes is formed according to task priority. It means that process with the highest priority is implemented first but integrally in relation to other processes. The rest of the priority-given processes are executed one after another according to their priority.

It is important to avoid priority-given process looping, as then it becomes impossible to implement background task and other priority-given processes of the queue.

This problem has the same solution. Every priority-given process has the same PDB structure (Process Descriptor Block) but this structure contains the process priority field in addition.

Designed diagnostic software allows to detect and repair situations, which can cause program failure, and also avoid looping in reserved parts of interrupts and priority-given processes in software development with the use of microkernel.

Literature

1. SH7201 Group Hardware Manual. Renesas 32-Bit RISC Microcomputer SuperH RISC engine Family/SH7200 Series R5S72011. – 2006. – 1208 p.

2. Renesas Interactive.—Access mode: http://www.renesasinteractive.com, free enter

3. SuperH RISC engine C/C++ Compiler, Assembler, Optimizing Linkage Editor. Compiler Package V.9.00 User's Manual. Renesas Microcomputer Development Environment System.- 2004. – 1105 p.

DATA TRANSMISSION IN INDUSTRIAL ETHERNET

Maria Alekseevna Ivashkina

Scientific supervisor: A.A.Zorkaltsev

Language supervisor: E.S. Samsonova

Tomsk Polytechnic University

E-mail: maria--06@mail.ru

In our days Ethernet technology predominates over all local networks. It is used in control systems of manufacture, enterprises, distributed objects, conforms to meeting real-time challenges and comes into operation in regional networks and Wide Area Networks (WAN). Ethernet ensures high degree of reliability with comparatively low cost. Ethernet is being continually developed and improved with invariable format of frames. In the first place improvements are directed at increasing of data transfer rate (DTR). New modifications of Ethernet technology for specific ranges of application are standardized. [1]

Industrial Ethernet opens up wide opportunities for solving problems in various fields. According to the Automation Research Corporation (ARC) Advisory Group yearly averaged growth coefficient of Industrial Ethernet products in world goods market will be 51,4 % in the next 5 years. [2]

As standard technology in building industrial networks and distributed control networks Ethernet enters the field of programmable controllers, adapter units with sensors and actuating units. Recently, the architecture of Ethernet in industrial application - Industrial Ethernet, supported by leading producers of automation equipments is widely discussed. As a universal mean of communication interfaces organization Industrial Ethernet offers full opportunities in realizing diverse topologies with different add-on devices of low cost, integrates with Internet Technology including such merits as high scalability and possibility of remote control. [3]

Ethernet or TCP/IP doesn't yet guarantee communication of devices. Ethernet provides capability of messages transmission only. Messages are transmitted by transport protocols. In Ethernet case it is basically TCP and UDP. However, transmission needs protocols of higher layers, too. Data of sensors and transducers could be packed in existing format of industrial network and be transmitted by means of TCP/IP. Architecture TCP/IP stack is shown on Fig. 1.
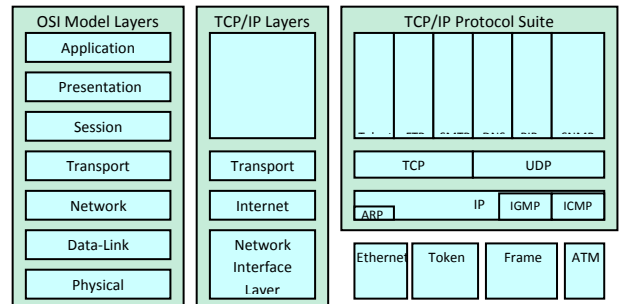

Fig. 1. Structures of OSI model and TCP/IP stack

Currently, there exist more than 20 profiles of Industrial Ethernet, basic profiles are Modbus/TCP, Ethernet/IP, Powerlink, PROFInet, SERCOS III, EtherCAT. Architectures of Modbus-TCP and PROFInet V3 are shown on Fig. 2 as an example.
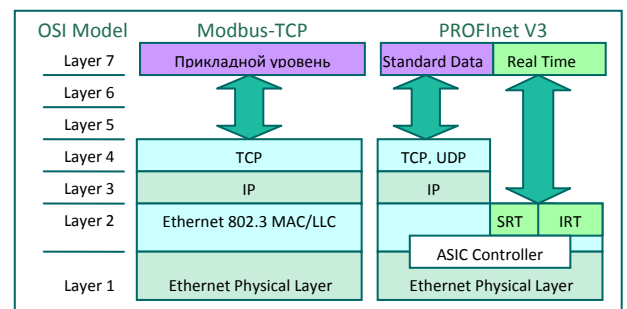

Fig. 2. Structures of OSI model, Modbus-TCP and PROFInet V3

In Modbus-TCP profile all data are transmitted through TCP/IP, in PROFInet V3 profile part of the traffic goes through TCP/IP, real time data goes directly to Ethernet layer. The same approach is used in other Industrial Etehrnet technologies, which provides real-time data transmission. In any realization TCP/IP stack is needed for work of Industrial Ethernet.

On basis of TCP/IP a big amount of products and devices are produced. Wide availability of network components, merging trend of automation systems of industry processes and widely spread network technologies open interesting opportunities of application usual global and local network protocols in enterprises. It simplifies solving problems of uniting heterogeneous environment of data transmission

and devices, helps to ensure their interaction and centralized control.

In Tomsk State University of Control Systems and Radioelectronics at Electronic Systems Department within university programme Renesas Technology Europe the Center of microprocessor-based systems was founded, where software developers research and elaborate applications on Renesas platform. The Renesas company is the first-rate producer of integrated microcircuits and is a leader among microcontroller producers.

Task of realization and TCP/IP stack work estimation on SH7201 platform of SH2A series from Renesas company with the use of µC/OS-II operating system exists within the framework of researching industrial network.

Microcontrollers from Renesas company with SH-2A kernel are used in industry, domestic appliances, office equipment, automotive electronics, etc. SH-2A kernel is modern 32-bit RISC platform with opportunity of working on frequency up to 200 MHz, is built on Harvard architecture base with 4 GB of uninterrupted address space. SH-2A can include hardware module of multiplication with opportunity of results accumulation. Command set and addressing routines were developed for ensuring highest possible productivity with programming in high level language C. CPU could execute under two commands per machine cycle. Increasing productivity is reached by using cache memory and five-level instruction pipeline. Conditional passage commands with waiting cycle is included in the regulation set for ensuring uninterrupted work of pipeline. Compiler for chips with SuperH structure optimizes glue code for minimizing pipeline breaks. [4]

Operating system µC/OS-II (Micro-Controller Operating System second edition) needed for realization of task was founded by Micriµm company, which has developed real time systems since 1992 and grants its source code of products for consumers for free for non-profit purposes. µC/OS-II can work on the majority of

8-bit, 16-bit, 32-bit and 64-bit microcontrollers. Basic feature of µC/OS-II real-time operating system is multitasking. µC/OS-II can control 64 tasks. Each task has a fixed unique priority. µC/OS-II is a priority-carrying preemptive real-time kernel. Kernel executes first-priority task, which is ready for performance. Execution time of all functions and services of µC/OS-II is determined. Execution time of all services doesn't depend on the amount of tasks, performed by the application. µC/OS-II is a scalable operating system. Thus one project could include only a of a service set, whereas another – a complete set. It enables to decrease workload of needed µC/OS-II proper memory: RAM (Random Access Memory) and ROM (read-only memory). [5]

In the report the features of real-time operating system µC/OS-II which influence TCP/IP stack performance will be examined. Also the estimates resources necessary for TCP/IP stack performance, results of researches with diverse criteria and comparison with other realizations will be presented.

▪ References

1. Вячеслав Виноградов: Системное развитие быстродействующих коммутируемых сетей Ethernet. Журнал «Современные технологии автоматизации», 1/2008.

2. Сергей Колесников: Технологии и протоколы передачи данных в промышленности: Industrial Ethernet. Журнал «Компьютер-Информ», 1/2003.

3. Компания КОЛАН: Ethernet в системах промышленной автоматизации [электронный ресурс]. Режим доступа: http://www.colan.ru/support/artview.php?idx=182, свободный.

4. Семейство микроконтроллеров и микропроцессоров SuperH. Брошюра. 2007 г. - 40с.

5. MicroC/OS-II: The real time kernel second edition /Jean J. Labrosse. CMPBooks, 1998 г. - 303с.

NEW RESEARCHES IN COMPUTER VISION

Arash Kermani

Supervisor: Spitsyn V.G, Professor

Tomsk Polytechnic University, 30, Lenin Avenue, Tomsk, 634050, Russia

E-mail: arash@tpu.ru

Abstract

Human vision as the fastest and the most developed image processor known is an ideal model of an image processor. The human visual system uses an internal model of the world to interpret what it sees. The aim of some researches in the area of computer vision is to develop some new methods for object recognition based on the way human visual cortex does it. The natural visual system uses an internal model of the work to interpret what is sees. The latest works attempt to develop adaptive feature detectors which can learn the model of the world from the input images.

Introduction

The visual cortex is a part of the outermost layer of the brain and refers to the primary visual cortex, V1 and extrastriate visual cortical areas such as V2, V3, V4, and V5. The first population of neurons to be activated by the visual stimulus is found in area V1. After processing in area V1, activity is relayed to a few other cortical areas located close to V1 which themselves transmit activity to additional cortical areas. After Hubel and Wiesel (1962, 1968) first showed that neurons in mammalian primary visual cortex (V1) are optimally stimulated by bars and edges, a large part of visual neuroscience has been concerned with exploring the response characteristics of neurons in V1 and in higher visual areas. However, such studies do not directly answer the question of why the neurons respond in the way that they do. Why does it make sense to filter the incoming visual signals with receptive fields such as those of V1 simple cells?

New Researches

An important approach in visual neuroscience considers how the function of the early visual system relates to the statistics of its natural input. It is found that the cortex does not simply seek to represent the sensory data efficiently, but it builds a probabilistic internal model for those data [4]. In such a framework, it is natural to think of neural networks not as simply transforming the input signals into coded representations, but rather as modeling the structure of the sensory data. The visual cortex expresses each observed data pattern approximately as some linear combination of the basis features.

One of the important works done in 2007 at the Center for Biological & Computational Learning at MIT under "Robust Object Recognition with Cortex-Like Mechanisms" is concerned with recognition of complex visual scenes, which is motivated by biology and closely follows the organization of the visual cortex [2]. This system follows a recent theory of the feed-forward path of object recognition in the cortex. They showed that a universal feature set, learned from a set of natural images "unrelated to any categorization task", achieves good performance in object recognition [2]. That is the artificial neural network responsible for image recognition was trained with some fundamental small pieces of natural images containing some basis features to prepare the network to interpret the input image (In fact, basis features act as filters and are very similar to Gabor filters [4]). It resulted in a much better performance of object recognition in natural images. Although this work was an important step in improving object recognition, it had a weakness; the statistics of basis features does not always match the satisfying statistics for recognizing objects in the working set.

A new research by Hamker [1] suggests learning the fundamental images (basis features) directly from the working set. This method is fully unsupervised and draws a model of what actually happens in the natural visual system. Unlike the usual feature detectors that depend on pre-defined features which cannot always describe the working set of images, the new feature detectors are able to adapt themselves with the nature of the input images and interpret them based on basis features which belong to the working set. During the training phase, several small random patches of images from the working set are fed to the first layer of the neural network and the network is trained to produce the same features using Hebbian Learning Algorithm. This layer then acts as a filter which reinforces the input patches similar to the training patches. This way we will have a clear image which then is used for contour and then object recognition in higher layers [4]. This is very similar to what happens in the primary visual cortex. In V1, images are filtered by feature detectors which detect features like bars and edges and then send this information to higher layers to be interpreted [4].

References

1. Jan Wiltschut and Fred H. Hamker, "Efficient coding correlates with spatial frequency tuning in a model of V1 receptive field organization", Visual Neuroscience (2009), 21–34

2. Thomas Serre, Lior Wolf, Stanley Bileschi, Maximilian Riesenhuber, and Tomaso Poggio, Member, "Robust Object Recognition with Cortex-Like Mechanisms", 2007, IEEE TRANSACTIONS ON PATTERN ANALYSIS AND MACHINE INTELLIGENCE, VOL. 29, NO. 3, MARCH (2007) 411-426

3. Internet tutorial in "The Physiology of the Senses", University of Western Ontario, Canada: http://www.physpharm.fmd.uwo.ca/undergrad/sensesweb/

4. Patrik O. Hoyer , Aapo Hyvärinen, "A Multi-Layer Sparse Coding Network Learns Contour Coding From Natural Images" 2002, Vision Research 42 (2002) 1593–1605

NETWORK CONGESTION CONTROL USING NETFLOW

Maxim A. Kolosovskiy

Supervisor: Kryuchkova E.N., PhD in physics and mathematics, professor

Altai State Technical University, 656038, Russia, Barnaul, Lenin pr., 46.

E-mail: maxim.astu@gmail.com

Abstract — the goal of congestion control is to avoid congestion in network elements. A network element is congested if it is being offered more traffic than it can process. To detect such situations and to neutralize them we should monitor traffic in the network. In this paper, we propose using Cisco's NetFlow technology, which allows collecting statistics about traffic in the network by generating special NetFlow packets. Cisco's routers can send NetFlow packets to a special node, so we can collect these packets, analyze its content and detect network congestion. We use Cisco's feature as example, some other vendors provide similar features for their routers. We consider a system, which collects statistical information about network elements, determines overloaded elements and identifies flows, which congest them.

Index Terms—Congestion Control, NetFlow, Network Monitoring, Traffic Measurements.

INTRODUCTION

The goal of congestion control is to avoid congestion in network elements. A network element is congested, if it is being offered more traffic than it can process. Congestion control is control of resources: routers CPUs, bandwidth of links, routers memory, etc. [1]

If we don't control our network, there is potential for a serious trouble. When some network element becomes congested, it processes traffic very slowly and some packets are lost. Therefore, users don't receive expected packets (or conformation of delivery) in the time limit. Users begin to resubmit packets and new packets cause further congestion. Such situation is called congestive collapse.

If we can't offer high-speed service to all users, we should restrict consumption of resources by users to avoid congestion. So, all users get satisfactory service continuously. If we permit unlimited using of resources, it can cause congestive collapse and all network services become unavailable.

NetFlow is Cisco's technology, which allows collecting detailed information about network traffic [2]. Most of Cisco's routers can generate special packets, which contain information about router's active traffic flows. Using NetFlow we can capture wide range of properties of network traffic: IP-addresses, ports, protocols, TCP-flags, ToS, etc.

STRUCTURE OF THE SYSTEM

We would introduce the system for network congestion control. The system collects information using NetFlow technology. The system helps:

a) To detect overloaded segments (or elements) of the network, which can initiate congestion.

b) To identify the cause of excessive load of these segments (or elements).

c) To make decisions about changing network parameters and to avoid congestive collapse.

The system consists of two applications:

A. **Collector** listens to certain UDP-port, receives NetFlow-packets and saves necessary fields of packets (source and destination IPs and ports, timestamps, protocols, number of Layer 3 bytes) to a file.

B. **Analyzer** reads data from the file, processes it and generates reports.
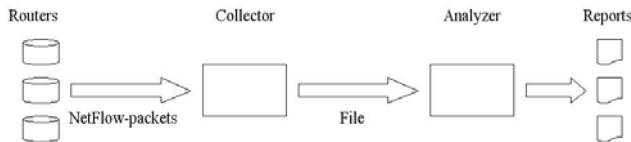
Let's look at the system structure on Figure 1.

Fig 1. The system structure. Routers send NetFlow-packets to the collector. The collector saves information from these packets to the file, the analyzer reads this file and builds reports.

USING OF THE SYSTEM

Using of our system consists of the following steps:

1) Configuring routers in the network to send NetFlow v5 packets to our NetFlow collector.
2) Collecting information about network flows for a long period.
3) Building reports by the analyzer about network traffic flows.

In the current system implementation the results of 3rd step are used by the network administrator,

We should repeat these steps periodically to control the network. If the system signals about overloaded elements, we should restrict traffic rates in these elements or to redistribute traffic between other elements. The system shows the most unloaded links and routers, this information helps us to redistribute traffic. The system also advises which traffic flows we should redirect. If the system signals that some elements can work more intensively, we may increase traffic rates in these elements. The system provides information about interaction between hosts and usage of services. The system shows which elements work as "bottleneck" and which elements idle.

We reviewed the information needs to control congestion and insert into the system the following types of reports (to make examples more clearly we use NetFlow packets, which are generated artificial):

A. The load of hosts

```
IP                   Total
10.1.12.2        2763.8 MB [6%-22%-23%-40%-3%-4%]
10.1.12.10       2777.6 MB [1%-22%-21%-33%-16%-3%]
10.1.12.12       4523.3 MB [5%-13%-22%-20%-13%-25%]
```

Using this report we can estimate the load of each host. We can replace our routers corresponding to their load. For each host we show its IP address, total traffic and a distribution of the traffic over different periods of a day (we assume that a day consists of six 4-hour periods). Hosts are sorted in increasing order by total   traffic.

B. The load of links

```
10.1.12.8 => 10.1.12.6              Total: 288.7 MB
10.1.12.1:29750  -> 10.1.12.6:12352  52% (151.1 MB)
10.1.12.13:29792 -> 10.1.12.4:23725  42% (121.9 MB)
10.1.12.8:20644  -> 10.1.12.14:16906  5%  (15.7 MB)
```

The example shows statistic for a link. We can see conversations, which are using maximal bandwidth. In this example we see, that first two conversations load the link most of all, so if we want to unload the link, we should change the path of one of these conversations. If we change the path of last conversation, it doesn't change the load of the link essentially.

C. The most unloaded links

```
1.      10.1.12.15 => 10.1.12.11          4.2 MB
2.      10.1.12.5 => 10.1.12.11          11.1 MB
3.      10.1.12.5 => 10.1.12.4           11.6 MB
4.      10.1.12.4 => 10.1.12.16          11.6 MB
5.      10.1.12.6 => 10.1.12.14          15.7 MB
```

We can use these links to unload other links.

D. Conversations

```
10.1.12.14:28542  ->  10.1.12.3:29828
 10.1.12.6  => 10.1.12.8   48.7 MB  (of 811.0 MB)
 10.1.12.7  => 10.1.12.12  48.7 MB  (of 416.5 MB)
 10.1.12.8  => 10.1.12.7   48.7 MB  (of 457.6 MB)
 10.1.12.14 => 10.1.12.6   48.7 MB  (of 481.1 MB)
 10.1.12.12 => 10.1.12.3   48.7 MB  (of 1104.3 MB)
```

Conversation is defined by four parameters: source and destination IPs and ports. For each conversation, we build the list of links, which are used for that conversation (in parentheses we show total traffic in the link).

E. Interactions with other hosts and protocol distribution

```
10.1.12.3
 10.1.12.14        62.3 MB (68%)
 10.1.12.4         13.5 MB (14%)
 10.1.12.16        10.4 MB (11%)
 10.1.12.6          4.8 MB (5%)
Total traffic:     91.0 MB
Protocols: TCP - 77%, UDP - 11%, Other - 11%
```

For each host we display the list of hosts, which interact with that host. We also display total traffic for each interaction. Last line contains protocol distribution for that host.

F. Input and output traffic

```
*** 10.1.12.1 ***
IN       165.8 MB [0%-0%-62%-2%-0%-34%]
OUT      292.2 MB [0%-4%-47%-47%-0%-0%]
IN&OUT   458.0 MB [0%-2%-53%-31%-0%-12%]
```

For each host we display input, output and total traffic. We also display distribution of the traffic over time (day is divided into six 4-hour periods).

G. Active ports of host

```
10.1.12.2
 :4157   473.9 MB (33%)
 :31890  438.1 MB (31%)
 :15681  237.1 MB (16%)
 :9015   149.3 MB (10%)
 :21435   64.6 MB (4%)
 :22222   27.4 MB (1%)
 :9390    10.2 MB (0%)
Total:  1400.6 MB
```

The system show all active ports and total traffic of the host. Each network service is assigned to one or more ports; so we can estimate how much traffic the service produces and consumes.

Use case: We are not satisfied by working of the service, which are located on *10.1.12.7* and uses port *32001*. We find hosts, which interact with *10.1.12.7* and find conversations, which are using port *32001*. So, we know links and routers, which support this conversation. We analyze the load of these elements and find "bottlenecks", which delay the service. We know conversations, which load bottlenecks. Finally, we change parameters of some network elements to unload bottlenecks.

Thus, these reports allow analyzing network traffic, to detect possible congestion and to make a decision about changes. We show elementary examples. These examples can be combined to produce tables that are more complex.

CONCLUSION

We have considered using NetFlow for network congestion control. Using our system network administrator obtains information about overloaded elements, but administrator must make a decision about balancing network load by himself. Thus, the next step is developing algorithms, which can propose explicit actions to unload congested elements, and include these algorithms into the system.

REFERENCES

1. Welzl M. *Network Congestion Control: Managing Internet Traffic.* New Sussex, England: John Wiley & Sons, 2005, 284 p.
2. Introduction to Cisco IOS NetFlow [Online]. Available: http://www.cisco.com.

APPLYING INVERSE-COMPOSITIONAL IMAGE REGISTRATION ALGORITHM

TO HEAD TRACKING WITH 6 DOF

O.A. Krivtsov.

Mentor: A.M. Korikov., Doctor of Science, Professor

Tomsk State University of Control Systems and Radioelectronics, 634050, Russia, Tomsk, Lenina st., 40

E-mail: olegkrivtsov@mail.ru

Introduction. Head tracking is a solution of the problem of determining the head configuration on video frames. It has various applications, such as 3D animation, human-computer interfaces, telecommunications, multimedia indexing, 3D model construction, face image stabilization, robotics etc.

One approach to head tracking with 6DOF is modeling the head as a rigid body (e.g. plane, cylinder or ellipsoid), initializing the head model's configuration on the first frame and determining its interframe motion using an image registration algorithm. In this paper, we show how to use an effective inverse-compositional registration algorithm (ICA) [1] in application to head motion with six degrees of freedom (6DOF).

Image registration using ICA. The ICA is used to determine the parameters of head motion between the 1st and the 2nd frames, …, *i-th* and (*i*+1)-th frames.

Let's take two subsequent grayscale video frames: the first one, I_i, is taken at time moment t_i, and the second one, I_{i+1}, is taken at the moment $t_{i+1} = t_i + \Delta t$. Head configuration $\mathbf{c}_i = (x, y, z, \alpha, \beta, \gamma)^T$ on the *i*-th frame is considered to be known. We need to estimate the configuration $\mathbf{c}_{i+1}$ on the frame I_{i+1}.

We can think of pixel intensity of an image as of function $I(\mathbf{x}, t)$, which depends on both pixel coordinates $\mathbf{x} = (x, y)^T$ and time *t* [2]. Then we can consider the pixel intensity of particular frame as the section of the function at time moment *t*: $I_i(\mathbf{x}) = I(\mathbf{x}, t_i)$, $I_{i+1}(\mathbf{x}) = I(\mathbf{x}, t_i + \Delta t)$.

Let some pixel $\mathbf{x}_n = (x_n, y_n)^T$ of *i*-th frame at t_i, belongs to the rectangular area Ω of the head projection (fig. 1, a). At the next time moment $t_i + \Delta t$ we take frame I_{i+1}, on which our pixel displaces to the new position $\mathbf{x}'_n = (x_n + \Delta x, y_n + \Delta y)^T$ (fig. 1, b).
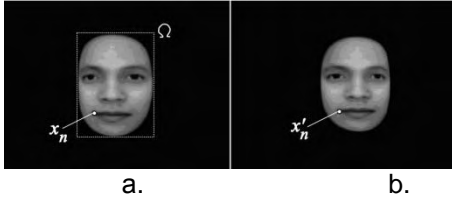
a.   b.

Figure 1. Interframe motion of pixel $\mathbf{x}_n$.

If we assume that illumination is constant and movement of the pixel between frames I_i and I_{i+1} is only because of head motion, than eq. (1) is true:

$$I(x_n, y_n, t_i) = I(x_n + \Delta x, y_n + \Delta y, t_i + \Delta t) \,. \tag{1}$$

Eq. (1) was first proposed by Lucas and Kanade [3] and defines the translational motion model $\mathbf{x}_n \to \mathbf{x}'_n$ for particular pixel. In general, there are many *parametric motion models* [4], starting from 2D translation and rotation to 3D projective models. So it is good idea to introduce the *generalized motion model* (also called warp function) $W(\mathbf{x}, \mathbf{p})$:

$$\mathbf{x}' = W(\mathbf{x}, \mathbf{p}) \,, \tag{2}$$

where $W(\mathbf{x}, \mathbf{p}) = \begin{pmatrix} W_x(\mathbf{x}, \mathbf{p}) \\ W_y(\mathbf{x}, \mathbf{p}) \end{pmatrix}$ is some vector-function, which maps pixel $\mathbf{x}$ on *i*-th frame to pixel $\mathbf{x}'$ on (*i*+1)-th frame, and depends on vector of motion parameters $\mathbf{p} = (p_1, p_2, ..., p_m)^T$. Let also constrain that $W(\mathbf{x}, \mathbf{0})$ maps $\mathbf{x}$ into itself: $W(\mathbf{x}, \mathbf{0}) = \mathbf{x}$.

Using the motion model (2), eq. (1) looks as follows:

$$I(\mathbf{x}_n, t_i) = I(W(\mathbf{x}_n, \mathbf{p}_n + \Delta \mathbf{p}), t_i + \Delta t) \,. \tag{3}$$

In the left part of eq. (3), $\mathbf{x}_n = W(\mathbf{x}_n, \mathbf{p}_n)$. In the right part, $\mathbf{p}_n = \mathbf{0}$ because of $W(\mathbf{x}; \mathbf{0}) = \mathbf{x}$. Eq. (3) depends on vector $\Delta \mathbf{p}$ nonlinearly, because $I(\mathbf{x}, t)$ depends on argument $\mathbf{x}$ nonlinearly. If the increment of argument is *infinitesimal*, eq. (3) can be approximated by replacing the function increment with its full differential:

$$I(W(\mathbf{x}_n, \mathbf{p}_n + \Delta \mathbf{p}), t_i + \Delta t) \approx$$
$$\approx I(\mathbf{x}_n, t_i) + \nabla I(\mathbf{x}_n, t_i) \mathbf{J}_W(\mathbf{x}_n, \mathbf{p}_n) \Delta \mathbf{p} + \frac{\partial I(\mathbf{x}_n, t_i)}{\partial t} t \tag{4}$$

here $\mathbf{J}_W(\mathbf{x}_n, \mathbf{p}_n)$ is the $2 \times m$ matrix of the first derivatives of vector-function $W(\mathbf{x}; \mathbf{p})$, calculated at $(\mathbf{x}_n, \mathbf{p}_n)^T$; vector $\nabla I(\mathbf{x}_n, t_i) = \left(\frac{\partial I(\mathbf{x}_n, t_i)}{\partial x}, \frac{\partial I(\mathbf{x}_n, t_i)}{\partial y} \right)$ is the spatial image gradient calculated at point $(\mathbf{x}_n, t_i)$; and scalar $\frac{\partial I(\mathbf{x}_n, t_i)}{\partial t}$ is the temporal image gradient at $(\mathbf{x}_n, t_i)$. Substituting eq. (4) into eq. (3), we have:

$$\nabla I(\mathbf{x}_n, t_i) \mathbf{J}_W(\mathbf{x}_n, \mathbf{0}) \Delta \mathbf{p} + \frac{\partial I(\mathbf{x}_n, t_i)}{\partial t} \Delta t = 0. \tag{5}$$

Eq. (5) is underconstrained linear equation of $\Delta \mathbf{p}$. Here Δt is known and can be set with 1 for simplicity. Assuming that function $W(\mathbf{x}, \mathbf{p})$ approximates the motion of every pixel $\mathbf{x} \in \Omega$ well, we can write the system of N equations (N is the count of pixels in Ω):

$$\left\{ \nabla I(\mathbf{x}_k, t_i) \mathbf{J}_W(\mathbf{x}_k, \mathbf{0}) \Delta \mathbf{p} + \frac{\partial I(\mathbf{x}_k, t_i)}{\partial t} = 0; k = 1, 2, ..., N \right. \tag{6}$$

If N is big, we have the overconstrained system of linear equations, the solution of which can be found using the method of the least squares:

$$\Phi(\Delta \mathbf{p}) = \sum_{n=1}^{N} w(\mathbf{x}_n) \left[\nabla I(\mathbf{x}_n, t_i) \mathbf{J}_W(\mathbf{x}_n, \mathbf{0}) \Delta \mathbf{p} + \frac{\partial I(\mathbf{x}_n, t_i)}{\partial t} \right]^2, \tag{7}$$

where $w(\mathbf{x}_n)$ is the scalar weight of the *n*-th term of the sum (weight of the pixel $\mathbf{x}_n$). It is obvious that the value of $\Delta \mathbf{p}$ which brings minimum to (7) is the closest to the solution of (6).

For the minimization of eq. (7) Gauss-Newton method can be used. The iteration scheme is as follows:

$$\Delta \mathbf{p} = -[\mathbf{H}_\Phi]^{-1} \nabla \Phi \,, \tag{8}$$

where $\Delta \mathbf{p}$ is the approximation of motion parameter increment; $\nabla \Phi$ and $\mathbf{H}_\Phi$ are (respectively) the gradient vector and the $m \times m$ matrix of the second derivatives (Hessian) of eq. (7):

$$\nabla \Phi = 2 \sum_{n=1}^{N} \left[w(\mathbf{x}_n) \left(G \Delta \mathbf{p} + \frac{\partial I(\mathbf{x}_n, t_i)}{\partial t} \right)^T G \right],$$

$$\mathbf{H}_\Phi = 2 \sum_{n=1}^{N} \left[w(\mathbf{x}_n) G^T G \right], \text{ where } G = \nabla I(\mathbf{x}_n, t_i) \mathbf{J}_W(\mathbf{x}_n, \mathbf{0}) \;;$$

The initial approximation of $\Delta \mathbf{p}^0$ is $\mathbf{0}$, because of constraint $W(\mathbf{x}, \mathbf{0}) = \mathbf{x}$.

Let's define the formula for the motion model $W(\mathbf{x}, \mathbf{p})$ for the case of 6DOF motion of a rigid body under perspective projection $\mathbf{P}$ (we use OpenGL formulations for the projection matrix). Let the point of the body having eye coordinates $\mathbf{X}_e = (x_e; y_e; z_e; 1)^T$ is projected into the pixel of the frame I_i having window coordinates $\mathbf{X}_w = (x_w; y_w; z_w)^T$. Let the point $\mathbf{X}_e$ moves into the new position $\mathbf{X}'_e = \hat{\xi}(\Delta \mathbf{p}) \mathbf{X}_e$, where $\hat{\xi}$ is the twist transform matrix [5]; $\Delta \mathbf{p} = (\omega_x, \omega_y, \omega_z, t_x, t_y, t_z)^T$ is the increment of the motion parameters vector.

Using OpenGL formulas of coordinate transformations, we can define the association between $\mathbf{X}_w$ and $\mathbf{X}'_w$, where $\mathbf{X}'_w$ is the window coordinates in of the $\mathbf{X}'_e$ projection:

$$\mathbf{X}'_w = WindTr \left(PerspDiv \left(\mathbf{P} \hat{\xi}(\Delta \mathbf{p}) \mathbf{P}^{-1} (2x_w / p_x - 1; 2y_w / p_y - 1; 2z_w - 1; 1)^T \right) \right)$$

where *WndTr* is window transform, *PerspDiv* is perspective division operation.

To reduce computational complexity of the formula, we save coordinates $\mathbf{X}_e$ for each pixel of $\mathbf{X}_w \in \Omega$, and then rewrite as follows:

$$\mathbf{X}'_w = WindTr\left(PerspDiv\left(\mathbf{P}\hat{\xi}(\Delta\mathbf{p})\mathbf{X}_e\right)\right). \tag{9}$$

Eq. (9) defines the motion model $W(\mathbf{x},\mathbf{p})$, and the components of the Jacobian $\mathbf{J}_W(\mathbf{X}_w,\mathbf{p})$ at point $\mathbf{p}=\mathbf{0}$ as calculated as follows:

$$\mathbf{J}_W = \begin{pmatrix} \varphi_1 x_e y_e & \varphi_1(-x_e^2 - z_e^2) & \varphi_1 y_e z_e & \varphi_1(-z_e) & 0 & \varphi_1 x_e \\ \varphi_2(y_e^2 + z_e^2) & \varphi_2(-x_e y_e) & \varphi_2(-x_e z_e) & 0 & \varphi_2(-z_e) & \varphi_2 y_e \end{pmatrix}$$

where $\varphi_1 = p_{11}p_x / 2z_e^2$, $\varphi_2 = p_{22}p_y / 2z_e^2$.

In eq. (5) we used only the linear part of function increment, so calculated $\Delta\mathbf{p}$ is *approximate*. We have to substitute $\Delta\mathbf{p}$ into the motion model function and *inverse*-warp the image I_{i+1}, by defining $I_{i+1}(\mathbf{x}) = I_{i+1}(W(\mathbf{x},\Delta\mathbf{p})) \quad \forall\mathbf{x} \in \Omega$. Then the $\Delta\mathbf{p}$ estimation should be repeated. The termination criteria for this iterative process is $\left\|\Delta\mathbf{p}^l\right\| < \varepsilon$, where l is the iteration number; ε is the desired accuracy. After the accuracy ε is reached, head configuration $\mathbf{c}_{i+1}$ can be extracted of the resulting warp function composition.

The used image warping formula can be named *inverse* one, comparing with the *forwards* formula $I_{i+1}(W(\mathbf{x},\Delta\mathbf{p})) = I_{i+1}(\mathbf{x}) \quad \forall\mathbf{x} \in \Omega$.

By warping the image I_{i+1} we make it more close to the image I_i. Of cource, it is possible to warp I_i instead of I_{i+1}, but the first way is more computationally effective, since the Hessian and spatial image gradient is constant accross the iterations.

In practice, when you deform the image I_{i+1}, and then deform the result of the deformation $I_{i+1}^{(1)}$ and so on, you can see that the image $I_{i+1}^{(l)}$ loses the quality and becomes blurred (l is the number of iteration). To preserve the good quality of warped image, always warp I_{i+1} and use the composition of warping functions

$W^l(\mathbf{x}) = W(...W(W(\mathbf{x},\Delta\mathbf{p}^1),\Delta\mathbf{p}^2),...,\Delta\mathbf{p}^l)$. For example, if the motion model looks like a matrix transform $\mathbf{X}'_e = \hat{\xi}(\Delta\mathbf{p})\mathbf{X}_e$, then the warp composition looks as the matrix multiplication.

Conclusion

In [1], image registration algorithms are divided into 4 classes: forwards additive, forwards compositional, inverse additive and inverse compositional. ICA is the most attractive because of less constrains on the warp function. ICA requires that the Jacobian is to be computed at $\mathbf{p}=\mathbf{0}$, the Hessian doesn't depend on $\Delta\mathbf{p}$, which reduces computational complexity, since the calculation is to be performed once.

In this paper, we have shown how the inverse compositional image registration algorithm can be used for tracking head with 6 DOF.

References

1. Baker S. Lucas-Kanade 20 Years On: A Unifying Framework: Part 1 / S. Baker, I. Matthews // CMU-RI-TR-02-16, Robotics Institute, Carnegie Mellon University. Pittsburg – 2002. – 47 p.
2. Zenik-Manor L. Optical Flow Field. Caltech, Oct. 2004. – 47 p.
3. Lucas B. An Iterative Image Registration Technique with an Application to Stereo Vision / B.D. Lucas, T. Kanade // Intnl. Joint Conf. Artif. Intell, 1981. – P. 674–679.
4. Szeliski R. Image Alignment and Stitching: A tutorial // Foundations and Trends in Comp. Graphics and Comp. Vision – Hanover, MA: Now Publishers Inc, 2006. – Vol. 2, No. 1. – P. 1–104.
5. Robust Full-Motion Recovery of Head by Dynamic Templates and Reregistration Techniques / J. Xiao, T. Moriyama, T. Kanade, J. Cohn // Intnl. J. Imaging Systems and Technology – N.Y.: Wiley. 2003. – Vol. 13. – P. 85–94.

DEVELOPMENT OF A COMPUTER MODEL OF A POWER PART

OF THE CONVERTER - SILICON RODS COMPLEX

R.K. Lidovskiy, A.G. Gorunov

Scientific Advisor: Ph.D. in Engineering Sciences A.G. Gorunov

Tomsk Polytechnic University, 634050, Russia, Tomsk, Lenin Avenue, 30

E-mail: lidovskiy@sibmail.com

Silicon - the basic semiconductor material used in modern microelectronics, power electronics, solar power engineering. State of polycrystalline silicon production (the main raw material), substantially determines the level of development of high-tech industries.

For the production of silicon Siemens-process is mainly used: in the channel gas-vapor mixture of silanes and hydrogen on the surface of the rods, that are heated to 1000–1200°C, the process of reduction of silane and the deposition of free silicon is occurred [1].

Analysis of existing technologies for high-purity polycrystalline silicon with the usage of direct current (DC) has showed the presence of a number of disadvantages:

–   Nonuniform temperature profile, which leads to nonuniform distribution of electric current in the rod. The central part of the rod is heated more than the surface layer. As a result, deposition of silicon on the rods is deteriorating, and the central part is heated to the melting temperature, that can lead to the destruction of the rod;

–   The presence of radial temperature gradient [2] not only limits the maximum radius of the obtained rods (about 150 mm), but also leads to substantial internal stresses in the volume of the rod, that can cause its destruction in the process of cooling down at the end of the technological process;

–   The high cost of electric energy in the process of hydrogen reduction.

Effective solution for these problems is the use of sources of high-frequency alternating current (AC) realizing the skin effect - the distribution of high-frequency electric current mainly in the surface layer, when it flows through a conductor.

In progress of works it is necessary to develop mathematical support, including mathematical models of the rods heating subsystem, hydrogen reduction installation base, with the use of pulsating current.

One of the important points in the modernization of technology is the development of power converter that meets specified technological parameters.

Modeling will be performed in the environment «Matlab / Simulink» with the library «Sim Power System» [3].

The first step is the simulation of power converter based on the use of direct electric current.

Generalized model of the power converter is shown on Fig.1. The chart contains a DC source (E), a power circuit (PC), the load (R), a choke (L).
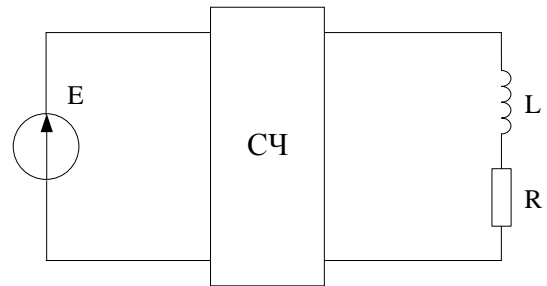
Fig.1. Generalized model of power converter

Current control block based on power transistors, controlled by high-frequency pulse, that forms a block of pulse-width modulation (PWM). Also, the device has a choke, which is connected in series with the transistors and with the load of the silicon rods. During the closed state of the transistor key, load circuit close the diodes that connected to the outputs of transistors in the opposite direction. Furthermore diodes perform a protective function - to protect the transistors from reverse voltage spikes that appear when you turning-off the power key.

Connection circuit of transistors is shown in Fig.2. It contains three power transistors (VT1-VT3) that are connected in parallel, pulse-width modulator (1), driver control (2), diodes (VD1-VD3) [4].
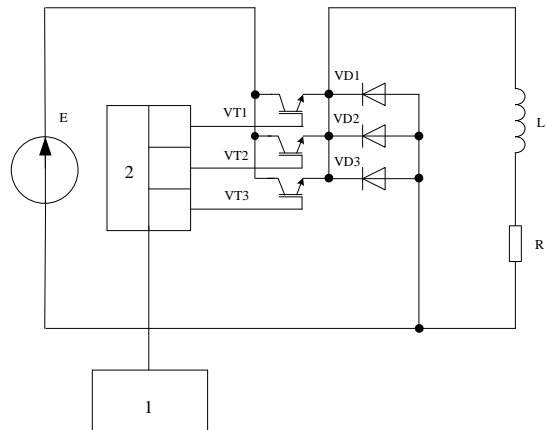
Fig.2. Connection circuit of transistors

Device operation include the following:

The voltage is input on the power transistors. The pulse-width modulator control their work and the current in the load and choke respectively. The current magnitude depends on the form of the pulse control signal of transistor. The longer the pulse for the opening of the transistor, the greater current magnitude in the load. The pulse duration depends on the selected current magnitude and carrier frequency.

The work of power key with three transistors models the work of power key in the circuit with one transistor (see Fig.3).
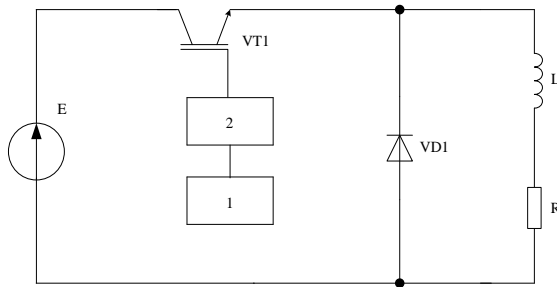
Fig.3. Connection circuit of one transistor

However, in the circuit with a group of transistors, they switches on in turn (see Fig.4).
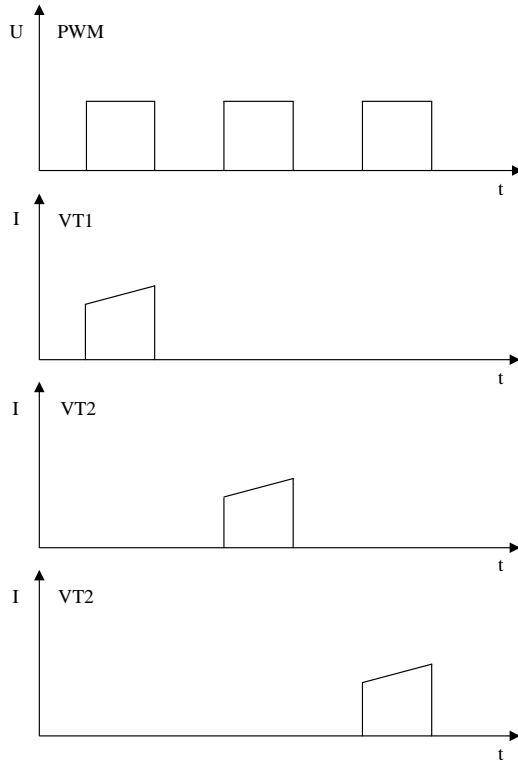

Fig.4. Diagrams of the PWM voltage and currents of transistors

Such circuit allows to reduce heat load on each transistor, which is an important factor in the device operating because when a voltage of about 220 V the pulse current in the transistor can reach 2 kA.

DC in the load is realized by applying of the choke and power diodes, that connected in the opposite direction relative to the power transistors (see Fig.5).
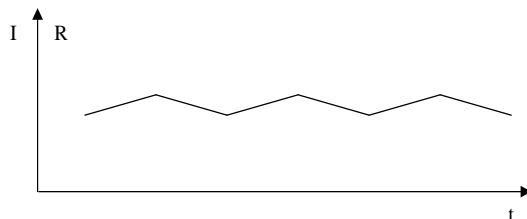
Fig.5. Diagram of the current in the load

Thus, the first phase of problem formulation on modeling the possibility of using high-frequency alternating current for heating the semiconductor cylindrical elements is completed. Further stages are:

−   Development of a mathematical model of the power converter of the subsystem heating rods, the base of hydrogen reduction installation, with the use of pulsating current. The mathematical support should include computer models that can simulate (calculate) the pulse shape of pulsed current according to the frequency and circuit parameters of the power converter;

−   Analysis of the technological process at different frequencies and shapes of current, in order to determine the optimal parameters of the curcit power converter;

−   Development of recommendations for using high-frequency current for heating the silicon rods to increase the efficiency of the technological process of polycrystalline silicon production;

−   Development of technical solutions to improve the program-technical tools of power converter of rods heating subsystem.

The main planned effect of the application of the results of developments are the following:

−   Considerable energy saving;

−   Decrease in equipment cost by eliminating of expensive chokes;

−   Alignment of the radial temperature profile in the rods;

−   Increase in the deposition rate of silicon, increase in productivity, decrease of process time.

References

1. E.S. Falkevich, E.O. Pulner, I.F. Chervony etc. Technology of semiconductor silicon - M.: Metallurgy, 1992. – 408p.

2. G. del Coso, I. Tobıras, C. Canizo, A. Luque. Temperature homogeneity of polysilicon rods in a Siemens reactor. / Journal of Crystal Growth 299 (2007) 165–170.

3. S.G. Hermann-Galkin Computer simulation of semiconductor systems in MATLAB 6.0. - St. Petersburg, 2001 pp. 148-150.

4. Pat. 2346416 RU, IPC N05V 1 / 02. Device for controlled heating of silicon bars / P.M. Gavrilov, M.G. Istomin, A.P. Prochankin etc. - Publ. 10/02/2009.

MATHEMATICAL MODELING OF THE SECURITIES MARKET

Lyudmila S. Makarova, Anastasia E. Dzyura

Scientific supervisor: Aleksandr V. Kozlovskih, Associate Professor, Ph.D.

Language supervisor: Ekaterina S.Samsonova,

Tomsk Polytechnic University, 634050, Russia, Tomsk, Lenin Avenue, 30

dzyura_nastya@sibmail.com

Introduction

The task of forecasting bid procedure in the stock market has not lost its relevance since the emergence of the stock market and stock exchanges as a mechanism for organization and management of investment processes. Currently, technical and fundamental analysis are considered traditional approaches to building stock projections. However, predictions derived from the classical methods of technical analysis often contradict each other and pose a potential investor in a deadlock. In addition, crises that arise in recent years in various financial markets around the world indicate a lack of effective management in the stock market.

Thus, the creation of reliable methods of predicting the pattern of the investment process has two objectives:

a) support of decision-making by individual bidders in the operations on the stock market;

b) taking adequate measures to control the market itself.

One of the most effective approaches to building a prediction system is to create a mathematical model of the process.

Problem setting

Source data are a common database - spreadsheet, which contains daily stock quotes, including the opening and closing prices of trades, minimum, maximum and average price of shares recorded in the trading day and trading volume.

Date	Volume	Minimum	Maximum	Close	Open	Average
23.03.98	56668700	1,82	1,99	1,98	1,85	1,93
24.03.98	25649300	1,98	2,03	2,00	2,00	2,00
25.03.98	20835000	1,97	2,01	2,00	2,00	1,99
26.03.98	18775100	1,94	1,99	1,99	1,99	1,97
27.03.98	26710900	1,97	2,00	2,00	1,98	1,99

Table 1. Source data

In graphical form the data are presented in Figure 1. Traditionally, trading volume is presented in the form of bar charts, and prices are in the form of vertical bars with marks of bid close.
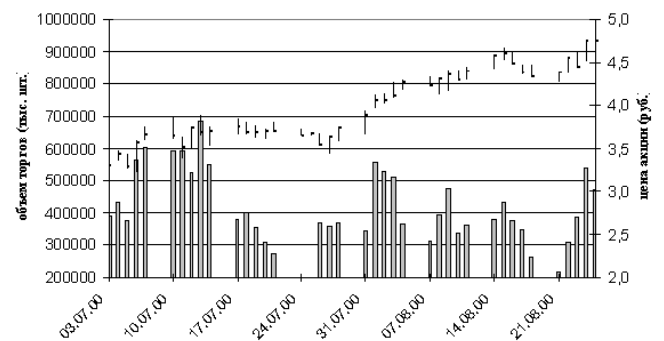
Fig1. Pictorial representation of source data

Suppose we want to build a forecasting system (predictor) with the foresight in 1 step from the original sample, i.e., to calculate the value of N +1- th h_{N+1} time series $h_1, h_2, h_3, ..., h_k, h_{k+1}, ..., h_{k+m}, ..., h_N$ of the system by N previous. To solve the problem we will use a three-layer neural network with $N_1 = m - 1$ neurons in the input layer and $N_3 = 1$ neuron in the output. In this case, the input data is represented as an m-1-dimensional z-vectors. Components of z-vectors $h_{k+1}, h_{k+2}, ..., h_{k+m-1}$ are fed to the N_1 input neurons, respectively (k in the learning process is chosen randomly from a sample at each step of training). At the output neuron quantity h_{k+m} is served as a desired outcome in the learning process. According to Takens theorem, for some values of m there must exist a function F, that

$$h_{k+m} = F\left(h_k, h_{k+1}, ..., h_{k+m-1}\right)$$

Now, if we want to continue the time series, it is enough to submit to the input of the network $h_{N-m+1}, ..., h_N$ components of time series and obtain the desired value of output - h_{N+1}.

Further, if the objective is a long-term prognosis, i.e. finding the values $h_{N+1}, h_{N+2}, ...$ can be handled as follows: each received output value of h used as input to the next step in testing. For example, to get the value h_{N+2} you

want to submit to the input values $h_{N-m+2}, \ldots, h_{N+1}$ etc.

In testing to verify the quality of training neural network values $h_{N+1}, h_{N+2}, \ldots$ calculated as forecast, compared with previously known values of the time series

Forecasting Lorentz system time series

The problem consists in determining the share price for several days in advance, based on available data for the previous time period. No less important is the result of evaluation of the trend appearance probability.

Chaotic behavior can be observed in very simple systems, such as a system of three ordinary differential equations. The so-called "Lorenz system serves the basic model and the test object of several techniques in studies on dynamic chaos:

$$\dot{X} = \sigma(X - Y)$$
$$\dot{Y} = rX - Y - XZ$$
$$\dot{Z} = XY - bZ$$

The trajectories of this system for all positive values of the parameters are in some areas in the phase space X, Y, Z, i.e. the system has an attractor and which is inside the sphere.

Fig. 2 and Fig. 3 show the normalized time series of Lorenz system.
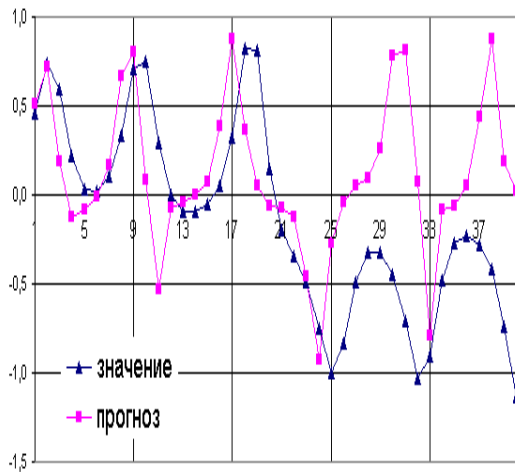
Fig. 2. Forecasting of time series values of the Lorentz system
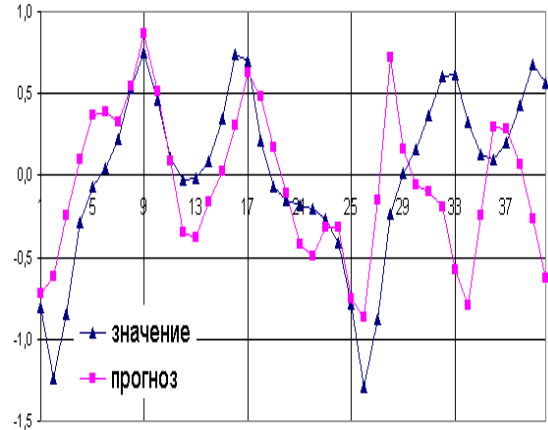
Fig. 3. Forecasting of time series values of the Lorentz system

Conclusion

Self-organization of people in the course of trading on the stock market leads to the formation of several groups of stakeholders in the investment process, determining the dynamics of the process in general. At the absence of intervention "from outside", this dynamic is easily predicted. Examples of such interference may be messages in the media, as well as the actions of large investors, which were not included in the training sample.

References

1. Document management and business processes [electronic resource]. - Mode of access: http://www.intellectika.ru/index.php, free.

2. Portal about consulting [electronic resource]. Mode of access: http://www.consult.ru/themes/default/publication.asp?folder=1924&publicationid=414, free.

3. Official site of the company DocsVision [Electronic resource]. Mode of access: http://docsvision.com/index.phtml?Name=Analytics

4. Official site consulting system DSS Consulting [Electronic resource]. Mode dosupa: http://www.dssconsulting.ru/index.phtml?id_page=81, free

5. Document management system and business процесами DocsVision 3.6 SR1. Brochure .2006 city-46s

FOLLOW-PHASE FREQUENCY ALGORITM OF TRACKING SEISMIC OF WAVES THE CONTROLLED QUALITY FUNCTION EXTENSION

Ekaterina V. Maneeva

Scientific adviser : Viktor P. Ivanchenkov, Associate Professor, Ph. D.

Language Supervisor : Ekaterina S. Samsonova,

Tomsk Polytechnic University, 634050, Russia , Tomsk, Lenin Avenue, 30

maneyka@sibmail.com

At present, to increase the efficiency and quality of processing seismic data obtained during the search for oil and gas fields is of great importance. Thus one of the most important elements of the development of software systems is the development of reliable methods and algorithms for tracking seismic waves. The most widely used are the tracking algorithms which mainly use energy characteristics of seismic waves as informative features. Recently, a number of spectral tracking algorithms, based on information properties of the phase spectra of reflected seismic waves is also proposed [2,3]. The research and application of phase-frequency algorithms (PFT) have shown that they allow to detect and provide signals to the background of intense noise in conditions of significant prior uncertainty. Among the proposed phase-frequency algorithms an algorithm with the equilibrium and nonequilibrium processing can be distinguished, which found application in data processing ground and borehole seismic survey [2]. The generalized quality function of these algorithms can be represented as:

$$L(\tau) = \sum_{k=1}^{m} W(f_k)\cos(\varphi_x(f_k) - 2\pi f_k \tau), \qquad (1)$$

where $W(f_k)$ - a weight function, $\varphi_x(f_k)$ - instant phase spectrum of allocated land seismic trace. Temporary provision of signals is measured by the extremum function position, which is formed when moving window analysis along the seismic trace (Figure 1).
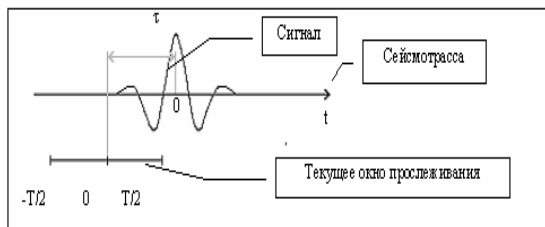
Fig.1. Diagram illustrating the phase-frequency tracking of seismic waves

For the balanced algorithm $W(f_k)$ is believed to equal one throughout the frequency band analyzed, for algorithms with non-equilibrium processing – the algorithm is defined in triangular or exponential form. As studies in the above algorithms have shown, the implemented quality functions have a relatively large extent and rather high level of side lobes. In the report phase-frequency tracking algorithm, which quality function length may vary to improve the resolution of signals in the area of their interference is considered. Given that the phase spectrum of seismic signals is close to the stationary spectrum the following constraints can be superimposed on the region of spectra summation current phase (Fig.2)

$$a(f) = 2\pi f \frac{T^*}{2} = \pi f T^*, \qquad (2)$$

Where T^* - defines the length (duration) of the quality function in the possible location of the signal.
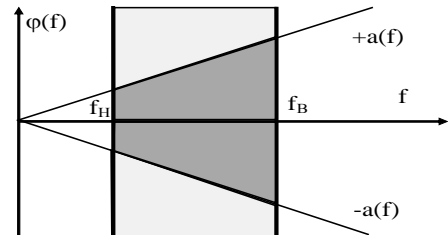

Fig.2. Summation area of the current phase spectra

The algorithm quality function can be represented in the following form:

$$L(\tau) = \sum_{k=1}^{m} F\left(\frac{\varphi_x(f_k,\tau)}{a(f_k)}\right), \qquad (3)$$

where $a(f_k)$ is limitations of $\varphi_x(f_k,\tau)$ the form (2). The $F\left(\dfrac{\varphi_x(f_k,\tau)}{a(f_k)}\right)$ function, called phase-changing function must satisfy the following condition:

$$F\left(\frac{\varphi_x(f_k,\tau)}{a(f_k)}\right) = 0, \ |\varphi_x(f_k,\tau)| > a(f_k), \qquad (4)$$

At signals tracking (Fig. 1.) small displacement of the window leads to a change in the current phase of the spectra, which are close to linear [3]. Therefore, imposing restrictions on the range of the current phase change in the spectra in the used algorithm the time length of the extremes of the quality function can be reduced. (Fig.3)
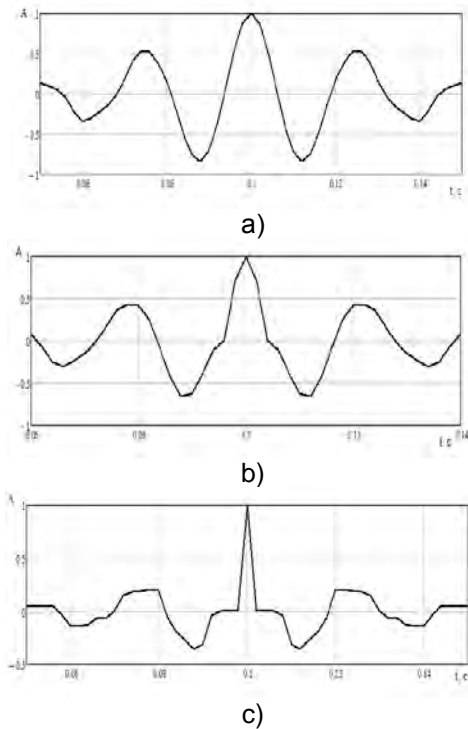
a)

b)

c)

Fig. 3. Quality function of PFT algorithm:

  a - the algorithm with the equilibrium processing,

  b, c - the algorithm with controlled length of the quality function (b - $T^* = 0.008\,c$, c - $T^* = 0.004\,c$)
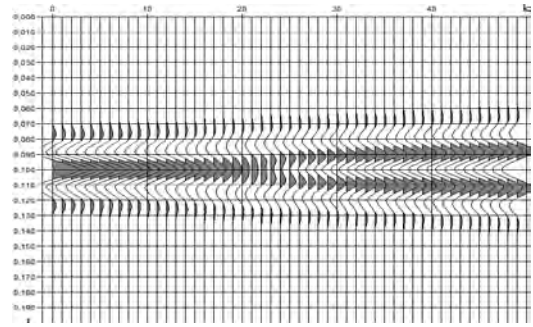

Fig. 4. Wave field model with the parameters of the signal ($t_0 = 0.1\,s$, $f_0 = 40\,Gc$, $\beta = 60$, $\varphi_0 = 0$)

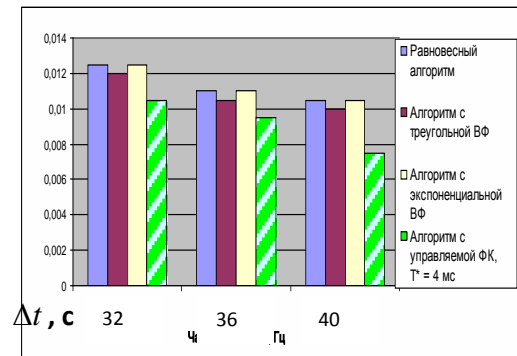Fig. 5. Evaluation of the resolving power of PFT algorithms depending on the values of fundamental frequency signals (BK - weight function, ФК - quality function)

As an example, in Figure 3 (a, b, c) of the quality functions for algorithm with equilibrium processing obtained in the same conditions (Fig.3 a) and proposed to the tracking algorithm (Fig. 3 b, c) are shown. They show that the application of the algorithm allows to significantly reduce the length of the main lobe of the quality function and side lobe level, thus improving the resolution of signals in their areas of intense interference.

To compare the resolving power of different PFT algorithms the study on models of wave fields in zones of interference emissions signals (Figure 4) was carried out. Fig. 5 shows the graphs $\Delta t = \varphi(f_0)$ defining the Δt signal resolution assessment depending on the f_0 harmonics frequency in their spectrum having the largest amplitude. They show that the proposed algorithm has the highest resolution. Also the research of resolving power of the algorithm when changing the number of its parameters and parameters of assignable signals. In general, studies have shown that the application of the proposed algorithm allows to increase the resolution of signals in approximately 1.5 times compared to the previously known PFT algorithms.

References

1. Boganik GN, Gurvich, II Seismic. - Tver: AIS, 2006. - 744 pp.

2. Ivanchenkov VP, Vylegzhanin ON, Orlov OV, Kochegurov AI, Kozlov AA Methods of frequency analysis of wave fields and their application to problems of processing seismic data / / Proceedings of the Tomsk Polytechnic University. - Tomsk, 2006. - T.309. - № 7. - S. 65 - 70.

3. Ivanchenkov VP, Kochegurov AI Determination of the temporal position of seismic signals to measure their phase-frequency characteristics / / geology and geophysics. - 1988. - № 9. - S. 77-83.

MAKING REPORTS IN OBJECT-ORIENTED
GEOGRAPHIC INFORMATION SYSTEMS FOR AGRIBUSINESS

Markov A.V., Sherstnev V.S.

Scientific supervisor: Sherstnev V.S.

Language supervisor: Pichugova I.L.

Tomsk Polytechnic University, 30, Lenin Avenue, Tomsk, 634050, Russia

E-mail: MarkovAV@tpu.ru

Nowadays, information technologies penetrate into all areas of human activity, even such seemingly unrelated sphere as agriculture. It is clear that a reasonable implementation of modern information technologies will simplify the collection and processing of statistical data and provide new tools for its analysis. Moreover, it will reduce errors and facilitate the routine work with documentation, thereby increasing labour productivity.

Since virtually all information on the resources of agriculture has spatial references, it is obvious that using geographic information technologies in this subject area is necessary and justified.

To meet the challenge of sustainable development of agricultural complex it is necessary to know precisely the current state of agricultural land, i.e. to conduct their monitoring. The collection of such information is performed by a number of centres and stations of the agrochemical service, which are the structural units of the Department of Plant Growing, Chimicalisation and Plant Protection of the Ministry of Agriculture of the Russian Federation. The main purpose of the agrochemical service is to monitor the fertility of agricultural lands. In the course of its activities the agrochemical service generates a large amount of various report documentation.

The authors of this paper are developing a geo-information system aimed at labour automation of the federal state agencies of agrochemical service, dealing with agricultural land analyzing in our country and its usage control. For the reason that there is a lot of official documentation, that is strictly regulated by directives but changed rather often, the proposed system is based on two-tier client-server architecture. The server part of the system consists of an application server with the installed DBMS of the company, and the automated workspaces designed for specialists are its clients. Due to the analysis of business processes at the enterprise, the authors did not find it necessary to use three-tier architecture with the Internet access. One of the main reasons behind this decision is that the basic life cycle of the data used by the system is located within one enterprise, whose premises are usually modest.

According to the functional needs of the system, the following subsystems are proposed: "Administrator", "Data entry", "Cartographic information preparation" (a subsystem of the surveyor and geodesist), "Data Analysis", "Output data". The main purpose of decomposing the system into subsystems and creating individual workstations for specialists of the agrochemical service is mainly to simplify the user interface. If necessary, it is possible to call functions of one subsystem from the other subsystems. For example, it is possible to inquire various reports from the input subsystem.
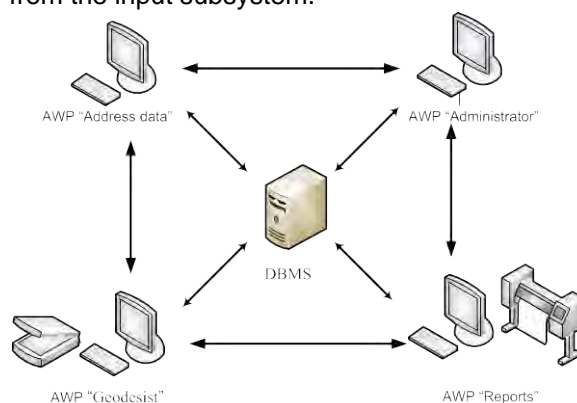

Pic.1. The overall structure of the system

One of the problems the developers have faced is the creation of high-quality and informative reports. The needs analysis shows that, as a rule, reports of two types are required. The first type of reports is "static" reports with almost unchanging pattern. The forms of these reports are often regulated by law, and they are assigned to be part of the routine circulation of documents in the organization. Unfortunately, most of the programs existing on the market today only contain built-in reports of this type, as they are intended to solve short-term tasks rather than strategic ones that involve a comprehensive analysis of cumulative and ever-changing data and long-range planning of company's activities. The problem of maintaining "static" reports comes to replacing the templates when it's time to update software application or to update existing forms of documentation.

In order to analyze and plan it is necessary to have a completely different type of reports – "dynamic". Their patterns are constantly changing; they provide graphical data representation, complex sorting, grouping and formatting. The main purpose of "dynamic" reports is to provide chief executive officers and top managers with comprehensive information in a convenient way for analyzing and planning company's activities. The necessity for complex reports, especially in the financial analysis, is very high. There is only one way to solve this problem, i.e. to give the user a simple, reliable, powerful tool so that he will be able to make the necessary reports quickly.

Traditional development tools are aimed at programmers, and they are too complicated for ordinary users. To solve this task it is better to apply a specialized report generator with user-friendly, intuitive interface, but with powerful tools for data processing and representation at the same time. A market leader among such programs is Crystal Reports by Seagate Software company. Also, a number of other up-to-date report generators, capable of working with a GIS, such as Fast Report, Stimulsoft Reports and Dream Report, have been considered. But after comparing their technical characteristics, Crystal Reports has been chosen.

Though Crystal Reports has a considerable amount of built-in functions for data processing, including functions for specialized statistical and financial analysis, it was necessary to write a large number of stored procedures running on the server side and providing the necessary data in the proper format.
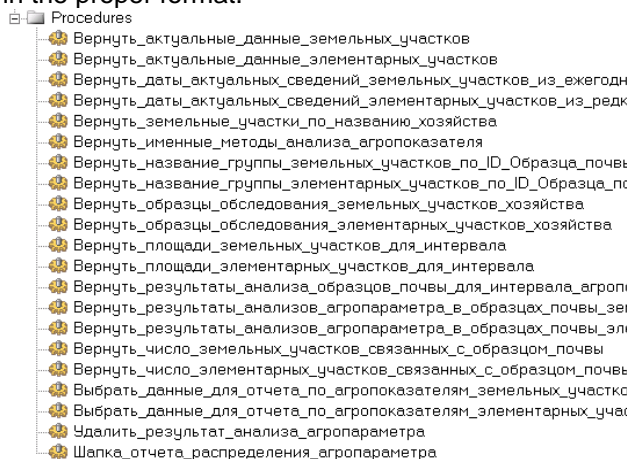
Pic.2. A list of stored procedures

Thus, a kind of intermediate interface between the database and the module for generating reports has been created.

Pic.3. A scheme fragment for stored procedures interaction

At present, there are several dozens of reports, created in accordance with the State Standards by developers. Moreover, there is the possibility to dynamically create new forms of reports and modify the existing ones by users themselves applying the standard editor built in Crystal Report.

References:
1. ESRI. ArcGIS Engine. [Electronic resource]. – 2010. – Access mode: http://www.esri.com/software/arcgis/arcgisengine/index.html
2. Crystal Reports and Xcelsius Software // Powerful Dashboarding and Reporting for IT and Business Users. [Electronic resource] – 2010. – Access mode: http://www.sap.com/solutions/sapbusinessobjects/sme/reporting-dashboarding/index.epx

GAS ODORIZATION

<u>Novak E.K.</u>, Faminkov I.A., Rudnicki V.A.

Scientific adviser: Yurova M.V., senior teacher of English

Tomsk polytechnic university, 634050, Russia, Tomsk, Lenina str. 30

E-mail: ege1992@sibmail.com

Odorization is a process of odorant delivery to gas stream on the output line of the gas distribution station for the purpose of giving the characteristic smell to gas.

Systems which realize odorization process called odorizing systems. Exist two different kinds of odorizing systems:

- Odorizing injection systems;
- Lapping odorizing system.

Odorizing injection systems

The odorizing injection system was specifically designed to guarantee a constant odorization rate regardless of the gas flow rate, the type of odorizer employed, and the required odorization rate.

The odorizing systems used up until now have several disadvantages from the point of view of operation as well as safety, as summarized below:

- Very low precision;
- Difficulties regarding calibration and regulation;
- Low operational flexibility;
- Difficulties in communications between men and machine.

The lack of precision inherent to the lapping system is compensated for by the system's operating principle. The electronic regulator receives the amount of gas dispensed and the amount of odorizer injected and, based on its programming parameters, it sets the number of impulses to be sent to the injector or the metering pump to guarantee the set odorization rate.

Lapping odorizing system

The odorizing system's functioning is based on a property that is common to all substances in the liquid state: the production of a certain amount of vapor. Basically the system consists of: a tank with a certain capacity, two connectors for adding odorizer, two connectors for connection to the main methane gas line, two connectors for the level, a connector for emptying the tank, a reinforced (reflection, magnetic) stainless steel level gauge, and a containment tank.

The choice of the odorization system is tightly correlated to the typology of the plant:

- Odorizing injection systems is the solution for the big installations;

- Lapping odorizing systems is ideal for small-medium installations. [2]

Odorization in automatic mode

Block of odorization (pic. 1) is intended for automatic delivery of odorant to gas stream on the output line of the gas distribution station, in proportion to its consumption.

Pic. 1. Block of odorization

Block of odorization provides:

- Automatic odorization of gas in proportion to its consumption;
- Storage of odorant resources in the container;
- Giving out the remote signal about lack of odorant;
- Discharge of odorant vapor in output pipes of gas distribution station when filling in;
- Accounting of used up odorant.

Block of odorization realizes odorization with automatic or manual modes. Odorization block can be done in three ways:

- With built-in system of technological measurement of gas consumption.
- With information about gas consumption from outside sources.
- For underground setup with gas consumption from outside sources.

When gas goes through the pipe, the pressure difference appears on the diaphragm of restriction (cress device) of commercial account

of gas. The pressure varies in proportion to gas consumption through the pipe.

Sensors of pressure difference provide analog signals to the automatic system of gas distribution station. When the definite quantity of gas go through, automatic system of gas distribution station will give the information about consumption of gas in the microprocessor of odorization block. This block will switch on the pump of the batch plant, and then introduction of odorant will go on in the stream of gas.

Block of odorization consist of:
1.   Batch plant, includes:
   - Batching membrane arrange;
   - Reducer of pressure difference;
   - Container.
2.   Service tank, contains reserve of odorant (160 liters) for period of service.
3.   Reserve container, contains 6.5 liters of odorant for period of fill up.
4.   Gaging container, controls gas consumption.
5.   Ejector, moves off the odorant's vapor and decrease of pressure in service tank.
6.   Observation port, is intended for visual control under the odorant entry to the output line then block of odorization set in automatic mode.
7.   Dropper, executes visual control under the odorant entry to the output line then block of odorization set in manual mode.
8.   Stop cocks, realize switching on and turning off some units.
9.   Safety valve, performs automatic pressure decreasing in service tank and communication of odorization block.
10. Filter and dump box, are intended for gas purification from mechanical additives and water.
11. Connecting boxes, join and branch power and supervisory cables, automatic and telemechanics systems. This boxes have implosion protection.
12. Block of control, controls under the batch plant in a few modes.
13. Heater, heats up elements of odorization plant. This element also has implosion protection. [1]

Odorizer nature

The odorizing substance is based on tetrahydrothiophene (99% THT) or mercaptan mixture (50% TBM, 50% THT). The consist of odorant depends on odorization method (pic. 2).

Tetrahydrothiophene (THT) Mercaptan Blends		
Component	Spotleak® 1013 (%)	Spotleak® 1039 (%)
THT	100	50
TBM	0	50
Odorization Method	Vaporization or Liquid Injection	Liquid Injection

Pic. 2. Odorizing substance consist

There is a formula for extent of odorization:

$$K = \frac{19.1 \cdot 1000}{V_n \cdot Q} 100\%,$$

where Q – consumption, V_n – used odorant volume. [3]

Odorization monitoring

Who manages a network gas needs to check out the odorization level many times in a day. Infact, two risks must be detected:
   - waste (for excessive use of odorant);
   - danger (for insufficient use of odorant).

There are many devices, destined to odorization monitoring. One of them – Edor (pic. 3), allows to control odorization constant from the web.

Pic. 3. Edor in use

Edor is the new sensor for the measurement of the amount of odorant in natural gas, used as remote station of survey. Two kind of odorant can be detected:
   - TBM: Mercaptans ;
   - THT: Tetrahydrothiophene.

Edor employs electrochemical cells developed for this application, specific for each odorant.

Thanks to Edor it's possible to control the state of odorization of network: the measures are normally carried out 4 times per day and sent out for remote control by SMS every day.

Edor is composed by:
   - Microprocessor unit with modem GSM (opt.: GPRS, PSTN, FTP, mail);
   - Data acquisition system analyzer unit;
   - Electrochemical cell easily replaced (SNAP-IN);
   - Time controlled electrovalve that drives the flow of sample gas from main line to sensor.

By means of a SW correction in temperature, standard precisions reached is less than 15%, with no interfering substances. With the accessory Sampling System (option SS), precisions of 10% can be reached, thanks to periodic autocalibration carried out by means of a cylinder of calibration gas connected to a second electrovalve. Without option SS, it is however possible the periodic calibration (one person calibration).

The Edor system can be installed in: odorization plants (to verify the intake of the odorant in gas), characteristic points (to measure the true condition of network), at the end of network (to have the real situation in critical points, through all the day). [2]

References:
1. Gas-distribution station operator workbook. GazpromTransgazTomsk. Tomsk, 2008.
2. http://www.cpl.it/en/product_services/gas/gas_odorization
3. http://www.arkema-inc.com/
4. http://www.tsctulsa.com/

THE DEVELOPMENT OF SOFTWARE FOR ORGANIZATION DATA EXCHANGE BETWEEN NODES OF CAN INDUSTRIAL NETWORK FOR MCU SH2A

Dmitry Obukhov, Maxim Rechkin

Scientific adviser: V.V. Ofitserov, M.V. Yurova

National Research University of Resource-Efficient Technologies "TPU"

obukhovds@gmail.com

Introduction

Controlled, reliable and safe connection is needed between elements of the technological process automation. Industrial networks are used for providing such connection. Industrial network is a network of the data transfer, which links different sensors, executive mechanisms, industrial controllers and predominantly used in automated systems of the technological process control. The most prevalent type of industrial network is CAN (Controller Area Network) [1].

Problem statement

The major modern controllers, for example SH7201 of Renesas Technology Company [2-3], have embedded network controller. CAN using experience in the systems of the technological process automation shows unadapted for particular problems interface using does not respond requires, which are presented to system reliable. So that the work aim is development software for organization data exchange between nodes of industrial network CAN for SH7201.

For the aim achievement are needed to solve follow problems:
- study RSK SH7201 and RCAN-ET module of SH7201 features;
- CAN protocols analysis making;
- determine data transfer between nodes algorithm developing;
- in HEW on program languages C and Assembler algorithm realization;
- software efficiency research making.

Study of IN CAN work

In practice CAN is network of "bus" topology [1]. CAN is used for communication so called nodes, consisting from CAN-controller, which provides interaction with network and realizes protocol, and CPU. The data transfer occurs by frames. Useful information in frame consists from ID (11 bit – standard format or 29 bit – expended format) and data field (8 bytes). ID is needed for priority determination at the attempt of the simultaneous data transfer by several nodes and contains frame information. The advantages of CAN – network are an opportunity of work in real time mode, realization simplicity and minimal costs for using, high stability to noises, transfer and receive errors control, wide rate diapason. The disadvantages are low rate for long network, big size of service data in the frame, absence of common standard for high level protocol. The last one we can classify as advantage, because such absence for common standard for high level protocol gives developers opportunity of the different CAN protocols design with any parameters.

RCAN-ET of SH7201 features [2]

The module RCAN-ET of SH7201 has follow features:
- supports CAN2.0B standard;
- has 2 biderictional, two-wire, sequenced data transfer channels;
- every channels has 16 programmable "mail boxes" (buffers);
- size of the data frame is 0 to 8 bytes;
- data transfer rate is up to 1 Mbits (clock frequency – 40 MHz);
- queue of data with ID;
- has flexible interrupt structure.

The module RCAN-ET consists from 4 common parts: MPI, transfer and receive buffers, buffer control registers set and CAN-interface.

Data transfer software requirements for RCAN-ET of SH7201

By the study of industrial network CAN operation principle, features RSK SH7201, network controller RCAN-ET of SH7201, interrupting structure, and developed base software requirements are produced:

- the 29-bit ID setting for the buffers. Using 29-bit ID the network with a large amount of nodes can be developed;
- data transfer rate (DTR) for hardware can be set from 250 Kbps;
- the biggest DTR is up to 1 Mbps. The 8-byte data time transfer with such DTR is 130 ms;
- the transfer and receive occur in real-time mode, that provides system determinacy;
- using the ring buffers for data transfer and receive. The transfer ring buffer forms the frames queue, which should be transfer. The receive ring buffer are used for the temporary data storage.

The data transfer algorithm development in industrial network

The common data transfer scheme from one node to another for industrial network is shown in the picture.
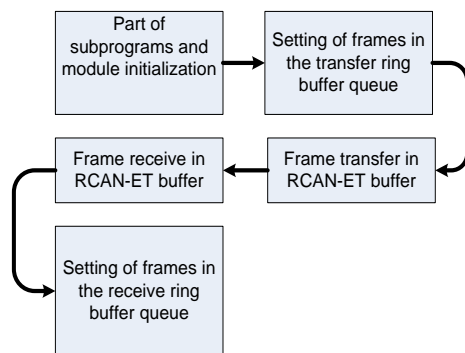
Pic. The common data transfer scheme between nodes in CAN – network

Firstly the frames (strings or data arrays) are defined which should be transferred to one or several nodes. The initialization section is executed by the next stage. It includes:

- microkernel initialization;
- two ring buffers initialization, which contain the transferred and received frames queue;
- MTU2 - timer initialization. This is used for data transfer through particular time (up to 100 ms). It provides determinate data exchange between nodes;

- RCAN-ET initialization. The necessary registers setting is happened and interrupt priority level is defined. After that the frames queue organization into the ring buffer occurs via special function call. This stages are executed in the main function (*void main()*), which also contains the background task (the part of code, which organized as infinite loop). The background task can consist of any quantity procedure calls or be empty.

Conclusion

By the study of industrial network work principles (CAN standard), the RSK SH7201 features with microcontroller on base of SH2A kernel and RCAN-ET and MTU2 modules, RCAN-ET and MTU2 interruption structures and CAN-protocols comparative analysis making obtained the follow results:

- the determine data transfer algorithm from one node to another requirements is developed;
- the procedures are realized in a integrated development environment HEWv4.0 using C, Assembler languages:

a) RCAN-ET-module channels initialization; MTU2 initialization;

b) two ring buffers initialization for frame transfer and receive;

c) frames queuing into the ring buffer for transfer;

d) frame transfer and receive procedures;

e) the receiving frames input into the receive ring buffer;

- testing, which shows software functionality

Literature

1. Description of CAN bus. — Access mode: http://itt-ltd.com/reference/ref_can.html, free enter
2. SH7201 Group Hardware Manual. Renesas 32-Bit RISC Microcomputer SuperH RISC engine Family/SH7200 Series R5S72011. – 2006. – 1208 p.
3. Renesas Interactive.—Access mode: http://www.renesasinteractive.com, free enter
4. SuperH RISC engine C/C++ Compiler, Assembler, Optimizing Linkage Editor. Compiler Package V.9.00 User's Manual. Renesas Microcomputer Development Environment System.- 2004. – 1105 p.

INVESTIGATION OF THE EFFICIENCY OF PARALLEL COMPUTING
BY THE EXAMPLE OF NUMERICAL SOLUTION OF DIFFERENTIAL EQUATION
IN MATLAB ENVIRONMENT

PA Ostrouhov, MV Troshin

Scientific supervisor: A.S. Ogorodnikov, associate professor, PhD

Language supervisor: E.S.Samsonova

Tomsk Polytechnic University, Russia, Tomsk city, Lenin Street, 30

E-mail: Orakul@sibmail.com

This article shows the efficiency of parallel calculations on the example of the numerical solution of ordinary differential equation of first order in the MatLab environment.

Around one million engineers and scientists around the world use MathWorks software solutions. Company products are used in leading technological and financial organizations, research institutes and educational institutions. MathWorks software is aimed at solving various engineering problems and accelerates the creation and implementation of innovative technologies for scientific research in the fields of medicine, ecology, air technology, energetics, education, etc. Recently MathWorks products are extensively used in the field of genetic engineering, the design of economical modeling and analysis of their stability in critical conditions, technologies testing, diagnostics and scientific forecasting [1]. MATLAB is the foundation of the entire family of MathWorks products.

In new versions of MATLAB an enhanced support for multicore and multiprocessor systems is included. MATLAB is an ideal environment for exploring and studying parallel computing, thanks to a multitude of specific examples illustrating the concept of parallel programming. Parallel computing technology is implemented by MathWorks with the use of two interrelated bump packs: MATLAB Distributed Computing toolbox and MATLAB Distributed Computing engine [2, 3]. We have considered this technology on the example of numerical solution of differential equations.

Differential equations are one of the main tools of mathematical modeling of physical and technical objects and processes. For example, let's consider the simplest case - an ordinary differential equation of the 1st order and solve the Cauchy problem for it.

The Cauchy problem for ordinary differential equations of the 1st order is to find the function $y = y(t)$, which satisfies this equation and initial condition $y(t_0) = y_0$, where t_0 and y_0 are set values. We use the Euler method for numerical integration (solution) of the differential equation. In this method, the derivative dy/dt is replaced by difference relation $\Delta y/\Delta t$ where t_0, y_0 calculations are accomplished by the following formula:

$$t_{k+1} = t_k + h;$$
$$y_{k+1} = y_k + hf(t_k, y_k).$$

where $h = \Delta t$ is a fixed lead.

The differential equation which is taken as an example has the form:

$$\frac{dy}{dx} = \frac{2y}{(x+1)} + e^x(x+1)^2.$$

The solution was made by two methods - sequential (on a single machine with one processor) and parallel (on two remote machines with one processor). To implement the second method the following settings must have been entered:

1. Start the mdce (on both machines);
2. Creating and running of jobmanager (on the same machine);
3. Formation of two workers for created jobmanager (one on each machine).

Here are the realization algorithms of both methods:

Sequential algorithm

```
function result = solve_equation(a, b, h, y0)
    mass(1) = y0; % Definition of initial values
    x(1) = a; % Initial value of x
    % Calculation of number of leads
    n = (b − a)/h;
    for i = 1 : n − 1
        % Calculation of next of x and y values
        x(i + 1) = x(i) + h;
        mass(i + 1) = mass(i) + h ∗ ( 2 ∗
            massixi+1+    expxi∗xi+    +12;


    end;
    result = mass; % Return of result
end
```

Parallel algorithm

```
function result = solve_equation_par(a, b, h, y0)
    mass(1) = y0; % Definition of initial values
    x = a; % Initial value of x
    % Calculation of number of leads
    n = (b − a)/h;
    for i = 1 : n − 1
        x = x + h; % Calculation of next of x value
        % Task for second worker
        if labindex == 2
            % Calculation of the first part of next y value
            tmp = h ∗ exp(x) ∗ (x + 1)^2;
            % Sending data to first worker
            labSend(tmp, 1);
            mass(i) = 0;
        end
% Task for first worker − process
if labindex == 1
            % Receiving data from second worker
            tmp2 = labReceive(2);
            % Calculation of resultant y value
            mass(i + 1) = mass(i) + tmp2 + h ∗
             mass(i) ∗ 2/(x + 1);
        end
    end
    result = mass; % Return of result
end
```

The comparative results of the above algorithms are presented in the form of a logarithmic dependence of the computation time from the number of iterations in Figure 1.
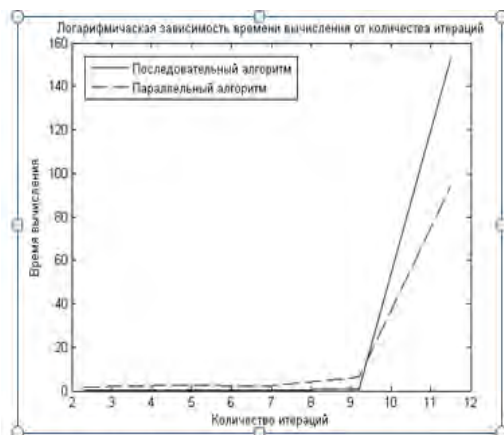
Fig. 1. Logarithmic dependence of the computation time from the number of iterations.

The above chart shows that the parallel algorithms lose to the sequential algorithm in time of calculations consistent with a small number of iterations. However, parallel algorithm significantly improves their performance compared to sequential algorithm with further increase in the number of iterations by reducing the integration step. This result illustrates the effectiveness of using parallel computing for numerical solution of differential equations. According to Amdahl's law, a further increase in the number of cores (processors) will not lead to better results, because this task may not be explicit parallelization. In our problem, some calculations can be made only by sequential calculations, which lead to the necessity of data exchange between processors.

In the future the design and testing of parallel algorithms for numerical solution of differential equations and systems of differential equations by methods of high order of accuracy and get access to the TPU cluster is planned.

References

1. Кетков Ю.Л., Кетков А.Ю., Шульц М.М. MATLAB 7: программирование, численные методы.-СПб.:БХВ-Петербург, 2005.
2. Distributed Computing Toolbox For Use with MATLAB.2004-2006 by The MathWorks, Inc., [Access mode]: http: // www. mathworks. com/ access/helpdesk/help/pdf_doc/distcomp/distcomp . pdf, free.
3. MATLAB Distributed Computing Engine For Use with MATLAB. 2004-2006 by The MathWork, Inc., [Access mode]:http: / /www. mathworks. com/access/ helpdesk/help/pdf_doc/mdce/mdce.pdf, free.
4. Parallel MATLAB Survey, [Access mode]: http://www.interactivesupercomputing.com/ref/par allelMatlabsurvey.php, free.

SYSTEM APPROACH TO THE FORMATION OF LAYERED GEOLOGICAL ABSORBING MEDIA MODELS

Margarita Pokrovskaya

Scientific supervisor: Viktor Ivanchenkov, Associate Professor, PhD

Language super visor: E.S.Samsonova

Tomsk Polytechnic University, 30 Lenin Avenue, Tomsk, 634050, Russia

sunpingvin@mail.ru

Widely used methods for solving the direct problems of seismic prospecting for homogeneous geological environments require the calculation of theoretical seismograms directly in the time domain [1]. In the study of geological layered media with absorption and dispersion it is advisable to perform calculations of wave fields in the spectral region and to pass to the time domain at the last stage of the study. The report covers the problems of formation of the layered absorbing media models within the accepted approach which is related to the representation of the medium as a linear system (linear filter) which introduces some changes in the vibrations passing through it [2]. Firstly, we illustrate the matter of our system approach by example for a simple model of the plane-parallel layered absorbing stratum (Fig. 1a).
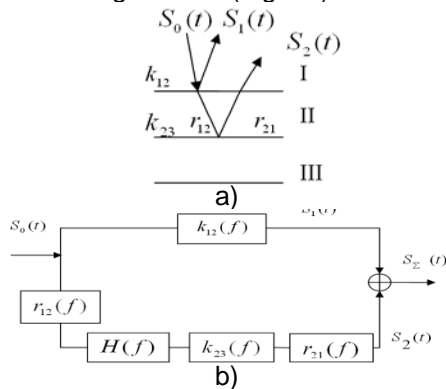
Fig. 1. a) model of plane-parallel layered absorbing stratum, b) $S_0(t)$ - incident wave; $S_1(t)$, $S_2(t)$ - signals reflected from the roof and the sole of the studied stratum II.

In case of normal wave incidence the reflection from the roof and the sole of the linear-nonelastic layer II in the ray approximation can be represented as an equivalent system (Fig. 1b).

The frequency response of such system can be represented as follows:

$$H_2(f) = r_{12}(f) \cdot H(f) \cdot k_{23}(f) \cdot r_{21}(f) + k_{12}(f) = \quad (1)$$

$$= |H_2(f)| e^{j\phi_2(f)},$$

where $k_{23}(f)$ and $k_{12}(f)$ are the reflection coefficients from the roof and sole of stratum II,

$r_{12}(f)$ and $r_{21}(f)$ are the refraction coefficients on the roof of stratum II, $H(f) = H_c(f) \cdot H_c^*(f)$ is the frequency response of the particular system which characterizes the wave propagation in the absorbing stratum II in two directions.

It is important to note that $k_{23}(f)$, $k_{12}(f)$, $r_{12}(f)$, $r_{21}(f)$ coefficients in the absorbing media are the complex functions of the f frequency. Wave spectrum reflected from the sole stratum II can be represented as follows:

$$S_2(f) = r_{21}(f) \cdot k_{23}(f) \cdot H(f) \cdot r_{12}(f) \cdot S_0(f) = \quad (2)$$

$$= |S_2(f)| e^{j\phi_s(f)},$$

where $\phi_S(f) = \phi_{r_{12}}(f) + \phi_{H_S}(f) + \phi_{k_{23}}(f) + \phi_{r_{21}}(f) + \phi_0(f), \quad (3)$

determines the phase spectrum of the reflected wave $S_2(f)$ which directly depends on the arguments of the refraction coefficient $\phi_r(f)$ and the reflection coefficient $\phi_k(f)$, as well as the PFC of the particular system $\phi_H(f)$ that determines the wave propagation in the absorbing layer, and the initial phase of the incident wave $\phi_0(f)$.

By analogy with the above described we can develop a model of the absorbing medium which consists of a random number of layers. Fig. 2 shows an equivalent system scheme which under the above assumptions characterizes the transmitting properties of the multilayer linear non-elastic absorbing medium.

This block diagram allows showing that the mathematical expression for the frequency response of this system is presented as follows:

$$H_\Sigma(f) = k_{L-1}(f) + \sum_{i=0}^{L-2} k_i(f) \prod_{n=i+1}^{L-1} H_n(f) r_{n,n-1}(f) r_{n-1,n}(f), \quad (4)$$

Complex reflection coefficient $k(f)$ and refraction coefficient $r(f)$ are specified in accordance with the relation given in [3], and the frequency response of the absorbing medium is determined in [2]:

$$|H(f)| = e^{-\alpha(f)2h}, \quad (5)$$

$$\phi_{_H}(f) = 4\pi f h \left[\frac{1}{V(f_0)} - \frac{\alpha(f)}{\pi^2} \ln \frac{f}{f_0} \right], \qquad (6)$$

where α is the absorption coefficient; h is the stratum depth; $V(f_0)$ is the propagation velocity at a certain frequency f_0.

The expression (4) can be used as a basis for calculation of the synthetic seismic track for a certain point on the observation surface.

$$S_{\Sigma}(t) = F^{-1}\{S(f)H_{\Sigma}(f)\} \qquad (7)$$

Here the expression $F^{-1}\{S(f)H_{\Sigma}(f)\}$ denotes the Fourier inversion operation.
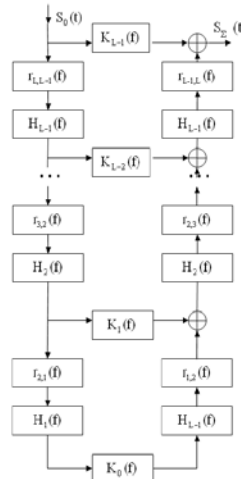
Fig. 2. Block diagram of the system that determines the transmitting properties of the multilayer absorbing medium.

Under the given number of layers and the distribution of petrophysical parameters, the set of model seismic tracks allows to develop the wave field and to use it for further researches.
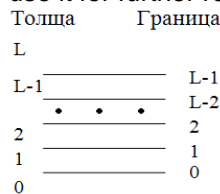
Fig. 3. Scheme of boundaries numbering and layers in the construction of the absorbing stratum numerical models.

In the numerical simulation of the absorbing media on personal computers the enumeration of layers should be done from the lower to the upper one (Fig. 3). There are significant problems caused by the large number of required computing operations. Fast algorithms for calculation of the synthetic wave fields in accordance with the method described in [4] were developed in order to solve these problems.

The algorithm is based on the recurrent calculation of the frequency response for "layer to layer" environment, i.e. calculation of the function:

$$R_i(f) = K_i + R_{i-1}(f) \cdot \tilde{H}_i(f), \quad i = \overline{1, L-1}. \qquad (8)$$

Here $R_0(f) = K_0(f)$;

$$\tilde{H}_i(f) = H_i(f) \cdot r_{n,n-1}(f) \cdot r_{n-1,n}(f), \qquad (9)$$

whereas $H_{\Sigma}(f)$ is determined by:

$$H_{\Sigma}(f) = R_{L-1}(f). \qquad (10)$$

This algorithm was implemented on a computer in Delphi environment. As an example, Fig. 4 shows the structure of two layered absorbing medium models and the synthetic seismograms calculated for them on the basis of the above mentioned approach (Fig. 5). The relevant speed of wave propagation in the layer, the rock density and the absorption parameters were used for simulation of each environment model layer.

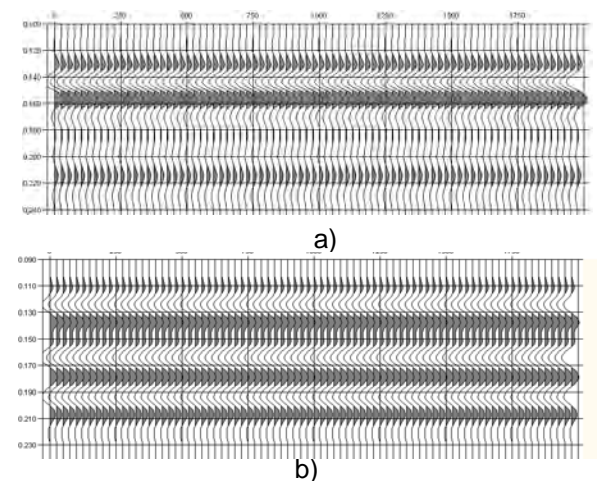*Fig. 4. Geological environment models.*

Fig. 5. Wave field for a model
a) gas-saturated sandstone; and
b) water-saturated sandstone.

The approach proposed and the method developed for simulation of the layered absorbing media are used for solving the direct geological problems as well as for studying of seismic data processing algorithms.

References

1. Gurvich I.I., Boganik G.N. Seismic prospecting. Textbook for high schools. Tver: AIS, 2006. 774p. 2. Averbukh A.G. Study of composition and properties of rocks in seismic prospecting. Moscow: Nedra, 1982. 232p.

3. Averbukh A.G., Trapeznikova N.A. Reflection and refraction of plane waves at normal incidence on the boundaries. // Physics of the Earth, № 9, 1972.

4. Lossovsky E.K. Theoretical seismograms for the idealized models of oil and gas deposits. 1 // Geophysical Journal, 1982, 4, № 5, 26-53p.

SAMPLING-BASED ALGORITHMS FOR THE MOTION PLANNING

Jaroslav Rozman*, František Zbořil**

Brno University of Technology, Department of Electrical Power Engineering, Technicka 8, 616 00
Brno, Czech Republic, www.feec.vutbr.cz/UEEN

Abstract— **This paper deals with the modern way of motion planning, with Sampling-Based Algorithms. It describes the decomposition of these algorithms into three parts – single query, multiple query and combined. It also describes particular parts of these algorithms like generating of the states in the free space, and connecting of the states. In the end it describes use of these algorithms and tasks solved in our university.**

I. INTRODUCTION

T HERE are a wide variety of the motion planning algorithms like the potential fields, roadmaps or cell decomposition. They all have advantages and also disadvantages. For example the potential fields are excellent for the motion planning of the autonomous robots. When we set the minimum of the function to the goal, this function will decline to it from all parts of the state space. The problem is, except the local minima, the computational complexity of this algorithm. We have to compute the values of the function in all configuration space. This means to divide the space into grids, the denser the more accurate, and iteratively compute the system of equations. The number of grids corresponds to the number of the equations. That's why this method is suitable only if we don't need change the goal or have a lot of the computational power. The solution would be not to compute all configuration space, but randomly chose some states and then check if the path between states lies in the free configuration space. And this is exactly what the sampling-based algorithms do.

II. SAMPLING-BASED ALGORITHMS

Sampling-based algorithms [1] can be divided into three groups. There are single-query, multiple-query and combined algorithms. They differ in the way they generate the samples and how they connect them to the roadmap. All these algorithms consist of several parts, sampling of the points from the configuration space, their connection to the roadmap and in the end the path finding.

A. The Configuration Space

The configuration space, as is probably clear, is the space of all possible configurations or positions of the robot. If the robot is simple four-wheel vehicle, the space is three dimensional, the x and y coordinate and the angle of the turning. If the robot is car-like vehicle, the turning of the front wheels adds fourth dimension. In the case of the robotic arms, every joint is one dimension, i. e. the arm with six degrees of freedom needs six dimensional space. The free configuration space is the space, where the robot doesn't collide with obstacles or with itself. When some state is generated, it is necessary to compute if the state lies in the free configuration space.

B. State Sampling

First important part of the sampling-based algorithms is the sampling of the states of the robot. The simplest and probably the most widespread way is the sampling of the states with the normal distribution. Other sampling strategies are sampling near the obstacles or sampling inside narrow passages. There is no problem in the sampling and path searching in the open areas, but in practice we also need the robot drive through narrow doors or passages. The normal sampling there would be impractical, because no connection through the narrow area would be probably created and the algorithm would probably create two separated parts of the roadmap.

The solution is the sampling inside the narrow passages, so called bridge test. It creates two samples and tests if both collide with the obstacles and if the point in the middle of the connection of these two samples lies in the free configuration space this point is added to the set of samples.

Good strategy for the samples generation is to impeach the density of the surrounding samples. The easiest way to compute this is to create the regular grid and compute the number of points in one cell. This approach ensures the exploration of the less occupied parts of the state space. In the work [2] created on our university, the

improvement of this approach was created. The cell that contains the obstacle has less samples then the cells which all lie in the free space. This means, that this cell will be chosen for the generating of the new samples more often, but the generating will be more often unsuccessful, because the free area of the cell wouldn't be so big. That's why the counter of the samples in the cell is decremented after every unsuccessful generating of the sample which lower the time needed for successful generation of the sample about one third.

C. The Samples Connection

The next part of the algorithm is to connect them to the roadmap. First we have to find k nearest neighbors and try to connect them to the processing sample. This is the task for the local planner, which has to ensure, that the path between two states is collision free, i. e. it belongs to the free configuration space. Two the most used approaches are incremental and subdivision. In the incremental case we advance from the first sample to the second sample about chosen distance *dist*. This distance has to be small enough to ensure, that it will detect even small obstacles. In the subdivision case we split the line between samples into two halves, test the point in the middle and continue in the recursive subdivision of the line. The subdivision testing is generally faster, because it use longer distances for the testing, while incremental proceeds in small distances.
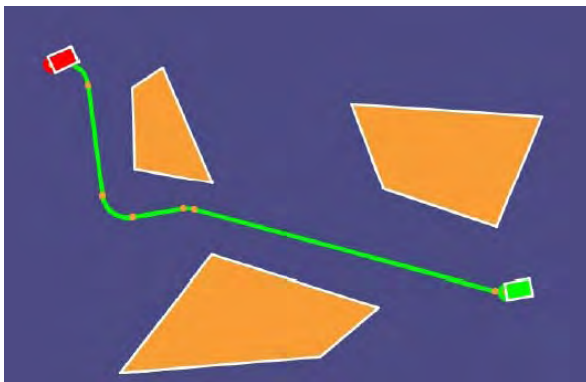
Fig. 2. Path for the non-holonomic vehicle with start and the goal point. Example from [3].

III. MULTIPLE-QUERY ALGORITHMS

The multiple-query algorithms first generate points in the space and after generating of a given number of samples it starts to connect them to a given number of the closest points. In the end the algorithm connects the starting point and the goal point. This means if we want to use different start or goal, we just delete the existing one and use the generated roadmap again. When the roadmap is created, we just perform some of the state-space searching, like Dijkstra's algorithm or A* to find the path. Example of this

group is the PRM (Probabilistic RoadMap planner).

IV. SINGLE-QUERY ALGORITHMS

Single-query algorithms add the start point to the one roadmap, the goal point to the second roadmap and then generate points and tries to connect these two roadmaps together. These algorithms are faster then multiple-query algorithms but when we want to find a path between different start or goal, we have to generate the points again. The examples of these algorithms are RRT (Rapidly-Exploring Random Trees) and EST (Expansive-Spaces Trees).

V. COMBINED ALGORITHMS

The SRT algorithm lies between single-query and multiple-query algorithms. It generates points and connects them to the roadmap as the multiple-query algorithms do, but for the connection of the samples it uses the single-query algorithms. If we suitably adjust parameters of this algorithm, it can converge to PRM, EST or RRT algorithm. The combined algorithms are one of the most powerful searching algorithms.
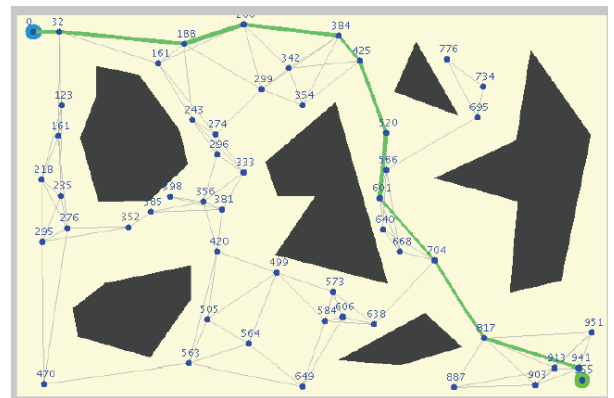

Fig. 1. Example of the samples generation and the found path in the multiple-query algorithm. This example is taken from [2].

VI. CONCLUSION

Sampling based algorithms have very wide area of the use. It can be used for the simple path planning for the autonomous robots or for the planning of the robotic arm motion.

Interesting use is in the control-based planning, where the weight and the momentum has to be taken into account. It is used in the car driving or in the space shuttle docking. Similar task will be solved in our university. Students will create docking algorithm for the small mobile robot, which will ensure automatic batteries recharging.

Another interesting task is the controlling of the nonholonomic vehicle, which is another project solved in our university. In the last year the www applet about nonholonomic and also

about planning of the motion of the flexible object was created. The students this year should reassume on this work and create program for controlling of the small RC car, which position will be detected by the overhead camera.

The last task currently solved in our university is the motion planning in the 3D space. As the analogy to the world famous α-shaped puzzle, the hedgehog in the cage, famous puzzle in the Czech Republic and also e. g. in the Japan, was chosen to demonstrate the benefits of the sampling-based algorithm. The hard part in these puzzles is the sampling in the narrow passages as was mentioned before.

As we can see the sampling-based algorithms are one of the most powerful algorithms and have great future in the complex motion planning tasks.

REFERENCES

3. Choset, H. et al.: Principles of Robot Motion, MIT Press, Cambridge, 2005, ISN 0-262-03327-5

4. Kvasnica, M.: Vizualizace hledání cesty pro robota, Bc. thesis, FIT VUT, Brno, 2008

5. Vozák P.: Vizualizace plánování cesty, Bc. thesis, FIT VUT, Brno, 2009

REFINING OF URANIUM AND ITS CONVERSION IN HEXAFLUORIDE

Sh.P. Samusenko, S.S. Mikhalevich, D.G. Rogozny

Scientific supervisor: Yu.A. Chursin ,

Tomsk Polytechnic University, 634050, Russia, Tomsk, Lenina str., 30

E-mail: AnopT@ya.ru

Uranium is widely distributed in nature. Ubiquitous presence of uranium is explained by its high chemical reactivity, good solubility of its salts, ability to participate in many chemical reactions and form compounds with many other elements.

The main objective of uranium technology is to obtain the enriched uranium in a form suitable for use in nuclear reactors. These forms are metallic uranium, uranium dioxide, uranium tetrafluoride. Particular technological scheme of uranium ores processing depending on type of final product is selected ifor different cases.

The term "yellow cake" is usually applied to a group of uranium sediments, so-called "diuranates", and refers to unrefined uranium oxide. In essence, the term "yellow cake" should be applied only to ammonium diuranate. The final product of leaching stage of fuel cycle, sometimes called "yellow cake", consists of crude U3O8. Purification of uranium oxide is needed to reach nuclear grade of purity before it will be converted into UF6 or metallic uranium by the chain UO_3, UO_2, UF_4.

Produced in the refining plants U_3O_8 is dissolved in nitric acid. This solution of $UO_2(NO_3)$ $26H_2O$ (UNH) is sent to operation of liquid extraction, usually consisting of a pulsating columns or mixer-settlers, in which an aqueous solution of uranyl nitrate interacts in counterflow with an organic extractant (as rule, tributyl phosphate (TBP)), diluted by kerosene or dodecane.

From the resulted product - complex of uranium with TBP, uranium is extracted back by diluted solution of nitric acid and concentrated by evaporation until the density of solution reach from 400 to 1000 grams per liter.

This solution is sent to calcination in furnace with a fluidized bed or to the installation of periodic action for producing of pure UO_3. Another variant of uranyl nitrate concentration is to neutralize it by gaseous ammonia and then to incinerate up to UO_3. Produced UO_3 is reduced to UO_2 with hydrogen in a fluidized-bed reactor according to the reaction:

$$UO_3 + H_2 \rightarrow UO_2 + H_2O$$
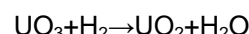
Part of received at this phase uranium can be used in the form of UO_2. The next step in the processing of uranium - its conversion into UF_4-form according to reaction with anhydrous HF:

$$UF_4 + F_2 \rightarrow UF_4 + 2H_2O$$
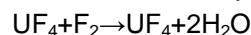
This reaction is conducted at temperatures from 300 to 500 ^{o}C in reactors with a fluidized bed or rotary kilns. This chemical reaction takes place in pulp ($UO_2/H_2O/HF$). Solid powder of UF_4 is converted into gaseous form of UF_6 in reaction with pure fluorine gas at temperature about 500 ^{o}C [1]:

$$UF_4 + F_2 \rightarrow UF_6$$
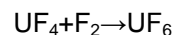
As part of conducted researches let's examine extraction methods for processing of uranium ores solutions and extraction uranium refining.

For the first time extraction process for the purification of natural uranium [2] was used Peligot in 1842, who used diethyl ether. The same ether was used in the United States 100 years later, in 1942, for fine purification of technical uranium mixed-oxide at "Mellinkrodt Chemical Works" plant in St. Louis during making the first atomic bomb. Firstly this method was used to obtain uranium oxide of nuclear purity with impurity content about 10^{-4}-10^{-5} %.

In 1947 John Whorf (USA) investigated the possibility to use TBP as extractant for natural uranium, and in 1950 - 1954 the processes of uranium extraction by TBP in diluent had been developed and tested on pilot plants. After that people began to use TBP in industry: 1954 - the U.S., 1955 - Canada, 1956 – France, 1957 - England, 1958 - West Germany. During some time Canada, France and Belgium used methyl isobutyl ketone for uranium refining.

Nowadays extraction processing of technological solutions after leaching of uranium ores are used on many plants (USA, Australia, Spain, Portugal, CIS, Russia). Scheme of extraction uranium processing at all plants are similar in common. However, variety of processing objects, solutions content, used extractants and equipment and local conditions create the uniqueness of each company.

In Russia usage of non-filtrational ion exchange sorption of uranium from pulps and method of sorption leaching of uranium ores gives great technical and economic effects. So methods combining sorption extraction and uranium concentration from ore pulps with subsequent extraction processing (purification) of desorption solutions to obtain pure final products are generalyused in russian uranium technology. Cation exchangers are used for sorption. For extraction alkylamines are used which sorbing uranium according to anion-exchange mechanism (see figure 1) [2].

Nowadays TBP is widely used for uranium refining in all countries of the world which have nuclear technology. The purpose of refining is to produce uranium compounds meeting specific requirements (conditions of impurities content in nuclear pure uranium).

Nowadays refining with application of extraction is the most widespread and effective method.
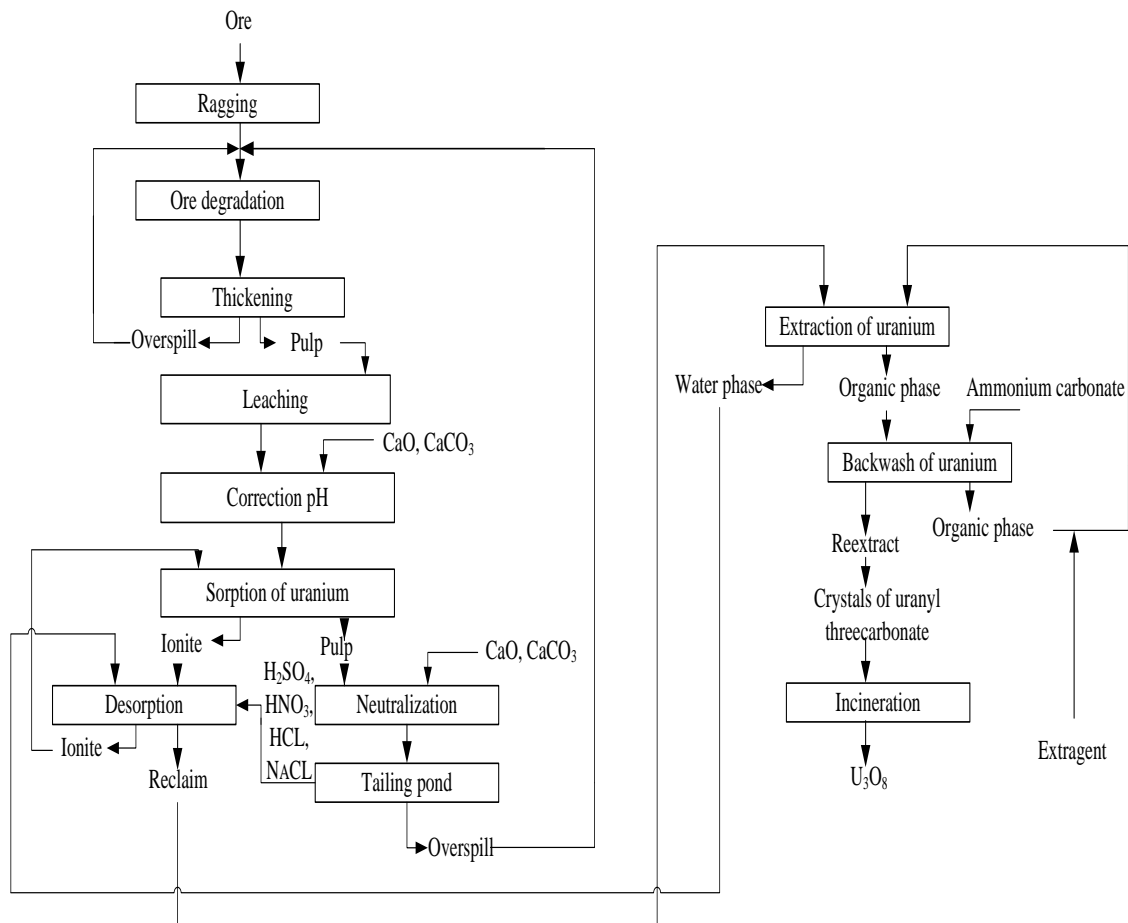

Figure 1. The technological scheme of obtaining U_3O_8, combining the sorption and extraction

As a rule extraction separation of substances does not result the solid phase. It is a great advantage in comparison to precipitation operations, as impurities capture excludes during formation of sediments. In the case of uranium extraction concentration is achieved

simultaneously with removing of impurities. Uranium extraction greatly reduces volume of waste solutions. Precipitation and crystallization of sediments is relatively long and complex process, whereas the extraction balance is usually established within few minutes. Presence of only liquid phases greatly simplifies instrumental design of process [2].

Basic laws of extraction process applying to refining is the same as for extraction processing uranium-ore solutions. However, requirements for extractive agents in refining are somewhat different due to several reasons: the uranium content in solutions is higher, so more concentrated solutions are used (e.g. 30-40% TBP in kerosene). Negligibly small distribution coefficients of impurities must be achieved. That means that extractant should have high separation ability associated with

the formation of uranyl nitrate sulphate (hexon, dibutyl carbitol, TBP are used).

The best extractant for uranium refining is supposed to be the solution of TBP in kerosene, CCl4, etc. Usually 30-40% solution of TBP in kerosene is used for refining.

REFERENCES
1. The Safety of the nuclear fuel cycle. [Электронный ресурс]: Paris : Nuclear Energy Agency, Organisation For Economic Co-operation And Development,1993.244 p. : ill ; 27 cm. – Режим доступа:http://catalogue.nla.gov.au/Record/2754849 - свободный.
2. Громов Б.В. Введение в химическую технологию урана: учебник для вузов. – М.: Атомиздат, 1978. – 336 с.

ADVANCED PARTIAL DIFFERENTIAL EQUATIONS SOLUTIONS

Václav Valenta[1], Václav Šátek [2], Jiří Kunovský[3]

Faculty of Information Technology, Brno University of Technology, Czech Republic, Brno, Božetěchova 2

[1] email: ivalenta@fit.vutbr.cz,

[2] email: satek@fit.vutbr.cz,

[3] email: kunovsky@fit.vutbr.cz

ABSTRACT

The paper is focused on the partial differential equations solutions. In term of advanced partial differential equations (PDE) we understand new ways of interpolation methods in combination with method of lines, when PDE is transformed to a set of ordinary differential equations (ODE).

Keywords: Differential equations, Continuous simulation, Modern Taylor Series Method

INTRODUCTION

The research group HPC ("High Performance Computing") has been working on extremely exact, stable and fast numerical solutions of systems of differential equations [1].

The extremely exact solutions are based on an original mathematical method which uses the Taylor series method for solving differential equations in a non-traditional way.

The "Modern Taylor Series Method" (MTMS) is based on a recurrent calculation of the Taylor series terms for each time interval. An important part of the method is an automatic integration order setting, i.e. using as many Taylor series terms as the defined accuracy requires. The MTMS also has some properties very favourable for parallel processing.

The MTMS has been implemented in II/2007 TKSL software[2].

PARTIAL DIFFERENTIAL EQUATIONS

Numerical methods of solving PDE's are based on approximations of the derivatives by differences are a main basic methods. Let us mention the Method of grids and the Method of lines. If we cover the space of independent variables with a grid of a finite number of nodes and replace the derivatives by differences using only values in chosen nodes, we will get the Method of grids and the solution of a PDE is transformed into the solution of a system of algebraic equations. If we leave the derivatives of one variable continuous and replace the derivatives of other independent variables by differences, we will get the Method of lines. Thus the solution of a PDE is transformed into the solution of a system of ordinary differential equations and the system can be solved by means of the Modern Tailor Series Method.

As an example the second derivative can be expressed using the symmetric formula for the three-point approximation

$$\frac{\partial^2 U(x,t)}{\partial x^2} = \frac{y_{k-1} - 2y_k + y_{k+1}}{(\Delta x)^2} \qquad (1)$$

Hyperbolic PDE

One of the most common hyperbolic PDE is the wave equation, which can be expressed in the basic form

$$b\frac{\partial^2 V(x,t)}{\partial x^2} = \frac{\partial^2 V(x,t)}{\partial t^2} \qquad (2)$$

With initial conditions

$$V(x,0) = \sin(\pi x) \wedge x \in <0,1>$$

$$\frac{\partial V(x,0)}{\partial t} = 0 \qquad (3)$$

As an example the string is divided into 10 segments and the figure show the solutions V1, V2, … V5 of the equation (Figure 1).

The equation may describe the swing of an ideal string of unit length, fixed at the external points to the x-axis which satisfies the boundary values and is released at time zero (thus having a zero velocity at time zero).

The analytic solution (at the midpoint of the string) is

$$V_5 = \cos(\pi.t) \qquad (4)$$
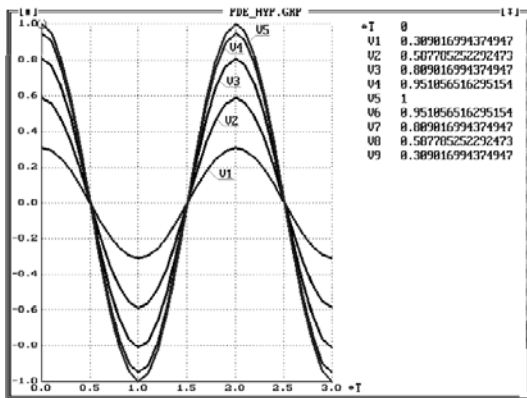
Figure 1 The solution of the hyperbolic equation

The Err function (the difference between numerical and analytical solution) of the solution V5 (at the midpoint of the string which is dividend into 10 segments) using a three-point approximation together with ORD is plotted in the Figure 2. ORD is number of Taylor series terms used.
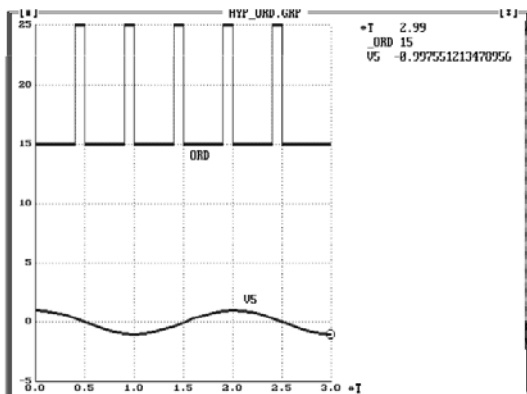
Figure 2 Err function for V5 midpoint

Elliptic PDE

Let's try to solve two-dimensional Laplace equation on domain

$$\Omega = <0,1> \times <0,1> \qquad (5)$$

The equation is in the form

$$\nabla^2.u = 0 \qquad (6)$$

Using the boundary conditions

$$u(x,0) = u(0, y) = u(1, y) = 0 \wedge$$
$$u(x,1) = \sin(\pi x) \qquad (7)$$

The analytic solution of this equation is

$$u(x, y) = \frac{1}{\sinh \pi} \sin(\pi x)\sinh(\pi y) \qquad (8)$$

Let's solve the two dimensional Laplace equation. We will use finite difference method. In this case we will cover the domain with a grid of nodes. In every node we replace derivation with the difference. The difference can be computed using three point approximation.

$$\frac{\partial^2 u(x, y)}{\partial x^2} \approx \frac{u(x+\Delta x, y) - 2u(x, y) + u(x-\Delta x, y)}{(\Delta x)^2} \qquad (9)$$

The result is a system of linear algebraic equations which can be solved using standard methods like Gauss-Seidel method.

We will add a time dimension and create a system of ordinary differential equations. This system of ODE will be solved using the *Taylor series method*. Then we will solve the this modified equation

$$\frac{\partial^2 u(x, y,t)}{\partial x^2} + \frac{\partial^2 u(x, y,t)}{\partial y^2} = \frac{\partial u(x, y,t)}{\partial t}$$

(10)

Finally nodes which are on border of domain are set using he boundary conditions and for node on the position [*I,j*], we create a ordinary differential equation in the form

$$u_{i,j}' = u_{i-1,j} + u_{i+1,j} + u_{i,j-1} + u_{i,j+1} - 4u_{i,j} \qquad (11)$$

In steady state, the derivation by time is equal zero and thus we indirectly found a solution.

The big advantage of the *Taylor series method* is that it can be run in parallel way. Every equation will be solved on a processor.

The next pictures display the graph of the solution. We can see that error of the numeric solution is smaller than the distance between nodes.
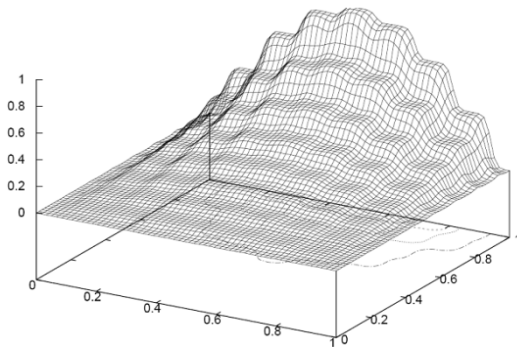
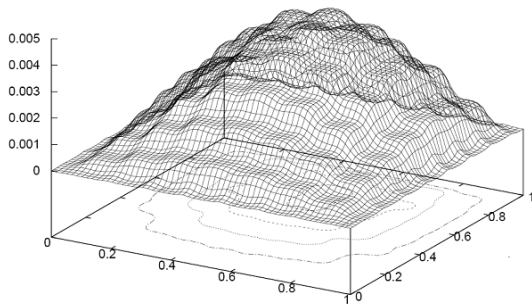*Figure 3 Laplace equation, 8x8 nodes*

Figure 4 Error Laplace equation 8x8 nodes

CONCLUSION

The most appropriate solution of PDE consists in combining more methods. Thanks to the combination of methods presented in this paper the error of solution is given only by the method of lines.

Acknowledgement:

REFERENCES

1. Kunovský J., *Modern Taylor Series Method*, FEI-VUT Brno, 1994, habilitation work.
2. Web sites, High Performance Computing, http:/www.itsolutions.cz/TKSL
3. Chung T. J., "Computational Fluid Dynamics", *Cambridge University Press*, 2002, ISBN 0-521-594116-2.

SEMIANALYTIC COMPUTATION IN TKSL

Václav Šátek[1], Michal Kadák[2], Jiří Kunovský[3]

Faculty of Information Technology, Brno University of Technology, Czech Republic, Brno, Božetěchova 2

[1] email: satek@fit.vutbr.cz,

[2] email: ikadak@fit.vutbr.cz,

[3] email: kunovsky@fit.vutbr.cz

ABSTRACT

The aim of our paper is to describe a new modern numerical method based on the Taylor Series Method and to show how to evaluate the high accuracy and speed of the corresponding computations. It is also the aim of our paper to show how to calculate finite integrals that are the fundamental part in signal processing, especially in Fourier analysis and how to use it for symbolic operations.

It is a fact that the accuracy and stability of the algorithms we have designed significantly exceeds the presently known systems. In particular, the paper wants to concentrate, using the previous results and latest development trends, on the simulation of dynamic systems and on extremely exact mathematical computations.

Keywords: *Differential equations, Continuous simulation, Modern Taylor Series Method, Finite integrals*

1 INTRODUCTION

The main idea behind the new developed Modern Taylor Series Method (MTSM) is an automatic integration method order setting, i.e. using as many Taylor series terms for computing as needed to achieve the required accuracy (more information in [1]).

The MTSM used in the computations increases the method order (ORD) automatically, i.e. the values of the terms are computed until adding the next term does not improve the accuracy of the solution. This new approach has been implemented in a simulation language TKSL [2]. In fact, the well-known rules of differential and integral calculus have been used.

MODERN TAYLOR SERIES METHOD

By a numerical solution of an ordinary differential equation (ODE)

$$y' = f(t, y) \qquad y(t_0) = y_0 \qquad (1)$$

we understand the finding of a sequence

$$[y(t_0) = y_0], [y(t_1) = y_1], ..., [y(t_n) = y_n]$$

The best-known and most accurate method of calculating a new value of a numerical solution of differential equation (1) is to construct the Taylor series in the form

$$y_{n+1} = y_n + h \cdot f(t_n, y_n) + \cdots + \frac{h^p}{p!} \cdot f^{[p-1]}(t_n, y_n)$$

(2)

where h is integration step.

COMPUTATION IN TKSL

Theoretical work on the numerical solution of ODEs by the Taylor series method has been going on for a number of years. The simulation language TKSL has been created to test the properties of the technical initial problems and to test an algorithm for MTSM.

Definite Integrals

Definite integrals and integral equations, due to the number of applications, are very important mathematical tools. Their solution using the MTSM is the subject of this chapter.

For all functions that have Taylor series the calculation of their integrals can be conducted indirectly via their derivatives. Thus, the problem of solving a definite one-dimensional integral taken as a function of the upper boundary can be transformed to solving a system of differential equations.

Example 1: Let a definite integral (3) be given

$$I = \int_0^\pi \cos(t)dt$$

(3)

The definite integral (3) can be rewritten in the form $I' = \cos(t)$, $I(0)=0$. The numerical solution of the integral (3) is obtained at the point corresponding to the upper boundary of the integral ($t_{max} = \pi$). The time function of the value of the integral I is in Figure 1. A particular calculation of the integral for T = π is in the right-hand part of this Figure 1. Numerical result represents the expected analytical value $I = 1$.
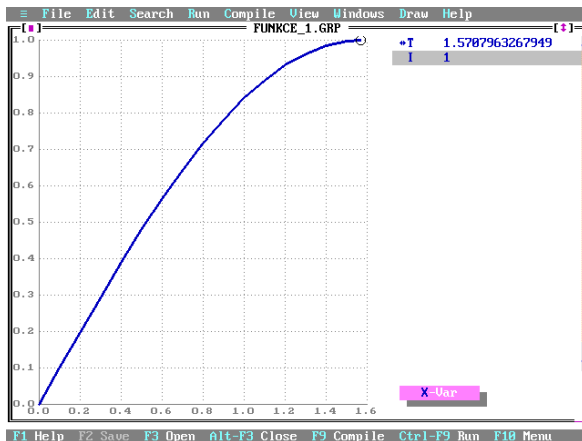

Fig. 8: Numerical solution of definite integral.

Symbolic Operations

A function $y(t)$ which is periodic of period 2π, is continuous except for a finite number of finite discontinuities in any interval of length 2π, and has a right-hand and left-hand derivative at every point may be expanded into a Fourier series

$$y(t) = \frac{a_0}{2} + \sum_{k=1}^\infty a_k \cos(kt) + \sum_{k=1}^\infty b_k \sin(kt)$$

(4)

where the Fourier coefficients are given by

$$a_0 = \frac{1}{\pi} \int_0^{2\pi} y(t)dt$$

(5)

$$a_k = \frac{1}{\pi} \int_0^{2\pi} y(t)\cos(kt)dt$$

(6)

$$b_k = \frac{1}{\pi} \int_0^{2\pi} y(t)\sin(kt)dt$$

(7)

The definite integrals can be rewritten in form:

$$a_k' = \frac{1}{\pi} y(t) \qquad a_k(0) = a_{k0}$$

(8)

$$a_k' = \frac{1}{\pi} y(t)\cos(kt) \quad a_k(0) = a_{k0}$$

(9)

$$b_k' = \frac{1}{\pi} y(t)\sin(kt) \quad b_k(0) = b_{k0}$$

(10)

The numerical solution of the integral is again obtained at the point corresponding to the upper boundary of the integral (t_{max} = 2π).

Example 2: In this example

$$f = 16 \cdot \sin^5(t) + 2 \cdot \sin^3(t) + \cos(2 \cdot t) + 5 \cdot \sin(3 \cdot t) + \quad (11)$$
$$+ \sin(t) \cdot (-10 + 2 \cdot \cos(t)) - \sin(5 \cdot t) - \sin(2 \cdot t)$$

Fourier coefficients a_0, a_1, a_2, a_3, a_4, a_5, b_1, b_2, b_3, b_4, b_5, have been calculated according to equations (8), (9), (10) in TKSL. It is very illustrative to have a look at the result in Figure 2 on the left, where $A_0 = 2$ as can be expected (for time $T = 2\pi$). Even though we are interested in values in $T = 2\pi$, time functions a_0, a_1, a_2, a_3, a_4, a_5, b_1, b_2, b_3, b_4, b_5 look very attractive. It is clear that values a_1, a_2, a_3, a_4, a_5, b_1, b_2, b_3, b_4, b_5 are negligible and thus, with respect to (4) our test equation (11) can be simplified into $f = 1$ as can be expected.

The results of Fourier coefficients computation using TKSL are in Figure 2 and Figure 3.
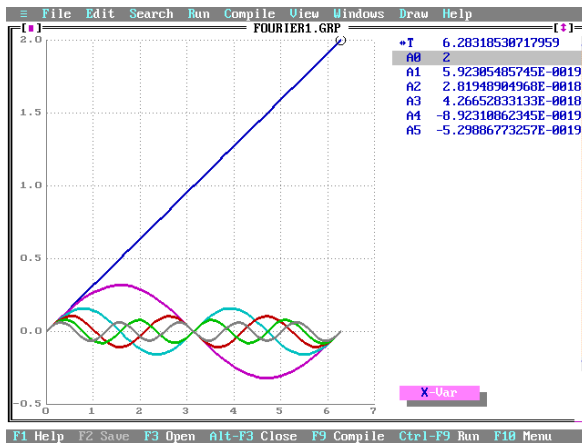
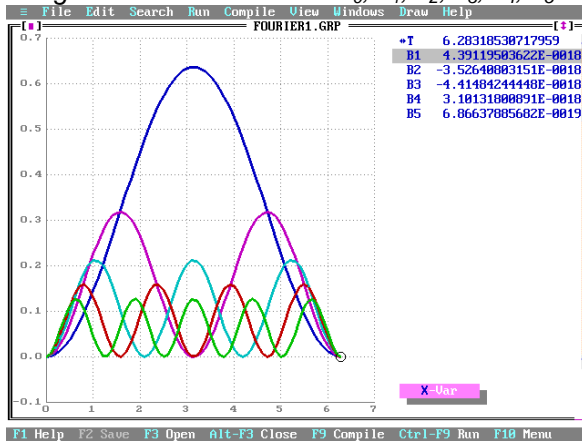Fig. 2: Fourier coefficients a_0, a_1, a_2, a_3, a_4, a_5.

Fig. 3: Fourier coefficients a_0, a_1, a_2, a_3, a_4, a_5.

CONCLUSION

The development project deals with extremely exact, stable and fast numerical solutions of systems of differential equations. It has been verified that the computation speed enabled by the newly developed Taylor series method is, while keeping the high accuracy, greater than that achieved by the algorithms currently used for numerically solving systems of differential equations. An important part of the method is an automatic integration order setting. Thus it is usual that the computation uses different numbers of Taylor series terms for different steps of constant length.

The Modern Taylor Series Method also has some properties very favourable for parallel processing. Many calculation operations are independent making it possible to perform the calculations independently using separate processors of parallel computing systems.

The idea of implementation of our fully original - highly accurate and fast algorithms into advanced programs, the creation of application programs and an analysis of problems requiring parallel processing will be a part of our research.

REFERENCES

[1] Kunovský J., *Modern Taylor Series Method*, FEI-VUT Brno, 1994, habilitation work.
[2] Web sites, High Performance Computing, http:/www.itsolutions.cz/TKSL
[3] Kunovský J., Šátek V., Kraus M., "New Trends in Taylor Series Based Computations", *In: Numerical Analysis and Applied Mathematics*, Rethymno, Crete, GR, AIP, 2009, p. 282-285, ISBN 978-0-7354-0705-3.

EXPLORING HISTORY WITH INFORMATION SYSTEMS

Ilya S. Solovyev, Evgeniya O. Schwarz

Scientific supervisor: Inna L. Pichugova, senior teacher

Tomsk Polytechnic University, 634050, Russia, Tomsk, pr. Lenina, 30

E-mail: ilya.s.solovyev@gmail.com

Information System (or IS) is historically defined as a 'bridge' between the business world and computer science, but this discipline is slowly evolving into a well-defined science. Typically, IS includes colleagues, procedures, data, software, and hardware (by degree) that are used to gather and analyze information. Specifically computer-based information systems are complementary networks of hardware/software that people and organizations use to collect, filter, process, create and distribute data. But it doesn't mean that IS can be useful only in business environment. Different spheres ranging from mapping to representing historical data can be supported by IS [1].

People have been accumulating and collecting historical information for many centuries. However, this information is stored far away from ordinary people who are interested in history and fascinated by it. But with the help of

IT it becomes possible to open up new horizons of our past and present.

It is impossible to imagine a historical event without any close connection to its geographic location. Thus, it doesn't mean much for us to know about, for instance, Alexander Macedonian as a historical figure without any foggiest idea what lands he conquered. Therefore, one of the most efficient tools to describe and represent historical events is Geo-Information System (GIS) implementation.

In the simplest terms, GIS can be described as a form of a database. What makes it unique is that every item of data in a GIS is linked to the representation of where the data refer to. Although GIS originated in the Earth Sciences, since the 1990s its use has increasingly spread to historical research and this field has become known as Historical GIS [2]. One of the original manifestations of this spread was the creation of National Historical GISs such as the Great Britain Historical (GBH) GIS and the US National Historical GIS in a number of countries. These are systems that hold changing administrative boundaries linked to censuses and other data published by using them. They usually cover most of the nineteenth and twentieth centuries. For example, the core of the GBH GIS is a systematic list of all the units historians know about. There are currently over 48,000 units linked by over 150,000 relationships. Although, it is not compulsory to know boundaries, the spatial extension was used to hold over 40,000 boundary polygons, with dates, for many units. A large part of the statistical holdings are being moved to this structure. Most collections of computerized statistics, including the old database, are divided into many separate tables and are designed mainly to allow researchers to download these datasets for further analysis. This system holds all statistical data values in a single column of a single table, with millions of rows, enabling them to be used very flexibly for mapping, graphing and reconstructing the source table. In general, the system aims to be a comprehensive description of Britain and its localities. One way to achieve this is to include approaching 10m. words of text: accounts of journeys around Britain, such as Celia Fiennes "Through England on a Side Saddle in the Time of William and Mary", cross-referenced by place to the rest of the system; over 90,000 entries from descriptive gazetteers published in the late 19th century, describing towns, villages and landmarks; and the main report from every census up to 1961 [3].

Increasingly, GISs are being focused on much smaller areas and on more qualitative sources. The Valley of the Shadow project and the Salem Witchcraft project include good examples of it. Both of these projects have created large archives on two counties on the eve of the American Civil War (the Valley of the Shadow) and the village of Salem, Massachusetts around the time of the witchcraft trials. Both of them independently saw the need to add a GIS component to their archive partly to help structure the data, and also because they realized that geography was important to their understanding of the research issues [2]. The Valley of the Shadow project details life in two American communities; one Northern and one Southern, from the time of John's Brown Raid through the era of Reconstruction. In this digital archive one may explore thousands of original letters and diaries, newspapers and speeches, censuses and church records, left by men and women in Augusta County, Virginia and Franklin County, Pennsylvania. Giving voice to hundreds of individual people, the Valley Project tells forgotten stories of life during the era of the Civil War.

The Valley of the Shadow differs from many other history websites. It is more like a library than a single book. There is no "one" story in the Valley Project. Rather, what a visitor will find are thousands of letters and diaries, censuses and government records, newspapers and speeches, all of which record different aspects of daily life in these two counties at the time of the Civil War. While exploring the extensive archive, the visitor can flip through the Civil War diary of a Valley resident, read what the county newspapers reported about the battle of Gettysburg, or even search the census records to see how much the average citizen owned in 1860 or 1870 [4]. The main page of the Valley of The Shadow archive is represented on the figure 1.
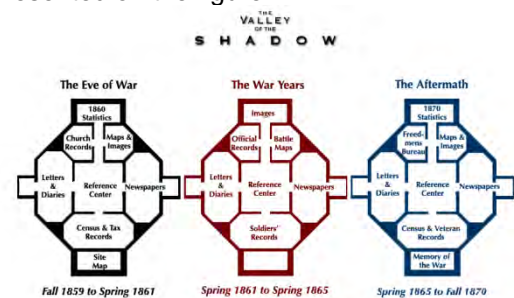

Figure 1. *The main page of Valley Archive*

The Valley of the Shadows project was supported in part by geo-information technologies. The cores of this system were diaries, newspapers, letters and different statistical data. The idea to represent all this data with the help of IT was successfully applied in another IT History project – Interactive Virtual History Timeline.

The British Library's new interactive timeline allows students to get a sense of change and chronology when studying historical events. Bringing together material from the Library's collections and using web-technology, users are

able to discover historical connections and create links in a multimedia experience [5].

Developed by the Library's Learning team in collaboration with historians and writers, the timeline includes some of the Library's key collection items from medieval times to the present day. They are records of political events, glimpses of everyday life and writings and speeches from some well-known historical and literary figures.

Scanning through centuries of images, audio-visual and printed material, users can explore various themed timelines: 'everyday life', 'music and literature' and 'politics, power and rebellion' on one screen.

The highlights of collection items featured include:

- Records of major events – from the Black Death and the Great Fire to the French Revolution and the abolition of the slave trade.

- Printed matter – the first English printed book, the first cookery manuscript, the first English bible and the first postage stamp.

- Public Life – posters, advertisements and illustrations documenting everything from public executions and magic shows to plague cures and séances.

- Campaigns – pamphlets and writings from activists such as Abolitionists, Chartists, Communists and CND marchers.

- Manuscripts – written by great figures in history including Henry VIII, Elizabeth I, Captain Cook, Beethoven, Wordsworth, Abolitionists, Florence Nightingale and Dickens.

- Maps – cities, military campaigns and imagined lands.

- Patents – including those for the Spinning Jenny, the bicycle and the machine gun [6].

Apart from the well-known collections items, the timeline also includes some of the Library's more unusual sources, opening up a new world of education and learning. They are a medieval Valentine's letter (1477); a 15th century recipe for custard (1440); a Renaissance anatomy book (1543), etc. These will allow everyone to become an expert as they explore and find fascinating links dating back to 1215.

Through the use of innovative Flash programming, users are able to dig deep into collection items, download information and images, view transcripts, add items to favourites and switch timelines and key events by pressing a button. This will allow for interesting and unique comparisons to be made between various aspects of social, political and cultural life. Users will also be able to focus on chosen topics such as political campaigns, technological changes, etc. Alternatively, they will be able to compare themes within one specific time period [5].

The British Library's Learning team is a world-leader in providing access to collection items and resources for students and teachers. Using its award-winning website that attracts 1.2 million visitors every year, the Learning team has consistently developed ways of giving users a chance to explore the Library's collections in a new light. Future developments include major resources to support English Language and Literature study.

Summing up, this research was aimed to find and affirm the great possibilities of information technologies that can be extremely useful not only in rather pragmatic business environment but also in studying our history.

References

1   Information System Discipline // Wikipedia, the free encyclopedia [e-resource]. – 2009. – Access mode: http://en.wikipedia.org/wiki/Information_systems_discipline

2   What is HGIS // The Historical GIS Research Network [e-resource]. – 2009. – Access mode: http://www.hgis.org.uk/what_is.htm

3   About GB Historical GIS // University of Portsmouth [e-resource]. – 2009. – Access mode: http://www.gbhgis.org/

4   Guide to the Valley: How to Use the Valley Project // The Valley of the Shadow [e-resource]. – 2009. – Access mode: http://valley.lib.virginia.edu/VoS/usingvalley/valleyguide.html

5   Teachers' orientation guide // Timeline: Sources from History [e-resource]. – 2009. – Access mode: http://www.bl.uk/learning/pdf/teachersnotes.pdf

6   Features of the Timeline // Timeline: Sources from History [e-resource]. – 2009. – Access mode: http://www.bl.uk/timeline

DATA PREPROCESSING FOR PERSON IDENTIFICATION BASED ON COLOR FACE IMAGES

Stepanov D.Y.

Scientific adviser: Lange M.M., Ph.D., ass.prof.

Moscow State Institute of Radioengineering, Electronics and Automation (technical university)

E-mail: DmitryStepanov@mail.ru

Introduction

Pattern recognition is used in such areas as: bioinformatics (molecular modeling, genomic analysis), data mining (data forecasting), document classification (table and scheme detection on images), remote sensing (object classification on images taken from the space), biometrical identification (person identification based on biometrical features) etc. [1].

Applied applications of biometrical identification used in criminalistics, banking area, security services [2]. Nowadays this problem is very important due to high level of economical crimes, fraud, terrorism etc.

There are a lot of methods which can be used for person identification by biometrical features, however, most of them are restricted by input data [3]. In general, person identification process involves information about: face, fingerprint, signature, eye, gesture, speech wave etc. (fig.1).
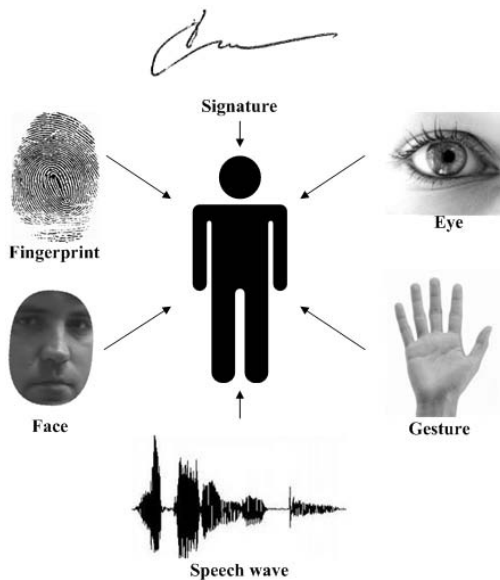
Fig.1. Biometrical features.

The problem of data preprocessing is still urgent for any recognition methods because the efficiency of recognition system depends on the quality of input data. Face recognition is the simplest way to identify person, inspite of it we are faced with the necessity to preprocess face images. But how we can do it in the right way?

Statement of problem

Let's restrict problem domain only by taking into consideration face images in color palette. We have to extract face outlines from color images excepting noises like haircut, beard, and ears of the person, which is not relevant for biometrical person identification.

Input data

In our case input data are presented by a set of color face images given by different expressions and views of a person (fig.2), see table 1.

Table 1

Expressions and views

Views \ Expressions	full face	raised head	hanged head	head rotation on the left	head rotation on the right	head bending on the left	head bending on the right
normal look	✔	✔	✔	✔	✔	✔	✔
closed eyes	✔	✔	✔	✔	✔	✔	✔
squinted eyes	✔	✔	✔	✔	✔	✔	✔
increased eyes	✔	✔	✔	✔	✔	✔	✔
smile	✔	✔	✔	✔	✔	✔	✔
opened mouth	✔	✔	✔	✔	✔	✔	✔
different positions of eyes		✔	✔	✔	✔		

All images differ from each other by age (time interval between shooting sessions), technical equipment of shooting (digital camera Olympus mju 810 and digital video camera Sony Handycam HDR-SR10E) and illumination (natural and artificial light, different angles of source of light). There are 2852 face images in database (31 persons, 96 realizations per person).

Fig.2. Input images.

Data preprocessing

Data preprocessing means face detection and noise erasing on input images. Our proposed procedure consists of follow steps: eyes detection, calculation of face geometrical characteristics and object of interest extraction [4].

We use eyes detection procedure of freeware *OpenCV* to find coordinates of left and right eyes $(x_L, y_L)(x_R, y_R)$ [5]. According to [6] this procedure gives one of the best results in comparison with other methods, moreover, we escape from developing a new technique to solve typical problem. Found coordinates are used to calculate distance *r*:

$$r = \sqrt{(x_R - x_L)^2 + (y_R - y_L)^2} \qquad (1)$$

and parameters of mask-oval which defines informative region of the face. Mask-oval is specified in coordinates (U, V) (fig.3b) calculated next way: axis *U* crosses the center of eyes line and is vertical to this line; center of mask-oval is specified by point on axis *U,* which is far from eyes line on βr where $\beta > 0$; axis *V* crosses this center and moves forward.

Mask-oval is defined by parametrical oval in coordinates (U, V):

$$\frac{U^m}{(\beta_u r)^m} + \frac{V^m}{(\beta_v r)^m} \le 1, \qquad (2)$$

where form parameter $m \ge 2$ and radiuses are specified by $\beta_u > 0$, $\beta_v > 0$ and distance *r* (1). Transformation of rotation and drift connects mask coordinates (U, V) and image coordinates (X, Y) by:

$$\begin{pmatrix} U \\ V \end{pmatrix} = \begin{pmatrix} -\sin\theta & \cos\theta \\ -\cos\theta & -\sin\theta \end{pmatrix} \begin{pmatrix} x - x_0 \\ y - y_0 \end{pmatrix}, \qquad (3)$$

where $x_0 = \frac{1}{2}(x_L - x_R) + \beta r \sin\theta$,

$$\sin\theta = \frac{y_R - y_L}{r}, \qquad y_0 = \frac{1}{2}(y_L - y_R) - \beta r \cos\theta,$$

$$\cos\theta = \frac{x_R - x_L}{r}.$$

If we specify parameters β, β_u, β_v, formulas (1) – (3) will allow us to find informative outline of face constrained by oval-mask (fig.3c).

The proposed procedure is invariant to rotation and drift of face images. Image scaling and light normalization can be carried out at the subsequent steps in recognition system.

Experimental results

For experiment, parameters in (2) and (3) were defined as *m* = 2.5, β = 0.5, β_u = 0.8, β_v = 0.6. Face outlines were extracted almost from all images (5% error, due to biometrical features of each person) excepting images with hanged head views (10% error, as it's difficult to describe triangle shape by mask-oval). As a result, it's advisable to exclude hanged head views of images from recognition system input.

Conclusions

In this paper a new method was proposed for face outline extraction from color images using freeware *OpenCV* for eyes detection purposes. This method allows us to normalize all input images to the onlygeneral presentation in which image noises (unimportant features) are deleted.

The method mentioned above was developed [4] and used in [7] for person identification using tree data structures [8].
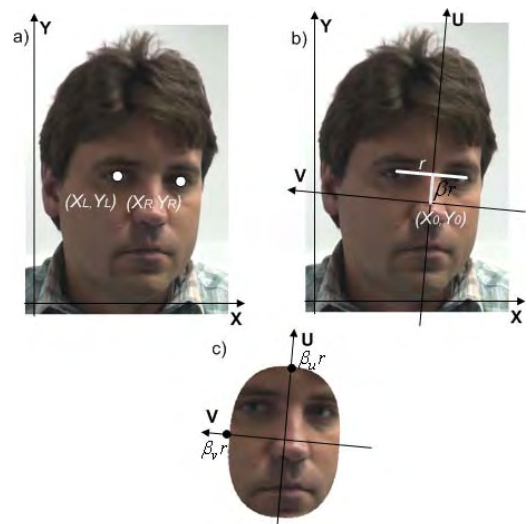

Fig.3. Basic steps to extract face outline.

a) eyes detection; b) calculation of face geometrical characteristics; c) object of interest extraction.

Literature

1. Jain A.K. Statistical pattern recognition: a review // IEEE Transactions on pattern analysis and machine intelligence, 2000 – Vol.22.

2. Stepanov D.Y. About pattern recognition in artificial intelligence // 3d Russian conference for students, post-graduates and young scientists "Artificial intelligence: philosophy, methodology, innovation".: Collection of reports – M.: Svyaz-Print, 2009. 382-385 pp. (in russian)

3. Stepanov D.Y. Data preprocessing and representation for person identification // 58th Annual technical conference of MIREA.: Collection of reports - M.: MIREA, 2009. 116-121 pp. (in russian)

4. Stepanov D.Y. Face detaction on images for person identification / M.: Software license №50200900489 from 02.06.2009 (in russian)

5. http://opencv.willowgarage.com/wiki/

6. Degtyarev N.A., Krestinin I.A., Seredin O.S. Comparative analysis of eyes detection algorythms // 14th Russian conference "Math techniques in pattern recognition".: Collection of reports – M.: Max-Press, 2009. 338-341 pp. (in russian)

7. Lange M.M., Stepanov D.Y. Multiresolution tree representation of multichannel images // 14th Russian conference "Math techniques in pattern recognition".: Collection of reports – M.: Max-Press, 2009. 376-378 pp. (in russian)

8. Lange M.M., Ganebnykh S.N. Tree-like Data Structures for Effective Recognition of 2-D Solids // IEEE Proceedings of ICPR-2004, Cambridge, England: IAPR, 2004. – Vol. 1.

ANALYSIS OF PHASE CORRELATION SEISMIC WAVES ALGORITHM

Yankovskaya N.G.

Scientific supervisor: D.Yu. Stepanov, associate professor

Language supervisor: E.S. Samsonova

Tomsk Polytechnic University, 634050, Russia, Tomsk, Lenina Street, 30

E-mail: abc-xwz@sibmail.com

At present seismic exploration is one of the main methods of geological and geophysical studies, in particular, in the search, exploration and development of oil and gas. Wide use of highly complex work for the implementation of seismic methods is conditioned by the fact that they can be used effectively to solve a wide range of problems arising at all stages of the exploration process [1].

In seismic exploration the following objectives are set: the determination of geological boundaries, prediction of material composition and physical state of rocks on the results of observations of artificially - excited vibrations of the earth (wave field). One of the main problems that arise in the interpretation of the wave fields is correlation of waves. It is the process of isolation, identification and tracking of waves in time and space on the seismograms and time sections [1]. Waves correlation algorithms are known [2, 3, 4], but their investigations are not enough published, so the objective of this work is to study the statistical reliability of the phase correlation algorithm.

For the experiments the well-known additive model of the wave field recorded along a single coordinate x will be used [3]:

$$Y(t, x) = S(t, x) + L(t, x),$$

where $S(t, x)$ implies a useful component of the wave field, which contains information the interpreter is interested in, $L(t, x)$ - disturbance; t – time coordinate. Disturbance will further believed as irregular noise. Generally

$$S(t, x) = \sum_i a_j S_j(t - \Delta t_i(x)),$$

where $S_j(t)$ –form of impulse j wave normalized to one; a_j – wave amplitude; $\Delta t_i(x)$ – time of waves arrival at the point of observation x (hodograph equation).

Phase correlation seismic waves algorithm.

The phase correlation algorithm is based on identification of phase correlation, i.e. the process of sequential tracing from one wave phase route to another which corresponds to the reflecting boundary [4].

Waves correlation is accomplished both by means of the individual seismograms, or their installations, and the converted records presented in the form of dynamic temporary or depth sections. If the registration is conducted on a uniform grid of observation with Δx increment and discretization on time with Δt increment, then the registered field can be represented as a

matrix of A_{NM}, where N is a number of cut routes, M is a number of readings over time.

The developed algorithm of the phase correlation of seismic waves is as follows:

1. Defining the starting correlation point: i – route number, t_0 – start time.
2. Clarification of waves situation on i route (arrival time t_i) – search of the nearest phase.
3. Transition to the next route ($i = i + 1$).
4. Search of possible positions of the wave on i route in $[t_{i-1} \pm \varepsilon]$ interval (an example on Fig. 1):

A) multitude of positive extrema $\{\tau_k\}_{k=1}^K$.

Б) multitude of negative extrema $\{\tau_k\}_{k=1}^K$.

B) multitude of curve amplitudes intersections with time axis $\{\tau_k\}_{k=1}^K$.
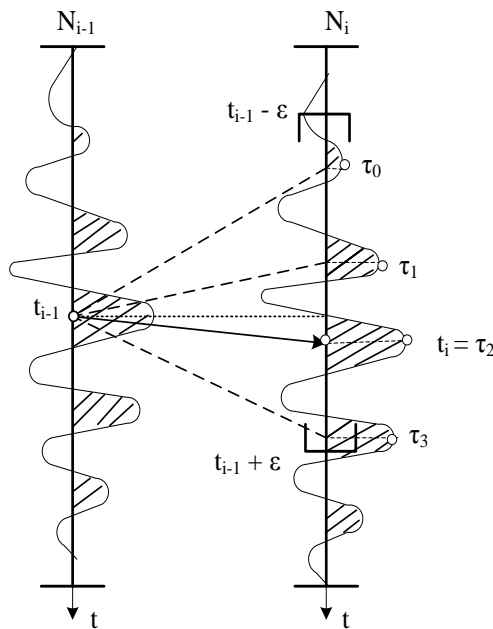
Fig. 1. Positive phase search by criteria of proximity to the previous point and amplitude module maximum

1. The choice of wave position on i route from the estimation set $\{\tau_k\}_{k=1}^K$ by the criterion. Possible phase selection criteria are the following:

A) proximity to the previous point:

$$t_i = \arg \min_{k=1,K} |\tau_k - t_{i-1}|.$$

B) amplitude module maximum (for positive and negative phase):

$$t_i = \arg \max_{k=1,K} |Y(\tau_k, x_i)|,$$

where x_i is a coordinate of i route.

If the amplitude of the found extremum is less than a prior specified minimum possible value of

the amplitude δ - algorithm performance completion.

2. If $i < N-2$, transition to item 3, otherwise – algorithm performance completion.

The resulting estimates $\{t_i\}_{i=0}^{N-1}$ determine the position of the seismic event on the wave field.

This algorithm of the phase correlation of seismic waves was accomplished in the mathematical package MathCad and tested on model seismic waves.

Investigation of algorithm accuracy on the models of useful component of the wave field without signals interference showed that the algorithm allows estimating the position of a wave with accuracy of a sampling increment, and the search interval should be chosen in correspondence to the curvature and slope of the hodograph.

In the study of disturbance influence experiments on a model of waves on the background of homogeneous uncorrelated Gaussian disturbance with given statistical characteristics were accomplished.

Fig. 2. Model wave with parabolic equation of the hodograph

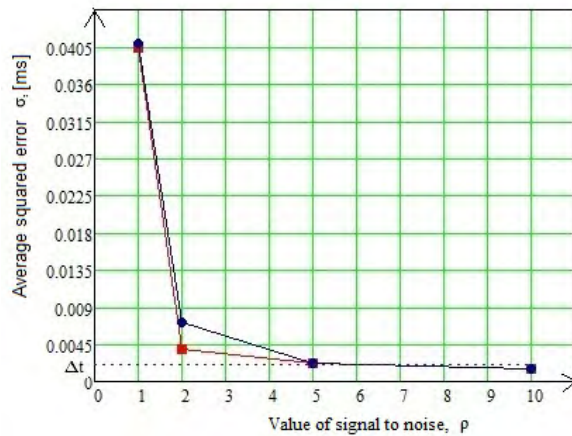*Fig. 3. Model of the wave field with disturbance, $\rho = 2$*

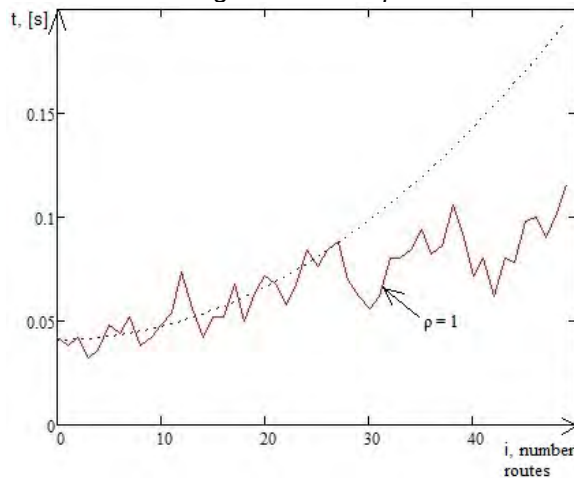*Fig. 4. Graph relationship accuracy algorithm of the ρ*

Fig. 5. Graph hodograph of wave and its evaluation

On Fig. 4 the results of the influence of intensity disturbance on the accuracy of correlation. By ρ ≥ 5 algorithm has the accuracy of a sample interval discretization. Choosing too large an interval search ε leads to error increase.

With the intensity of disturbance (ρ ≤ 2) algorithm becomes unstable, and the results are incorrect (an example on Fig. 5).3

References:

1. В.И. Бондарев. Сейсморазведка. – Екатеринбург: Изд-во Уральского ГГУ, 2007. – 690 с.
2. Н.Г. Туганова Алгоритм фазовой корреляции сейсмических волн //Молодежь и современные информационные технологии: Сборник трудов VII Всероссийской научно-практической конференции студентов, аспирантов и молодых ученых - Томск, 25-27 февраля 2009. - Томск: СПб Графикс, 2009.
3. В.П. Номоконова. Сейсморазведка. Справочник геофизика. – т. 2. – М.: «Недра», 1990. – 400 с.
4. И.И. Гурвич, В.П. Номоконова. Сейсморазведка. – М.: «Недра», 1981. – 464 с.

AUTOMATIC CONTROL SYSTEM OF COMP LEX UNIT
FOR NATURAL GAS PREPARATION

Vasin D.V., Molkin A.S.

Scientific advisor: Rudnitskiy V.A.

Tomsk Polytechnic University

E-mail: vasindv@sibmail.com

An important part in a technological process of uninterrupted gas supply for consumers is preparation of natural gas for transportation. Complex unit for natural gas preparation (CUNGP) provides clearing of gas of impurity and its drainage for pumping on the gas main pipeline. [1]

CUNGP includes following technological objects which are intended for gas preparation:
- a building of switching armature;
- a distribution platform of methanol;
- a technological building of gas preparation;
- gas-measuring station;
- shed of glycol regeneration;
- a technological pumping station;
- servicing units.

Functionally it is possible to describe the work of control object as follows (fig. 1).

Unstripped gas from gas welt clusters arrives on loops of clusters on station of switching armature (SSA). From gas-collecting collector of SSA gas arrives in the technological building, where gas consistently is separated (clearing of mechanical impurity and condensed moisture)

and absorbed (clearing of the respirable and soluted moisture). In total in the technological building there are four parallel working technological lines. On an exit from the technological buildnig gas passes gas-measuring station (GMS) for the purpose of the commercial account of the flow. For measurement of gas flow intellectual flowmeters "Floboss" with controllers ROC407 are used, which send information in system through the controller of gas-measuring station S7-414. [1]

Automatic control system of CUNGP (ACS CUNGP) is capable to solve following problems:

- collection and primary information processing of analogue and discrete sensors;
- indirect measurement of technological parametres;
- engineering-and-economical performance of CUNGP;
- formation of databases of subsystems;
- the analysis of preemergencies;
- supervision of technological process;
- supervision of operation of protection and blocking;
- automatic protection and blocking;
- automatic switching on of the reserve equipment;
- control of technological process;
- supervision of working capacity of technology. [2]

For the decision of these problems the hierarchical three-level SCADA-system (fig. 2) is used.
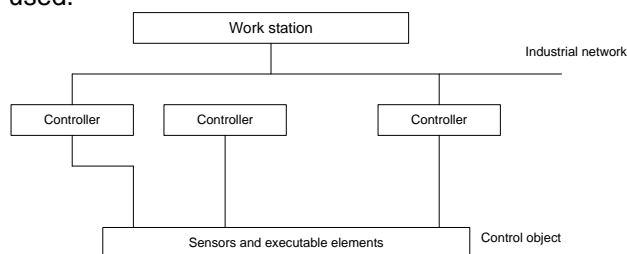
Fig. 2 Structure of three-level SCADA-system

At the lower level following technology of ACS are used:

- sensors with unificated current signal 4-20 mA and a kind of implosion protection «intrinsically safe electric circuit»;
- control valves from "ROTORK" and blocking valves from «ROTORK» and «LEDEEN» (data exchange with them using protocol the report "MODBUS"). [3]

At the level of controllers industrial microprocessor facility SIMATIC - S7-400H, SIMATIC S7-300, S7-417-4H from "SIEMENS" are used. [1]

At the high level software SCADA is used which is structured according to executable algorithms and elements. For each executable element (the valve, the pump, the engine, etc.)

126

individual subprogram programs is realised having the unificated interface with calling program. For realisation of each of the basic algorithms of start-up and closedown (normal and emergency) the subprogram is written tracing its performance and operating transition to its next stage. The general program analyzes generated commands by subprograms of the executable algorithms of performance of the next stages and through the unificated interface, which operates a call of subprograms of executable elements. Such construction of application software provides the structure having a minimum of branchings. Thus it is reached transparent, clear and easily modernised architecture of the application software. Some algorithms is executed jointly by several controllers. For synchronisation of their work data exchange between them on network Ethernet by means of the mechanism of exchange Ethernet Global Data is provided. [4]

Control of CUNGP is executed in an automatic mode (on complex algorithms), or on commands of the operator from high level workstations. The operator interface represents the screen form executed in SCADA package on which all objects of CUNGP and executable elements are represented. Besides, on the screen form signals of the prevention of occurrence of emergencies, system of the fire warning are located. Also on the screen form basic parametres of technological process which are traced by system of automatics and the operator are located. Controllers receive the technological information from the sensor(s). This information arrives on the high level where its gathering, storage, supervision and display is carried out. In case of divergence of any parametres of technological process for the established limits, automatics in the light and sound form notifies the operator on possibility of occurrence of an emergency, emergency protection is actuated, the system begins to work in emergency mode. Then the operator should interfere immediately in this technological process and return its parametres on the established level by means of the operator interface (i.e. to return system in a normal mode). The operator sends control signals to the controller which controls executable element(s). If it is impossible to make it, the operator should shoot a trouble all possible means. Besides, ACS looks for work of the operator and, in case of fulfilment of erroneous actions by him, blocks them.

Thus, usage of ACS CUNGP allows:

- to raise reliability and stability of system work at the expense of an exception of the human factor;
- optimum to use the process equipment;
- material resources conservation. [3]

References

1. automationdrives.ru/as/.../7_11_ASY_Pod-gotovka_gaza_Beregovoi.pdf
2. www.cta.ru/cms/f/326760.pdf
3. http://www.gazauto.gazprom.ru
4. http://www.advantekengineering.ru/index.php?option=com_content&task=view&id=31&Itemid=44
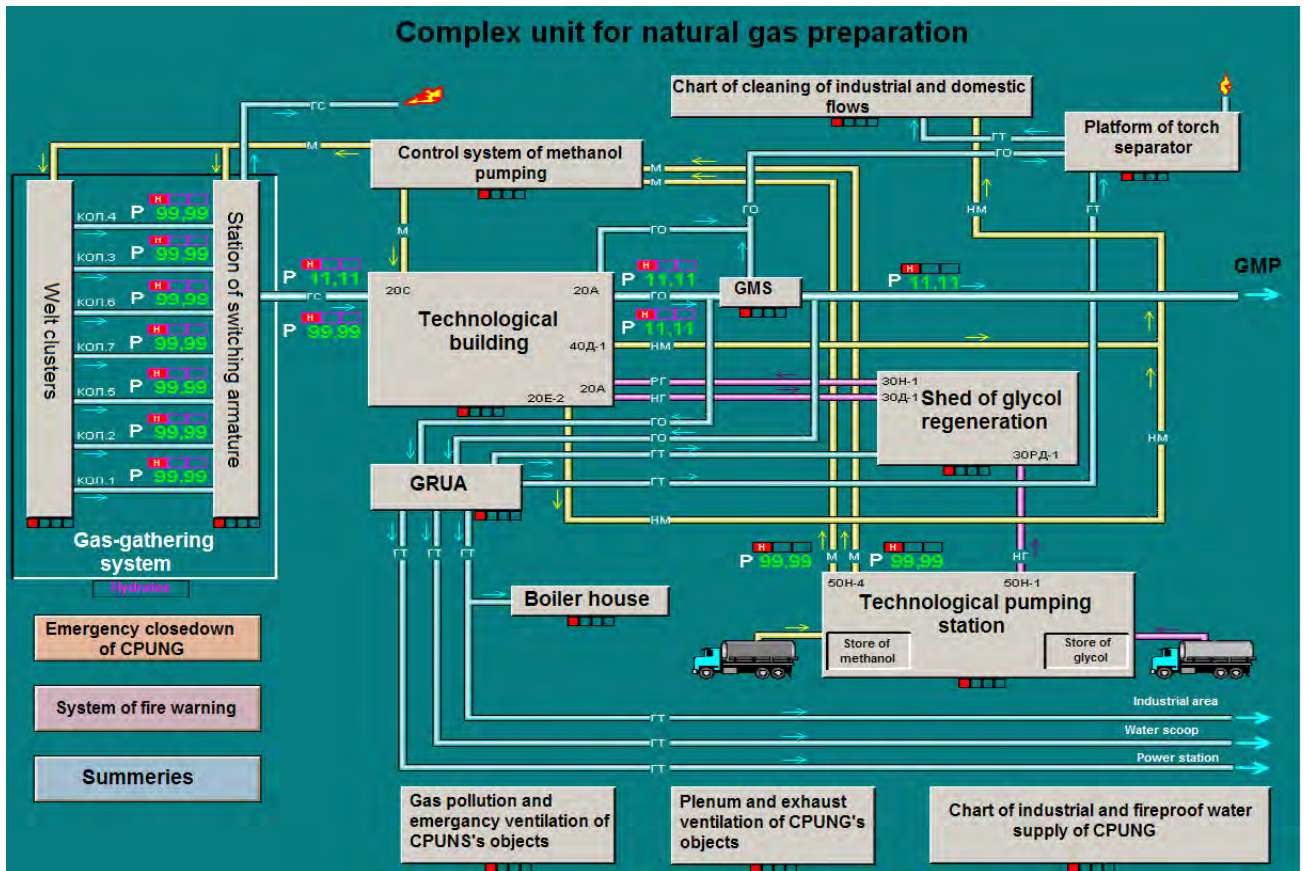
Fig. 1 Function chart of control object

DEVELOPMENT OF TESTING AREA FOR MODELING REAL TIME CONTROL BASED ON "FESTO" EQUIPMENT

Zhuravlev D.V, Berchuk D.Y., Scientific advisers: Mickailov V.V., Yurova M.V.

Tomsk Polytechnic University, Lenin st. 30, Tomsk

At automation of any technological process, one of the most important, complex and expensive problems are adjustment and debugging algorithms of work of the controller at interaction with the real equipment. Nowadays the software of controllers allows directly to debug program of the controller. Debugging of the controller at interaction with the equipment of control object should be spent on the control object that is very costly and dangerous procedure owing to stated below factors:

1. Necessity break manufactures for carrying out of debugging;

2. An opportunity of failure of the equipment because of incorrectly adjusted program.

The most successful way of the decision of this problem is using range with a part of the real equipment on which it is possible to test key stages of algorithm. Tests of the basic stages of algorithm are reduced with risk of occurrence of a supernumerary situation on real object, allow to finish algorithm, not interfering in real technological process.

The basic purpose of our work is creation range on the basis of the equipment "Festo" firm using on faculty IKSU TPU AVTF. During

127

creation of the stand it is necessary to solve a number of labour-consuming problems:

1. Completion of an available equipment;

2. The description of opportunities of range;

3. Creation of laboratory works rate for studying a speciality " Automation of technological process and manufacture ".

Now stands of firm "Festo" have following characteristics:

1. The station of mixing - allows to make mixing of three components in the proportions set by the program of the controller. 6 capacitor sensors of a level, 3 spherical valves, 2 pumps, system of emergency switching-off are located at station.

2. The station of heating - allows to mix a liquid, to create necessary temperature conditions for performance of the recipe. The station has 2 capacitor sensors of a level, 2 pumps, 1 electromixer, 1 heating element, 1 analog sensor of temperature, system of emergency switching-off.

3. The station of pouring - allows to dose out and spill the received liquid in special tanks. The station has a tape the conveyor, 3 one-beam sensors of position, 2 capacitor sensors of a level, analog acoustic the sensor of a level, 1 pump, 1 dosing out valve, 1 separator pneumatic.

Each of stations is controlled by controller Siemens S7-300.

Within the limits of the given work we shall consider algorithm of maintenance of a continuity technological process and control in real time.

Necessary properties of control systems are provided by means of controllers interruption systems.

Controller Simatic Siemens S7-300 has huge functional maintenance of interruptions. In the given controller are realized:

1. Interruptions on time of day (Time-of-Day Interrupts),

2. Cyclic interruptions (Cyclic Interrupts),

3. Hardware interruptions (Hardware Interrupts),

4. Interruptions with a delay of time (Time-Delay Interrupts),

5. Diagnostic interruptions (Diagnostic Interrupt) and interruptions of asynchronous mistakes (Asynchronous Error Interrupts).

Let's consider more in detail each type of interruption and its applicability to algorithm of controllers Simatic Siemens S7-300 work for the decision of a automation of mixing problem.

Interruptions on time of day are used, if it is necessary to address to the process started with periodicity in day. Such process can be clearing of any valve, for example. However, in application to the equipment of firm " Festo " the given type of interruption can be applied only in the special program of the user.

Cyclic interruptions allow to carry out the certain processes with the set cyclicity, for example, time in 1 second. Such interruptions should be used, for example, for movement of the conveyor at process of liquids flood.

Hardware interruptions allow to create operating conditions, proceeding from a condition of the hardware of the equipment. The given type of interruption should be used for all processes depending on values, registered by sensors. Thus, for algorithm of the decision of a problem of mixing with use of the equipment of firm " Festo " it is necessary to use the given type of interruption for all conditions, for example, at filling a tank it is necessary, that there was an interruption on demand of the level sensor, and in the program of interruption it is necessary to open drain valve.

Diagnostic interruptions and interruptions of asynchronous mistakes are used for elimination of mistakes and submission of the signal system about refusal of the equipment. In the program of interruption there should be instructions either on elimination of a malfunction or on inclusion of the alarm system.

Thus opportunities of system of interruption of controller Siemens S7-300 allow to provide completely continuous process.

Let's consider algorithm of work of controller S7-300 with maintenance of continuous technological process on an example of the decision problem of automation mixing.

At use of interruptions the basic program considerably becomes simpler. It aspires to carrying out only the basic function, all other conditions and transitions will be organized by means of interruptions, that considerably facilitates process of programming controller. Necessity of concrete interruptions can be found out at testing the equipment and is easily added, practically without change of the basic program. It is obvious, that most simple and reliable realization of algorithm will be use of hardware interruptions.

Let's consider the algorithm providing a continuity of technological process. The algorithm of work of the equipment consists of 3 mainframes:

1. Check of readiness of the equipment to start-up,

2. Start of the equipment according to the recipe of the user,

3. End of the program.

The first block includes check of all conditions of start, such as presence of a liquid in initial tanks, an opportunity of filling of the tank for mixing, check of indications of sensors (absence of the indication of the charge, the closed spherical valves).
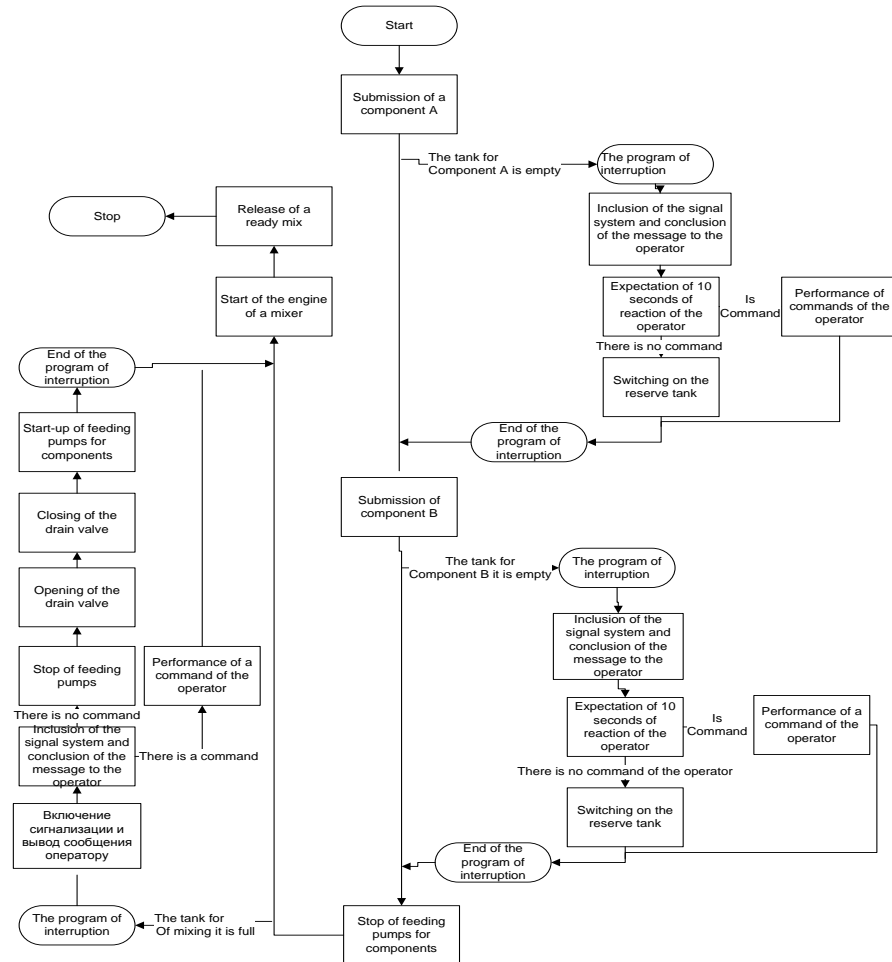
Fig.2. Algorithm of using interruptions

In the same block can be used and diagnostic functions of the controller, for example, check of quantity of starts of the pump for correct maintenance service of the equipment.

The second block realizes the recipe of the user. As an example the recipe mixing serially two components (fig. 2) is shown.

The third block checks readiness of the equipment for switching-off and if it is required, disconnects the equipment. Spherical valves are closed, the engine of a mixer is switched off, the final valve is closed.

The system of interruptions is realized by means of functional blocks OB40 - OB47 in the environment of development STEP7. Each interruption has the priority, the prioritiest is block OB47. Algorithms of work of interruptions include the actions described on fig. 2.

Process, at use of system of interruptions is represented on fig. 2.

Thus, the system of interruptions in the controller is capable to provide a continuity of technological process and to provide reliable performance of the program of the user at all stages of work.
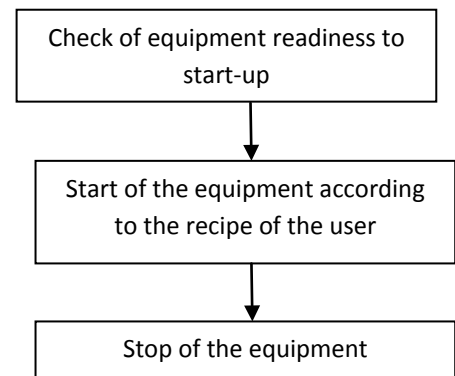
Fig.1. The generalized algorithm of the equipments
work

References

1. Bernhard Schellmann, Jьrgen Helmich. Festo Didactic's Learning System. Bottling station. Festo Didactic GmbH & Co. KG, 73770 Denkendorf, Germany, 2006.

2. Программирование с помощью STEP 7 V5.0. Siemens AG 1998.

PRINCIPLE OF OPTIMIZATION METHODS FOR ASSESSING THE LAW ON SPEED DATA OF VERTICAL SEISMIC PROFILING

Zhukova, MS

Scientific supervisor: Stepanov DY, Ph.D., Associate Professor

Language supervisor: E.S. Samsonova

Tomsk Polytechnic University, 634050, Russia, Tomsk, Lenin Avenue, 30

semeikaju@mail.ru

Vertical seismic profiling (VSP) - a type of 2D seismic survey, during which the sources of seismic waves are located on the surface and receivers are placed in drilled wells (Fig. 1).
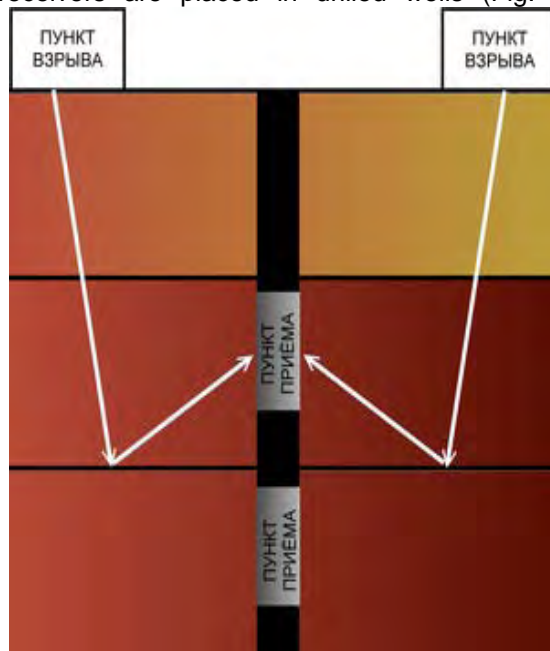

Fig.1. Schematic diagram of the method of vertical seismic profiling

The method is widely implemented in practice industrial geological and geophysical work and firmly entrenched in the complex seismic studies.

Among the main objectives of the GSP there exists the task of estimating the speed characteristics of the medium on which research problems borehole vicinity, refinement and structural models, task prediction of the material composition of rocks are solved. Thus, the accuracy of constructing high-speed applications with high requirements of the law are produced.

Estimate of the rate environment for a certain time of arrival of the direct wave refers to the so-called inverse problems, building models of environments according to the obtained field data.

Isotropic medium is a region of space, the physical properties of which do not depend on the direction. We confine ourselves to a model of a homogeneous and isotropic medium with a horizontally-layered structure (Fig. 2) and consider possible the options for constructing algorithms to determine the waves velocity law.

Speed in a single-layer medium

Let the beam pass through a single layer (top) environment with a known location of excitation (PX) and reception (PP) points and the specified time of arrival of the first entry. It is obvious that the speed of this wave is described by the equation

$$V = \frac{\sqrt{L^2 + \Delta h^2}}{t} \qquad (1)$$

where Δh is thickness, L is the distance to the PV in the vertical, t - the arrival time of first entry.

Speed in a multilayer medium

Assume that we know the velocity $(V_1, V_2, ..., V_{n-1})$ of (n-1) upper layers and t_n - the arrival time of P-wave on the boundary of the n-th and (n +1)-th layer. The speed in the n-th layer should be found. Model of the environment is shown in Fig. 1. The thickness of each layer is $(\Delta h_1, \Delta h_2, ..., \Delta h_n)$.

We can calculate the time of waves arrival in the PP, located in the n-th layer, and the distance L, which P-wave passes through the horizontal using the following equations [1,2]:

$$t_n = \sum_{k=1}^{n} \frac{\Delta h_k}{V_k \sqrt{1 - p^2 V_k^2}}, \qquad (2)$$

$$L = \sum_{k=1}^{n} \frac{p V_k \cdot \Delta h_k}{\sqrt{1 - p^2 V_k^2}} \qquad (3)$$

where $p = \frac{\sin(\alpha_1)}{V_1} = \frac{\sin(\alpha_2)}{V_2} = ... = \frac{\sin(\alpha_n)}{V_n}$,

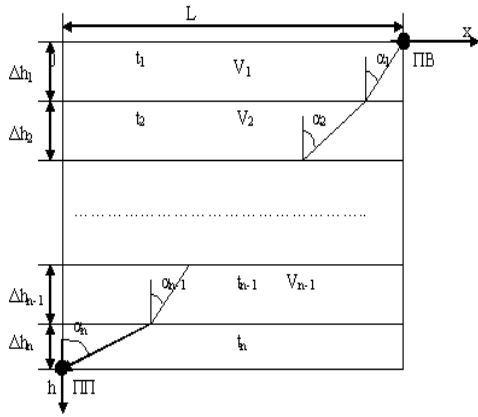α_i is the angle of beam incidence от the boundary between media i and (i +1).

Fig. 2. Model of horizontally layered medium

Typically, the assessment rates, the calculations are carried out only on the hodograph of direct longitudinal waves. Average speed is calculated as V_cp = Δh / t. Verticalization is realized using the formula:

$$t_k = t_{пад} * \cos \propto + \Delta t_{ПВ}$$

where $\Delta t_{ПВ}$ - is static correction, α - the angle of straight beam with the vertical: tgα = Δh / L

In practice, any point of explosion is at least a small take-away from logged well, so the condition of the vertical angle is observed only at great depths. The effects of velocities anisotropy at the first stage is often neglected.

It is known that the estimation of the rate as calculation of the first time derivative of the distance function is considered to be incorrect and unsustainable task. The slightest deviation in the observed data leads to large error estimates of the rate.

In order to solve the problem of evaluating the speed of light anisotropy of the medium, it is necessary to solve the system (2-3). This system of equations for the parameters exposure has a very complicated structure, and, therefore simplifies the equations themselves, and only then the decision is received.

The most frequently used approaches for solving direct and inverse problems is to replace the system of equations (2-3) with approximate expressions, for example by using Taylor power series:

$$F(p) = t_n - \sum_{k=1}^{n-1} \frac{\Delta h_k}{V_k \sqrt{1 - p^2 V_k^2}} - \frac{\Delta h_n}{V_n(p)\sqrt{1 - p^2 V_n^2(p)}}$$

As a rule, series are limited to the first three members. Neglecting the residual components of the Taylor series, given inaccuracy value is received due to the fact that they are not always small. Therefore, such problem solution is not always accurate. For more accurate solution of (2,3) optimization methods can be applied:

Solution of nonlinear equations system by optimization methods

In order to solve any problem of optimization methods, you must have an objective function. In our case it will depend on the composite parameter p:

$$F(p) = 0 \tag{4}$$

where

$$F(p) = t_n - \sum_{k=1}^{n-1} \frac{\Delta h_k}{V_k \sqrt{1 - p^2 V_k^2}} - \frac{\Delta h_n}{V_n(p)\sqrt{1 - p^2 V_n^2(p)}}$$

- objective function obtained from equation (2). Let's xpress the desired speed V_n from equation (3):

$$V_n(p) = \frac{L - \sum_{k=1}^{n-1} \frac{p V_k \cdot \Delta h_k}{\sqrt{1 - p^2 V_k^2}}}{p \cdot \sqrt{\Delta h_n^2 + \left(L - \sum_{k=1}^{n-1} \frac{p V_k \cdot \Delta h_k}{\sqrt{1 - p^2 V_k^2}}\right)^2}} \tag{5}$$

For the upper layer expression (5) is similar to (1). For the second and subsequent layers it's necessary to solve nonlinear equation (4) with (5) numerical optimization methods. Solution (4) is the unknown factor p and the speed Vn. In solving equation (4) should it should also be considered that, $p \geq 0$ because, $\sin(\alpha_i) > 0$; $\alpha_i \in (0, \frac{\pi}{2})$, $V_i > 0$ if $p = 0$ then it has a direct drop in beam waves, $p \neq \frac{1}{V_k}, k = \overline{1,n}$ because at points $p = \frac{1}{V_k}$ the function F (p) experiences discontinuity of 2 kind,

$$0 \leq p < \min_{k=1,n}\left(\frac{1}{V_k}\right) = \frac{1}{\max_{k=1,n}(V_k)}.$$

Thus we have an objective function and constraints to find solutions to a composite parameter p. Using one of the known techniques of optimization, with sufficient accuracy the solution to (2-3) can be found.

The principle of the algorithm of the rate-based optimization methods presented in this report is intended to be applied to assess the high-speed properties of anisotropic media according to vertical seismic profiling. This method, in contrast to the well-known, based on Taylor series expansion, involves finding a solution to the given parametric equations, rather than their approximations. This suggests a significant reduction in errors of the resulting approximation.

References:
1. Гальперин Е. И. Вертикальное сейсмическое профилирование. 2-е изд., доп. и перераб. - М., Недра, 1982. 344с.
2. Сейсморазведка. Справочник геофизика /Под ред. И.И.Гурвича, В.П. Номоконова. – М..:Недра, 1981. – 464 с.
3. Речкин М.С., Алгоритм оценки скоростного закона по данным ВСП // МиСИТ:

Сборник трудов VII Всероссийской научной конференции студентов, аспирантов и молодых ученых – Томск, 25-27 февраля 2009

– Ч.1.- Томск: Издательство «СПб Графикс», 2009. С.179-180.

Section VIII

MODERN PHYSICAL METHODS IN SCIENCE, ENGENEERING AND MEDICINE

PLANTS OF ISOTOPE RECTIFICATION

A.V. Abramov

Research supervisors: A.A. Stepanov, A.V. Tsepilova

Tomsk Polytechnic University, 634050, Russia, Tomsk, Lenin Avenue, 30

E-mail: artyom_a@sibmail.com

Introduction

At present time one of the most pressing problems for the heavy-water reactors is the problem of heavy water purification from hydrogen isotopes accumulating over time.

The problem of tritium accumulation is more complicated for the heavy-water reactors. The annual rate of tritium (in the moderator of power reactors 2.5 Ku / kg D_2O per year; in research nuclear reactors 1.0 - 4.0 Ku / kg D_2O per year) is on the same level or higher than accepted tritium concentration (2.0 Ku/ kg D_2O) in heavy water, which raises the need either to make its replacement and related costs for the purchase of heavy water (approximately $ 6 million / year in PINP, about $ 50 million / year for the replacement of moderator in the reactor project CANDU), or make heavy water rectification from tritium and maintain the tritium concentration on the set level using the isotope rectification plant.

The main problems

Heavy water rectification from tritium is much more difficult problem because firstly the tritium concentration in heavy water is low (very diluted solutions), secondly the rates of separation for heavy hydrogen-tritium mixtures have essentially lower values comparing with protium-heavy hydrogen mixtures and thirdly the tritium is radioactive and radiotoxic in water form and especially in the form of other compounds (hydrogen sulfide, ammonia, etc.) used as working matter in the production of heavy water. Besides, these compounds are exposed to radiolysis under the action of its own radiation. These factors should be considered when choosing the method for resulting tritium concentration. All of these problems very complicate and do more expensive heavy water rectification from tritium. That's why and because of comparatively lower values of neutron flow and accordingly a small velocity of tritium formation and accumulation the water rectification from tritium was not executed, and tritium wastes formed after dilution were dropped into the environment [2].

Rectification column

Rectification is used in industry for direct separation mixtures of volatile liquids, partially or wholly soluble in one another widely.

The main point of the rectification is a mixture separation from two or several liquids with different boiling point of one or more liquids in a more or less pure form. It is achieving by heating and evaporation of mixture, followed by repeated heating and mass exchange between liquid and vapor phases. As a result more volatile component fraction transform in vapor from the liquid phase and less volatile component fraction transforms in a liquid from the vapor phase.

The process of rectification is realized in the rectification plant including rectification column, fractionating column, refrigerator-condenser, heater of initial mixture, collector of the distillate and vat residue. Fractionating column, refrigerator-condenser, heater of initial mixture are used as usual heat exchangers. The plant basic unit is a rectification column, where rectify liquid vapor is rise from the bottom up, and towards to vapor from the top streams the liquid applied to the top part of the plant as a condensate. In most cases the resulting product is a distillate (condense in a fractionating column vapors of volatile components, leaving from the top of the column) and vat residue (less volatile components in liquid form, flowing from the bottom of the column).

Industry has used the bubble (fig. 1.a), screen (fig. 1.b), nozzle (fig. 1.c), membranous tubular columns and centrifugal membranous rectifier. It differs by construction of internal arrangement of device, whose purpose is ensuring interaction between liquids and pair. This interaction occurs under pair bubbling through the liquids layer on plate (bubble or screen) or under pair and liquids surface contact on checker filling or liquids surfaces flowing down fine layer [1].
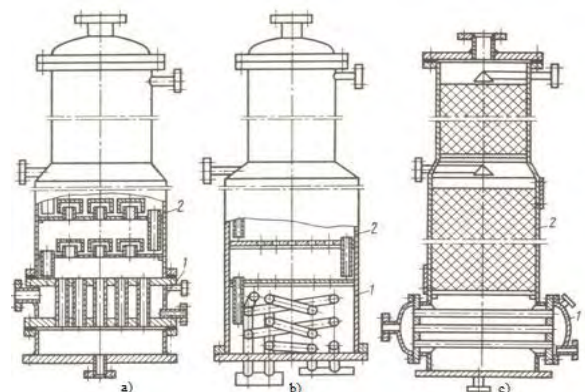

Fig. 1. The construction of rectification columns

Principle of operation, current status and prospects of development

The operation principle of the plant represents the following process. As the catalytic reaction of isotopic exchange between water vapors and heavy waters, $DTO + D_2 = DT + D_2O$ $HDO + D_2 = HD + D_2O$ at a temperature of 200 centigrade degree we have the heavy water removal from tritium and protium and it transfer in gas phase. (fig. 2)

Fig. 2. The plant of isotope rectification

The heavy water degree of tritium extraction is limited to the above reaction equilibrium constant and with three-stage rectification is about 30%. The rectified heavy water from tritium and protium returned to reactor. A mixture of hydrogen isotopes: D_2, DT, HD after admixture rectification and cooling about 25 K is delivering in low-temperature column [2]. As a result because of the process of mass exchange between gas and hydrogen isotopes liquid mixture we have a tritium concentrate at the bottom of the column, and protium - against at the top of the column. Depleted from tritium and protium heavy hydrogen stream returns to catalytic reaction unit of isotopic exchange. From the top of the cryogenic column we have the protium concentrate selection but from the bottom of column - the concentrate or pure tritium.

Nowadays in working plants of isotope rectification tritium extraction degree is comparatively small and for deeper tritium extraction it is necessary to use the cascade of big amount exchange steps "steam-hydrogen". It does the system unmanufacturable. That's why these plants could not be used for deep heavy-water rectification from tritium and light-water waste.

Deep reactor heavy water and heavy-water waste rectification from tritium can be realize on base of catalytic isotope exchange in system "liquid water-hydrogen" on hydrophobic catalyst with use electrolytic cell as a centre of phases circulation and/or gas generator [4]. The process can be realized in catalytic isotope exchange column instead of devices cascade which used in working plants in France and Canada. It allows greatly simplifying the technological plant model and doing its more practically feasible. However there is still no full-scale demonstration of both isotope exchange process and in combinations with low-temperature column which concentrate the tritium. So this process is realized nowhere in the world until.

At present times in institute of nuclear physics in Petersburg on a pilot heavy water plant of isotope rectification for reactor PIK perform an investigation for making practice plant of double-purpose not having while analogue in world:

- maintenance of constant tritium and protium concentration in water for reactor PIK on determined level with guarantee safety level of tritium concentrations in heavy water and its isotope purity (not less than 99,8% D_2O) and

- for conversion polluted by tritium heavy-water and light-water waste of exterior origin with deep rectification its from tritium [5].

Conclusion

Now the development of nuclear technology (atomic power-plant construction with heavy-water reactors such as the Canadian project CANDU, creating high assembly-line production heavy-water nuclear research reactors, the accumulation of tritium contaminated heavy and light waste, including resulting by the removal nuclear weapons) give rise to an annual rate of formation and accumulation man-caused tritium on a global scale (kilograms or tens of millions of Ku per year) has become more than in order exceed than the rate of its natural way (0.2 kg or $2 \cdot 2 \cdot 10^5$ Ku per year). The situation becomes complicated by development of thermonuclear power. Globally the tritium is not having important influence on the flora and fauna yet due to its low emissions to the atmosphere. However because of the locations of nuclear plants especially the heavy-water reactors and plants for processing nuclear fuel there is a potential risk of tritium environmental pollution and risk of radiation exposure for personnel above the permissible limits.

References:

1.   I.A. Alexandrov, Rectification and absorption devices, vol 2, M., 1971;

2.   V.D.Trenin, I.A.Alekseev, I.A.Baranov, K.A.Konoplev et.al. Full-Scale Experimental Assembly for Hydrogen Isotopes Separation Studies by Cryoogenic Distillation: Assembly and Results of the Studies. FUSION TECHNOLOGY, vol.28, No 3, 761, (1995).

3.   I.A.Alekseev, S.P.Karpov, V.D.Trenin. Zeolite Cryopumps for Hydrogen Isotopes Transportation. FUSION TECHNOLOGY, vol.28, No 3, 499, (1995).

4. V.D.Trenin, I.A.Alekseev, K.A.Konoplev et al. Full-Scale Experimental Facility for the Development Technologies for the Reprocessing of Tritium Contaminated Light and Heavy Water Wastes by CECE Process and Cryogenic

Distillation. FUSION TECHNOLOGY, vol.28, \ No 3, 767, (1995).
5. http://www.pnpi.spb.ru

VAVILOV-CHERENKOV RADIATION

N.S.Timchenko, O.O. Batkova

Scientific Supervisor: N.V. Demyanenko, senior teacher; L.G. Syhih, assistant PF

Tomsk Polytechnic University, Russia, Tomsk, Lenin str., 30, 634050

E-mail: tns@sibmail.ru

The authors have chosen Cherenkov-Vavilov radiation for the topic of the article, because it is of great scientific relevance and connected with future profession and scientific activities. On the basis of Cherenkov-Vavilov radiation the experimental methods widely applied in nuclear physics were developed. These methods are used for detection of particles and for research of their nature.

Luminescence is radiation which is the excess over the thermal radiation of the body at a given temperature and has a length considerably exceeding the period of light waves.

For the occurrence of luminescence it is required, therefore, any energy source that is different from the equilibrium internal energy of the body, corresponding to its temperature. To maintain the steady-state luminescence this source must be external. Transient luminescence may occur during the transition of the body in the equilibrium state after the pre-excitation (damping of the luminescence). As follows from the definition, the term luminescence refers not only to the individual radiating atoms or molecules, but also to their collections - bodies.

Elementary acts of molecular excitement and emission light can be the same in the case of thermal radiation and luminescence. The difference lies only in the relative number of various energy transitions. The definition of the luminescence should also include that this concept applies only to bodies having a certain temperature. In the case of strong deviation from thermal equilibrium to talk about the temperature equilibrium or luminescence does not make sense. [7]

Especially important is the special case of luminescence, observed by the radioactive radiation (β- And γ-rays). As shown by Pavel Cherenkov, who worked under the guidance of Vavilov, the glow of this type occurs in a wide variety of substances, including those in pure liquids, with little brightness depends on their chemical composition. This radiation has the polarization and orientation along the direction of motion of the particle. Having found that the radiation does not undergo quenching Vavilov came to the conclusion that it is not luminescence, as previously thought, and its origin is connected with the movement of electrons through matter. A full explanation of the phenomenon was given in the theoretical study of Tamm and Ilya Mikhailovich Frank, which showed that the emission must take place if the electron velocity exceeds the phase velocity of light in this matter.

Let the electron moves uniformly with velocity υ through a substance, such as water.

When an electron moves through a substance is, of course, the interaction of electrons with atoms of matter, with the result, which is part of the energy of the electron can indulge in the atoms, causing ionization or excitation. However in the given case these kinds of energy losses are not of the interest. As shown by a detailed examination of the electric field generated by a moving electron other forms of waste energy electron can take place. Consider the case. Let an electron moving at high speed along the axis of a hollow canal made in the matter, so it did not have direct clashes with the atoms of matter. It appears, however, that if the channel diameter is much smaller than the wavelength of light, all the same electron loses energy in the form of light radiation through the surface, covering the axis of the cylindrical channel. In this case we can assume for simplicity completely transparent environment, so that the flow of radiation pass through it. The radiated energy is, of course, borrowed from the energy of the moving electron, whose velocity is expected to decline as a result of inhibition of the electron in its own field. It is this radiation is a pure Cherenkov radiation.

The calculation shows that the reported emission and the associated inhibition occurs only when the electron velocity υ is greater

than the phase velocity of light in a medium c and stops when the electron velocity is reduced to that speed. Calculating the electric and magnetic field of a moving electron with "superluminal" speed of an electron and forming the Poynting vector, you can calculate the flux of radiation emitted by electrons.
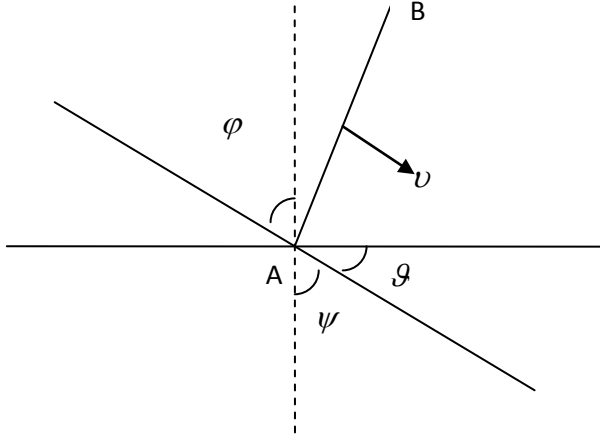

Figure 1.

Vavilov-Cherenkov radiation can be caused not only by moving particles, but any excitement, spreading faster than the phase velocity of light in the environment. Suppose, for example, that at the boundary of the medium of the incident wave with a flat front AB (Fig.1). Along the interface will run at speeds of outrage $V = \upsilon_1 \sin \varphi$ where υ_1 - Phase velocity of light in the first medium. It will initiate the second medium Vavilov- Cerenkov angle ϑ to the interface. Angle ϑ determined from the relation $\cos \vartheta = \dfrac{\upsilon_2}{V}$ where υ_2 - Phase velocity of light in the second medium. Noting that $\cos \vartheta = \sin \psi$. So we find $\dfrac{\sin \psi}{\sin \varphi} = \dfrac{\upsilon_2}{\upsilon_1}$. Thus, the refraction of light can be interpreted as the effect of Cherenkov excited in the second medium of the incident wave. The reflection of light can be here considered. In this case, the speed of the wave front of V coincides with the phase velocity υ. Also we find that $\vartheta = 0$ i.e. wave front propagates without change of direction. [6]

Effects similar to Vavilov-Cerenkov radiation have long been known in hydrodynamics and aerodynamics. If, for example, the vessel moves along the surface of calm water with speed exceeding the speed of wave propagation in the water, then the appeared under the rostrum waves being behind it, form a flat cone of waves, whose disclosure angle depends on the ratio of the vessel speed and the velocity of surface waves. When moving the projectile or aircraft at supersonic speeds the acoustic emission occurs ("roots"), the laws of distribution of which are also associated with the formation of the so-called "Mach cone". These phenomena are complicated by the complexity of the equations of aerodynamics. [1]

Vavilov-Cerenkov radiation has found diverse applications in experimental nuclear physics and elementary particle physics. It established the so-called Cherenkov counters, i.e. detection of relativistic charged particles, radiation which is recorded by a photomultiplier. The main purpose of Cherenkov counters - the separation of relativistic particles with the same momentum, but different velocities. Suppose, for example, the beam consists of relativistic protons and mesons, which passes through a uniform transverse magnetic field. Destinations past trajectories of particles will be determined only by their impulses, but will not depend on their velocities. With the help of diaphragms can be identified protons and mesons with the same momentum. Because of the differences of mass velocity π-mesons υ_π would be a bit more speed protons υ_p. If the resulting beam sent to the gas and pick up the refractive index n of gas so that it $\upsilon_\pi \rangle \dfrac{c}{n} \rangle \upsilon_p$. Then π-mesons will produce Cerenkov radiation, and protons - no. Thus, the counter will only register π-mesons, but it will not register the protons.

Despite the extreme weakness of light, the light receivers are sensitive enough to register the radiation generated by a single charged particle. The devices that allow for the Vavilov-Cerenkov radiation to determine the charge, velocity and direction of motion of a particle, its total energy were created. This radiation is of great practical importance and it is widely used for the control of nuclear reactors.

Vavilov-Cerenkov radiation has found various applications in the experimental nuclear physics and the physicist of elementary particles. It is the basis of the action of the so-called Cherenkov counters, i.e. detectors of the relativistic charged particles which radiation is registered by means of photo multipliers. The main objective of Cherenkov counters is separation of relativistic particles with identical impulses, but different speeds.

Let, for example, the bunch consisting of relativistic protons and mezons, passes through a homogeneous transverse magnetic field. Trajectories directions of the passing particles will be defined only by their impulses, but will not depend on their speeds. By means of diaphragms it is possible to allocate protons and

mezons with identical impulses. Because of mass difference the speeds of mezons will be a little bit more than speeds of protons. If the obtained bunch is directed into gas and a parameter of refraction n of gas mezons will give Vavilov-Cherenkov radiation, and protons will not. Thus, the counter will register only mezon, but will not register protons.

Despite of extreme weakness of a luminescence, the receivers of light are sensitive enough to register radiation, induced by the only charged particle. Devices which allow to determine charge, speed and a direction of a particle moving, its full energy by Vavilov-Cherenkov radiations have been developed. Application of this radiation for the control of nuclear reactors operation is practically important.

Cherenkov radiation can be observed by unaided eye at small research nuclear reactors often established at the bottom of pool to provide radiation protection. The core of a reactor in this case is surrounded by effective blue luminescence, which is Cherenkov radiation under under the action of fast particles emitted as a result of nuclear reaction.
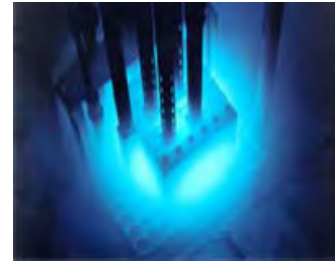
Picture 1. Vavilov – Cherenkov radiation

REFERENCES

1. Antonov-Romanovsky V.V. "Optics and Spectroscopy", 1957.
2. Stepanov B.I. "Classification of secondary emission", 1959.
3. Prinsgeym P. "Fluorescence and fosforentsentsiya", 1951.
4. Levshin V.L. "Photoluminescence of liquids and solids," 1951.
5. Moskvin A.V. "Cathodoluminescence", 1949.
6. Landsberg G.S. "Optics" ,1976
7. Sivukhin D.V. "The course of general physics. Optics ",1985

NUCLEAR WEAPONS IN THE 21st CENTURY IN THE USA

Churkina, A.E., Kakhanova, A.A.

Scientific Supervisor: Tsepilova, A.V., Sukhikh, L.G.

Tomsk Polytechnic University, Russia, Tomsk, Lenina st., 30, 634050

E-mail: cheerful-student@sibmail.com

In the given text the interesting theme of NUCLEAR WEAPONS in the USA and its application is considered. The question of non-proliferation of NUCLEAR WEAPONS remains now especially unclosed. During the Cold War, the greatest security concern of the United States was the military capabilities of the Soviet Union. Potential threats from China and regional states such as North Korea were considered to be lesser included cases that could be addressed by the capabilities deployed to counter the Soviet threat. The current global security environment is radically different. The primary national security challenge the United States is facing now is the nexus of violent extremists and regional states of concern that have, or seek to attain, weapons of mass destruction (WMD).

The United States seeks to assure its allies and friends that the U.S. nuclear deterrent continues to serve as the ultimate guarantor of their security, obviating any need for them to develop nuclear weapons on their own. Credible U.S. nuclear capabilities and the security commitment to allies remain an indispensable part of U.S. efforts to limit nuclear proliferation [2].

Early in his first term, President Bush called for a fundamental reorientation of the United States' strategic force posture [6]. In recognition of the changed security environment the President directed the Department of Defense (DoD) to develop a portfolio of strategic capabilities–including missile defenses and advanced conventional strike assets–and to size the nuclear force to meet 21st century requirements.

Nuclear forces continue to represent the ultimate deterrent capability that supports U.S. national security. U.S. nuclear weapons deter potential adversaries from the threat or use of weapons of mass destruction against the United States, its deployed forces, and its allies and friends [1]. In the absence of this "nuclear umbrella," some non nuclear allies might perceive a need to develop and deploy their own nuclear capability.

One of the questions to consider is whether the USA still needs nuclear weapons.

The world has changed a great deal in the last decade and a half. The Cold War stand-off with the Soviet Union is over, and Russia is no longer an ideological adversary. The United States has made historic reductions in its operationally deployed strategic nuclear forces and plans to reduce them to a level of 1,700 to 2,200 by 2012, as called for by the Moscow Treaty [3]. The U.S. has also greatly reduced its non-strategic nuclear forces and the total nuclear warhead stockpile. These significant nuclear reductions are fully warranted in the new security environment.

The United States continues to maintain nuclear forces for two fundamental reasons. First, the international security environment remains dangerous and unpredictable, and has grown more complicated since the dissolution of the Soviet Union. Political intentions can change overnight and technical surprises can be expected. Second, nuclear weapons continue to play unique roles in supporting U.S. national security [6]. Although not suited for every 21st century challenge, nuclear weapons remain an essential element in modern strategy.

U.S. nuclear forces have served, and continue to serve, to: 1) deter acts of aggression involving nuclear weapons or other weapons of mass destruction; 2) help deter, in concert with general-purpose forces, major conventional attacks; and 3) support deterrence by holding at risk key targets that cannot be threatened effectively by non-nuclear weapons. Because of their immense destructive power, nuclear weapons, as recognized in the 2006 National Security Strategy, deter in a way that simply cannot be duplicated by other weapons [4].

The role nuclear forces play in the deterrence of attack against allies remains an essential instrument of U.S. nonproliferation policy by significantly reducing the incentives of a number of allied countries to acquire nuclear weapons of their own.

It is also necessary to say a few words about the emerging security environment.

Although trends in the security environment are uneven, we live in a complicated and dangerous world. Challenges that the United States may confront in the decades ahead include:

• States of Concern: States that either have or seek weapons of mass destruction and the means to deliver them and whose behavior is outside of international norms;

• Violent Extremists and Non-State Actors: Non-state organizations that are motivated by goals and values at odds with our values, and that resort to violent means to further their goals; some seek WMD and the means to deliver them; and

• Major Existing Nuclear States Outside of NATO: China and Russia are each modernizing their nuclear capabilities; the future political direction of each remains uncertain [5].

The United States is engaging Russia in important areas of common interest (e.g., counter-terrorism, clear security and nonproliferation), and does not consider Russia to be an adversary. However, despite diligent U.S. efforts to improve relations with Moscow, Russia's transition to a more democratic state with a less confrontational, more cooperative foreign policy has seen recent setbacks [6]. Greatly assisted by profits from its oil and natural gas resources, Russia continues to modernize its strategic nuclear forces.

Even as the United States and its allies work to engage Russia cooperatively, and to promote greater transparency and predictability with respect to nuclear forces and other military capabilities, considerable uncertainty remains about Russia's future course. Recent statements by former President Putin have highlighted Russia's nuclear modernization program and operational readiness (e.g., the resumption of Russian longrange bomber patrols near U.S. and allied territories). Former President Putin's statements, together with Russia's across-the-board modernization of its strategic capabilities, increase concern regarding Russia's intentions. Russia has also threatened to target possible future U.S. ballistic missile defense sites in Eastern Europe [3]. In light of these uncertainties, maintaining a nuclear force second to none, consistent with the Moscow Treaty, remains a prudent approach. For the same reasons, continuing U.S. security commitments to NATO and other allies –including the commitment of U.S. nuclear capabilities– remain vital.

Let us now consider some ways of Managing Risk and the U.S. Nuclear Posture.

To help manage geopolitical, operational, and technical risks, the United States relies on three inter-related aspects of its nuclear posture: 1) the composition of the operationally deployed nuclear delivery systems and their capacity to deliver nuclear weapons; 2) the size, yield, and mix of the nuclear stockpile that supports the operational force; and 3) the ability of the supporting infrastructure to maintain, produce, and repair nuclear weapon delivery systems and warheads.

Finally let us consider the baseline, i.e. the planned strategic nuclear force for 2012.

The United States maintains a triad of strategic nuclear forces that includes land-based ICBMs, SSBNs armed with SLBMs, and long-range bombers able to deliver both tandoff cruise missiles and gravity bombs. (The United States also maintains a small nonstrategic nuclear force, consisting of dual-capable aircraft deployed in

NATO countries, and some non-deployed, nuclear-armed sea-launched cruise missiles.)

The planned composition of the U.S. strategic nuclear force in 2012 is:
- 450 Minuteman III ICBMs;
- 14 Ohio class SSBNs; and
- 20 B-2 and 56 B-52 bombers [5].

The current stockpile of nuclear warheads includes sufficient quantities of each warhead type to support deployed nuclear forces. Additionally, because the United States does not have the ability to produce new warheads, a pool of non-deployed warheads is retained to be used in cases of reliability failures and as a hedge against adverse political developments.

Subsequently, the stockpile analysis has been refined and the planned 2012 stockpile size reduced further to the lowest total since the Eisenhower Administration, and a quarter of its level at the end of the Cold War.

In the conclusion it can pointed out that the United States is making historic reductions in its deployed nuclear forces and its nuclear stockpile. The resulting nuclear force, along with a portfolio of advanced conventional offensive and defensive strategic capabilities, will support the goals of assurance, dissuasion, and deterrence, and allow the United States to respond decisively against aggression should deterrence fail.

The future security environment is characterized by a broad range of uncertainties; some current trends are not favorable. The future direction that states may take, including some established nuclear powers with robust nuclear force modernization programs, could adversely affect U.S. security and that of U.S. allies and friends [4]. The United States seeks to assure its allies and friends that the U.S. nuclear deterrent continues to serve as the ultimate guarantor of their security, obviating any need for them to develop nuclear weapons of their own. Credible U.S. nuclear capabilities and the security commitment to allies remain an indispensable part of U.S. efforts to limit nuclear proliferation.

REFERENCES

1. John C. Baker, Non-Proliferation Incentives for Russia and Ukraine , Adelphi Papers, no. 309 (New York: Oxford University Press, 1997).
2. Simpson, John and Darryl Howlett. eds., The Future of the Non-Proliferation Treaty , (St. Martin's Press, New York, 1995).
3. Bailey, Alison, Jeanine Czubaroff, and Robert Ginsberg, Posterity and Strategic Policy: A Moral Assessment of Nuclear Policy Options (Lanham, MD: University Press of America, 1989).
4. Beigbeder, Yves, Judging War Criminals: The Politics of International Justice, by Yves Beigbeder, Theo Van Boven (New York: St. Martin's, 1999).
5. Russel J. Dalton et al., Critical Masses: Citizens, Weapon Production, and environmental Destruction in the United States and Russia (Cambridge, Mass.: MIT Press, 2000).
6. http://www.nuclearfiles.org/

INTERNATIONAL THERMONUCLEAR EXPERIMENTAL REACTOR

Dolgov A.S., Nikienko A.V.

Scientific supervisor: Stepanov B.P., Ph.D., Associate Professor; Ermakova Ya.V, teacher.

Tomsk Polytechnic University, 634050, Russia, Tomsk, Lenin str., 30

E-mail: ellsworth@sibmail.com

Over the past 50 years, immense progress has been made in the fields of plasma science and fusion technology. Fusion is the merging of two light atomic nuclei into a heaver nucleus, with a resultant loss in the combined mass and a massive release of energy. Still, harnessing fusion power and delivering it for industrial applications remains one of the greatest challenges of our time.[1]

ITER (originally the International Thermonuclear Experimental Reactor) is an international tokamak (magnetic confinement fusion) research/engineering project that could help to make the transition from today's studies of plasma physics to future electricity-producing fusion power plants. It builds on research done with devices such as DIII-D, EAST, ADITYA, KSTAR, TFTR, ASDEX Upgrade, Joint European Torus, JT-60, Tore Supra and T-15. The incredibly complex ITER Tokamak (Pic.1) will be nearly 30 metres tall, and weigh 23 000 tons.[2]
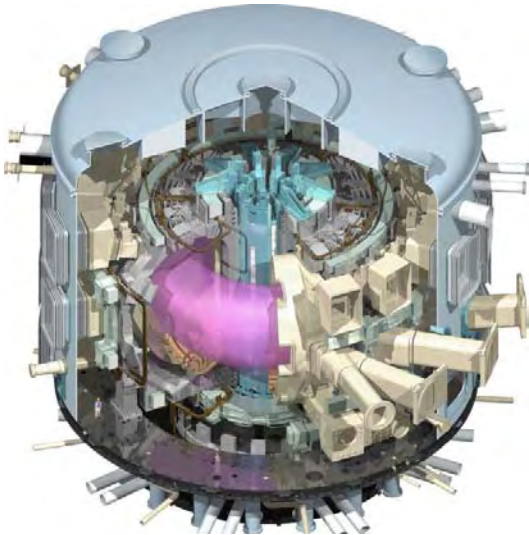
Pic.1. The ITER

One of the tasks awaiting ITER is to explore fully the properties of super hot plasmas - the environment in which the fusion reaction will occur - and their behavior during the long pulses of fusion power the ITER machine will enable.

The challenge will be very great. ITER's plasma pulses will be of a much longer duration than those achieved in other devices, creating intense material stress. ITER will be used to test and validate advanced materials and key technologies for the industrial fusion power plants of the future.

ITER, which incorporates the experience of all previous fusion machines, will take fusion to the point where industrial applications can be considered for providing mankind with a cleaner, safer, and unlimited source of energy.[1]

ITER is a large-scale scientific experiment that aims to demonstrate that it is possible to produce commercial energy from fusion.

In the formula given below Q symbolizes the ratio of fusion power to input power. $Q \geq 10$ represents the scientific goal of the ITER project: to deliver ten times the power it consumes. From 50 MW of input power, the ITER machine is designed to produce 500 MW of fusion power - the first of all fusion experiments to produce net energy.[2]

ITER is based on the 'tokamak' concept of magnetic confinement, in which the plasma is contained in a doughnut-shaped vacuum vessel. The fuel - a mixture of Deuterium and Tritium, two isotopes of Hydrogen - is heated to temperatures in excess of 150 million°C, forming a hot plasma. Strong magnetic fields are used to keep the plasma away from the walls; these are produced by superconducting coils surrounding the vessel, and by an electrical current driven through the plasma.

The ITER Magnet System (Pic.2) comprises 18 superconducting Toroidal Field and 6 Poloidal Field coils, a Central Solenoid, and a set of Correction coils that magnetically confine, shape and control the plasma inside the Vacuum Vessel. Additional coils will be implemented to mitigate Edge Localized Modes (ELMs), which are highly energetic outbursts near the plasma edge that, if left uncontrolled, cause the plasma to lose part of its energy.

The 48 elements of the ITER Magnet system will generate a magnetic field some 200 000 times higher than that of our Earth.
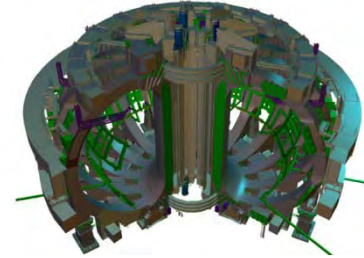

Pic.2. The ITER Magnet System

The large stainless steel Vacuum Vessel (Pic.3) provides an enclosed, vacuum environment for the fusion reaction. It is a hermetically-sealed container inside the Cryostat that houses the fusion reaction and acts as a first safety containment barrier. In its doughnut-shaped chamber, or torus, the plasma particles spiral around continuously without touching the walls.

The Blanket (Pic.4) covers the interior surfaces of the Vacuum Vessel, providing shielding to the Vessel and the superconducting Magnets from the heat and neutron fluxes of the fusion reaction.
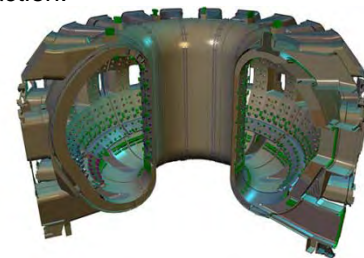
Pic.3. The Vacuum Vessel

The neutrons are slowed down in the Blanket where their kinetic energy is transformed into heat energy and collected by the coolants. In a fusion power plant, this energy will be used for electrical power production.
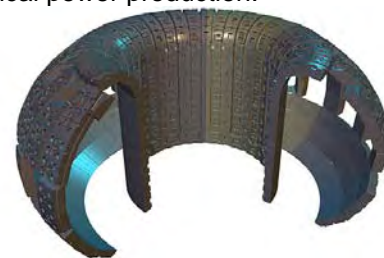

Pic.4. The Blanket

The Divertor (Pic.5) is one of the key components of the ITER machine. Situated along the bottom of the Vacuum Vessel, its function is to extract heat and Helium ash — both products of the fusion reaction — and other impurities from the plasma, in effect acting like a giant exhaust system. It will comprise two main parts: a supporting structure made primarily from stainless steel, and the plasma-facing components, weighing about 700 tons. The plasma-facing components will be made of Tungsten, a high-refractory material.

Pic.5. The Divertor

An extensive diagnostic system (Pic.6) will be installed on the ITER machine to provide the measurements necessary to control, evaluate and optimize plasma performance in ITER and to further the understanding of plasma physics. These include measurements of temperature, density, impurity concentration, and particle and energy confinement times.

The ITER Tokamak will rely on three sources of external heating (Pic.7.) that work in concert to provide the input heating power of 50 MW required
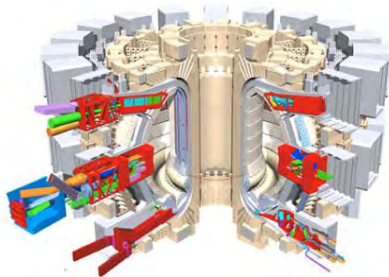
Pic.6. The Diagnostic System

to bring the plasma to the temperature necessary for fusion. These are neutral beam injection and two sources of high-frequency electromagnetic waves.
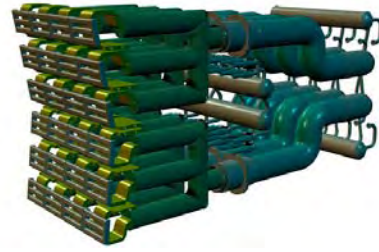
Pic.7. The External Heating Systems

The Cryostat (Pic.8) is a large, stainless steel structure surrounding the Vacuum Vessel and superconducting Magnets, providing a super-cool, vacuum environment. It is made up of two concentric walls connected by horizontal and vertical ribs. The space between the walls is filled with Helium gas at slightly above one atmosphere that acts as thermal barrier. The Cryostat is 31 metres tall and 36.5 metres wide.[3]
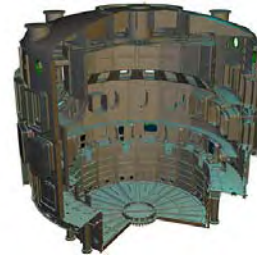
Pic.8. The Cryostat

During its operational lifetime, ITER will test key technologies necessary for the next step: the demonstration fusion power plant that will capture fusion energy for commercial use.[4]

REFERENSES:

1.   The ITER Organization. The Science http://www.iter.org/sci/Pages/Default.aspx.
2.   The ITER Organization. The Project http://www.iter.org/proj/Pages/Default.aspx.
3.   The ITER Organization. The Machine http://www.iter.org/mach/Pages/Tokamak.aspx.
4.   P. Kamenski, D. Davenport, E. Hitt. Thinking inside the box// Wisconsin Engineer. - 2006. - №11.

RADON IMPACTS ON PREMISES

O.B. Elovikova , E.A Noskova

Supervisor: M. E. Silaev, associate professor, PhD.

Ya. V. Ermakova, teacher

Tomsk polytechnic university, 634050, Russia, Tomsk, 30 Lenin str.

E-mail: olga210988@yandex.ru

What is the radon in our life?

We are all permanently exposed to natural radioactivity. This is the radioactive radiation which comes from space (cosmic radiation) and from the natural radioactive elements that can be found in our environment (terrestrial radiation). The human being is fully adapted to this natural level of radiation, so in most cases natural radioactivity doesn't pose a health risk.

This is completely different as far as the naturally occurring gas Radon is concerned. Radon is radioactive and it is continually produced from the natural decay of uranium that is found in nearly all soils. Some amounts of Radon gas are present everywhere in the soil, water and air. Particularly high Radon levels occur in regions where the soil or rock is rich in uranium. It can enter the indoor air where it accumulates in poorly ventilated areas.

There are two main reasons, why Radon has become a health concern in our days:

• Currently, much emphasis is put on isolating buildings to save energy. Unfortunately, these sealings also reduce the exchange of indoor and outdoor air. Radon can therefore build up to high levels!

• In contrast to former generations, people nowadays spend roughly 80% of the lifetime indoors. The exposure time to indoor Radon has risen dramatically!

Out of these reasons Radon doesn't just make the largest contribution to the dose of natural radiation received by the human being (fig. 1) but it is even considered the second
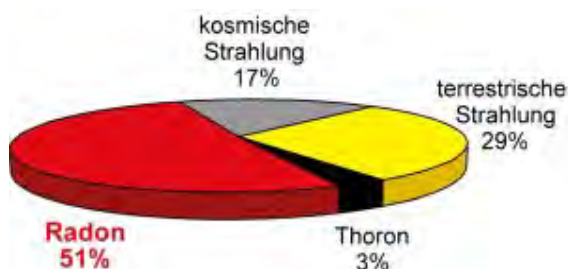
leading cause for lung cancer after smoking. Approximately 5-15% of all lung cancer cases are due to high Radon levels! [1]

Fig. 1 Diagram of natural radiation

How Radon enters a building?

Because of Radon is a gas, a fraction of the Radon produced in the soil can find its way into a building through cracks in the foundation, loose-fitting pipe penetrations, sump openings, crawl spaces, and the like. (fig. 2) [2]

During colder seasons when windows are closed and heaters are on the difference in temperature between the indoor air and the outdoor air causes a thermal stack effect. Warm air rises in a house and creates a vacuum in the lower portions of the building. This suction on the lower level, such as a basement, draws Radon gas from the soil into the building.

Fig. 2 Route of exposure to radon in the room

The concentration of Radon and Radon daughters in the indoor air depends on:
• the amount of uranium and radium in the soil
• cracks in the walls and foundation of the building
• loose-fitting pipe penetrations
• the impermeability between the different floors
• the existence of a concrete floor in the cellar

The concrete floor and walls in the basement slow down the movement of Radon from the soil into the building. However, cracks in the floor, wall slab joints, and openings around plumbing and electrical conduits allow Radon to enter a building.

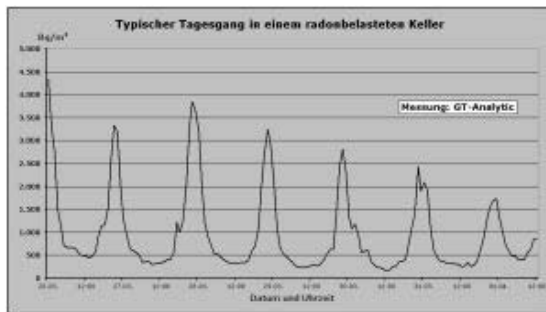**How does the content of radon in the building change in different season?**

Fig. 3 Daily variations of Radon

Radon levels frequently show significant daily variations. Because Radon is a gas, changes in the atmospheric pressure also affect its emission from the ground and its accumulation in the building air. But it is also the habits of the occupants which contribute a lot to the variations in Radon concentrations. When doors and windows are opened during the day, Radon is diluted with fresh air and indoor Radon levels will decrease. On the other hand during the nighttime, if doors and windows are closed Radon levels can build up again.

The fig. 3 shows daily variations of Radon levels over one week in a cellar of a house with very high Radon concentrations.

In addition to the daily variations, Radon levels in a building also show seasonal variations. In contrast to the summertime, indoor Radon concentrations are significantly higher during the winter months because:

• Due heating of the rooms, warm air ascends in the house and creates a state of negative pressure in the lowest floor. This thermal stack effect causes the suction of Radon gas from the soil into the building.

• The frozen ground makes it more difficult for the Radon gas to escape into the atmosphere. It will find an easier way for migration through the cellar of a house.

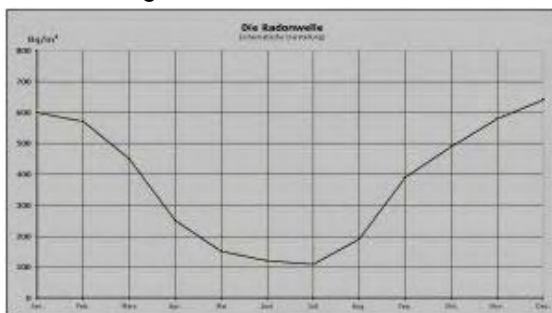• Homes and working places are less aerated during the colder season.

Fig. 4 "Radon wave"

The resulting seasonal change in indoor Radon concentrations is also called the "Radon wave" as shown in the figure on the right. (fig. 4)

What consequences of a high content of radon in buildings?

Radon levels in the outdoor air are relatively low however, when Radon enters a house it can build up to levels which pose a significant health risk to the occupants.

When Radon undergoes the process of radioactive decay, new particles like Polonium (Po-218 & Po-214), radioactive Lead (Pb-214 & Pb-210) and Bismuth (Bi-214) are created. These Radon decay products are also called "Radon daughters" and unlike to the Radon gas they are solid particles. The problem is, that the Radon daughters are radioactive substances, too! Most of the Radon daughters become attached to tiny dust particles (aerosols) in the indoor air. When these particles are inhaled, a fraction of them is deposited in the lungs. Inside the lung, Radon daughters emit alpha particles that are absorbed in the nearby lung tissues. The resulting radiation dose increases the risk of lung cancer.

Radon gas is chemically unreactive. It does not react with body tissues. While some inhaled Radon does dissolve in the body fluids, the resulting concentration is so low that the radiation dose from the Radon gas itself is negligible. It is the Radon decay products that cause the damaging health effects when breathed in!

The greater the amount of Radon in the air, the greater is the potential of developing lung cancer, because: More Radon means, that also more Radon daughters will be produced which can be inhaled and retained in the lungs. The radiation dose to the lung tissue increases and so does the risk of lung cancer. The mortality rate for lung cancer is about 90%![3]

What measures to reduce the level of radon?

The level of the indoor Radon concentration depends mainly upon the ease at which Radon can migrate into the house and move within the house as well as on the amount of suction force exerted by the building on the soil beneath.

A reduction of the Radon level can be achieved by:

• Sealing cracks and joints in the floor and walls which are in contact to the soil.

• Sealing of openings around plumbing and electrical conduits through which Radon can enter the building.

• Sealing of walls between occupied and unoccupied rooms.

• Sealing with concrete of exposed earthen floors in basement areas.

How to choose a location for the building?

A prediction of precise radon levels which may occur in a future building is not possible. On the other hand the constructor can consult local authorities and gain information about the radon potential in the region. Radon measurements in

neighbouring houses may also give information about radon levels, that can be expected.

Especially in areas with a known high Radon potential it is recommended to consider a Radon mitigation system at the planning of a new house. This will be the best way for a reliable Radon reduction, technical wise as well as from the financial point of view.

A very good mitigation method is a drainage system which permanently removes Radon gas from the soil beneath the building's foundation. The drainage tubes can be connected to a fan if necessary or simply left open if enough Radon is removed through natural airflows.[1]

References:

1.   About Radon [internet-resource], regime of access: www.radon.at, free
2.   It's Your Health – Radon [internet-resource], regime of access: http://www.hc-sc.gc.ca/hl-vs/iyh-vsv/environ/radon-eng.php   , free
3.   Health Risks- Radon [internet-resource], regime of access: http://www.epa.gov/radon/healthrisks.html , free

SPECTRAL COMPOSITION OF NEUTRON AND PHOTON RADIATION SOURCES IRRADIATED STANDARD, REGENERATE AND MOX FUELS IN COMPARISON

Beloshickij K.V., Gnetkov F.V., Nefedov S.A.

Research supervisor: Bedenko S.V., assistant, Ermakova Ya.V., teacher.

Tomsk Polytechnic University, 634050, Russia, Tomsk, Lenin Avenue, 30

E-mail: gnetkov@mail.ru

State of research.

Prolonged operation of a large fleet of power reactors leads to the formation of a large quantity of spent nuclear fuel (SNF). There are two methods for storing SNF: long-term storage and recycling. At present, the choice of strategy for dealing with spent nuclear fuel remains debatable, but in any case the necessity to ensure the safe handling of spent nuclear fuel remains valid. This determines the feasibility and significance, of the research detailed characteristics of the radiation field, formed by SNF [1].

The return of uranium and plutonium into the nuclear fuel cycle has been studied for a long time. Currently, 33 reactors in France, Germany, Belgium and Switzerland use such fuel with a load of ~ 30%.

Nuclear power engineering in Russia is based on the VVER and RMBK reactors. State-of-the-art capabilities of fuel processing allow to separate uranium and plutonium into two fractions that may lead to their different use. Thus, released in processing spent nuclear fuel of VVER-440 reclaimed uranium on the RT-1 plant is mixed with uranium obtained from spent fuel of the BN-600, and it is used to produce fuel for RBMK-1000, containing up to 2,6% U^{235}.

The peculiarity of regenerated uranium is that except for the isotopes of U^{234}, U^{235} and U^{238} there are U^{232} and U^{236} in the fuel, which after the first recycle degrade the radiation characteristics

of spent nuclear fuel at all stages of the nuclear fuel cycle. The content of U^{236} and U^{232} will increase by the re-use of regenerated uranium in nuclear reactors, that may lead to the complication of radiation environment near such nuclear fuel.

This work is devoted to the computing calculated researches of radiation characteristics of the advanced fuel used in VVER, PWR and BWR reactors at the stages of its storage, transportation and processing.

The procedure of calculating the neutron and γ-component of the radiation characteristics of SNF of VVER, BWR and PWR reactors.

Alpha particles appear as a result of α-decays of heavy atoms. β-particles - in β-decays of heavy atoms as well as fission products, γ-quanta appear in all types of decays. In addition, the contribution to the generation of γ-rays is made by irradiated structural materials. Neutrons are created by spontaneous fission of actinides, (α, n)-reactions on the light elements and the reaction (γ, n).

To provide the radiation protection, the problems concerning the shielding from highly energetic γ-rays flows characterized by a high penetrating power and intensity were solved in the first place. Protection against γ-radiation of SNF automatically provides the protection against the α- and β-radiation, since these types of ionizing radiation have much less penetrating

ability. But it did not provide the protection against the neutron radiation (especially in respect of fast neutrons), for which the materials used in the design of protection against γ-radiation, are actually "transparent." For this reason, the neutron and γ-radiation is considered in this paper.

Fuel nuclide composition was calculated using the ORIGEN-S (SCALE 5.0) program, 27-group system of constants, the library of the evaluated nuclear data ENDF / B-IV.

While preparing the constants for the calculating of the spectral composition of the neutron and photon radiation sources in the nuclear fuel, multigroup approximation in one-dimensional cylindrical geometry was used. The neutron spectrum was calculated using the 27-group nuclear data library ENDF4, the spectrum of photon radiation is determined in the 18-group approximation 18GrpSCALE. In the process of burnout constants may repeatedly be recalculated taking into account changes in the spectrum and released power.

ORIGEN-S is widely used in world practice for the calculations of radiation sources in the spent fuel assembly, but ORIGEN-S does not account for the mechanism of neutrons via (γ, n)-reaction.

The source of high-energy γ-rays is the spontaneous fission of actinides. Taking into account the probability of formation γ-rays of high energy (~0.4% [4]) and a relatively high concentration of actinides [3] in the spent fuel, where the reaction passes (γ, n), it is impossible completely eliminate the formation of secondary neutrons by this mechanism [5].

Specific intensity of neutron radiation, caused by the occurrence of (γ, n)-reaction is determined by the relation:

$$Q_j^{\gamma,n}(Z) = A_k^{\gamma}(Z) \cdot \sigma_i^{\gamma,n} N_i(Z)/\mu_j(Z), \text{ neutron/(s·g)},$$

where $A_k^{\gamma}(Z)$ - specific rate of γ-rays generation emitted by the nuclide k, γ-quanta / (s · g); $N_i(Z)$ - the nuclei concentration of actinide i in the compound, cm^{-3}; $\sigma_i^{\gamma, n}(E)$ - a microscopic cross-section (γ, n)-reaction on the actinides i, cm^2; $\mu_j(Z)$ - full rate of interaction γ-rays for the compound j, including photonuclear interaction, cm^{-1}.

The values of reaction cross sections was evaluated using the Bohr's mechanism, when describing the formation of an intermediate nucleus with subsequent emission of fission products [7].

$$\sigma_i^{\gamma,n} = \sigma_{0i}^{\gamma,n}(\Gamma_i/2)^2(E_0/E_i)^{1/2}/((E_i - E_{0i})^2 + (\Gamma_i/2)^2),$$

where $\sigma_{0i}^{\gamma,n}$ - the maximum value of the resonance cross-section of actinide i; Γ_i - resonance half-width of the actinide i; E_{0i} - energy of the resonance peak of actinide i.

The accuracy of the cross sections (γ, n)-reaction near the resonance is in the range from 3 to 40%. The procedure and results of the calculation are described more detailed in the works [1, 4, 6].

Initial data for the calculation.

The nuclide composition was computed for standard, regenerated and MOX fuel irradiated in WWPR-1000, PWR and BWR reactors. The initial nuclide composition of the standard fuel is the following (mass, %): U^{234} - 0,036, U^{235} - 4, U^{238} - 95,964. Source nuclide composition of the recycled fuel, mass %: U^{232} - 2·10^{-7}, U^{234} - 0,043, U^{235} - 4,139, U^{236} - 0,463, U^{238} - 95,355. The initial nuclide composition of MOX fuel (mass %): U^{235} - 1,5, U^{238} - 94,5, Pu - 4. Isotopic composition of Pu: Pu^{239} - 70%, Pu^{240} - 25%, Pu^{241} - 5%.

The results of calculations.

Fuel is irradiated in a reactor about 1100 effective days (fuel cycle with the duration of 3x365 effective days). The calculated value of the burn-up depth was amounted to 56,69 MW· d / t. The SNF isotopic composition of VVER, PWR and BWR reactors was calculated and analyzed. The spectral structure of neutron and photon radiation sources in the spent fuel of these reactors was determined. Neutron and γ-component of the radiation characteristics of spent nuclear fuel of VVER, PWR and BWR reactors was obtained for the burnouts - 28, 40 and 57 MW· d / t and agings - 2, 3 and 7 years. The mechanism of neutron formation via (γ, n)-reaction was taken into account when calculating the intensity of neutron radiation.

The calculated data shows that the MOX fuel irradiated in PWR reactors has the highest activity. Irradiated recycled fuel (first recycle) of BWR reactors has the lowest activity, because it is necessary to increase the quantity of U^{235} in order to compensate U^{236} in the recycled fuel. So, the amount of U^{238} will be less.

The neutron component of the SPF radiation characteristics calculated in this work is understated and the error does not exceed 20-30%, because the error in determining the concentration of Cm^{244} in the spent fuel assemblies of BWR reactor while using 27-group constants library is 24%.

The error in determination the characteristics of the gamma radiation component does not exceed 8-10%, as the concentration of fission products, which are the main gamma emitters, is defined by SCALE much more precisely.

Summary.

Analysis of the calculation results showed that the neutron and γ-component of the radiation characteristics of the regenerated fuel (after the first recycle) practically does not differ from similar characteristics of standard fuel for the same mode of irradiation.

Reuse of regenerated uranium will lead to the increase of the unrecoverable fission products and actinides, as well as the increase of U^{232}, which would lead to complication of the radiation environment at all stages of the nuclear fuel cycle, but this fuel will have an inner self protection from uncontrolled use and distribution.

While calculating the dose characteristics it is neccesary to take into account the energy spectrum of neutrons (in particular from (α, n)-reactions on oxygen, since the spectrum of neutrons significantly "tougher" in comparison with the spectrum of spontaneous fission neutrons).

Radiation characteristics of irradiated MOX fuel are 2-7 times greater (depending on the burn-up and fuel type) than the characteristics of irradiated state and regenerated fuel.

The greatest activity will have MOX fuel irradiated in PWR reactors, the lowest - SNF of BWR reactors.

References.

1. Шаманин И.В. Гаврилов П.М., Беденко С.В., Мартынов В.В. (a, n)-реакции и поле нейтронного излучения облученного керамического ядерного топлива // Известия Томского политехнического университета, 2009. - т.315 - № 2. - с. 75-78.

2. Гарбачев Б.А., Ганев И.Х., и др. Обращение с облученным топливом РБМК-1000 и ВВЭР-1000 при развитии ядерной энергетики. – Атомная энергия, 2001, т. 90, вып. 2, с. 121 – 132.

3. K. Okumara, T. Mori. Validation of a continuous-energy Monte-Carlo burn-up code MVP-BURN and its application to analysis of post irradiation experiment. Journal of Nuclear Science and Technology. Vol. 37, N2, 2000.

4. Схемы распадов радионуклидов. Энергия и интенсивность излучения: Публикация 38 МКРЗ: В 2 ч. Ч. 2. Кн. 1: Пер. с англ. – М.: Энергоатомиздат, 1987. – 432 с.

5. Беденко С.В., Мельников К.В., Шелепов Е.Н. Расчетно-экспериментальное определение сечений (n)-реакций, протекающих в ОЯТ // Современные техника и технологии: Труды XIII Междунар. научно-практ. конф. студентов, аспирантов и молодых ученых – Томск, 26-30 марта 2007. – Томск: ТПУ, 2007. – С. 16–18.

6. Варламов В.В., Песков Н.Н., Руденко Д.С., Степанов М.Е. Сечения фотонейтронных реакций в экспериментах на пучках квазимоноэнергетических аннигиляционных фотонов. Препринт НИИЯФ МГУ 2003-2/715.

7. Шаманин И.В., Гаврилов П.М., Беденко С.В., Мартынов В.В. Нейтронно-физические аспекты проблемы обращения с облученным ядерным топливом с повышенной глубиной выгорания //Известия Томского политехнического университета, 2008. - т.313 - № 2. - с. 62-66.

APPLICATION OF THE EXPERIMENTAL INSTALLATION BASED ON BETA–SPECTROMETER "ASPECT" "BETA–1C" WITHIN THE SCOPE OF RESEARCH ABOUT SPECTROMETRIC DETECTION OF ^{90}SRIN THE ENVIRONMENT

Kadochnikov S.D.

Supervisor: Ermakova Ya.V.; Scientific Advisor: Silaev M.E.

Tomsk Polytechnic University, Russia, 634050, Tomsk, Lenin Avenue, 30

E-mail: foqsis@gmail.com

RADIONUCLIDE STRONTIUM-90

Strontium-90 (^{90}Sr) is a radioactive nuclide of the chemical element strontium which has atomic number 38. Perhaps it is one of the most well-known beta-emitters, which, nevertheless, has a wide application in industry and medicine. For example, there are radio-electronic industry, pyrotechnics, metallurgy, metallothermy, food industry and production of magnetic materials. Radioactive strontium is used for production of nuclear power batteries, atomic hydrogen power, radioisotope thermoelectric generators, etc. Also it is widely used for manufacturing verification sources for radiation monitoring equipment, applied in the military and civil defense.

^{90}Sr is a radioactive isotope is with a half life of 28.9 years. [1] ^{90}Sr undergoes β-decay, turning into a radioactive ^{90}Y with a half-life of 64 hours. Complete disintegration of ^{90}Sr, which was

emitted into the environment, will take several hundred years.

History is that radiation hygiene gives much attention to this radionuclide due to the several reasons. The first one is that ^{90}Sr has a substantial part in the mixture of products of a nuclear explosion. Secondly there was the nuclear accidents at the production association "MAYAK" in the southern Urals in 1957 and 1967, when a considerable quantity of ^{90}Sr was thrown into the environment. And finally, there are some features in the behavior of this radionuclide inside the human body. Strontium is a chemical analogue of calcium and is capable to be deposited in the bones. Long-term radiation effects of ^{90}Sr and ^{90}Y affect bone and bone marrow, which leads to the radiation sickness, tumors of hemopoietic organs and bones.

^{90}Sr and ^{90}Y in complex is almost pure β-source. [2] Beta-emission can be easily stopped with relatively thin (about 1 mm) layer of aluminum or steel in contrast to the γ-rays. But

Figure 1. Detecting unit of beta-spectrometer "ASPECT" "Beta–1C"

there is no effective protection from destructive influence of the β-sources embedded in the human skeleton.

There is no any difference between chemical reactions of radioactive and non-radioactive isotopes of strontium. Strontium is a natural part of microorganisms, plants and animals. In spite of everything strontium compounds accumulate in the skeleton. It delayed less than 1% in the soft tissues. The way of strontium income affects the magnitude of the deposition of it in the skeleton. The behavior of strontium in the body is determined with a lot of factors: kind of isotope, sex, age, pregnancy and others. For example, the skeleton of man deposits more strontium than

the skeletons of women. There are different ways how strontium can get inside the body: in food and water, with the air or through open wounds and skin lesions.

Because of the specific impact on the human body, and also the properties to accumulate in bones regulations for ^{90}Sr have low values of maximum allowable concentrations which are differ by an order from the same of magnitudes for ^{137}Cs and ^{40}K. It is important to add that the ^{137}Cs and ^{40}K have the beta-activity and thus cause significant errors in determining the ^{90}SR, if they are with it in one test sample. [3,4]

IDENTIFYING RADIONUCLIDE

In the laboratory of the Department of Applied Physics we have is a beta-spectrometer "ASPECT" "Beta-1C" (figure 1). Its measuring of radionuclide activity is based on method of scintillation spectrometry. Continuous β-spectrum of the sample containing β-emitting radionuclides is decomposed into components using computer program. Decomposition is carried out by the spectra of standard sources of each radionuclide, which are measured in the same geometry as the test sample and activity of which has certified value. The decomposition coefficients are found to be proportional to the activity of radionuclides in the sample. [5] With this installation, we can carry out an express qualitative and quantitative analysis of the content of ^{90}Sr in the sample, without resorting to expensive and unattractive radiochemical methods.

From the theory of physics we know that any radionuclide can be identified with three physical characteristics: a type of radioactive transformations, decay energy and a half-life. [6] In studies involving the use of radioactive detectors, identifications were based only on energy of radiation of the main components and/or half-life, because usually in advance it is known exactly what radionuclides may be contained in a test sample.

Working with spectrometric tools is important to take into account the background. The background is a reading of detector in the absence of the investigated radiation source (test sample). The background takes place due to cosmic radiation, radioactivity of construction materials, false electrical pulses, as well as the presence of other radioactive samples in the operating room, in the air and polluted parts of the measuring device. Level of background depends on the design of the detector and its service life period and also increases during the operating time.

As opposite to ^{90}Sr, ^{137}Cs and ^{40}K always demonstrate a γ-radiation. In the scheme of two-stage β-decay ^{90}Sr $\rightarrow$ ^{90}Y $\rightarrow$ ^{90}Zr, which ends with a stable nuclide, the excess energy of the nucleus can be emitted with γ-rays. But this

contribution is negligible and we may ignored it. [7,8]

In the process of measuring the activity of β-emitters, which also emit γ-rays, it is important to determine the γ-background. Plotting the attenuation of β-particles curve we can account the γ-background. The residual activity, which does not change with further increase in the thickness of the absorber, can make it possible to be value the γ-component. [6]

In process of measurement it is also important to take into account the weakening of the radiation in time. This phenomenon of radioactive substance is understood as a complex of self-dissipation and self-absorption effects. However, self-weakening correction can be ignored if the thickness of the sample did not exceed 20 mcg/cm^2 for radionuclides with low β-radiation energy and 1 mg/cm^2 for radionuclides with high β-radiation energy. [6] The experimental installation is designed to use a thin source of ^{90}Sr – ^{90}Y complex with thickness no more than 10 mg/cm^2. [5]

Decay energy is identified differently depending on the nature of nuclear radiation. However, the most accurate values of the maximum energy of the β-spectrum can be obtained only by using β-spectrometers.

RESEARCH

The priority of my research is to run the experimental installation and measure a minimal activity which can be detected with it. Analysis of the results will determine the accuracy and sensitivity of the installation.

For further research it is important to find β-emitting samples of ^{90}Sr and other radionuclides, with calibrations and without it. Successful use of this spectrometric device involves deep understanding of the physics of the measuring process and many hours of practical work.

Previous experience of working with spectrometers "ASPECT", in which experimental results are processed with the «LSRM» software, gives a reason to make suggestion that processing may be not entirely correct. Because of the expected results of the measurements often are not confirmed in practice. It can be

suppose that the reason for this lies in the additional errors that had not been eliminated in the process of calibration. There is still no clear understanding of the algorithm of calculation errors during the functioning in normal mode using division of the analyzed range to several energy intervals. Applications of the measurement procedures need to be analyzed with the assistance of professional literature about the processing of measurement results. [9]

REFERENCES

1. Стронций-90 [Электронный ресурс] – режим доступа: http://traditio.ru/wiki/Стронций-90. – 25.02.2010.

2. Радионуклид: стронций-90 [Электронный ресурс] – режим доступа: http://www.chornobyl.ru/ru/exclusion-zone/8-radionuclide/13-strontium-90.html – 25.02.2010.

3. Беспамятнов Г. П. Предельно допустимые концентрации вредных веществ в воздухе и воде. – М: Химия, 1975.

4. Bob Russ. Draft Euratom Directive on the Control of High Activity Sealed Radioactive Sources (HASS) // J. Radiol. Prot. – 2001. – Т. 21. – №2. – С. 193-194.

5. Активность бета-излучающих радионуклидов в счетных образцах. Методика выполнения измерений на сцинтилляционном спектрометре / Под редакцией Ю.И. Брегадзе. – Менделеево, 1996.

6. Лукьянов В.Б., Симонов Е.Ф. Измерение и идентификация бета-радиоактивных препаратов. – М: Энергоатомиздат, 1982.

7. Голубев Б.П. Дозиметрия и защита от ионизирующих излучений. – М: Атомиздат, 1976.

8. Активность радионуклидов на счетных образцах. Методика выполнения совместных измерений на гамма-бета-спектрометре с использованием программного обеспечения «LSRM» / Под редакцией В.С. Алекандрова. – Менделеево-Дубна, 2000.

9. Кунце Х.-И. Методы физических измерений. – М: Мир, 1989.

ELECTRON BEAMS AND GAMMA RAYS APPLICATION FOR TREATMENT OF ONCOLOGICAL DISEASES

Karengina M.N.

Scientific Advisor: Sukhikh L.G., assistant; Demyanenko N.V., senior teacher

Tomsk Polytechnic University, Russia, Tomsk, Lenin str., 30, 634050

E-mail: grima88@mail.ru

The present article deals with radiation therapy applied in modern medicine for treatment of oncological diseases. The authors have considered different methods of radiation treatment such as gamma-radiation (based on Cobalt-60) and electron beams (used in linear accelerators). Also the authors have provided the explanatory notes to the main notions of radiation medicine and nuclear physics. The article is based on the considering of two methods of cancer treatment that allows to represent different approaches to the problem of radiation therapy application for cancer treatment.

Radiation therapy is sometimes called radiotherapy, X-ray therapy radiation treatment, cobalt therapy, electron beam therapy, or irradiation uses high energy, penetrating waves or particles such as X-rays, gamma rays, proton rays, or neutron rays to destroy cancer cells or keep them from reproducing.

The purpose of radiation therapy is to kill or damage cancer cells. Radiation therapy is a common form of cancer therapy. It is used in more than half of all cancer cases. Radiation therapy can be used:

- alone to kill cancer
- before surgery to shrink a tumor and make it easier to remove
- during surgery to kill cancer cells that may remain in surrounding tissue after the surgery (called intraoperative radiation)
- after surgery to kill cancer cells remaining in the body
- to shrink an inoperable tumor in order to and reduce pain and improve quality of life.
- in combination with chemotherapy.

Radiation therapy is a local treatment. It is painless. The radiation acts only on the part of the body that is exposed to the radiation. This is very different from chemotherapy in which drugs circulate throughout the whole body. There are two main types of radiation therapy. In external radiation therapy a beam of radiation is directed from outside the body at the cancer. In internal radiation therapy, called brachytherapy or implant therapy, where a source of radioactivity is surgically placed inside the body near the cancer [1].

Radiation therapy works by damaging the DNA (deoxyribonucleic acid) of cells. The damage is caused by a photon, electron, proton, neutron, or ion beam directly or indirectly ionizing the atoms which make up the DNA chain. Indirect ionization happens as a result of the ionization of water, forming free radicals, notably hydroxyl radicals, which then damage the DNA. In the most common forms of radiation therapy, most of the radiation effect is through free radicals. Because cells have mechanisms for repairing DNA damage, breaking the DNA on both strands proves to be the most significant technique in modifying cell characteristics. Because cancer cells generally are undifferentiated and stem cell-like, they reproduce more, and have a diminished ability to repair sub-lethal damage compared to most healthy differentiated cells. The DNA damage is inherited through cell division, accumulating damage to the cancer cells, causing them to die or reproduce more slowly.

One of the major limitations of radiotherapy is that the cells of solid tumors become deficient in oxygen. Solid tumors can outgrow their blood supply, causing a low-oxygen state known as hypoxia. Oxygen is a potent radiosensitizer, increasing the effectiveness of a given dose of radiation by forming DNA-damaging free radicals. Tumor cells in a hypoxic environment may be as much as 2 to 3 times more resistant to radiation damage than those in a normal oxygen environment. Much research has been devoted to overcoming this problem including the use of high pressure oxygen tanks, blood substitutes that carry increased oxygen, hypoxic cell radiosensitizers such as misonidazole and metronidazole, and hypoxic cytotoxins, such as tirapazamine. There is also interest in the fact that high-LET (linear energy transfer) particles such as carbon or neon ions may have an antitumor effect which is less dependent of tumor oxygen because these particles act mostly via direct damage [2].

For treatment of cancer diseases two various methods such as gamma radiation and electron beams are used. With Cobalt-60 units gamma rays are emitted from a radioactive source with a 5.26-year half-life. The dose rate is constantly decreasing as the source decays and the source needs to be changed every 5 years. A typical teletherapy Cobalt-60 source is a cylinder of diameter ranging from 1.0 to 2.0 cm and is

positioned in the cobalt unit with its circular end facing the patient. Both isocentric (Theratron 780) and column-mounted (Eldorado 8) units exist. The advantage of isocentric machines is that the patient is positioned only once for the treatment and then the source located in the head of the machine is rotated around the patient. The Cobalt-60 source emits radiation constantly (as opposed to linear accelerators or orthovoltage units) and the source must be shielded when the machine is in the off position. The Cobalt-60 source decays to Nickel-60 with the emission of beta particles (E_{max} = 0.32 MeV and two photons per disintegration of energies 1.17 and 1.33 MeV (average energy 1.25 MeV); the gamma rays constitute the useful treatment beam. With an average energy of 1.25 MeV, there are a number of advantages of Cobalt-60 over orthovoltage. There is greater penetrability for more deeply seated tumors due to the higher energy. There is uniform dose deposition in bone and soft tissue (versus orthovoltage). There is a dose build-up region such that maximum dose is not deposited until 0.5 cm below the skin surface resulting in what is termed a "skin-sparing" effect (there is less skin reaction than with orthovoltage). Treatment of superficial tumors and potential tumor cells in surgical incisions requires the placement of a tissue-equivalent material (bolus; superflab; wet gauze) over the site to allow dose build-up to occur and maximum dose deposition at the skin level. In this setting there will then be loss of the skin-sparing effect and increased radiation reaction in the skin. The source-to-skin distance is typically 80 cm so larger field sizes are possible than with orthovoltage. This is one of the most reliable radiation therapy machines because of their mechanical and electric simplicity. A radioactive material license is required for operation. Also, there is a low level of exposure to radiation with a Cobalt-60 unit due to a minor persistent leak of radiation from the source despite the shielding; time spent in the room should be limited to the extent that is possible.

Collimators (two pairs of heavy metal blocks) are use to alter the field size. Other beam modifying devices include the use of lead blocks (preformed or custom made; placed on a tray that is located near the head of the machine and is between the radiation source and the patient) or wedges (used to differentially absorb the photon beam to provide more uniform dose distribution in the tumor and normal tissues; specifically in situations where there is a slope in the patients contour; the use of wedges requires computer planning) [3].

By eliminating the metal target used in linear accelerators, high-speed electrons can be used for radiation therapy. Because the dose of radiation delivered by electrons diminishes rapidly with tissue depth, treatment with electrons is desirable for tumours that are situated within a few centimeters of the skin surface or that overlie radiation sensitive normal tissues (e.g. spinal cord). The energy of the electron beam is chosen according to the desired depth of tissue penetration. Electrons are also combined with photon irradiation to deliver a homogenous dose of radiation to a desired tissue depth. In addition, some radiation centers in developed world are using a single high-dose Intraoperative electron treatment for unresectable abdominal tumours. Direct surgical exposure of the tumour reduces the dose of radiation delivered to normal tissues, thereby reducing the toxicity of treatment [4].

Linear accelerators utilize X-rays (also referred to as photons) or electron beams. Linear accelerators use high-frequency electromagnetic waves to accelerate charged particles, i.e., electrons, to high energies through a tube; the electrons can be extracted from the unit and used for the treatment of superficial lesions; or they can be directed to strike a target to produce high-energy X-rays for treatment of deep-seated tumors. The energy is higher and varies depending on the machine specifications with a range of 4-25 MeV. With the higher energy there is an even greater skin-sparing effect with maximum dose deposited at a depth related to the energy of the photons. The source-to-skin distance is 80-100 cm, and the relatively large source-to-skin distance allows treatment of large fields. It is also possible to treat large volume tumors more uniformly due to the depth dose characteristics. The relatively small focal spot limits the penumbra of the beam, and results in a relatively sharper edge to the treatment field. High output from the machine shortens the treatment time for individual patients and allows treatment of a larger number of patients per day [3].

Linear accelerators can potentially be equipped with a multileaf collimator allowing the shape of the field to match the shape of the target. Multileaf collimators consist of a large number of pairs of narrow rods with motors that drive the rods in or out of the treatment field thus creating the desired field shape. Units without multileaf collimators have two sets of jaws that can move independently but basically allow the formation of a square or rectangular field, and further modification of the field requires the use of lead blocks [4].

An optimal use of the available modern linear accelerators and other teletherapy machines, in particular conformation therapy, will improve the outcome of the radiotherapy treatments in some groups of patients. The side effects and complications will certainly be reduced. Optimization of the treatments with linear accelerators will be facilitated by further

improvement in their technical performance and reliability. In addition, several companies have designed specific types of linear accelerators and Cobalt-60 teletherapy machine for specific purposes.

References

1.   Lica, Lorraine. "Radiation Therapy." Gale Encyclopedia of Cancer. The Gale Group Inc. 2002. Encyclopedia.com. 3 Nov. 2009 - http://www.encyclopedia.com.

2.   Edward   C.   Halperin,Carlos   A. Perez,Luther W. Brady. Perez and Brady's Principles and Practice of Radiation Oncology.

3.   Radiation Therapy Today: Options and Applications - Access mode: http://www.vin.com, free.

4.   Radiation   Oncology   Physics   :   A Handbook for Teachers and Students / editor E. B. Podgorsak ; sponsored by IAEA — Vienna : International Atomic Energy Agency, 2005.670 p.

FLOATING NUCLEAR POWER PLANT – PROSPECT OF NUCLEAR INDUSTRY

Karyakin E.I. , Murigin M. E.

Supervisor: Ermakova Ya. V.; Advisor: Chertkov U.B.

Tomsk polytechnic university, 634050 Tomsk, Lenin Avenue 30

E-mail: evgeny.karyakin@gmail.com

All over the world the Renascence of nuclear industry is observed. Nowadays 442 nuclear reactors with power of almost 369 billion kV are maintained in 30 countries in the world. Nuclear power plants (NPP) produce 16% of world's electricity. As vice director of MAGATE U. Sokolov told in July of 2005, in near 15 years more than 130 nuclear blocks will be built. And general capacity of NPP will rise to 430 billion kV. Share of nuclear energy in world's energy balance will increase till 30%. [1]

As for Russian nuclear industry is concerned, presently, there are 10 operating NPP, most of them are located in the European part of the country. They produce 17% of the electricity generated in the country. The development prospects of the nuclear industry of Russia are specified by the federal target program "Development of Nuclear Industry of Russia in 2007-2010 and -2015" and other documents. This program says that by 2025 the share of nuclear power plants in the total electricity production in Russia should be increased from 16% to 25% and that 26 new reactors should be built during the period. [2]

In many Russian regions it is impossible to build land NPPs as such projects would require preparing construction site, delivering equipment and materials, building and maintaining social infrastructure. So, one of the most prospective projects is floating nuclear power plant (FNPP). FNPP is a flush decked non-self-propelled ship with two KLT-40S reactors manufactured by Nizhniy Novgorod Machine Building Plant. The length of the vessel is 144 meters, the width – 30 meters, the tonnage – 21,500 tons.

Floating NPP can be used for production of electric and thermal energy and can desalinate water (from 40,000 to 240,000 cubic meters of fresh water). The electric capacity of each reactor is 35MW, thermal capacity is 140 Gcal. The service life is 38 years (3 12-year cycles with repairs in between).

The use of floating NPPs is mostly expedient in regions lacking own fuel resources or experiencing difficulties in delivering them (Far North and Far East of Russia, island states of Asian-Pacific). There are six potential sites for floating NPPs: Arkhangelsk, Kamchatka, Chukotka, Yakutia, Krasnoyarsk and Primorsk regions. Decentralized energy supply zones cover almost 2/3 of Russia' territory. The living standard of the local population – mostly small ethnic communities – heavily depends on energy supply and industrial production. On the other hand, these areas are abundant in mineral resources: Chukotka alone has mineral resources worth $1trl. Their development also needs energy.

One of the most important points is that FNPP is designed in such a way that its high reliability and safety are ensured both under normal operating conditions and in power transients. However, its core fuel contains highly enriched uranium (20% and more).

The use of low enrichment uranium is feasible at the expense of the application of higher U content dispersion fuel, for example, at the expense of increasing the volume fraction of UO_2. To further increase the power resources and cost-effectiveness of the core consideration will also be given to an option using a high U content metallic fuel, U-Mo, U-Mo-Si, U-Nb-Zr (the uranium content of the fuel composition being more than 8 g/cm^3).

The application of > 20% enriched U requires the following: [3]

– calculate the physical and thermo physical characteristics of the core;

– formulate the requirements for design, quantity of fissile material, stability and service parameters of fuel rods;

– ensure the criticality safety of floating plant reactor using low enrichment fuel;

– establish the specific requirements for the systems of the reactor unit and plant;

– study the specificity of the spent fuel management;

– develop the design of the higher uranium content fuel element as applied to the KLT-40 reactor;

– develop the technology of the fuel element fabrication;

– validate the fuel element design as applied to the specified burn-up and operating conditions;

– develop the design of burnable absorber pins as applied to the KLT-40 reactor;

– develop the technology of the burnable absorber pins;

– validate the burnable absorber design as applied to the specified operating conditions.

The power resource of this core has to ensure the cost-effective operation of the plant and be maximal as far as it is possible in terms of the serviceability and safety to provide for the minimal reactor reloads and risk of the unsanctioned access to fuel assemblies upon their handling.

Safety and ecological compatibility of floating NPP

Floating NPP with KLT-40S reactor is ecologically friendly source of energy. The annual radiation dose produced by such a plant is just 1 microSv/year with the natural radiation background affecting a man being 2,4 milliSv/year. [4]

In case of off-design accident at floating NPP the maximum irradiation dose for the personnel is 0,25 milliSv, for the population (in the monitoring zone) – 75 microSv.

This is no more than 0,01% of the natural radiation background. The activity of the nearby water cannot exceed 0,1 Bq/l, which is 100 lower than the allowed activity of drinking water.

Among the non-radiation effects a floating NPP can have on the environment are the effect of discharge of heat into nearby waters, electromagnetic and acoustic effects.

The discharge of heat in case of full capacity:

— into the air by ventilation system – 270KW;

— into nearby waters by generator cooling system – 1650KW;

— into nearby water by turbine cooling system – 90MW.

In winter discharge of circulation water can produce ice-holes: the maximum area of such holes is 44,000 m^2 but usually it is no more than 5,000 m^2. The heat emitted by the ventilation systems is not dangerous for the environment.

The chemical, electromagnetic and acoustic impacts the equipment of a floating NPP can have on the environment are localized by design solutions and special measures and are not dangerous for the environment and population.

The project is based on "build-own-operate" scheme. Russia is not only building the plant but will also ensure its normal operation, maintenance once in 12 years, decommissioning and disposal. The project has done through all legislative examinations and ecological inspection. The plant can stand not only design but also off-design accidents like earthquake or falling plane.

Economic expediency of floating NPP

The use of floating nuclear power plants is economically effective in regions where the expenses for transportation of fuel are at least 50% higher than its cost. In the future the initial capacity of the plant (70MW) will be raised to 300-400MW due to the use of unique technologies designed for nuclear submarines. [2]

The use of floating NPP is economically expedient for the following reasons:

— the construction of floating NPP costs as much as the construction of a plant working on organic fuel;

— the period of construction is much shorter (3-3,5 years);

— the reactor is assembled by specialized manufacturer and delivered to the site;

— very little construction and installation work done onsite;

— the operation is based on shift regime;

— maintenance of the plant and treatment of radioactive waste is carried out by specialized companies;

— the biggest advantage of floating NPP over other sources of energy is the cost of 1KW/h – 1.5-2 RUR, which is much lower than the cost of coal, gas, masout or diesel fuel;

— the investment cycle of this project is much shorter due to minimum construction and installation work onsite;

— high quality of the reactor and its construction on turn-key basis by specialized company;

— the plant can be stationed very close to the potential consumer;

— the plant is operated on a shift basis;

— decommissioning is easy (stopped plant is towed to a specialized enterprise for disposal).

The economic profitability of floating NPP is obvious: the government saves money on

transportation of organic fuel to remote regions. The nuclear industry has all necessary infrastructure for building, maintaining, decommissioning and disposing of floating NPP and training operating personnel.

In case of serial production, the cost of the second and the following plants will be 15%-20% lower, which will make it even more profitable.

Conclusion

After disaster at the Sayano-Shushenskoye hydro energetic station the lack of electricity is felt even more. Several regions of Siberia, Far North and Far East still need energy. If project of FNPP will be successful and it will become real it could be sufficient solution. The project and it's business plan is already proven in all inspections, also some investors are found. India, Malaysia and some island states are interested in such a project, but even if some Russian FNPP would be sold abroad, Russia will have rights and obligations to operate it and to prevent propagation of nuclear materials.

Materials

1. Russia creates alternative energetic/ 20.06.2007 «The Truth», Moscow, translation.
2. FNPP/ Project "Rosenergoatom", Moscow, 20.10.2007.
3. Floating NPP with low enrichment fuel/ Project ISTC, Moscow, 2008.
4. Floating NPP will be safer/ 17.04.2007 "RiaNovosti", Moscow.

HEAVY CHARGED PARTICLES APPLICATION FOR THE TREATMENT OF ONCOLOGICAL DISEASES

Ya.A. Leonyuk

Scientific Advisor: Sukhikh L.G., assistant; Demyanenko N.V., senior teacher

Tomsk Polytechnic University, Russia, Tomsk, Lenin str., 30, 634050

E-mail: leonyu4ka@sibmail.com

The term heavy charged particle refers to those energetic particles whose mass is one atomic mass unit or greater. This category includes alpha particles, together with protons, deuterons, fission fragments, and other energetic heavy particles often produced in accelerators. These particles carry at least one electronic charge, and they interact with matter primarily through the Coulomb force that exists between the positive charge on the particle and the negative charge on electrons that are part of the absorber material [1].

Nowadays cancer is becoming common in the world.

One of the most important tasks within this field is the investigation of possibilities for oncological pathologies early diagnostics.

The present-day oncology diagnostics of tumours consists of two stages: population mass examination in order to reveal tumours or their signs, and thorough examination of comparatively small groups selected during the screening in order to make the diagnosis more exact [2].

The future of ion therapy will be best realized by clinical trials that have ready access to top-quality delivery of both protons and heavier ions that can be accurately shaped for treatment of a specific pathology, and which will permit direct randomized-trial comparison of the effectiveness of the various ions for different diseases.

There are two main factors motivating the work in particle radiotherapy. One is the better depth-dose distribution and lateral localization of the radiation dose that can be achieved with charged particles of the mass of the proton or greater. The second reason for using charged particles lies in the presumably more favorable radiobiologic properties of high linear energy transfer (LET) radiation.

The latter provided the main impetus for the extensive clinical work that was conducted using fast neutron radiation, since, at best, the depth-dose and lateral dose localization properties of fast neutrons approximate those of megavoltage photon beams. High-LET radiation is generally thought to offer advantages in treating malignant tumors for the following reasons: 1) they are better able to kill hypoxic cells because they are less dependent on the so-called "indirect", free radical-mediated form of cell killing; 2) cells are less capable of repairing damaging events induced by high-LET radiation (including both sublethal and potentially lethal damage); and 3) there is less variation in radiosensitivity across the cell cycle, hence the therapeutic effect of high-LET radiation is not as dependent on cells "redistributing" themselves into sensitive phases of the cell cycle during the course of therapy [3].

The majority of the studies performed with charged particles have been performed with protons or α-particles. Protons and helium nuclei,

with relatively low linear-energy-transfer (LET) properties, have consistently been demonstrated to be beneficial for aggressive (high-dose) local treatment of many types of tumors. Protons have been applied to the majority of solid tumors, and have reached a high degree of general acceptance in radiation oncology after three decades. However, some 15% to 20% of tumor types have proven resistant to even the most aggressive low-LET irradiation. For these radio-resistant tumors, treatment with heavier ions (e.g., carbon) offers great potential benefit. These high-LET particles have increased relative biological effectiveness (RBE) that reaches its maximum in the Bragg peak.

The Bragg peak is a pronounced peak on the Bragg curve which plots the energy loss of ionizing radiation during its travel through matter. For protons, α-rays, and other ion rays, the peak occurs immediately before the particles come to rest. This is called Bragg peak, for William Henry Bragg who discovered it in 1903.

When a fast charged particle moves through matter, it ionizes atoms of the material and deposits a dose along its path. A peak occurs because the interaction cross section increases as the charged particle's energy decreases.

The phenomenon is exploited in particle therapy of cancer, to concentrate the effect of light ion beams on the tumor being treated while minimizing the effect on the surrounding healthy tissue [4].

The future of ion therapy will be best realized by clinical trials that have ready access to top-quality delivery of both protons and heavier ions that can be accurately shaped for treatment of a specific pathology, and which will permit direct randomized-trial comparison of the effectiveness of the various ions for different diseases. The current status and the anticipated future directions of the role of particle therapy in medicine is a complex subject that involves a very intimate interplay of radiobiology, accelerator physics and radiation oncology.

Heavy charged particles represent the ultimate that the physicist can contribute to the development of radiation sources for therapy.

Of the heavy charged particles, protons are the least expensive to accelerate and can be manipulated to give a sharply defined high-dose volume with a rapid fall-off of dose outside the target area. The biological properties of protons do not differ significantly from X- rays.

High-energy heavy ions offer the greatest flexibility and allow localized dose distributions and also, with the higher Z particles, a substantial reduction of the oxygen enhancement ratio can be achieved.

The ultimate choice of particle depends upon what turns out to be the most important factor in radiotherapy-an improved localization of dose or a reduction in the dependence of cell killing on the presence of molecular oxygen [2].

Radiation therapy is one of the main methods to treat this disease. It is recommended to be applied in 50-70% of cases, as an independent method or combined with other methods of treatment (for example, surgery and chemotherapy). The list of indications to apply it is constantly growing.

Hadron therapy method is a technique for treatment of oncological diseases by exposure to nuclear particles (protons, ionized atoms etc.). Protons diminish 2-3 times the radiation load on the normal tissue around the tumour, in comparison to gamma-rays. The proton (hadron) therapy method is very sensitive and allows treatment of deep seated tumours, including those in brain, with minimal impact on healthy tissues.

Proton-beam therapy (PBT) is one of the most promising and fast developing trends in modern radiation medicine. The physical-technological, medical-biological and clinical research held in recent years showed that, provided a number of requirements are observed, PBT permits higher clinical results (in comparison to the conventional radiation sources) bringing down at the same time the treatment course expenses. In some cases PBT is the only method of treatment with no alternative. To date, about 50 thousand patients with various oncological and other severe diseases have taken a PBT course. The proton-beam therapy in oncology has become a real alternative to surgery [5].

Hadron therapy research has been conducted in Dubna since 1967. The method of 3D conformal proton radiation therapy and radiosurgery has been developed here and is successfully applied on the basis of the computer (CT) and magnetic resonance tomography (MRT), and 3D exposure scheduling.

This method of 3D conformal therapy was developed for irradiation of neoplasms situated in the vicinity of radiosensitive vitals. In this method, the maximum delivered dose distribution coincides with the target shape with high accuracy. The dose drops sharply beyond the target boundaries. It allows the irradiation of localizations which could not be treated by traditional radiotherapy [5].

Unfortunately humans are not yet aware of totally safe means to fight malignant tumours. In the final analysis all resources that kill a tumour cause varying degrees of harm to healthy cells; they destroy the tissues of the heart, kidneys, testicles and so on. Sometimes the most effective kind of therapy and, strange though it may seem, the least harmful to the patient, is the so-called optimal beam therapy, in the course of which the dose required to treat the tumour is received by

the tumour itself, while the patient's remaining organs and tissues receive a minimum dose load.

Naturally the developers of the beam therapy apparatus are doing their utmost to optimize where possible the dose distribution and, to do this, to increase the accuracy of its calculation. In an ideal situation a beam is required which would hit the tumour directly and which would rapidly weaken beyond its outer limits.

It is clear that only a computer is able to resolve such a non-uniform task as the planning of remote beam therapy. In principle methods already exist in other applied fields to calculate the spread of radiation effects and the algorithms and programs required to solve other tasks. Under their direct application to resolve tasks in radiation therapy planning, they ensure high precision but are so difficult to implement that it would take one PC not minutes but tens of hours to solve such a task. It is understood that such terms are unacceptable for the purposes of practical medicine.

Latest researches in oncological diseases sphere showed that to treat cancer is much easier if it is defined in the earlier stages. If the medical course of treatment is carried out on earlier stages, then according to European statistics, in 80-85 cases out 100 it allows to prolong life of the patient [6].

In order to treat cancer first of all the patient undertakes the examination in one of the oncological clinics with the best specialists and laboratories.

After carrying out this diagnostics the doctors can say for sure what methods of treatment can be applied in this particular case.

The efficiency of each method is in the individual approach and program of patients' treatment. Patients should not be in depression – it lessens the resistibility of the body. Thanks to the precise diagnostics and modern methods of treatment it is possible to treat cancer.

References
1. Wilson RR. Radiological use of fast protons. Radiology 1946;47:487.
2. Nowakowski VA, Castro JR, Petti PL, et al. Charged particle radiotherapy of paraspinal tumors. Int J Radiat Oncol Biol Phys 1992;22:295–303.
3. Austin-Seymour M, Munzenrider JE, Goitein M, et al. Progress in low-LET heavy particle therapy: intracranial and peracranial tumors and uveal melanomas. Radiat Res Suppl 1985;8:S219–S226.
4. Zeman EM. Radiation biology. In: Gunderson LL, Tepper JE, eds: Clinical Radiation Oncology. New York, NY: Churchill Livingstone; 1997.
5. Protons force out the lancet .[url]. – Access mode http://mtk.jinr.ru, free
6. History of Radiation Oncology.[url]. – Access mode http://radonc.stanford.edu/resources/links.html, free

INFLUENCE OF WATER CAVITIES INSIDE THE FUEL ASSEMBLY OF MEDIUM POWER REACTOR ON NEUTRON-PHYSICAL CHARACTERISTICS

Marchenko V.O., Timoshin S.V., Kazak N.I

Scientific Supervisor: Chertkov Yu.B., Ph.D., Associate Professor, Ermakova Ya.V., Teacher

Tomsk Polytechnic University, 634050, Russia, Tomsk, Lenin str., 30

E-mail: timoshin@tpu.ru

The distribution analysis of energy release in the existing variant of the fuel element of the medium-power reactor shows the high nonuniformity of the energy release distributions over the fuel assembly cross section. At the reactor power of 100 MWt such nonuniformity leads to is that at the surface of the most intense fuel elements in the active zone, heat flux density (which is the average on the fuel element perimetre) reaches limiting values - 15 MWt/m^2, and at the fuel elements surface in the middle of the fuel assembly it is about 8 MWt/m^2.

In the given work it is offered to replace some fuel elements that are in the centre of each fuel assembly of the medium-power reactor by the water neutron trap. Under the replacement after removing of inefficiently used fuel elements, water cavities are formed, where neutron flux burst increasing the energy release in the environmental cavity. And such increase compensates the amount of energy which is lost at the expense of fuel elements removal. As a result coefficients of energy release distributions over the fuel assembly cross section essentially decrease, averages of these distributions raise and, reactivity margin of a reactor increases. In stead of the removed fuel elements the zirconium alloy hollow tube, muffled from below to reduce

flow section for the coolant should take place. In the given water cavities it is possible to place not only existing experimental channels, but also it is essential to increase their quantity [1, 3].

To carry out neutron-physical calculations MCU-RR program [3] was used. It is intended for the solution of equation of neutrons and photons transfer by Monte-Carlo method in research reactors on the basis of estimated nuclear data in three-dimensional geometry without including any approximates in the geometry description of the considered system and physics of particles and substance interaction. Influence of water cavities inside the fuel assembly, containing fuel elements with loading 6g ^{235}U was examined.

The cartogram shown in fig. 1 has been considered for the active zone with fuel elements that have increased loading on ^{235}U. The maximum value of heat flux density from the fuel elements surface (14.5 MWt/m^2) is observed in cell 75. Therefore all calculating distributions of energy release and neutrons flux density are considered for this cell [2, 4].

Fig.2. Reactivity dependence of medium-power reactor on the number of removed from a fuel assembly fuel elements.

a) The Cavity (24 fuel elements were removed) in a fuel assembly

b) The Cavity (43 fuel elements were removed) in a fuel assembly

c) The Discharged lattice fuel elements in the heart of fuel assembly; 30 fuel elements were removed

d) The Cavity (24 fuel elements were removed) in a fuel assembly

Fig.1. Examples of installations of water cavities inside a fuel assembly in the medium-power reactor.

Table 1.
Engineering and economical characteristics of regular and offered (with water traps in fuel assembly) variants of an active zone in the medium-power reactor:

Parametre	Value of parametre		
	Regular active zone (in fuel element 5 g ^{235}U)	1 stage of modernisation (in fuel element 6 g ^{235}U)	fuel assembly with a water cavity (in fuel element 6 g ^{235}U)
Core density of fuel element on uranium, g/sm^3	2.22	2.64	2.64
Initial mass of ^{235}U in an active zone with fresh fuel, kg	29.24	35.09	30.72
Average burning out in the beginning of campaign, %	14.7	19.0	21.5
U-235 mass in an active zone, kg	24.94	28.42	24.12
Change of average burning out of fuel for one campaign, %	4.25	3.54	3.96
Average burning out at the end of campaign, relative units	18.95	22.5	25.5

Average burning out in unloaded fuel assembly, relative units	33.6	41.5	47.0
Average of new fuel assembly, necessary for indemnification of burning out for campaign, pieces	4.03	2.68	2.68
Annual requirement for fuel, kg ^{235}U	96.9	77.2	67.7

The research of standard rebuilt characteristics of the active zone in the medium-power reactor and the zone composed from fuel assembly, containing water cavities is carried out. Characteristics of the experimental channels in the active zone and reflector are considered. When creating water cavities inside the fuel assembly reactivity margin increases in ~1.5 $\square_{eff}$, nonuniformity of energy release distributions decreases from ~2.5 till ~1.8. But because of the increase of negative effects of the reactance maintained the reactor's operation (effect of stationary poisoning ^{135}Xe, the rate of reactivity loss on fuel burning out) the duration of campaign can be reduced to ~10 %.

Thermal neutrons flux density in experimental channels of reflector and central block decreases no more than in 3 %. Irradiated fuel assembly which is unloaded from an active zone the average fuel burnup increases in about 5% and nonuniformity of its distributions by the assembly cross section decreases. The requirement for fresh reactor assemblies with fuel assembly with water cavities practically coincides with similar values for the update active zone (1 stage). But its annual requirement for fuel (^{235}U) is less in ~12 %.

REFERENCES:

1. Ю. Б. Чертков. Обоснование энергетических и теплофизических характеристик реактора СМ при модернизации активной зоны: автореферат диссертации на соискание ученой степени кандидата физико-математических наук: спец. 01.04.14 / — Томск, 2009. — 22 с.

2. А.А. Цыканов, В.Г. Дворецкий, Ю.Ю. Косвинцев и др. Материаловедческие исследования отработавшего топлива ИЯР СМ в обоснование концепции модернизации активной зоны. Сб. докладов на VII Российской конференции по реакторному материаловедению, 8-12 сентября 2003 г., Димитровград.

3. Е.А. Гомин, М.И. Гуревич, Л.В.Майоров, С.В. Марин. Описание применения и инструкция для пользователя программой MCU-RR расчета методом Монте-Карло нейтронно-физических характеристик ядерных реакторов. Препринт ИАЭ-5837/5. Москва, 1994.

4. А.Г. Калашников, В.М. Декусар. Об эффективной модификации метода переменных направлений. Вопросы атомной науки и техники. Сер. Физика и техника ядерных реакторов. 1985, вып. 5.

DETERMINATION OF NOBLE METALS IN ORE BY TETRAFLUOROBROMATE OF POTASSIUM

Maslova L.S., Matyskin A. V.,

Advisor: Ostvald R.V., Shagalov V.V., Manuylova E.V.

Tomsk Polytechnic University , 634050, Russia, Tomsk, 30 Lenin Avenue

E-mail: Matyskin@sibmail.com

Noble metal – it is metal which has high corrosion resistance, high melting point and which is also stable in process of oxidation even at high temperatures. Noble metal is scientific definition, people say precious metals because these elements are rare and expensive.

One of the first precious metals which have been known from ancient time is gold. As you know this metal has beautiful glitter, color and it does not oxidize in the air. Gold is one of the most expensive metals which has wide field of applications in industry and medicine. Besides this, gold gives aesthetic pleasure.

Assay analysis is method of determination of noble metals in ore, treatment of products, nuggets and in finished products by using of chemical-metallurgical processes. Assay analysis is based on property of melted metallic lead to dissolve noble metals with obtaining of low-melted alloy. To separate noble metal and lead

we can use cupellation process. Cupellation process means that lead and other base metals are easily oxidized at high temperatures by air-oxygen and turn into oxides. But gold is noble metal and it will not turn into oxide even at high temperatures, so we can easily separate gold from oxides. So, assay analysis includes blend preparation, crucible melting at temperature 1000^0C, cupellation, and dissolution of obtained regulus in nitric acid and burning and weighting of gold sample.

Besides assay analysis there are many methods which are used for determination of noble metals in ore, such as: emissive spectral analysis, atomic absorption, spectrophotometric analysis and radioactivation analysis. Scientific analytical centre in Tomsk polytechnic university deals with measurement of mass concentration of elements in natural water, drink water and atmospheric precipitation. Method, which this centre uses, is atomic emission spectrometry with inductive-coupled plasma.

Atomic emission spectroscopy analysis is a way of determination of elementary composition which uses optical linear radiation spectra of atoms and ions of analyzed sample. It is the most accepted and highly sensitive method of identification and quantitative determination of elements of impurity in gases, liquids and solids. It is widely used in different fields of science and engineering. If we compare atomic emission spectroscopy analysis with other optical-spectral and physical-chemical methods, we can say that our method has important advantage: possibility of nondestructive, fast and quantitative determination of almost all elements in large interval of concentrations with good accuracy. Besides this it is possible to use small mass of sample.

But all these methods have disadvantages. In case of assay analysis it is long analysis time and high melting processes temperature. If we want to use atomic emission spectroscopy we need specific equipment. But the main problem of determination of noble metals in solid natural and technological materials is sophisticated preparation of sample. The efficiency of sample preparation depends on the completeness and rate of transferring gold and platinum group metals into solution, melt or another homogenized state. In this case decomposition of a matrix with the oxidation of noble metals is the most important and the most difficult stage.

In 25 years to solve this problem analytical chemists devoted their attention to oxidative fluoridation as an alternative to assay melting. Fluorine oxidants give an opportunity to remove impurity when opening ore. It was found that complex macro base__can be efficiently decomposed with various fluorine oxidants. Choice of reagent and condition of decomposition depend on physicochemical properties of the test matrix.[1]

There are different possibilities of fluorination of noble metals. Reaction of fluorination of noble metals goes in different ways. Part of noble metals easily reacts with almost all fluorine oxidants. Types of obtained fluorides in this reaction depend on nature of fluorine oxidants, on its phase state, on type of reaction vessel, on process temperature and pressure, on complexing and on composition of macro base. Fluoridation of noble metals take place in flow systems with gaseous fluorine oxidants, in open systems with liquid fluorine oxidants and in isolated systems. Practice shows that it is better for economical reasons to use liquids for fluoridation, because we don't need any special equipment if we deal with liquids and to mix gas with liquid we need special, expensive conditions.

Bromine trifluoride is the only one liquid fluorineoxidant, which is known in engineering and which can be used in laboratory for fluoridation of noble metals without any special conditions. Other fluorine halogens (as BrF_5 and ClF_3) in normal conditions have high partial pressure and as a result low boiling point. Because of this reason it is dangerous and uneconomic to use such oxidants. In analytical practice dissolution of ground samples in liquid bromine trifluoride with quantitative oxidation of all noble metals is possible, because in these samples all noble metals are small particles, which are distributed in all volume of sample.

The main aim is to research interaction of noble metals and tetrafluorobromate of potassium ($KBrF_4$). Melt of bromine trifluoride and of tetrafluorobromate of potassium is used for decomposition of different samples, which are difficult to decompose, in system "solid-liquid" $KBrF_4$ is solid substance which is almost safe in analytical practice. It has strong oxidative properties by incongruent melting (It is about $350-400^0$C). In case we posses 8-10 times more of $KBrF_4$ it allows us to decompose and fluorinate almost all materials. $KBrF_4$ suits for oxidative fluoride decomposition of all noble metals in all oxide and sulfide matrix in geological and technological samples. Advantage of using of $KBrF_4$ in decomposition of all joint hinges is lack of loss of noble metals. Oxidation of metals takes about 30-80 minutes, it depends on dispersion of joint hinge. Temperature of process $300-450^0$C can be reached by simple electric stove if we use crucible which is covered by heat-insulating bonnets.

Thermodynamic research of interaction of noble metals with $KBrF_4$ at temperatures 180-190^0C showed that if we have ratio oxidant-noble metal 2:1 − 4:1, we will get total fluoridation and as a result formation of hexafluocomplex of noble metals:

$$KBrF_4 + Au \rightarrow KAuF_4 + 1/2Br_2 \ (t = 280\text{-}320°C)$$

Analysis of determination of noble metals in ore with tetrafluorobromate of potassium is shown in diagram

```
┌──────────┐  ┌──────────────────────────────────┐
│  Sample  │  │ Tetrafluorobromate of potassium  │
└──────────┘  └──────────────────────────────────┘
          │           │
          ▼           ▼
    ┌─────────────────────────────┐
    │   Mixing in graphite crucible │
    └─────────────────────────────┘
                 │
                 ▼
    ┌─────────────────────────────┐
    │  Alloying at temperature 450 ⁰C │
    └─────────────────────────────┘
                 │
                 ▼
    ┌─────────────────────────────┐
    │  Neutralization of excess of KBrF₄ │
    └─────────────────────────────┘
                 │
                 ▼
    ┌─────────────────────────────┐
    │  Separation of soluble fluorides │
    └─────────────────────────────┘
                 │
                 ▼
    ┌─────────────────────────────┐
    │   Extraction concentration   │
    └─────────────────────────────┘
                 │
                 ▼
    ┌─────────────────────────────┐
    │    Quantitative analysis     │
    └─────────────────────────────┘
```
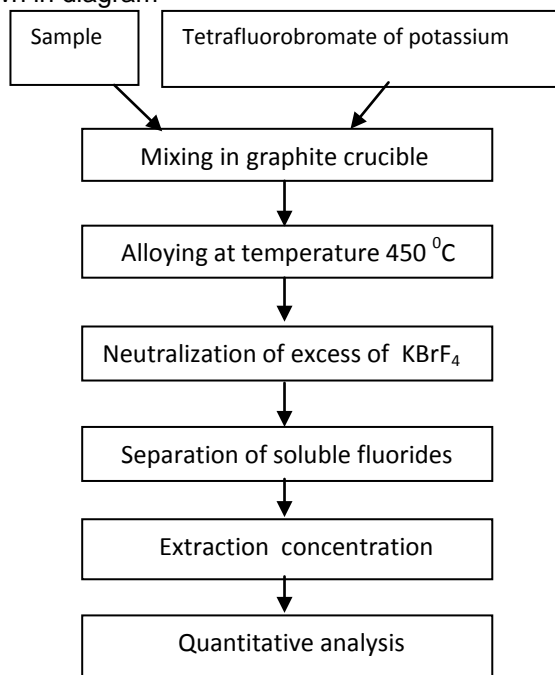
Determination of noble metals in samples which are treated by fluorine technology satisfies all recent requirements. Using of fluorination allows deciding complicated analytical tasks for which it is impossible to apply traditional methods. In development of this area it is expected for various optimized methods of oxidative fluoride decomposition and next conversion of fluorides in useful forms to emerge as a main procedure of preparation of samples for transferring noble metals to oxidized stage.

On the one hand fluorination method is expensive for most analytical laboratories, but on the other hand it will save energy and time in industry. Besides, this method allows spending less chemical reagents. All this factors are economically sound in industry.

References

1. V.N. Mitkin, Fluorine Oxidants in the Analytical Chemistry of Noble Metals/ журнал аналитической химии, том 56, №2, 2001.

2. С.В. Воробьёва, Лабораторные методы определения благородных металлов в рудах, продуктах горно-металлургического производства и сплавах/ методическое руководство, Оренбургский государственный университет, 2004.

3. А.И. Бусев, И.П. Ефимов, Словарь химических терминов/ пособие для учащихся, Просвещение, 1971.

DESTRUCTION OF LONG-LIVED RADIOACTIVE WASTE

Noskova A.O.

Scientific advisor: N.V. Demyanenko, senior teacher

Tomsk Polytechnic University, 634050, Russia, Tomsk, Lenin str., 30

E-mail: pr0fy@sibmail.com

All activities associated with human civilization consume naturally occurring resources and produce waste materials. Whereas the influence of animal life is confined to its natural habitat that of all human activities, especially industrial activities, has strongly influenced the biosphere and atmosphere particularly in densely populated areas such as Europe. Since the industrial revolution, man has made increasing use of fossil energy and mineral resources which have been depleted and to a certain extent been transformed into waste products polluting the human environment and suspected of exerting a detrimental impact on global climate. Age-old historical trends, now accentuated by ecological concern, have boosted the pressure for a reduction of waste output and of its noxiousness. Reduction and recycling of wastes are one of the most recent trends in resource management and have been pioneered by the nuclear community since the early days of nuclear power. Undoubtedly because of the small volumes of waste it generated, nuclear industry has been a leader in pursuing "containment and disposal" rather than the more common "dilution and dispersal" strategy. From this point of view, the nuclear establishment, aware of its social and long-term responsibility, has always carefully considered the future management of irradiated fuel discharged annually from some 400 commercial nuclear power plants now in operation worldwide including ~120 GWe nuclear electric capacity operational in Western Europe and 45 GWe operational in the ex-USSR and East

European countries. Various means of management types are considered for each of the main irradiated fuel constituents discharged from LWRs - uranium, plutonium, actinides and fission products:

• uranium, constitutes about 96% of the fuel unloaded from commercial power reactors. In the case of light water reactors, the most widespread type of reactor in Europe and in the world, the spent fuel on discharge contains still 0.90% enriched in the fissile isotope 235 whereas natural uranium contains only 0.7% of this isotope;

• plutonium, constitutes about 1% of the weight of discharged fuel, it is a fissile material which can be used as fuel in present and future commercial reactors;

• minor actinides constitute about 0.1% of the weight of discharged fuel. They consist of about 50 % neptunium, 47 % americium and 3 % curium, which are very radiotoxic;

• fission products (iodine, technetium, neodymium, zirconium, molybdenum, cerium, cesium, ruthenium, palladium, etc.) constitute about 2.9% of the weight of discharged fuel. At the present stage of our knowledge and our technological capacity, they are considered as the final waste form of nuclear power production, unless a specific use is found for the non-radioactive platinum metals.

• All the physical reactions which produce energy take place within the fuel sub-assembly itself, enclosed inside a strong metallic cladding. Thus all the waste resulting from these reactions remains confined during the discharge of the spent fuel, within the cladding of the discharged sub-assembly. If this sub-assembly is considered as waste, its volume is 10 000 times smaller than the wastes from coal.

• Radioactive decay, which is a natural physical process, takes place in fission products, minor actinides and plutonium in the same way as it occurs in the uranium of the earth's crust and other naturally occurring radioactive elements. As a result, the inventory of the radioactive products contained in irradiated fuel is not fixed for ever: these products will gradually disappear by natural disintegration after periods of time specific to the isotope of interest (for example, half lives are 18.1 years for the curium isotope 244, 24 000 years for the plutonium isotope 239, 2.14 million years for neptunium). It must be pointed out that the products resulting from the decay of these isotopes are themselves radioactive and that a long series of radioactive decay processes must follow one another in order to finally produce a stable element. Irradiated fuel management must therefore take into account a very long-term evolution of the residual radioactivity.

The destruction of plutonium and the minor actinides

Plutonium destruction

With the nuclear power stations currently in operation, a fraction of the plutonium separated in reprocessing plants is used as fuel in pressurized water reactors (PWRs). Good use is thus made of the fissile nature of this plutonium by replacing part (one third) of the enriched uranium oxide sub-assemblies by MoX sub-assemblies (Mixed oxide: mixed uranium and plutonium oxides) when reloading a part of these reactors. In this way, the plutonium inventory jc stabilized as electricity is produced. During this successive recycling in conventional PWRs. however, an increasing proportion of the plutonium isotopes 238, 240 and 242 are formed, and these are neutron absorbers.

Because of this, successive recycling may be limited to just once or twice. This, however, slows down the growth of the plutonium inventory by 30 % compared to what it would be without the use of MoX fuel in PWRs. Moreover, in view of the time required for fuel fabrication, plant residence, and interim storage before reprocessing, the use of MoX fuel postpones by 15 to 30 years the time when the question of how to eliminate the plutonium by other means must be addressed. It must also be noted that experiments have shown that it should be possible to process recycled plutonium so as to increase the number of recycling stages.

Depending on the proportion of the U238 isotope in the core, a fast reactor can therefore be a breeder, a regenerator or a plutonium burner. Moreover the neutronic characteristics of these reactors allow them to use plutonium containing a high proportion of the even-numbered isotopes and therefore to burn plutonium of various origins, notably plutonium which has already been recycled one or more times in a PWR.

Destroying long-lived fission products

As fission products are not fissile, their transmutation into stable elements has to be carried out by specific nuclear reactions induced by particles such as neutrons, protons, photons or light nuclei. The probability of these reactions is very low: therefore very long irradiation time or very high fluxes must be used to obtain acceptable results. Maybe it will be possible to burn fission products in moderated sub-assemblies in the outer core zone of a fast reactor. otherwise the designing of high-flux reactors in which actinides and fission products could be treated simultaneously has apparently come up against difficulties that cannot be easily overcome. The use of particle accelerators or systems coupling

161

a proton accelerator with a sub-critical reactor are therefore now being envisaged. Research is in progress, particularly in the US and in Japan, but the technological uncertainties of such projects are considerable.

Conclusions

The partitioning and transmutation of minor actinides and fission products has been identified as being an alternative strategy for the long-term management of long-lived radioactive waste from power reactors. In order to be able to determine whether partitioning and transmutation can become a viable alternative to the largely proven existing strategies of direct disposal and reprocessing (with no partition of minor actinides and fission products), a considerable amount of investigation will be necessary.

In order to be able to define the best strategies for efficient use of the world's natural uranium resources and for the long-term management of long-lived radioactive waste, it is the duty of the scientific community in Europe to consider all the viable technical possibilities. This paper has identified the main areas where research into partitioning and transmutation are needed:

- continuation of studies on deep geological repositories;
- optimization of LWR core design, fuel and/or fuel cycle to minimize the total amount of long-lived radionuclides produced in irradiated fuel;
- development of advanced reprocessing techniques with a view to waste incineration or chemical stabilization;
- optimization of Fast Reactors with the objective of maximizing plutonium and actinide consumption;
- feasibility studies of devices able to significantly reduce the inventories of long-lived radioactive products and to put them to use.

The nuclear power scientific community is studying these various avenues.

In France, advanced actinide reprocessing and subsequent incineration is being studied, notably in view of carrying out a possible scientific demonstration in Superphenix. In the United States, a dry method of actinide partitioning is being studied in Argonne as well as incineration by means of accelerators.

In Japan, a vast project OMEGA will cover all the above strategies. Research is being carried out worldwide on the most suitable management methods for the remaining radioactive waste which will eventually lead to final deep geological repository disposal of high-level fission product waste. International collaboration is being set up for all these research issues. It should thus be possible in the future to reduce even further the volume and toxicity of the final waste products remaining from nuclear power production.

References

1. Kashkovsky V.V. Applied ecology and safety radiation. Tomsk, 1998.
2. Ryzhakova N.K. Nucleus physics and its exhibits. Tomsk, 2007.
3. http://www.nea.fr
4. http://nuclphys.sinp.msu.ru

ALTERNATIVE ENERGY SOURCES IN THE USA

A.V. Rumyantsev

Scientific advisor: N.V. Demyanenko, senior teacher

Tomsk Polytechnic University, 634050, Russia, Tomsk, Lenin str., 30

E-mail: Smarrt@sibmail.com

We get energy from different things. These things are called energy sources. Some of these energy sources, like coal and gas, have a limited supply. These are called non-renewable sources or fossil fuels. Fossil fuels supply energy for transportation, industrial manufacturing, heating of buildings, and the production of electricity. As of the beginning of the twenty-first century, fossil fuels (fuels formed over millions of years from the remains of plants and animals) provide more than 85 percent of the total energy used around the world [1].

However, the reserves of coal, oil, and natural gas are limited; in fact, they are called non-renewable resources because once the supplies that are available are used up, they cannot be replaced. It is predicted that at the current rate of energy consumption, available reserves of oil and natural gas will be greatly decreased during the twenty-first century. Coal is more plentiful, but its use can contribute to environmental problems such as global warming (an increase in Earth's temperature over time). Because of growing energy demands in developing nations as well as the energy needs of industrialized societies, it will become increasingly necessary to turn to alternative sources of energy in the future. Conserving energy and using it more efficiently are additional ways of addressing the energy problem.

Some of the energy sources, like wind and sunlight, will never run out so they are important sources of energy for the future. These are called renewable or alternative energy sources [1].

Alternative energy is energy provided from sources other than the three fossil fuels: coal, oil, and natural gas. Alternative sources of energy include nuclear power, solar power, wind power, water power, and geothermal energy, among others.

Let us consider different kinds of alternative energy sources.

Nuclear power

Nuclear power is an alternative energy source that can be obtained from either the splitting of the nuclei of atoms (nuclear fission) or the combining of the nuclei of atoms (nuclear fusion). In either of these two reactions, great amounts of energy are released. Nuclear power plants use a device called a nuclear reactor in which uranium or plutonium atoms are split in controlled fission reactions. The heat energy released is captured and used to generate electricity. As of 2000, there were 110 operating nuclear power plants in the United States. France relies on nuclear power for more than 70 percent of its electricity production.

Controlled nuclear fusion is believed by many scientists to be the ultimate solution to the world's energy problems. The energy released in fusion reactions is many times greater than that released in fission reactions. To date, however, the technology has not been developed to make use of this source of energy.

Although nuclear power is a clean, cheap, and relatively safe means of providing energy, public concern over safety issues has brought the construction of new nuclear power plants to a virtual halt in the United States. The nuclear accidents at Three Mile Island in Pennsylvania in 1979 and at the Chernobyl nuclear power plant in Ukraine in 1986 (in which a large amount of radioactive material was released into the atmosphere) prompted fears of similar disasters occurring elsewhere. In addition, there is the problem of storing radioactive nuclear waste safely so that it does not pose a threat to humans or the environment.

Water power

The power of moving water, or hydropower, is a clean and efficient means of generating electricity. Water falling through dams powers water turbines that are hooked up with electric generators. The energy is then distributed across vast electrical networks. Canada, the United States, and Brazil lead the world in hydroelectricity production. The building of dams has an environmental impact, however, causing flooding of land above the dams and disrupting the normal flow of water below them, which can affect the natural ecosystem (a community of organisms and their environment) of a river [2].

Wind power

Wind power is one of the earliest forms of energy used by humankind. Windmills were used on farms in the early part of the twentieth century to pump water and generate electricity. Now considered an alternative energy source, wind power is being harnessed by modern windmills with lighter, stronger blades. Single giant windmills capable of providing electricity to several thousand homes [2].

With new technologies being developed to improve windmill performance and efficiency, wind power is a promising, clean, cheap, and abundant source of energy for the future.

Solar power

Solar power, or energy from the Sun, is a free, abundant, and nonpolluting source of energy. Solar energy can be used to heat buildings and water and to produce electricity. However, the Sun does not always shine, and the process of collecting solar energy and storing it for use at night and on cloudy days is difficult and expensive.

Solar energy systems can be either passive or active. In a passive solar heating system, a building captures and stores the Sun's heat because of the way it is designed, the materials it is made of, or the heat-absorbing structures it possesses. An example of a passive system is a building with large windows facing south (that allow sunlight to enter) and with thick walls that store heat and release it at night.

Active solar energy systems use pumps or fans to circulate heat obtained by solar collectors. A solar collector is a device that absorbs the energy of the Sun and converts it to heat for heating buildings and water. Flat-plate collectors are mounted to the roofs of buildings and used for space heating. They are made of a heat-absorbing plate, such as aluminum or copper, covered by glass or plastic. Water or air circulating in the collector absorbs heat from the plate and is carried to a heat storage tank. The stored heat is circulated or blown over cold rooms using pumps or fans. A conventional heating system is used as a backup when solar heat is not available. Solar heating of water is accomplished using a collector, a hot water storage tank, and a pump to circulate water.

Sunlight can be captured and converted into electric power using solar cells (called photovoltaic cells). Solar cells are usually made up of silicon and can convert light to electric current. They are used in space satellites to provide electricity, as well as in watches and pocket calculators. Solar panels made up of solar cells have been installed in some homes, and solar cells are used as energy sources in lighthouses, boats, and other remote locations.

Solar power plants—using energy from the Sun to produce steam for driving turbines to generate electricity—could potentially replace fuel-driven power plants, producing energy without any environmental hazards. In California, a solar power facility—using collectors made of large motorized mirrors that track the Sun—produces electricity to supplement the power needs of the Los Angeles utilities companies [2].

Geothermal energy

Geothermal energy is the natural heat generated in the interior of Earth and released from volcanoes and hot springs or from geysers that shoot out heated water and steam. Reservoirs of hot water and steam under Earth's surface can be accessed by drilling through the rock layer. The naturally heated water can be used to heat buildings, while the steam can be used to generate electricity. Steam can also be produced by pumping cold water into rock that is heated by geothermal energy; such steam is then used to produce electric power.

Tidal and ocean thermal energy

The rise and fall of ocean tides contain enormous amounts of energy that can be captured to produce electricity. In order for tidal power to be effective, however, the difference in height between low and high tides needs to be at least 20 feet (6 meters), and there are only a few places in the world where this occurs. A tidal station works like a hydropower dam, with its turbines spinning as the tide flows through them in the mouths of bays or estuaries (an arm of the sea at the lower end of a river), generating electricity. By the end of the twentieth century, tidal power plants were in operation in France, Russia, Canada, and China [2].

Ocean thermal energy uses the temperature change between the warmer surface waters and the colder depths to produce electrical power.

Biomass energy

Certain biomass (the sum total of living and dead plants, animals, and microorganisms in an area) can be used as fuel to produce heat energy. Wood, crops and crop waste, and wastes of plant, mineral, and animal matter are part of the biomass. The biomass contained in garbage can be burned to produce heat energy or can be allowed to decay and produce methane (natural gas). In Western Europe, over 200 power plants burn rubbish to produce electricity. Methane can be converted to the liquid fuel methanol, and ethanol can be produced from fermentable crops such as sugar cane and sorghum. Adequate air pollution controls are necessary when biomass is burned to limit the release of carbon dioxide into the atmosphere [2].

Other sources of alternative energy

Other sources of alternative energy include hydrogen gas and fuel cells. Hydrogen gas is a potential source of fuel for automobiles, as well as a potential source of energy for heating buildings and generating electricity. Although hydrogen is not readily available, it can be produced by separating water into hydrogen and oxygen in a process called electrolysis. A disadvantage of using hydrogen gas as fuel is that it is highly flammable [3].

Fuel cells are devices that produce electric power from the interaction of hydrogen and oxygen gases. They are used to provide electricity in spacecraft and are a potential alternative energy source for heating buildings and powering automobiles.

The recent energy problems that are happening everyday in the world make us rethink the manner in which energy is used and saved. The effort conducted at conserving this resource makes people to reevaluate their choices on consumption. The truth is there is really not that much energy to waste and current natural energy sources today cannot be renewable. Using alternative energy sources can solve these energy problems. The advancement in technology gives rise to alternative energy sources such as wind power, solar power; especially they are renewable energy sources [3].

References:

1. World Energy Assessment (2001). Renewable energy technologies, p. 221.
2. United Nations Environment Program *Global Trends in Sustainable Energy Investment 2007: Analysis of Trends and Issues in the Financing of Renewable Energy and Energy Efficiency in OECD and Developing Countries*, p. 3.
3. The Rise of Renewable Energy

REAL-TIME RECONSTRUCTION AND VISUALISATION

OF PLASMA SHAPE SYSTEM FOR KTM TOKAMAK

Sankov A.A., Malahov A.V., Khokhryakov V.S.

Supervisor: Pavlov V.M., Assoc., PhD

Tomsk Polytechnic University, 30, Lenin Avenue, Tomsk, 634050, Russia

E-mail: sankov@sibmail.com

1. Introduction

The Kazakhstan Tokamak for Material Testing studies (KTM) is designed for modeling plasma-material interactions in divertor region under conditions expected for ITER. [1] The device enables divertor plates to be changed without disturbance of vacuum.

Coordination of the research programs of Russian Globus-M, T-15M, TSP-AST tokamaks and KTM gives unique possibilities for support of the ITER project, developing fusion physics and technology.

Creation and putting into operation the KTM tokamak before realization of ITER project can make KTM the basis of international cooperation in plasma material interaction investigations. It can give an important investment to the elongated plasma confinement database

The KTM Parameters and Discharge scenario

Major plasma radius R, m	0.86
Minor plasma radius a, m	0.43
Plasma current IP, MA	0.75
Pulse duration $\square$t$_{pl}$, s	2-4
Additional heating power Paux, MW	5
Heat flux at divertor plates, MW/m^2	2-20

The information of the magnetic field around plasma is collected with 36 magnetic and 12 flux loops.

Development of methods for plasma's magnetic surface recovery using external magnetic measurements is necessary for normal operation of tokamaks. [2] It is also necessary to control the position and shape of the plasma in real time, and for solving other physical diagnosis and analysis in the interval between the discharges of the tokamak

2. Objectives and Specifications

To develop reconstruction system, we need to have a set of specialized numerical algorithms that process external magnetic measurements data with varying speed and accuracy of calculations. More simple and fast algorithms (with a characteristic time of a few milliseconds, ON-LINE mode) is required to determine the shape and position of the plasma in order to control the discharge.

More complex and less high-speed algorithms are used to determine the equilibrium plasma parameters and plasma boundary after experiment (OFF-LINE mode).

The main objective of this work is the adaptation and verification of algorithms and software based on the filament current method, to solve the problem of determining the plasma boundary according to the external magnetic measurements.

To provide real-time reconstruction, plasma shape and position should be calculated every 3 ms or less.

3. Filament Current Method

The problem is formulated as follows: find the coordinates and the amplitudes of current filaments so that deviation of the actual plasma surface from the reconstructed surface would be minimal. This deviation could be calculated as follow [3]:

$$\Delta = K_b \sum_{k=1}^{N} \left[\left(B_n^k - \overline{B}_n^k\right)^2 + \left(B_\tau^k - \overline{B}_\tau^k\right)^2 \right] + K_f \sum_{j=1}^{M1} \left(\Psi_j - \overline{\Psi}_j\right)^2 \quad (1)$$

where:

$\overline{B}_n^k$ – magnetic probe measurement at magnetic probe position;

B_n^k – calculated magnetic field at magnetic probe position;

$\overline{\Psi}_j$ – flux at control point;

Ψ_j – calculated flux at control point;

N – number or magnetic probes;

M1 – number of flux loops;

nj – number of discretized points along plasma's contour;

K_b, K_f – constants;

Flux function could be calculated using Green's function (a poloidal flux function for toroidal filament current in axisymmetric geometry)

$$\psi(r_v, z_v) = G(r_v, z_v)I_{c_i} =$$

$$= \sum_{i=1}^{N} I_{c_i} \frac{\mu_0}{\pi} \sqrt{\frac{r_{c_i} r_v}{k^2}} [(1 - \frac{k^2}{2})K(k^2) - E(k^2)]$$

where:

r_v, z_v – flux loop position (coordinates);

r_{c_i}, z_{c_i} – filament current position (coordinates);

$$k^2 = \frac{4r_v r_{c_i}}{(r_v + r_{c_i})^2 + (z_v - z_{c_i})^2};$$

$K(k^2), E(k^2)$ – Elliptic Integrals:

$$K\left(k^2\right) = \int_0^1 \frac{dt}{\sqrt{\left(1-t^2\right)\left(1-k^2 t^2\right)}}; E\left(k^2\right) = \int_0^1 \sqrt{\frac{1-k^2 t^2}{1-t^2}} dt$$

For magnetic field:

$$B_r(r_v, z_v) = \sum_{i=1}^{N} \frac{\mu_0}{2\pi} I_{c_i} \frac{z_v - z_{c_i}}{r_v \sqrt{(r_v - r_{c_i})^2 + (z_v - z_{c_i})^2}} [-K(k^2) + \frac{r_{c_i}^2 + r_v^2 + (z_{c_i} - z_v)^2}{(r_{c_i} - r_v)^2 + (z_{c_i} - z_v)^2} E(k^2)]$$

$$B_z(r_v, z_v) = \sum_{i=1}^{N} \frac{\mu_0}{2\pi} I_{c_i} \frac{1}{r_v \sqrt{(r_v - r_{c_i})^2 + (z_v - z_{c_i})^2}} [K(k^2) + \frac{r_{c_i}^2 - r_v^2 - (z_{c_i} - z_v)^2}{(r_{c_i} - r_v)^2 + (z_{c_i} - z_v)^2} E(k^2)]$$

[3] In order to find filament currents we use moments of the plasma current density distribution:

$$Y_m = \mu_0 \oint_L (f_m \cdot B_\tau + g_m \cdot r \cdot B_n) dl$$

where:

B_τ – tangential component of the magnetic field;

B_n – normal component of the magnetic field;

f_m, g_m are defined with equations:

$$\Delta^* f = \frac{\partial^2 f}{\partial z^2} + \frac{\partial^2 f}{\partial r^2} - \frac{1}{r}\frac{\partial f}{\partial r} = 0 \quad (2.1)$$

$$\Delta g = \frac{\partial^2 g}{\partial z^2} + \frac{\partial^2 g}{\partial r^2} + \frac{1}{r}\frac{\partial g}{\partial r} = 0 \quad (2.2)$$

Functions:

$f_0 = 1$; $g_0 = 0$;
$f_1 = z$; $g_1 = -\ln(r)$;
$f_2 = r^2$; $g_2 = 2z$;

are acceptable for equations 2.1 - 2.2 [3].

$$\overline{Y}_0 = \frac{Y_0}{\mu_0 I_p} = 1$$

$$\overline{Y}_1 = \frac{Y_1}{\mu_0 I_p} = \frac{z_1 + z_2}{2} = z_c$$

$$\overline{Y}_2 = \frac{Y_2}{\mu_0 I_p} = \frac{r_1^2 + r_2^2}{2} = r_c^2$$

Coordinates r_c, z_c, define plasma centre. We use this position as an initial approximation for further iterative process. To get more accurate results plasma boundary parameterized with follow equations [4]:

$$\begin{cases} r = R_0 + a \cdot \cos(t + \delta \cdot \sin t), \\ z = Z_0 + b \cdot \sin t \end{cases} \quad (3)$$

where parameters R_0, Z_0, a, b, δ should be defined during iterative process.

Optimization

In order to make the algorithm faster, gradient descent method is used. [5] This is a numerical approach to find minimum of the function we have. Gradient descent method based on partial derivatives.

Possible algorithm is shown below:

$$\Delta \rightarrow F(R_0, Z_0, a, b, \delta)$$

Δ function is defined with the (1)

$$X^0(x_1^0, x_2^0, ..., x_n^0) \rightarrow X^1(x_1^1, x_2^1, ..., x_n^1)$$

$$x_n^1 = x_n^0 - \frac{\partial F(X)}{\partial x_n}$$

$$x_n^{i+1} = x_n^i - \frac{\partial F(X)}{\partial x_n}$$

Summary and Further Work

A special program in C++ Builder 6 was designed using methods and algorithms which were described before.

Input data for the program is an array with magnetic probes and flux loops measurements. Output data: plasma boundary parameters (3).

There is an opportunity to save reconstructed plasma shape and magnetic field configuration to the Bitmap file in the program. In the Figure 1 reconstruction result is shown.
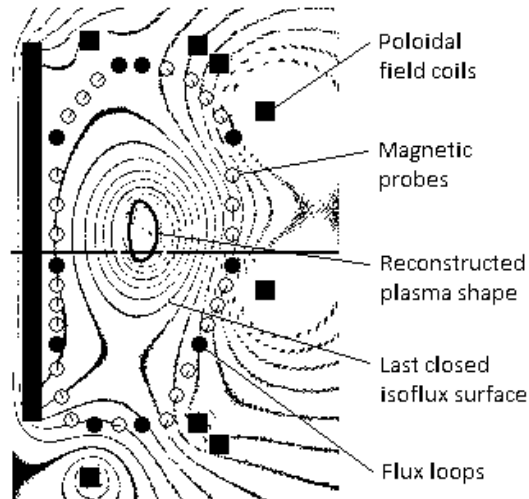
Fig.1 Reconstructed configuration of the flux.

Different current effects which take place in the real plasma discharge experiment could be taken into account (the effect of eddy current, camera's inductive current etc.)

References

[1] KTM project (Kazakhstan Tokamak for Material Testing) / E.A.Azizov, Moscow, 2000;
[2] Initial implementation of a multivariable plasma shape and position controller on the DIII–D tokamak / D.A. Humphreys, International Symposium on Computer-Aided Control System Design, September 25–27, 2000, Anchorage, Alaska;
 [3] Итоговый научно-технический отчёт по теме: «Разработка и адаптация алгоритмов и программного обеспечения определения формы и положения плазменного шнура по магнитным измерениям в токамаке КТМ» / А.А. Кавин, СПб, 2008. – 10 с.;
[4] В.А. Глухих, В.А. Беляков, А.Б. Минеев Физико-технические основы управляемого термоядерного синтеза. Спб, Изд-во Политехнического университета, 2006, 348с.
[5] Лесин В.В., Лисовец Ю.П. Основы методов оптимизации. – М.: Изд-во МАИ, 1995. – 344 с.

THE PROBLEMS OF NON-PROLIFERATION IN THE FULL NUCLEAR FUEL CYCLE WITH CANDU REACTOR

Sednev D.A, Sokolovskaya E.A.

Supervisor: Demyanyuk D.G., associate professor, PhD.

Ermakova Ya.V., teacher

Tomsk polytechnic university, 634050 Russia, Tomsk, 30 Lenin str.

E-mail: sednev@sibmail.com

The CANDU ("CANada Deuterium Uranium") reactor is a Canadian-invented, pressurized heavy water reactor developed initially in the late 1950s. CANDU is a reference to its deuterium-oxide (heavy water) moderator and its use of uranium fuel (originally, natural uranium). One of the design features – on-power refueling. [1] General technical data of the CANDU reactor are represented in Table 1.

Table 1. General technical data of CANDU reactor

Type	PHWR
Length of bundle	495.3 mm
Weight of bundle	23.7 kg
Weight of uranium per bundle	19.2 kg
Elements per bundle	37
Fuel material	Natural UO_2
Fuel bundles in core	4560
Fuel bundles per channel	12
Nuclear moderator	D_2O
Primary coolant	D_2O

Today there are 29 CANDU reactors in use around the world, and a further 13 "CANDU-

167

derivatives" in use in India (these reactors were developed from the CANDU design after India detonated a nuclear bomb in 1974 and Canada stopped nuclear dealings with India). Locations of the CANDU reactors can be found in Table 2.

Table 2. The number of CANDU reactors in countries

Country	Number of reactors
Canada	17
South Korea	4
China	2
India	2
Argentina	1
Romania	2
Pakistan	1

Some countries, which possess the CANDU reactor, are in tense geopolitical situation. The striking example can be South Korea which is adjacent to nuclear capable North Korea. This fact can induce South Korea to develop its own nuclear program. The following ways of possible goal achievements can be identified: 1) To carry out covert plans of nuclear weapons program; 2) To develop own full nuclear fuel cycle with the intention to further withdrawal from NPT and openly produce nuclear weapon 3) Combination of two previous ways. The most feasible is the second way of the development.

The potential threats of violence of the nonproliferation regime by the country generating a full nuclear fuel cycle in the CANDU reactors are investigated in this work.

The main problem of the CANDU reactor is the production of plutonium per megawatt - day is about twice as high as in LWRs and the fraction of heavier isotopes in the plutonium is smaller - about 25 per cent. [2] As is well-known nuclear weapons can be made with weapons-grade plutonium that is plutonium which contains more than 93 per cent of isotope of plutonium 239.

In fact the question concerning the plutonium application of the so-called power quality used in nuclear weapons has been discussed for a long time. Moreover it was confirmed that the extracted plutonium from the spent fuel of the power reactor was unable to use for producing nuclear warheads.

However, according to the last researches, which have been carried out in the field of the evaluation of potential threats of the spent fuel from the point of proliferation of nuclear materials, plutonium of any isotopic composition is practically suitable for the production of nuclear warheads of different efficiency level. [4] In the CANDU reactors plutonium with the content 67 per cent of isotope 239 is accumulated. [3] The comparison of critical masses of the warheads, which are produced from weapons-grade

plutonium and reactor grade plutonium are represented in Table 3.

Table 3. Critical mass of plutonium

Isotope	Weapon grade plutonium	Reactor grade plutonium
Pu – 238	0.012	0.024
Pu – 239	0.938	0.584
Pu – 240	0.058	0.240
Pu – 241	0.0035	0.112
Pu – 242	0.00022	0.039
Critical mass, kg	10.7	13.5

As we can see, the quantity of plutonium, which can be accumulated in the CANDU reactor, has no great differences from the weapons-grade plutonium. Thus, the issue about the alleged inability of the military use of plutonium extracted from spent nuclear fuel nuclear power plants and nuclear research facilities has been closed. [4] Also, the country can try to enrich plutonium up to the necessary level to make more completed nuclear charge. This goal can be achieved by applying the enrichment technologies. Such technologies are developed by the country for the production of the heavy water, which is the integral part of the full nuclear fuel cycle with the CANDU reactors, where it is used as a moderator. The country can get the technology of the enrichment of plutonium in a short period of time because of there can be similarities in the methods of the enrichment. The technologies can be found on the principle of the difference in atomic masses. In addition, the heavy water offers interest for the proliferation itself as the irritation of it produces tritium, which is the weapons-grade material used to generation the thermonuclear weapon.

As a result of that, the heavy water reactor in conjunction with the full nuclear fuel cycle is a dangerous object in terms of the nonproliferation regime (accumulation of the significant amounts of the weapons-grade plutonium on the basis of the use of natural uranium; generation of tritium). [4]

Another one feature of CANDU reactor is on-power refueling. This feature threatens to nuclear non-proliferation regime. CANDU reactors are refueled continuously, instead of every 18–24 months as in case with LWRs. This means that international monitoring of the fuel is more expensive. [2] This monitoring includes the following points: the IAEA comprehensive safeguards and additional protocol; commitments to effect international nuclear non-proliferation norms and guidelines such as the Nuclear Suppliers' Group Supply Guidelines; bilateral treaties concerning nuclear co-operation

for peaceful purposes; and national policies and laws regarding exports. [5]

Nowadays, the main aspect of international monitoring will be considered more detailed. The IAEA safeguard system is the basis of providing the non-proliferation regime. The main purpose of the safeguards system of the International Atomic Energy Agency is to provide credible assurance to the international community that nuclear material and other specified items are not diverted from peaceful nuclear uses. [6] Comprehensive Safeguards Agreements and Additional protocol are two fundamental documents, which ensure that the states perform their commitment to non-proliferation regime. Every country has to sign Comprehensive Safeguards Agreements, if it intends to use nuclear power plants legally. This fact allows IAEA apply safeguard system. Also many countries signed Additional protocol, which shows the intention of the state to support the nuclear non-proliferation regime. This protocol gives more wide authority to the IAEA inspectors. For instance, this authority includes verification possibility of an object without prior warning, access rights and sampling in any parts of object, which stands under the IAEA safeguards. With Additional protocol the IAEA can provide strengthen guaranty of the non-proliferation regime.

Methods and equipment for the IAEA safeguards of the CANDU reactors consist of the installed by the IAEA technology for surveillance and item accountancy verification reviewed either through the IAEA inspections or through the remote monitoring supplemented by the unannounced inspections. It is possible to track every CANDU fuel bundle throughout its life cycle, as well as detecting with high probability any undeclared irradiation and movement of fuel bundles. [5] Examples of common IAEA Safeguards Equipment for CANDU are Core Discharge Monitor, Spent Fuel Bundle Counter, and Spent Fuel Verifier.

Thereby we can see that the creation by the state of the own full nuclear fuel cycle with the use of CANDU reactor is dangerous from nuclear non-proliferation point of view. Nowadays, only the installation of such objects under the IAEA safeguards with signing Additional protocol can guarantee that the state hasn't intention to switching civil technology. When we tell about risks of switching, we mean that the state can use civil technology in military purposes by uncontrolled and hidden way.

If we try to estimate the risk of proliferation, we should notice that it depends not only on technical characteristics of equipment, technology or material, but also on the recipient country. Export of sensitive products is dangerous procedure for the non-proliferation regime, if the recipient country is the so-called threshold country, which carry out plans of own nuclear weapon program. All these factors should be taken into account by states, which pass their nuclear technology to other countries.

References:

1. The evolution of CANDU® fuel cycles and their potential contribution to world peace [internet-resource], regime of access: http://www.nuclearfaq.ca/brat_fuel.htm, free

2. SIPRI Yearbook 2007 Appendix 12C. Fissile materials: global stocks, production and elimination [internet-resource], regime of access: http://www.sipri.org/yearbook/2007/files/SIPRIYB 0712C.pdf, free

3. И.Н.Бекман Ядерная индустрия Лекция 19 Топливные циклы [internet-resource], regime of access: http://www.profbeckman.narod.ru/RH0.files/20_2. pdf, free

4. Экспортный контроль товаров, применяемых в ядерных целях [internet-resource], regime of access: http://excon.minatom.ru/excon_files/textbook/GL-04.doc, free

5. CANDU®: Setting the Standard for Proliferation Resistance of Generation III and III+ Reactors [internet-resource], regime of access: http://www.nuclearfaq.ca/Whitlock_IAEA_conf_Oct_2009.pdf, free

6. The Safeguards System of the International Atomic Energy Agency [internet-resource], regime of access: www.iaea.org/OurWork/SV/Safeguards/safeg_system.pdf, free

RADIOACTIVE WASTE

Sharafutdinova Yu.R.., Nikiforova Yu.V.

Research supervisors: Silaev M.E., associate professor, PhD., Ermakova Ya.V., teacher

Tomsk Polytechnic University, 634050, Russia, Tomsk, Lenin str., 30

E-mail: Yurlik@sibmail.com

Nowadays the problem of a radioactive waste recycling is one of the major problems in nuclear power. This problem has arisen with the development of scientific and technical progress, in particular since the construction of atomic power stations. Especially now it is of great importance, the reason is the dismantling of a great number of atomic power stations all over the world (according to the IAEA, it is more than 65 reactors of atomic power stations and 260 reactors used in the scientific purposes).

Radiation comes from naturally occurring radioactive elements, left over from the formation of the Earth, and from cosmic radiation. Every day we are exposed to radiation from rocks and soil, cosmic radiation from outer space, the air we breathe, the water we drink and wash in, and the food we eat. There are radioactive elements in our muscles and bones. This natural radiation, known as background radiation, is a part of our everyday lives. [1]

Radioactive materials have a variety of important uses in medicine, industry, agriculture, and as well as in our homes.

Too high radiation dose can be harmful. For the population it is 1mSv/year, but no more than 5mSv/year during the next 5 years; for the personnel of group A - 20mSv/year, but no more than 50mSv/year during the next 5 years. So, while using radioactive materials, we should be cautious.

The use and production of radioactive materials generate radioactive waste which must be managed safely and appropriately. It is necessary to handle them according to the regulations and rules. Radioactive wastes are products containing radioactive materials, which are not used in future.

Radioactive waste should be reduced to minimal volumes, and be contained, for instance within metallic, corrosion resistant canisters.

Containers for radioactive waste must do three things:

- Prevent wastes from escaping into the environment;
- Absorb hazardous radiation;
- Allow heat to escape. [2]
- Radiation occurs naturally from the decay of particular forms of some elements (radioisotopes). There are three main types of radiation alpha, beta and gamma. Radioactive emission takes place as an atom disintegrates.

Radioactive wastes are formed:

✓ During the operation and the enterprises decommissioning of a nuclear fuel cycle (extraction and processing of radioactive ores, fuel elements production, power generation on a nuclear atomic power plant, processing of the spent nuclear fuel);

✓ In the course of realization of military programs for the nuclear weapon creation, preservation and liquidation of defensive objects and rehabilitation of the territories polluted as a result of the enterprises activity for nuclear materials production;

✓ During the operation and dismantling of the ships of a navy and civil fleet with nuclear power installations and bases of their service;

✓ During the use of isotope production in national economy and medical institutions;

✓ As a result of carrying out of nuclear explosions for the national economy benefits, during the mining operations, fulfillment of space programs, and also because of the accidents on nuclear objects. [3]

As a result of reprocessing 1 ton of the spent nuclear fuel (in recalculation to uranium) the following quantity of radioactive waste is formed:

- Liquid:
- highly level waste – 45 m^3;
- Intermediate level waste – 150 m^3;
- Low level waste – 2000 m^3;
- Solid:
- the 3rd of the active group – 1000 kg;
- the 2nd of the active group – 3000 kg;
- the 1st of the active group – 3500 kg;
- Gaseous – 0,23 curie per year. [4]

The half-life of a radioisotope is the time taken for half of its atoms to decay. So something with a long half-life such as uranium 238 (a half life of 4.5 billion years) gives out very low levels of radiation albeit over a geological time scale. Something with a short half life such as radon 220 (half life 56 seconds) emits very much more radiation over a shorter time. [5]

- The radioactive wastes are divided according to their life time:

Long-living – the half-life period is more than 100 years;

Intermediate-living – a half-life period from a year till 100 years;

Shorted-living – the half-life period is less than 1 year.

- Radioactive wastes are devided into some categories on activity:

Low level waste there are less than 0,1 curie/m^2;

Intermediate level waste from 0,1 to 100 curie/m^2;

High level waste more than 100 curie/m^2.

- The radioactive waste can be also liquid, solid and gaseous.

The division of waste into the categories is established by the regulatory enactment. Radioactive wastes are dangerous for people, therefore regulations and rules of handling with them are established by the International committee on radiating protection, IAEA (the International Atomic Energy Agency) and National regulations and rules. There are main sanitary rules of work with radioactive substances and other sources of an ionizing radiation and Sanitary rules of handling with radioactive wastes, regulating the order of collecting, disposal, storage and burial places of radioactive waste. Handling safety with radioactive waste is regulated by the safety standards.

There are some methods of a radioactive waste, disposal such as save in long-term land storage, deep holes, rock melting, direct pumping – in (applies only for a liquid waste), disposal into the sea, disposal under the ocean floor, disposal into motions zones, disposal into the ice sheets, disposal into space. Some proposals are only developed by the scientists all over the world. The others have already been forbidden by the international agreements. A lot of scientists investigating the given problem appreciate the idea of radioactive waste burial in the geological environment. [3]

Geological formations are currently studied for radioactive waste that is either heat emitting, or contains a certain amount of long-living radionuclides. Surface sites are currently considered for low-level radioactive waste. There are 2 types of geological burial - surface or deep disposal. [6]

The current approach is to develop a multibarrier system to contain and isolate the radioactive waste from the biosphere. The immobilized waste (most widely within cement or glass) is inserted into a canister, and disposed in either geological formations (= natural rocks) or surface sites.

The idea is a multiple barrier concept:

- The waste, either as a ceramic oxide (e.g. the spent fuel itself) or through vitrification (separated HLW from reprocessing) is immobilised.

- It is then sealed in a corrosion resistant canister such as stainless steel or copper

- Finally it is buried in a solid rock formation.

classified as low-level, medium-level or high-level wastes, according to the amount and types of radioactivity in them. Sources of waste and their treatment are shown in Table 1.

Level	Composition	Treatment
Low LLW	Building materials from nuclear installations. Discarded protective clothing, paper towels and wrappings.	Compacted in drums before disposal in landfill site (Drigg, Cumbria).
Interm ediate	Fuel cladding, filter materials, small items of equipment.	Cut up, packed in cement inside stainless steel drums.
High HLW	Nitric acid solutions containing fission products, separated during reprocessing.	Concentrated by evaporation, stored in stainless steel tanks inside thick concrete walls. Water-cooled. Some is vitrified (turned into solid blocks of glass) before storage.

Table 1. Sources of waste and their treatment. [7]

- Like all industries, the thermal generation of electricity produces wastes. Whatever fuel is used, these wastes must be managed in ways which safeguard human health and minimise their impact on the environment. Nuclear power is the only energy industry which takes full responsibility for all its wastes, and costs this into the product.

Radioactive wastes comprise a variety of materials requiring different types of management to protect people and the environment. They are normally classified as low-level, intermediate-level or high-level wastes, according to the amount and types of radioactivity in them.

Under the modern socio-psychological condition of the society any proposals concerning radioactive waste are perceived as the most dangerous "environmental pollution" for a man and biosphere and meet the reaction of immediate emotional rejection. This reaction can be understood as natural, but in any case it is impossible to estimate it as constructive. We would like to point out, that from year to year the quantity of the radioactive wastes only increases.

And nowadays the recycling problem is still very urgent.

Referents:

1. Radioactive waste. [internet-resource], regime of access: http://www.ret.gov.au/resources/radioactive_waste/radiation_radioactive/Pages/RadiationandRadioactiveWaste.aspx, free

2. Radioactive waste. [internet-resource], regime of access: http://resources.schoolscience.co.uk/nirex/wastech2pg2.html, free

3. Обращение с радиоактивными отходами. [internet-resource], regime of access: http://profbeckman.narod.ru/RR0.files/L23_2_12.pdf, free

4. Обращение с радиоактивными материалами и отработанным ядерным топливом в производстве ядерно-топливного цикла. [internet-resource], regime of access: http://www.yabloko.ru/Publ/Atom/atom00010.html Обращение с РАО и ОЯТ на предприятиях ЯТЦ, free

5. Radioactive waste. [internet-resource], regime of access:
http://www.world-nuclear.org/info/inf60.html, free

6. Disposal of radioactive waste. [internet-resource], regime of access: http://www.sckcen.be/fr/Notre-Recherche/Research-domains/Disposal-of-radioactive-waste, free

7. Radioactive waste. [internet-resource], regime of access: http://resources.schoolscience.co.uk/nirex/wastech2pg2.html, free

RADIUM AND RADON IN THE ENVIROMENT

A.D. Valevech, A.E. Shepeleva

Scientific Supervisor: N.V. Demyanenko

Tomsk Polytechnic University, Russia, Tomsk, Lenin str., 30, 634050

E-mail: Proka3nica@mail.ru

Lenka123@mail2000.ru

The present article provides a brief review of radium and radon in the environment. Over the past decade, many studies on radium and radon influence on the environment and human health have been reported in Russia and abroad. The authors have analyzed some of the publications published abroad in order to deepen the knowledge of radon risks and summarize the experience of foreign scientists. The objective of the present paper was to analyze the impacts and risks of radon for environment and human health.

Residues from the oil and gas industry often contain radium and its daughters. The sulfate scale from an oil well can be very radium-rich. It is the case that the water inside an oil field is often very rich in strontium, barium and radium while seawater is very rich in sulfate so if water from oil well is discharged into the sea or mixed with seawater the radium is likely to be brought out of solution by the barium/strontium sulfate which acts as a carrier precipitate. [1]

The majority of the dose is caused by the decay of the polonium (^{218}Po) and lead (^{214}Pb) daughters from ^{222}Rn. It is the case that by controlling the daughters that the dose to the skin and lungs can be reduced by at least 90%. This can be done by wearing a dust mask, and wearing a suit to cover the entire body.
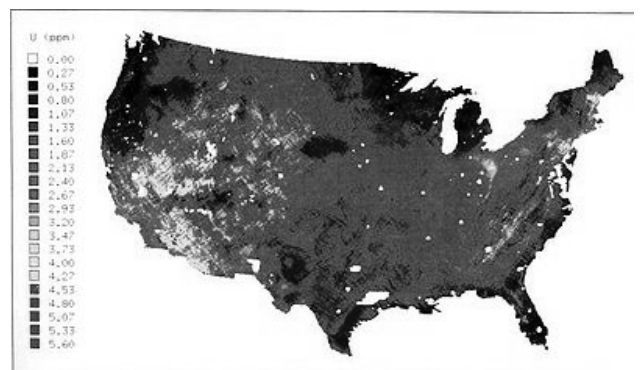
Рисунок 1. Predicted country median concentration.

Note that exposure to smoke at the same time as radon and radon daughters will increase the harmful effect of the radon. In uranium miners radon has been found to be more carcinogenic in smokers than in non-smokers.
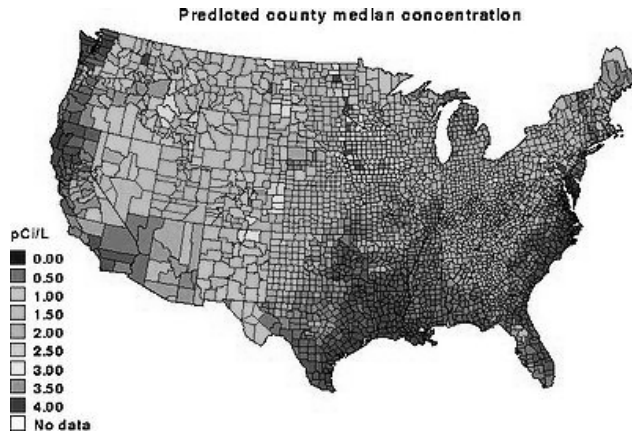
Рисунок 2. A map showing concentration of Uranium in U.S. soils, in parts per billion.

On average, there is one atom of radon in 1×10^{21} molecules of air. Radon can be found in some spring waters and hot springs. The towns of Misasa, Japan, and Bad Kreuznach, Germany boast radium-rich springs which emit radon. Unsurprisingly, Radium Springs, New Mexico does too.

Radon exhausts naturally from the ground, particularly in certain regions, especially but not only regions with granitic soils. Not all granitic regions are prone to high emissions of radon, for instance while the rock which Aberdeen is on is very radium rich the rock lacks the cracks required for the radon to migrate. In other nearby areas of Scotland (to the north of Aberdeen) and in Cornwall/Devon the radon is very able to leave the rock.
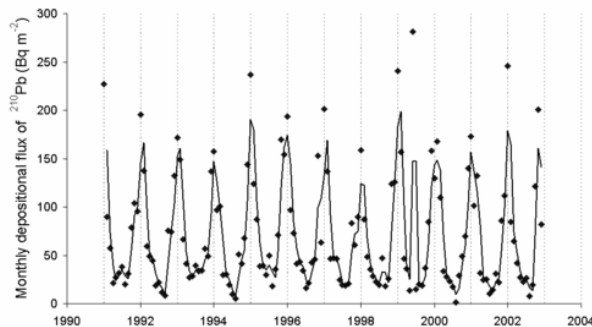
Рисунок 3. A graph of the deposition rate observed in Japan.

Radon is a decay product of radium which in turn is a decay product of uranium. It is possible to get maps of average radon levels in houses, these maps assist in the planning of radon mitigation measures for homes.

Note that while high uranium in the soil/rock under a house does not always lead to a high radon level in air, a positive correlation between the uranium content of the soil and the radon level in air can be seen.

Radon is related to Indoor air quality as it blights many homes. The radon (^{222}Rn) released into the air decays to ^{210}Pb and other radioisotopes, the levels of ^{210}Pb can be measured. It is important to note that the rate of deposition of this radioisotope is very dependent on the weather. Here is a graph of the deposition rate observed in Japan (M. Yamamoto *et al.*, *Journal of Environmental Radioactivity*, 2006, **86**, 110-131).

Well water can be very radon-rich, the use of this water inside a house is an additional route allowing radon to enter the house. The radon can enter the air and then be a source of exposure to the humans, or the water can be consumed by humans which is a different exposure route. [2]

The water, oil and gas from a well often contain radon. The radon decays to form solid radioisotopes which form coatings on the inside of pipework. In an oil processing plant the area of the plant where propane is processed is often one of the more contaminated areas of the plant as radon has a similar boiling point as propane.

Because uranium minerals emit radon gas, and their harmful and highly radioactive daughter products, uranium mining is considerably more dangerous than other (already dangerous) hard rock mining, requiring adequate ventilation systems if the mines are not open pit. During the 1950s, a significant number of American uranium miners were Navajo Indians, as many uranium deposits were discovered on Navajo reservations. A statistically significant subset of these miners later developed small-cell lung cancer, a type of cancer usually not associated with smoking, after exposure to uranium ore and radon-222, a natural decay product of uranium. The radon, which is produced by the uranium, and not the uranium itself has been shown to be the cancer causing agent. Some survivors and their descendants received compensation under the Radiation Exposure Compensation Act in 1990.

Currently the level of radon in the air of mines is normally controlled by law. In a working mine, the radon level can be controlled by ventilation, sealing off old workings and controlling the water in the mine. The level in a mine can go up when a mine is abandoned, it can reach a level which is able to cause the skin to become red (a mild radiation burn). The radon levels in some of the mines can reach 400 to 700 kBq m^{-3}. [3]

A common unit of exposure of lung tissue to alpha emitters is the Working level month (WLM), this is where the human lungs have been exposed for 170 hours (a typical month worth of work for a miner) to air which has 3.7 kBq of ^{222}Rn (in equilibrium with its decay products). This is air which has the alpha dose rate of 1 working level (WL). It is estimated that the average person (*general public*) is subject to 0.2

173

WLM per year, which works out at about 15 to 20 WLM in a lifetime. According to the NRC 1 WLM is a 5 to 10 mSv lung dose (0.5 to 1.0 rem), while the OECD consider that 1 WLM is equal to a lung dose of 5.5 mSv, the ICRP consider 1 WLM to be a 5 mSv lung dose for professional workers (and 4 mSv lung dose for the general public). Lastly the UN (UNSCEAR) consider that the exposure of the lungs to 1 Bq of ^{222}Rn (in equilibrium with its decay products) for one year will cause a dose of 61 µSv. This overview of the working level month is based upon the book by Jiří Hála and James D. Navratil (ISBN 80-7302-053-X).

In humans a relationship between lung cancer and radon has been shown at exist (beyond all reasonable doubt) for exposures of 100 WLM and above. By using the data from several studies it has been possible to show that an increased risk can be caused by a dose as low as 15 to 20 WLM. Sadly these studies have been difficult as the random errors in the data are very large. It is likely that the miners are also subject to other effects which can harm their lungs while at work (for example dust and diesel fumes).

The danger of radon exposure in dwellings was discovered in 1984 by Stanley Watras, an employee at the Limerick nuclear power plant in Pennsylvania. Mr. Watras set off the radiation alarms on his way *into* work for two weeks straight while authorities searched for the source of the contamination. They were shocked to find that the source was astonishingly high levels of Radon in his basement and it was not related to the nuclear plant. The risks associated with living in his house were estimated to be equivalent to smoking 135 packs of cigarettes every day.

Depending on how houses are built and ventilated, radon may accumulate in basements and dwellings. The European Union recommends that action should be taken starting from concentrations of 400 Bq/m^3 for old houses, and 200 Bq/m^3 for new ones.

The National Council on Radiation Protection and Measurement (NCRP) recommends action for any house with a concentration higher than 8 pCi/L (300 Bq/m³).

The United States Environmental Protection Agency recommends action for any house with a concentration higher than 148 Bq/m^3 (given as 4 pCi/L). Nearly one in 15 homes in the U.S. has a high level of indoor radon according to their statistics. The U.S. Surgeon General and EPA recommend all homes be tested for radon. Since 1985, millions of homes have been tested for radon in the U.S. By adding a crawl space under the ground floor, which is subject to forced ventilation the radon level in the house can be lowered.

In the conclusion the authors would like to note that contradictory explanations concerning the discovery of the given element cause a great interest to basic efficiency indexes and leads to some problems. The main problem is that radon is ubiquitous. At present this problem can't be solved by the existing methods. [4]

REFERENCE

1. A.R. Denman, J.P. Eatough, G. Gillmore and P.S. Phillips, Assessment of Health Risks To Skin and Lung Of Elevated Radon Level in Abandoned Mines, *Health Physics*, 2003, **85**, 733.

2. G.K. Gillmore, P. Phillips, A. Denman, M Sperrin and G. Pearse, *Ecotoxicology and Environmental Safety*, 2001, **49**, 281.

3. J.H. Lubin and J.D. Boice, *Journal Natl. Cancer Inst.*, 1997, **89**, 49. (Risks of indoor radon)

4. N.M. Hurley and J.H. Hurley, *Environment International*, 1986, **12**, 39. (Lung cancer in uranium miners as a function of radon exposure).

GIF AND INPRO FOR ENERGY IN FUTURE

A.I. Sitdikova

Scientific Advisor: M.E. Silaev, professor, Ya.V. Ermakova, teacher

Tomsk Polytechnic University

30, Lenin Avenue, Tomsk, 634050, Russia

E-mail: Alexandra.Sitdikova@gmail.com

The world's population is expected to expand from 6.7 billion people today to over 9 billion people by the year 2050, all striving for a better quality of life. As the earth's population grows, so does the demand for energy and the benefits that it brings: improved standards of living, better health and longer life expectancy, improved literacy and opportunity, and many others. Simply

expanding the use of energy along the same mix of today's production options, however, does not satisfactorily address concerns over climate change and depletion of fossil resources. For the earth to support its population while ensuring the sustainability of humanity's development, we must increase the use of energy supplies that are clean, safe, cost effective, and which could serve for both basic electricity production and other primary energy needs. Prominent among these supplies is nuclear energy.

To meet these challenges and develop future nuclear energy systems, the Generation IV International Forum (GIF) is undertaking necessary R&D to develop the next generation of innovative nuclear energy systems that can supplement today's nuclear plants and transition nuclear energy into the long term. Generation IV nuclear energy systems comprise the nuclear reactor and its energy conversion systems, as well as the necessary facilities for the entire fuel cycle from ore extraction to final waste disposal. Generation IV systems can be broadly divided into fast and thermal reactors that address the above challenges with differing emphasis and technology.

The Generation IV International Forum (GIF) was initiated in 2000 and formally chartered in mid 2001. It is an international collective representing governments of 13 countries where nuclear energy is significant now and also seen as vital for the future. Most are committed to joint development of the next generation of nuclear technology. Led by the USA, Argentina, Brazil, Canada, China, France, Japan, Russia, South Korea, South Africa, Switzerland, and the UK are charter members of the GIF, along with the EU (Euratom). Most of these are party to the Framework Agreement (FA) which formally commits them to participate in the development of one or more Generation IV systems selected by GIF for further R&D. Argentina and Brazil did not sign the FA, and the UK withdrew from it; accordingly, within the GIF, these three are designated as "inactive Members." Russia formalized its accession to the FA in August 2009 as its tenth member, with Rosatom as implementing agent.

After some two years' deliberation, GIF (then representing ten countries) late in 2002 announced the selection of six reactor technologies which they believe represent the future shape of nuclear energy. These were selected on the basis of being clean, safe and cost-effective means of meeting increased energy demands on a sustainable basis, while being resistant to diversion of materials for weapons proliferation and secure from terrorist attacks: gas-cooled fast reactors, lead-cooled fast reactors, molten salt reactors (the Molten Salt Fast Neutron Reactor, the Advanced High-Temperature Reactor), sodium-cooled fast reactors, supercritical water-cooled reactors, very high-temperature gas reactors.

In addition to selecting these six concepts for deployment between 2010 and 2030, the GIF recognized a number of International Near-Term Deployment advanced reactors available before 2015.

Most of the six systems employ a closed fuel cycle to maximize the resource base and minimize high-level wastes to be sent to a repository. Three of the six are fast neutron reactors (FNR) and one can be built as a fast reactor, one is described as epithermal, and only two operate with slow neutrons like today's plants.

At least four of the systems have significant operating experience already in most respects of their design, which provides a good basis for further R&D and is likely to mean that they can be in commercial operation well before 2030.

The International Project on Innovative Nuclear Reactors and Fuel Cycles (INPRO) brings together nuclear technology holders and users to jointly consider international and national actions that would result in the required innovations in nuclear reactors, fuel cycles or institutional approaches. In addition, INPRO plays an important and unique role in helping its Members better understand the national, regional and global implications of future nuclear energy systems´ development. To support that development, INRPO looks decades ahead and plays a key role in fostering innovation in technologies and institutional infrastructure.

INPRO was established in 2000 to help ensure that nuclear energy can meet the energy needs of the 21st century. At present, 30 IAEA Member States (including Algeria, Italy and Kazakhstan who joined in 2009) and the European Commission comprise the INPRO membership. The countries represent 65% of the world population.

The INPRO methodology, which can be used to assess a country's existing or planned nuclear energy system, helps Member States to determine if their nuclear energy system meets national sustainable development criteria. The INPRO methodology encompasses seven assessment areas: economics, infrastructure, waste management, proliferation assistance, physical protection, safety and the environment, including impact of stressors and resource depletion.

INPRO plays and important role in understanding

- the future development of nuclear energy systems from a national, regional and global perspective, and

• the role of innovation in technologies and institutional arrangements in support of this development.

Relationships between INPRO and GIF are very often asked question. The web sites on each side have comprehensive information on this. In essence, GIF is an international development activity by technology holders, whereas INPRO has unique value as:

• A forum by both technology holders & users including countries not yet operating nuclear power plants.

• Addressing issues other than development.

• Having viewpoint from users.

• Paying attention to the needs of developing countries.

Their complementary relationship has been recognized in various occasions including G8 Summit in St. Petersburg in July 2006. Because the IAEA has a unique role (by statute) in safety and safeguard, the IAEA has been contributing GIF by sending experts to GIF working groups. INPRO has been participating in GIF Policy Group as observer. Occasionally interface meetings have been held and joint action plan has been established to create synergy by working together in such areas as use of IAEA Safety Standards for preliminary assessments of GIF systems, use of the GIF economic model ECONS by IAEA GCR group for cost estimates of GCRs, providing IAEA's HEEP code for non-electric application to GIF. Future synergy could be developed, subject to discussion by both sides in interface meeting and INPRO Steering Committee (All the GIF members are members of INPRO. Through the national delegations to INPRO, GIF can express its expectations on synergy with GIF in the INPRO Steering Committee). This synergy could be created by utilizing unique value and activities by the IAEA and INPRO in the following areas, but not limited to:

1) Enhancing interface between technology users and holders of innovative nuclear energy system, IAEA/INPRO bringing users'/Developing Countries' point of view, and GIF bringing potentially available innovative technologies. This may include an assessment of selected GIF system using INPRO methodology from user's point of view.

2) Enhancing interface in the areas of safety, security and safeguard for establishing technologies to meet expectation for innovative systems, which could include assessments of GIF systems against IAEA Safety Standards.

3) Joint discussion on future reference deployment scenario of Generation IV systems.

4) Subsequent joint consideration of institutional and infrastructure conditions to enable expanded use of GIF systems including closed fuel cycle. Further cooperation with INPRO and IAEA could benefit GIF when it considers the use of Generation IV systems in countries not yet operating nuclear power as of today. Given the situation that currently more than 60 countries are considering embarking on nuclear power programme, GIF may consider what is the role of GIF in it and if GIF needs to re-orient its direction to meet the needs of all including the newcomers.

Many of the world's nations, both industrialized and developing, are driving the growth of nuclear energy. Some 43 new units are under construction in 11 countries, and more are preparing to move forward. They are confident that nuclear energy is a valuable option for their energy security in the future. However, challenges still exist to further large-scale use of nuclear energy: (1) nuclear energy must be sustainable from the standpoint of its utilization of nuclear fuel resources as well as the management and disposal of nuclear waste, (2) the units must operate reliably and be economically competitive, (3) safety must remain of paramount importance, (4) deployment must be undertaken in a manner that will reduce the risk nuclear weapons proliferation, (5) new technologies should help meet anticipated future needs for a broader range of energy products beyond electricity, and (6) governments need to support the revitalization of their nuclear R&D infrastructures. Solving of these challenges is the main goal of GIF and INPRO, and future relationships between two these innovative projects play important role for nuclear energy in future.

REFERENCES

1. GIF R&D Outlook for Generation IV Nuclear Energy Systems, Aug 2009
2. http://www.world-nuclear.org/info/inf77.html
3. http://www.gen-4.org/GIF/About/index.htm
4. "Nuclear Engineering International" Judith Perera, January 2004
5. http://www.iaea.org/OurWork/ST/NE/Downloads/files/INPRO_GC52Briefing.pdf
6. http://www.gen-4.org/GIF/About/documents/40-Session3-7-Omoto.pdf

POTENTIAL OF THE HTGR IN SUSTAINABLE DEVELOPMENT.

Sychov V.S., Martynov S. A.

Scientific advisors: Nesterov V.N., Ermakova Ya.V. teacher

Tomsk Polytechnic University , 634050, Russia, Tomsk, 30 Lenin Avenue

E-mail: martins88@sibmail.com;

Even now, over 2 billion people have no electricity at all. To ensure a reliable supply of electricity that does not produce greenhouse gases will likely require other technologies besides strictly renewable sources. Among the advanced technologies that have been proposed to fill some of the niches is that of the High Temperature Gas Cooled Reactor (HTGR) [1].

While the HTGR has various safety advantages, it has never received the large development effort compared to water-cooled reactors. There were several reasons for focus on the water-cooled reactor. The first was that water-cooled reactors were much more practical for use in submarines, which was the principal driver for nuclear power development in the late 40's and early 50's. The second factor was simply that water and steam properties are well understood and have been studied for a longer time than helium gas. Another reason is that as fossil fueled plants (especially natural gas combustion turbines) are currently much cheaper to build than HTGRs. Of course, in a carbon-free, sustainable development context, fossil fuels would likely need to be phased out. Therefore, technologies such as the HTGR would be more competitive in a non-carbon energy market[2].

The 13 MWe AVR was operated in Germany from 1966 to 1988. This prototype was the first of the "pebble bed" reactors. Pebble bed reactors are essentially an assembly of balls (about the size of a tennis ball) that contains the TRISO fuel (Figure1).
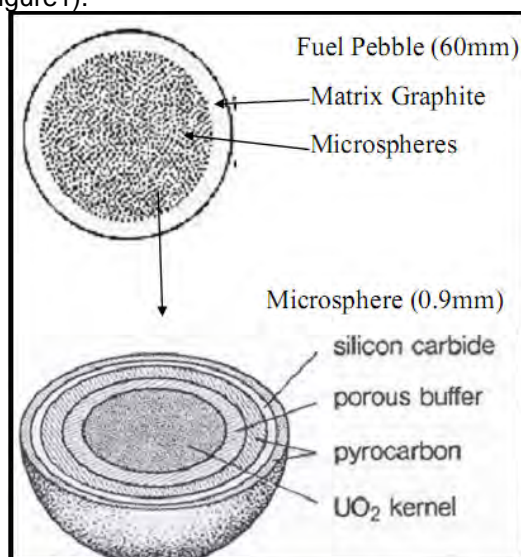
(Figure1. TRISO Fuel Particle - "Microsphere").

Pebble bed reactors have the advantage of online refueling by pneumatic insertion and removal of pebbles from the core. Germany's largest pebble bed reactor was the 296 MWe Thorium High Temperature Reactor (THTR) which operated from 1985 to 1988.

In the US, HTGR design used fuel rods contained in hexagonal graphite blocks. While sacrificing online refueling, hexagonal blocks allow for enhanced fuel accountability (i.e., better for non-proliferation) and more certain core geometry control [3].

Why the HTGR is under consideration again after these mixed results from the various prototypes? For nuclear energy to contribute to sustainable development, smaller, safer reactors that do not need large quantities of water would be ideal in many developing countries that have higher population densities. With important lessons learned on helium circulation, using smaller reactors, and successful demonstration of the safety of HTGR fuel, a new generation of HTGR prototypes has arisen which may be able to fill the gaps in sustainable energy needs.

The main two prototypes operating currently are the HTTR in Japan and the HTR-10 in China. The HTTR is a 30 MW thermal reactor built in Japan that uses the hexagonal block fuel similar to that used in the previous US designs. HTTR has been operating since 1998. The purpose of the HTTR is to investigate the potential of hydrogen production using the higher temperatures provided by HTGR technology [4].

HTR-10 was built in China and is a 10 MW thermal reactor that uses the pebble bed design. HTR-10 has been operating since 2000. The reactor will be used to perform experiments in the use of process heat and electric power production. These prototypes continue to provide valuable data for both hexagonal block and pebble bed HTGR development. Besides these small research devices, new designs that permit greater safety and modularity are under serious consideration in several countries. These programs represent the future potential of the HTGR [5].

Past designs of HTGR power plants used indirect steam cycles to produce power. Helium was passed through a heat exchanger to make steam for turbines. New designs take advantage of the advances in engineering materials that allow for turbine blades to be used in the main helium system. This will allow for both greater

efficiency and cost savings from eliminating the steam system, as well as significant savings in water use to produce electricity. In addition, these newer HTGRs may be small and simple enough to permit factory construction and greater modularity. This is similar to current gas turbines that are factory built and quickly installed at the power plant site [6].

Hexagonal block designs are also being considered. The main effort centers on the Gas Turbine - Modular Helium Reactor (GT-MHR) (Figure2).
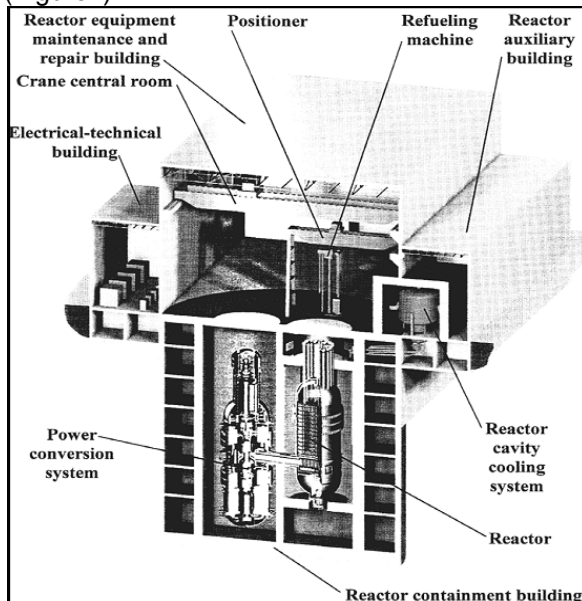
(Figure2. Gas Turbine - Modular Helium Reactor (GT-MHR)).

This effort is an evolution from the previous US designs . The reactor would produce approximately 150 MWe. It would not have online refueling capability, however the hexagonal blocks would be arranged in an annular pattern, in other words a "donut" of fuel containing blocks with "empty" graphite blocks in the center and surrounding the outside. This annular configuration would serve as a further absorber of excess heat should a loss of coolant occur [7].

In the Netherlands, a more unusual pebble bed reactor is being studied. Called NEREUS , this design is both smaller (8 MWe) and would not have online refueling capability. Instead the fuel design would permit longer periods of operation between refuelings (three years). The main objective for the NEREUS design would be either for commercial ship propulsion or could be used for small remote villages. NEREUS has even been studied for desalination due to both its longer periods between refueling and greater portability [8].

The Pebble Bed Modular Reactor (PBMR) project in South Africa is probably the most publicized of the current efforts. A decision is expected from the South African government by late 2002 or early 2003 whether to construct the prototype. The prototype would be approximately 150 MWe and would have online refueling capability. If built, this project would answer many questions on the feasibility of both helium turbines as well as the economics of the pebble bed reactor. In addition, the South African effort may provide impetus for other HTGR projects [9].

The important aspects of the HTGR design are its higher efficiency, greater safety than standard water-cooled reactors, and lesser water requirements due to the use of helium as the main coolant. The primary reason for the enhanced safety of the HTGR is the use of the TRISO fuel particles that contain the nuclear fuel inside multiple layers of special materials such as silicon carbide (used for inside coatings of high performance devices such as aircraft jet engines) [10].

All of the HTGR designs can easily absorb the excess heat generated in an accident by virtue of the high temperature coatings and smaller size of the reactors. This essentially means that the HTGR designs currently being studied would avoid any of the consequences of accidents such as the Three Mile Island or Chernobyl. Smaller reactors that cannot meltdown or explode combined with a lower water requirement mean that the HTGR could supply carbon-free power, desalinated water, or process heat depending on the particular needs.

The HTGR fuel is also better designed for disposal. The safety, modularity, and simpler design make the HTGR a path by which nuclear power may make substantial contributions to future sustainable development. This article will briefly discuss the early projects, current activities, and future potential of the HTGR to contribute to sustainable development [11].

• This article has presented a summary of the HTGR as an alternative to renewable energy sources when such sources are either unavailable or inadequate for the particular need. While the designs presented were not all inclusive, they represent the spectrum of efforts in progress to provide energy needed for sustainable development efforts. While no single energy technology can be a panacea for global energy needs, HTGRs represent an opportunity for nuclear energy to make a relevant contribution to a more sustainable world [12]

References

1.   http://www.uic.com.au/nip64.htm.
2.   http://www.uic.com.au/nip64.htm.
3.   http://www.jaeri.go.jp/english/temp/tem.
4.   http://www.inet.tsinghua.edu.cn/english/proj ect/htr10.htm.
5.   http://ftortechnology.ru/f891.html.
6.   http://www.ga.com/gtmhr.

7. Платонов П.А., Новобратская И.Ф., Туманов Ю.П., Карпухин В.И. Влияние степени совершенства графита на изменение его свойств при облучении / Атомная энергия, 1979., т.46 – С. 248-254.
8. http://www.romawa.nl.
9. http://www.pbmr.co.za.
10. Engle G.B. Eatherly W.P. High Temperateres High Pressures / 1972, v.4.
11. http://web.mit.edu/pebble-bed.
12. http://www.uic.com.au/ne3.htm

CERN EXPERIMENTS

Vedeneyev V.Y.

Scientific instructor: Suhih L.G., teacher, Demyanenko N.V., senior teacher

Tomsk Polytechnic University, 634050, Russia, Tomsk, Lenin ave., 30

E-Mail: brainsplash@sibmail.com

CERN is an international laboratory for particle physicists and provides some of the most technologically advanced facilities for their research into the basic building blocks of the Universe. Specialist facilities that would otherwise be difficult or impossible for individual nations to build include advanced particle accelerators, such as the Large Hadron Collider, and facilities for the production of exotic forms of matter, including antimatter. CERN has established a reputation at the forefront of research, proven through its experiments, past and present.

The Large Hadron Collider (LHC) is a gigantic scientific instrument near Geneva, where it spans the border between Switzerland and France about 100 m underground. It mainly consists of a 27 km ring of superconducting magnets with a number of accelerating structures to boost the energy of the particles along the way.

Two beams of subatomic particles called 'hadrons' – either protons or lead ions – will travel in opposite directions inside the circular accelerator, gaining energy with every lap. Physicists will use the LHC to recreate the conditions just after the Big Bang, by colliding the two beams head-on at very high energy. Teams of physicists from around the world will analyse the particles created in the collisions using special detectors in a number of experiments dedicated to the LHC.

But how does it work? Inside the accelerator, two beams of particles travel at close to the speed of light with very high energies before colliding with one another. The beams travel in opposite directions in separate beam pipes – two tubes kept at ultrahigh vacuum. They are guided around the accelerator ring by a strong magnetic field, achieved using superconducting electromagnets. These are built from coils of special electric cable that operates in a superconducting state, efficiently conducting electricity without resistance or loss of energy. This requires chilling the magnets to about -271°C – a temperature colder than outer space! For this reason, much of the accelerator is connected to a distribution system of liquid helium, which cools the magnets, as well as to other supply services.[1]

The six experiments at the LHC are all run by international collaborations, bringing together scientists from institutes all over the world. Each experiment is distinct, characterized by its unique particle detector.

The two large experiments, "ATLAS" and "CMS", are based on general-purpose detectors to analyze the myriad of particles produced by the collisions in the accelerator. They are designed to investigate the largest range of physics possible. Having two independently designed detectors is vital for cross-confirmation of any new discoveries made.

Two medium-size experiments, "ALICE" and "LHCb", have specialized detectors for analyzing the LHC collisions in relation to specific phenomena.

Two experiments, "TOTEM" and "LHCf", are much smaller in size. They are designed to focus on 'forward particles' (protons or heavy ions). These are particles that just brush past each other as the beams collide, rather than meeting head-on.

The "ATLAS", "CMS", "ALICE" and "LHCb" detectors are installed in four huge underground caverns located around the ring of the LHC. The detectors used by the "TOTEM" experiment are positioned near the "CMS" detector, whereas those used by "LHCf" are near the "ATLAS" detector.[2]

About "ATLAS"

"ATLAS" is a particle physics experiment at the Large Hadron Collider at CERN. Starting in

late 2009/2010, the "ATLAS" detector will search for new discoveries in the head-on collisions of protons of extraordinarily high energy. "ATLAS" will learn about the basic forces that have shaped our Universe since the beginning of time and that will determine its fate. Among the possible unknowns are the origin of mass, extra dimensions of space, unification of fundamental forces, and evidence for dark matter candidates in the Universe.

"ATLAS"

"ATLAS" is one of two general-purpose detectors at the LHC. It will investigate a wide range of physics, including the search for the Higgs boson, extra dimensions, and particles that could make up dark matter. "ATLAS" will record sets of measurements on the particles created in collisions their paths, energies, and their identities.

This is accomplished in "ATLAS" through six different detecting subsystems that identify particles and measure their momentum and energy. Another vital element of "ATLAS" is the huge magnet system that bends the paths of charged particles for momentum measurement.

With the same goals in physics as "CMS", "ATLAS" will record similar sets of measurements on the particles created in the collisions – their paths, energies, and their identities. However, the two experiments have adopted radically different technical solutions and designs for their detectors' magnet systems.

The interactions in the "ATLAS" detectors will create an enormous dataflow. To digest these data, "ATLAS" needs a very advanced trigger and data acquisition system, and a large computing system.

More than 2900 scientists from 172 institutes in 37 countries work on the "ATLAS" experiment (December 2009).[1]

"ALICE" (A Large Hadron Collider Experiment)

For the "ALICE" experiment, the LHC will collide lead ions to recreate the conditions just after the Big Bang under laboratory conditions. The data obtained will allow physicists to study a state of matter known as quark-gluon plasma, which is believed to have existed soon after the Big Bang.

All ordinary matter in today's Universe is made up of atoms. Each atom contains a nucleus composed of protons and neutrons, surrounded by a cloud of electrons. Protons and neutrons are in turn made of quarks which are bound together by other particles called gluons. This incredibly strong bond means that isolated quarks have never been found.

Collisions in the LHC will generate temperatures more than 100 000 times hotter than the heart of the Sun. Physicists hope that under these conditions, the protons and neutrons will 'melt', freeing the quarks from their bonds with the gluons. This should create a state of matter called quark-gluon plasma, which probably existed just after the Big Bang when the Universe was still extremely hot. The "ALICE" collaboration plans to study the quark-gluon plasma as it expands and cools, observing how it progressively gives rise to the particles that constitute the matter of our Universe today.

A collaboration of more than 1000 scientists from 94 institutes in 28 countries works on the "ALICE" experiment (March 2006). [1]

"CMS" (Compact Muon Solenoid)

The "CMS" experiment uses a general-purpose detector to investigate a wide range of physics, including the search for the Higgs boson, extra dimensions, and particles that could make up dark matter. Although it has the same scientific goals as the "ATLAS" experiment, it uses different technical solutions and design of its detector magnet system to achieve these.

The "CMS" detector is built around a huge solenoid magnet. This takes the form of a cylindrical coil of superconducting cable that generates a magnetic field of 4 teslas, about 100 000 times more that of the Earth. The magnetic field is confined by a steel 'yoke' that forms the bulk of the detector's weight of 12 500 tonnes. An unusual feature of the "CMS" detector is that instead of being built inside the underground, like the other giant detectors of the LHC experiments, it was constructed on the surface, before being lowered underground in 15 sections and reassembled.

More than 2000 scientists collaborate in "CMS", coming from 155 institutes in 37 countries (October 2006).[3]

"LHCb" (Large Hadron Collider beauty)

The LHCb experiment will help us to understand why we live in a Universe that appears to be composed almost entirely of matter, but no antimatter.

It specializes in investigating the slight differences between matter and antimatter by studying a type of particle called the 'beauty quark', or 'b quark'.

Instead of surrounding the entire collision point with an enclosed detector, the "LHCb" experiment uses a series of sub-detectors to detect mainly forward particles. The first sub-detector is mounted close to the collision point, while the next ones stand one behind the other, over a length of 20 m.

An abundance of different types of quark will be created by the LHC before they decay quickly into other forms. To catch the b-quarks, "LHCb" has developed sophisticated movable tracking

detectors close to the path of the beams circling in the LHC.

The "LHCb" collaboration has 650 scientists from 48 institutes in 13 countries (April 2006).[1]

"TOTEM" (Total Elastic and Diffractive Cross Section Measurement)

The "TOTEM" experiment studies forward particles to focus on physics that is not accessible to the general-purpose experiments. Among a range of studies, it will measure, in effect, the size of the proton and also monitor accurately the LHC's luminosity.

To do this "TOTEM" must be able to detect particles produced very close to the LHC beams. It will include detectors housed in specially designed vacuum chambers called 'Roman pots', which are connected to the beam pipes in the LHC. Eight Roman pots will be placed in pairs at four locations near the collision point of the "CMS" experiment.

Although the two experiments are scientifically independent, "TOTEM" will complement the results obtained by the "CMS" detector and by the other LHC experiments overall.

The "TOTEM" experiment involves 50 scientists from 10 institutes in 8 countries (2006).[3]

"LHCf" (Large Hadron Collider Forward)

The "LHCf" experiment uses forward particles created inside the LHC as a source to simulate cosmic rays in laboratory conditions.

Cosmic rays are naturally occurring charged particles from outer space that constantly bombard the Earth's atmosphere. They collide with nuclei in the upper atmosphere, leading to a cascade of particles that reaches ground level.

Studying how collisions inside the LHC cause similar cascades of particles will help scientists to interpret and calibrate large-scale cosmic-ray experiments that can cover thousands of kilometres.

The "LHCf" experiment involves 22 scientists from 10 institutes in 4 countries (September 2006).[1]

List of used sources:
1. www.cern.ch – electronic resource;
2. www.lhc.cern.ch – electronic resource;
3. www.uslhc.us – electronic resource.

Section IX

QUALITY MANAGEMENT CONTROL

INTEGRATED MANAGEMENT SYSTEM

Kanina E. A., Sakun T. S.

Advisors: Venyukova G. A., associate professor; Alekseev L. A., associate professor.

Tomsk Polytechnical University, 634050, Russia, Tomsk, Lenin av., 30

E-mail: smile753@sibmail.com

The work is devoted to the theme «Integrated management system». The main objectives are to investigate integrated management system, to reveal its basic advantages and to estimate efficiency of introduction of this system at various enterprises.

Recently the problem of introducing integrated management system (IMS) has become more and more urgent for the Russian companies which faces a serious competition on the part of western companies and domestic one, confirmed by the certificates the achievement in the field of quality management, ecology and professional safety.

A management system is the framework of processes and procedures used to ensure that an organization can fulfill all tasks required to achieve its objectives.

Management system standards provide a model to follow in setting up and operating a management system.

IMS is a management system that integrates all of your systems and processes into one complete framework, enabling you to work as a single unit with unified objectives. Integrated management provides a clear picture of all aspects of your organization, how they affect each other and their associated risks. It also means less duplication and makes it easier to adopt new systems in the future. Integrated management is relevant to any organization, regardless of size or sector, looking to integrate two or more of their management systems into one cohesive system with a holistic set of documentation, policies, procedures and processes.

A typical integrated management system might include:
- ISO 9001 (Quality Management)
- ISO 14001 (Environmental Management)
- OHSAS 18001 (Occupational Health & Safety)
- ISO/IEC 27001 (Information Security)
- ISO 22000 (Food Safety)
- ISO/IEC 20000IT Service Management
- A quality management system (QMS) can be expressed as the organizational structure, procedures, processes and resources needed to implement Quality Management. QMS includes next elements:
- Organizational structure
- Responsibilities
- Procedures
- Processes
- Resources

ISO 9000 is a family of standards for quality management systems. It consists of standards and guidelines relating to quality management systems and related supporting standards. ISO 9000 includes the following standards:
- ISO 9000:2005 Quality management systems – Fundamentals and vocabulary describes fundamentals of quality management systems which form the subject of the ISO 9000 family, and defines related terms.
- ISO 9001:2008 Quality management systems – Requirements is intended for use in any organization regardless of size, type or product (including service). It provides a number of requirements which an organization needs to fulfill to achieve customer satisfaction through consistent products and services which meet customer expectations. It includes a requirement for continual (i.e. planned) improvement of the quality management system for which ISO 9004:2000 provides many hints.
- ISO 9004:2000 Quality management systems - Guidelines for performance improvements covers continual improvement. This gives you advice on what you could do to enhance a mature system. This document states very specifically that it is not intended as a guide to implementation. An example of a Practical Guide to ISO 9001 presentation can be found here ISO 9001 a Practical Guide to Implementation

Environmental management system (EMS) refers to the management of an organization's environmental programs in a comprehensive, systematic, planned and documented manner. It includes the organizational structure, planning and resources for developing, implementing and maintaining policy for environmental protection. The ISO 14000 family addresses various aspects of environmental management.

ISO 14004:2004 provides guidelines on the elements of an environmental management system and its implementation, and discusses principal issues involved.

ISO 14001:2004 specifies the requirements for such an environmental management system. Fulfilling these requirements demands objective evidence which can be audited to demonstrate that the environmental management system is operating effectively in conformity to the standard.

The systematic ISO 14001:2004 approach

requires the organization to take a hard look at all areas where its activities have an environmental impact. And it can lead to benefits like the following:

- reduced cost of waste management;
- savings in consumption of energy and materials;
- lower distribution costs;
- improved corporate image among regulators, customers and the public;
- framework for continual improvement of environmental performance.

Occupational health and safety management system should aim at: the promotion and maintenance of the highest degree of physical, mental and social well-being of workers in all occupations; the prevention amongst workers of departures from health caused by their working conditions; the protection of workers in their employment from risks resulting from factors adverse to health; the placing and maintenance of the worker in an occupational environment adapted to his physiological and psychological capabilities; and, to summarize the adaptation of work to man and of each man to his job. OHSAS 18000 is an international occupational health and safety management system specification. It comprises two parts, 18001 and 18002 and embraces BS8800 and a number of other publications.

Integrated management provides a clear picture of all aspects of your organization, how they affect each other and their associated risks. It also means less duplication and makes it easier to adopt new systems in the future. Integrated Management is relevant to any organization, regardless of size or sector, looking to integrate two or more of their management systems into one cohesive system with a holistic set of documentation, policies, procedures and processes. Typically, organizations most receptive to this product will be those who have maturing management systems and who wish to introduce other management systems to their organization with the benefits that those bring.

We had practice in Tomsk Distributing Energy Company which implements an integrated management system. It includes Quality Management, Environmental Management and Occupational Health & Safety. The benefits of IMS:

- encourages risk management;
- gives you a competitive edge;
- attracts investment;
- improves and protects brand reputation;
- raises stakeholder perception and satisfaction.

- The IMS ensures bigger coordination inside organization, intensifies synergetic effect. It means that the common result is higher then the sum of individual results.
- The IMS minimizes functional separation in organization which arises with autonomous management systems.
- IMS creation is not so difficult then creation of two or more parallel systems.
- The organization management system is simpler because the number of external and internal connections in the IMS is less then summarized number of connections in different systems.
- The number of documents is reduced.
- The staff involving degree is higher.
- The IMS auditing is simply, briefly and cheaper because of information doubling liquidation.
- The costs of IMS are lower than the costs of individual management systems.

So, integrated systems of management have much greater advantage in comparison with separately taken systems of quality. And each enterprise applying to be on a high level of development in conditions of modern economic, political and social conditions should inculcate IMS.

References

1. Pyzdek, T, "Quality Engineering Handbook", 2003, ISBN 0824746147
2. Godfrey, A. B., "Juran's Quality Handbook", 1999, ISBN 007034003
3. "Good Business Sense Is the Key to Confronting ISO 9000" Frank Barnes in Review of Business, Spring 2000.
4. ISO 9000:2005 Quality management systems – Fundamentals and vocabulary
5. ISO 9001:2008 Quality management systems – Requirements
6. ISO 9004:2000 Quality management systems - Guidelines for performance improvements
7. ISO 14001:2004 Environmental management systems – Requirements with guidance for use
8. ISO 14004:2004 Environmental management systems -- General guidelines on principles, systems and support techniques
9. OHSAS 18001:2007 Occupational health and safety management system – Requirements
10. http://www.iso.org
11. http://www.wikipedia.ru
12. http://www.bsigroup.com

RUSSIAN HIGHER EDUCATION SYSTEM: TRADITIONS AND INNOVATIONS

Mertins K.V.

Supervisor: **Venukova G.A.**

Tomsk Polytechnic University

E-mail: mertinskv@tpu.ru

Abstract In the article the analysis of existing Russian system of higher education is given. The problems to be solved for introducing the training credit-rating system ofthe educational process organization in technical university to improve the education quality, are presented.

Key words: education quality, credit-rating system of training, educational process.

Introduction

Over the last ten years, the system of higher education has undergone considerable change in the following areas:

- goals - with an orientation towards the needs of the market, society, and individuals;

- structure - decentralization (in contrast to Soviet centralized planning);

-autonomy of higher educational institutions - introduction of private higher education; four- and two-year programs in parallel with the traditional five-year program; elimination of a bias towards engineering specialties;

-financing - diversification of financial sources instead of reliance solely on state financing;

-content - increasing the humanitarian components in the curriculum, and diversifying programs and courses. [1]

Before considering higher education system transition to a new paradigm one should answer a question: what merits and drawbacks are there in the Russian traditional higher education system?

The traditional system of higher education based on principles of integrity, sequences and continuity of knowledge, was been introducing for a long time. In the Soviet society higher education was very prestigious. But it was not so mass.

Fundamental training in the field of natural sciences made it possible to make improbable investigations in the field of physics, mathematics, chemistry, electronics and to create innovative technologies in the field of astronautics.

However, among the drawbacks of Russian education system the following ones may be distinguished:

-unability to operate updated equipment due to poverty in RF;

- insufficient comprehension by Russian students of their own significance in comparison with foreign students. Europe students in contrast to Russian students are known to influence on educational process by their own activities.

- still bad quality of foreign languages mastering.

The trainers are considered to be the subjects of educational process: they define the purposes and educational problems, their maintenance, principles, methods, tools and modes of studying. A student is an object of studying. His role is more often passive and is reduced to mastering, storing and temporary use of the information learnt. Students and trainers with their own point of views, different from the standard one , are not accepted and rejected away by such system of training.

The contradiction between traditional practice of the organization of educational process in higher school, on the one hand, and new requirements to education quality by designing and using new technologies, including module-rating technology, on the other hand, has defined a research problem.

Our further discussion is concerned with the model of higher educational training process organization.

Findings

It is obviously that changes in structure and harmonization of national system of higher education assumes: introducing multistage model of education and credit-rating -modular structure of educational process, developing new system of quality maintenance, academic mobility of students and trainers. Separating the outcomes from curriculum content and assessment tasks are likely to lead to artificiality and rigidity, and, thus, there is the necessity of making the system of continuous assessment for trying to avoid injustice with respect to students.

Credit-rating system of educational process organization promotes optimum planning of the maintenance and methodical provision of disciplines taking into account the outcomes. Stimulating the development of various technologies and forms of studying, the system promotes implementing the variability of the curriculums providing individuality of the training trajectory. Moreover, using continuous assessment liberalizes educational process and focuses it on the student stimulating independent work. To improve the process of quality estimation of educational programs development, modern systems of a quality management of

educational services is established, promoting integration of the higher school into the world system of higher education.

Results

As for educational system development at Tomsk Polytechnic University it is characterized by integration into the European educational community to join the countries supporting Bologna Process. The establishment of a credit system is directly linked to its capacity to promote mobility.

Jurding from mentioned above the credit-modular system organization experiment at Tomsk Polytechnic University should be described. Four departments of TPU had taken part in experiment by 2009. In 2005 The Institute of Electrical Engineering was the first to begin the integration into Bologna Process. The Faculty of Computer Science and Engineering, the Faculty of Electrophysics and Electronic Equipment, the Faculty of Chemistry and Chemical Engineering were also joined. In 2010 all the syllabus at the university should be in conforming with the credit-rating system, based on Europe Credit Transfer System (ECTS), and competence approach. It has to be said that learning outcomes are sets of competences, expressing what the student will know, understand or be able to do after completing the learning .process.

Credit system can only work as means of transfer and accumulation of educational attainments within parts of a course programme, providing a course programme is sub-divided into a number of relatively small parts (courses, modules, units, etc.) and the assessment of educational achievements is similarly sub-divided according to those parts, whereby the overall attainments assessment is cumulative.

ECTS credits are quantitative values allocated to all educational components of a study programme (such as modules, course units, placements, dissertation work, etc.). They reflect the quantity of academic work each course unit requires in relation to the total quantity of work necessary to complete a full year of academic study at the institution (e.g. lectures, practical work, seminars, tutorials, fieldwork, private study – in home or library – and examinations or other activities to be assessed).

The system relies on the convention that 60 credits measure the workload of a full-time student during one academic year. The student workload of a full-time study programme in Europe amounts in most cases to 36/40 weeks per year and in those cases one credit stands for 25 to 30 working hours. Workload refers to the notional time an average learner might expect to complete the required learning outcomes. Credits in ECTS can only be obtained after completion of the work required and appropriate assessment of the learning outcomes achieved. [2]

The key components of a credit transfer system have been identified as units and modules: A unit is intended to denote the elementary (or smallest) part of a curriculum and a module is understood to describe the elementary (or smallest) part of a learning pathway. Credits can be considered as a quantitative measurement allocated to qualification units and/or modules and/or to part or full qualifications.

The allocation of ECTS credits is based on the official length of a study programme cycle. The total workload necessary to obtain a first cycle degree lasting officially three or four years is expressed as 180 or 240 credits. [3]

One should underline that the credit system of training rather essentially changes work of trainers, puts before necessity of their constant self-improvement and self-training, developing new methodical maintenance of educational process. The main working principle of the contemporary trainer is not only purposeful influence on the student, its personal installations, but optimum activities of students. According to the credit system training should be based on:

- interactive methods of training;
- sufficient and constantly updated portfolio of methodical and didactic materials;
- constant personal and professional growth of the trainer;

New, perspective forms of the educational process organization are connected with information technology to be actual for higher education. Students are able to use modern computers, instruments a communication facility, to search and reception of the information, to problem solving in difficult situations. Traditional work forms are filled with the new maintenance as time is saved due to application of information and communication technologies, for providing personal contact between of trainers and students is very important for their vocational training .

The credit technology is interesting and because it provides strength to the teacher creatively working as his individuality is underlined, and as for the student, wishing to get proper education? It gives spectrum of possibilities.

Conclusion

Credit-rating system of the organization of educational process described above resulted in reforms have never been fully analyzed and reported. Implementing this system by introducing the advanced mechanisms and technologies of training causes the necessity of

structural transformations in traditional higher educational system.

References

1. http://www.hse.ru/lingua/en/rus-ed.html
2.http://europa.eu.int/comm/education/programmes/socrates/ects_en.html
3. Curriculum, assessment and qualifications .- an evaluation of current reforms - prepared by Michael Irwin, New Zealand. business roundtable for the education forum/ may 1994

Section X

HEAT AND POWER ENGINEERING

HEAT TRANSFER AND HYDRODYNAMICS IN THERMOSYPHON

M.A. Al-Ani

Supervisor: Professor G. V. Kuznetsov

Thermal Power Engineering,TPU

E-mail: maathe_a@yahoo.com

Abstruct:

Heat transfer and hydrodynamics of two phase closed thermosyphon (TPCT) is studied in this paper using finite difference technique method of stream function and vorticity. The mathematical model is formed for both vapor phase and liquid film in a non-dimensional form. The effect of Rayleigh number Ra is studied and its effect on the Nusselt number on the lower and upper end of the thermosyphone

Introduction:

A two phase closed thermsyphon (TPCT) Fig 1 has advantages of simple structure, good performance, and easy manufacture, and widely used in a heat recovery systems and other fields of heat exchange.

In this paper we assumed the main length is Ny= 1, and the working fluid us the water A two-phase closed thermosyphon (TPCT) is passive high performance heat transfer device. It is a closed container filled with a small amount of a working fluid (Fig. 1). In such a device, heat is supplied to the evaporator wall, which causes the liquid contained in the pool to evaporate. The generated vapor then moves upwards to the condenser. The heat transported is then rejected into the heat sink by a condensation process. The condensate forms a liquid film which flows downwards due to gravity. The main advantage of TPCTs is that no mechanical pumping is needed. As a consequence, they are cheap and reliable[1].

Mathematical Model:

Equations of continuity, momentum and energy for the gas and liquid phase are[2]:

$$\frac{\partial u}{\partial x} + \frac{\partial \upsilon}{\partial y} = 0 \qquad (1)$$

$$\rho\left(\frac{\partial u}{\partial t} + u\frac{\partial u}{\partial x} + \upsilon\frac{\partial u}{\partial y}\right) = -\frac{\partial p}{\partial x} + \mu\left(\frac{\partial^2 u}{\partial x^2} + \frac{\partial^2 u}{\partial y^2}\right) \qquad (2)$$

$$\rho\left(\frac{\partial \upsilon}{\partial t} + u\frac{\partial \upsilon}{\partial x} + \upsilon\frac{\partial \upsilon}{\partial y}\right) = -\frac{\partial p}{\partial y} + \mu\left(\frac{\partial^2 \upsilon}{\partial x^2} + \frac{\partial^2 \upsilon}{\partial y^2}\right) + \rho\beta g(T - T_o) \qquad (3)$$

$$\rho C_p\left(\frac{\partial T}{\partial t} + u\frac{\partial T}{\partial x} + \upsilon\frac{\partial T}{\partial y}\right) = \lambda\left(\frac{\partial^2 T}{\partial x^2} + \frac{\partial^2 T}{\partial y^2}\right) \qquad (4)$$

Equation of conduction for solid phase:

$$\rho C_p \frac{\partial T}{\partial t} = \lambda\left(\frac{\partial^2 T}{\partial X^2} + \frac{\partial^2 T}{\partial Y^2}\right) \qquad (5)$$
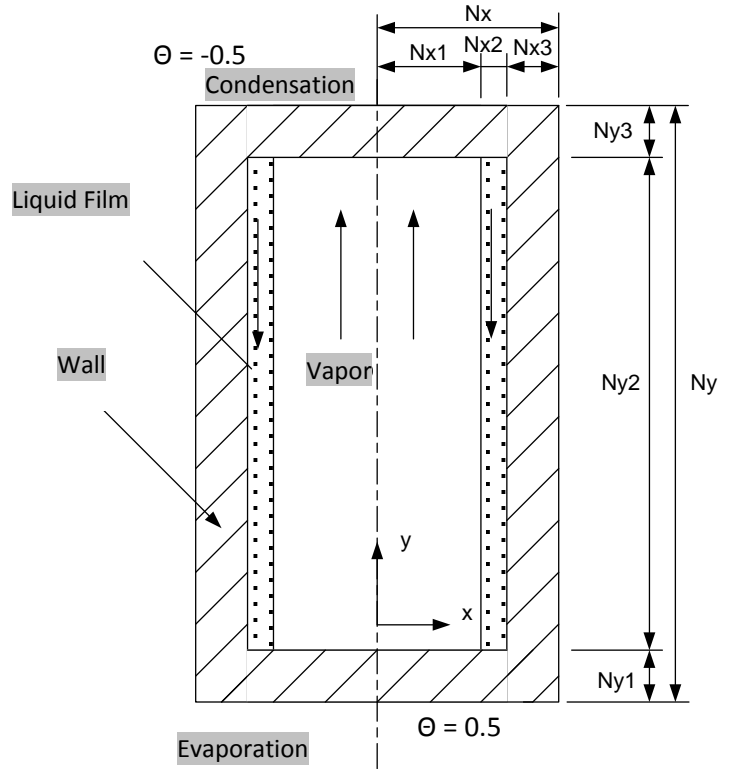
Fig. 1 – Thermosyphon

Equations 1-4 may be written in another form without pressure, in rectangular coordinate the set of equations can be written in term of variables (ω.ψ) :

$$\rho\left(\frac{\partial \omega}{\partial t} + u\frac{\partial \omega}{\partial x} + \upsilon\frac{\partial \omega}{\partial y}\right) = \mu\left(\frac{\partial^2 \omega}{\partial x^2} + \frac{\partial^2 \omega}{\partial y^2}\right) + \rho\beta g\frac{\partial T}{\partial x}$$

(6)

$$\frac{\partial^2 \psi}{\partial X^2} + \frac{\partial^2 \psi}{\partial Y^2} = -\omega \qquad (7)$$

Stream function φ and vorticity ω are:

$$u = \frac{\partial \psi}{\partial y}, \upsilon = -\frac{\partial \psi}{\partial x}, \omega = \frac{\partial \upsilon}{\partial x} - \frac{\partial u}{\partial y}$$

To set the equations 4-7 in non-dimension form

the following relations are used:

$$X = \frac{x}{L}, Y = \frac{y}{L}, \tau = \frac{t}{t_o}, U = \frac{u}{V_o}, \Theta = \frac{T - T_o}{\Delta T}, \Psi = \frac{\psi}{\psi_o}, F_o = \frac{at_o}{L^2},$$

$$\Pr = \frac{v}{a}, \Omega = \frac{\omega}{\omega_o}, V_o = \sqrt{g\beta\Delta TL}, \psi_o = V_oL, \omega_o = \frac{V_o}{L}, Ra = \frac{g\beta(T_H - T_L)L^3}{va}$$

Mathematical model for thermosyphon in non-dimension form are:

$$\frac{\partial\Omega}{\partial\tau} + U\frac{\partial\Omega}{\partial X} + V\frac{\partial\Omega}{\partial Y} = \frac{1}{\sqrt{Gr}}\left(\frac{\partial^2\Omega}{\partial X^2} + \frac{\partial^2\Omega}{\partial Y^2}\right) + \frac{\partial\Theta}{\partial X} \quad (8)$$

$$\frac{\partial^2\Psi}{\partial X^2} + \frac{\partial^2\Psi}{\partial Y^2} = -\Omega \quad (9)$$

$$\frac{\partial\Theta}{\partial\tau} + U\frac{\partial\Theta}{\partial X} + V\frac{\partial\Theta}{\partial Y} = \frac{1}{\sqrt{Ra\cdot\Pr}}\cdot\left(\frac{\partial^2\Theta}{\partial X^2} + \frac{\partial^2\Theta}{\partial Y^2}\right) \quad (10)$$

For solid phase :

$$\frac{\partial\Theta}{\partial Fo} = \Delta\Theta = \left(\frac{\partial^2\Theta}{\partial X^2} + \frac{\partial^2\Theta}{\partial Y^2}\right) \quad (11)$$

The average Nussel number at the wall of thermosyphon is calculated by the form:

$$\overline{Nu} = \int_0^{Nx}\frac{\partial\Theta}{\partial X}dY \quad (12)$$

Boundery Conditions :
Non-dimensional B.C.for equations 8-11are[2,3] :

$$X = 0, \quad 0 \le Y \le 1, \frac{\partial\Theta}{\partial X} = 0, \Psi = 0$$

$$X = \frac{Nx}{Ny}, \quad 0 \le Y \le 1, \frac{\partial\Psi}{\partial X} = 0, \frac{\partial\Theta}{\partial X} = 0$$

$$X = Nx1, \quad \frac{Ny1}{Ny} \le Y \le \frac{Ny1 + Ny2}{Ny}, \frac{\partial\Theta_1}{\partial X} = \lambda_{2,1}\cdot\frac{\partial\Theta_2}{\partial X},$$

$$\left.\frac{\partial\Psi}{\partial X}\right|_\Gamma = \left.\frac{\partial\Psi}{\partial X}\right|_{\text{ж}}, \eta_\Gamma\cdot\Omega_\Gamma = \eta_{\text{ж}}\cdot\Omega_{\text{ж}}$$

$$X = \frac{Nx1 + Nx2}{Ny}, \quad \frac{Ny1}{Ny} \le Y \le \frac{Ny1 + Ny2}{Ny}, \frac{\partial\Theta_2}{\partial X} = \lambda_{3,2}\cdot\frac{\partial\Theta_3}{\partial X},$$

$$\left.\frac{\partial\Psi}{\partial X}\right| = 0, \Psi = 0$$

$$Y = (0, Ny1/Ny), \quad 0 \le X \le \frac{Nx}{Ny}, \Theta = 0.5$$

$$Y = (Ny1 + Ny2/Ny, 1), \quad 0 \le X \le \frac{Nx}{Ny}, \Theta = -0.5$$

To solve the equations 8-11 we used finite difference technique method of alternative variables [4-6].

Results.
In the present work we set the thickness of the liquid layer W=Nx2/Ny=0.01,aspect ratio of diameter (width) to height Nx/Ny = 0.25, the height of thermosyphon = 1.

We assumed that the working fluid is a water. In Fig 2 we see distributions of stream functions lines, temperature lines, and velocity field for Rayleigh number Ra, $8*10^5$, $8*10^5$, $8*10^4$, $8*10^3$,and constant temperature on the top and botton of the thermosyphone, Θ = -0.5 and 0.5 respectively.Increasing the Rayleigh number increas the value of stream function, increas the value of Nusselt number from 1.33 for Ra=$8*10^3$ to4.88 at Ra=$8*10^4$ and 8.45 for Ra=$8*10^5$.
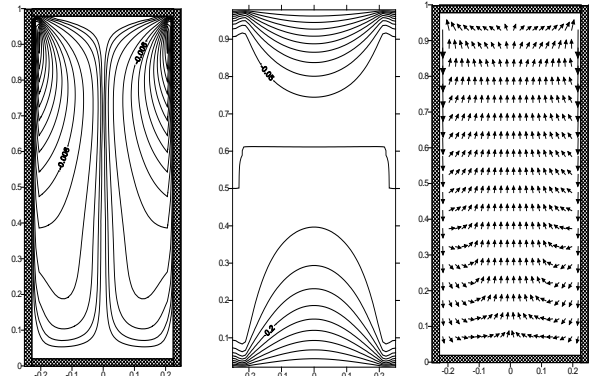
Fig.(2-a)-Ra=$8*10^3$,
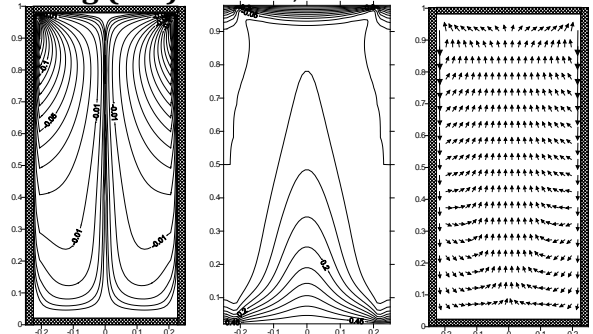
Fig.(2-b)-Ra=$8*10^4$
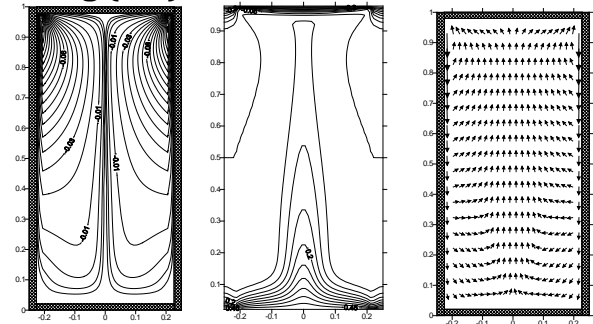
Fig.(2-c)-Ra=$8*10^5$

References:

1. Hichem F., Jean-Louis J., An experimental and theoretical investigation of the transient behavior of a two-phase closed thermosyphon, Applied Thermal Engineering 23 (2003) 1895–1912

2.M.K.Bezrodny, I. L. Pioro, T.O.Kystyuk.Trnsfer presses in two-phase thermosyphon systems. Theory and practice, Kiev 2005.

3. Zhu H. Experimental study on transient behavior of semi-open two-pahse thermosyphon. Journel of Zhejiang university science 2004 5(12):1565-1569.

4. Роуч П. Вычислительная гидродинамика. М. Мир, 1980-616 с.

5. Самарский А.А.Теория разностных схем 1977-655 с.

6. В.М.Пасконов, В.И.Полежаев, Л.А.Чудов. Численное моделирование процессов тепло и массообмена.1984.

INFLUENCE OF FUEL BURNUP ON ENERGY RELEASE DISTRIBUTION OVER HEIGHT OF FUEL ELEMENT IN MEDIUM POWER REACTOR

Kazak N.I., Timoshin S.V., Marchenko V.O.

Scientific Supervisor: Chertkov Yu.B., Ph.D., Associate Professor, Ermakova Ya. V, Teacher

Tomsk Polytechnic University, 634050, Russia, Tomsk, Lenin str., 30

E-mail: timoshin@tpu.ru

In the given work the results of calculated testing of fission products distribution (FP) over the height of an active zone depending on the depth of fuel burnup in two test fuel assemblies of medium power reactor, and also changes of this distribution in process of irradiation are submitted. When the average fuel burnup was reached (38 % - 40 %), the peak value in some fuel elements was 74 %. The results of calculations are compared to the experimental ones. The agreement of calculation and measurement results shows that the developed advanced model gives satisfactory descriptions of the processes of fuel isotope change in process of irradiation.

To receive comparative data on working capacity of fuel elements with the increased uranium content, material science researches of two spent fuel assemblies in medium power reactor are conducted [1]. One of them was standard, where the mass of ^{235}U in fuel elements was 5 g, and the second - tested, with the increased mass of ^{235}U up to 6 g in fuel elements. Earlier used calculating models of the active zone described geometry and material structure approximately, using a homogenization principle that simplified the description and reduced expenses of time for carrying out calculations, but brought a certain error in results and did not allow to receive the information about energy release and burning out in each fuel element of an active zone. On the basis of MCU-RR program [2] the calculating model which allows to describe each fuel element in details by specific registration zones is created.
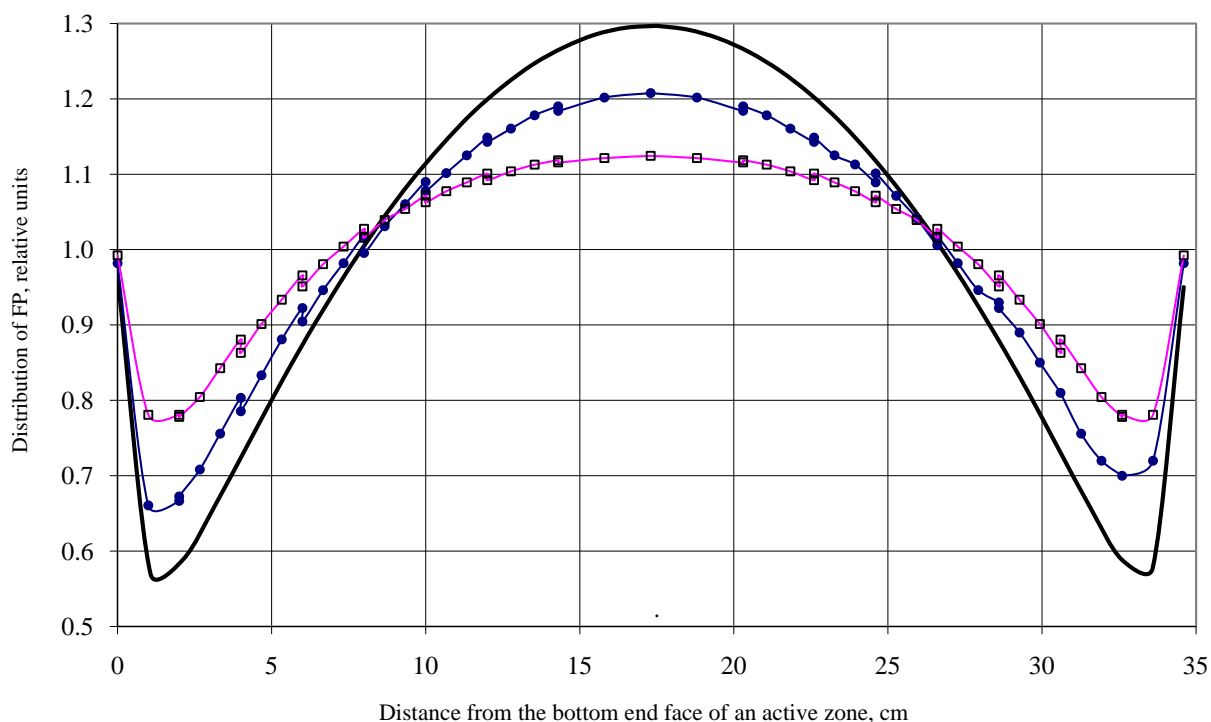
Fig. 1 Distribution of FP over the height of fuel elements at different average values of burning out

The research objective consisted in testing the calculating model on experimental data and getting the information on change of distribution of fission products (FP) over the height of an active zone and burning out of ^{235}U in fuel assemblies the course of tests. Such

information will allow to calculate temperature distribution by the kernel volume correctly and to interpret the results of materials science researches.

With the help of RZA program [3] in two-dimensional multigroup model of medium power reactor (r, z - geometry) the distributions of fission products (FP) over the height of an active zone which depend on the depth of fuel burning out have been received. In fig. 1 the distribution of FP normalized on the average value are given at beginning of irradiation (burning out of 0.1 %), on burning out which is approximately equal to an average for outgoing fuel of medium power reactor (38 %) and deep, close to maximum reached burning (74 %). Fuel burning out is understood as a full decrease of ^{235}U as a result of fission processes and radiative capture in relation to its initial quantity. According to the received calculating results it follows, that in process of burning out of ^{235}U the distribution of FP over height of fuel elements becomes flat.

Data obtained in the experiments for a considerable quantity of fuel elements have been used for the calculation of average high distribution. Comparison of calculating and experimental distributions of FP over the height of an active zone can be made by data given in fig. 2.

Distance from the bottom end face of an active zone, cm
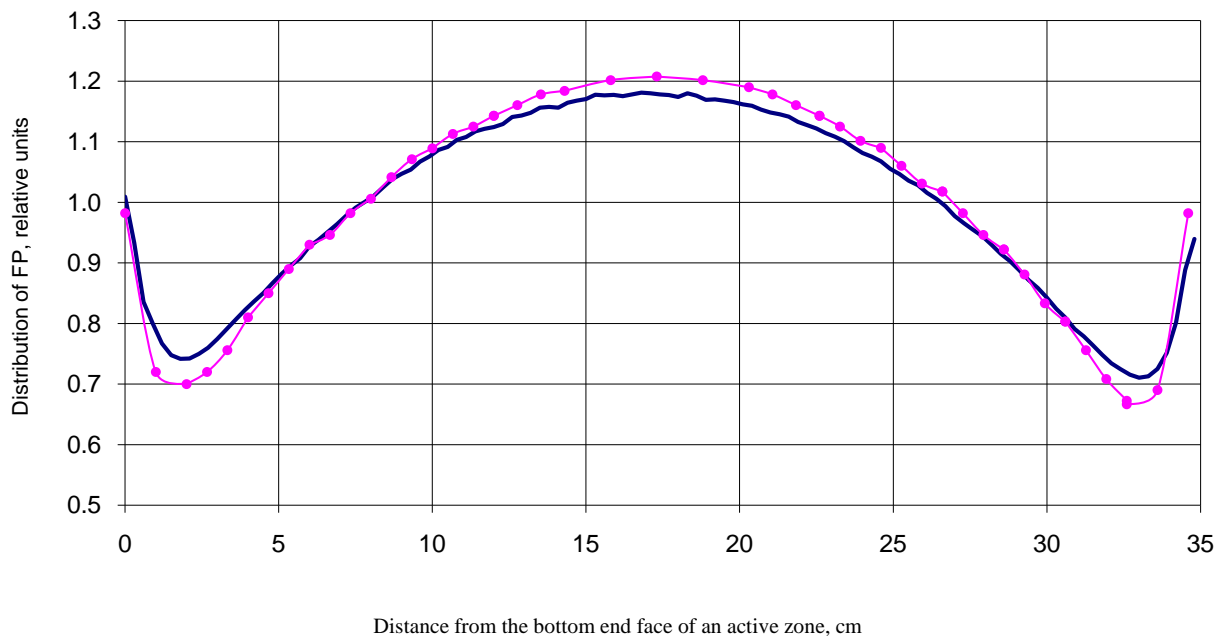
Fig. 2 Comparison of average experimental and calculating distributions of FP over the height of an active zone

The dark blue line-experiment, pink line- RZA program

The difference of calculating values from the experimental does not exceed 2,3 % in the peak region and 5,7 % in the valley region of these distributions.

The agreement of calculation and measurement results shows that the advanced model of an active zone used in calculations gives satisfactory descriptions of behavior of distribution of fission products over the height of an active zone and burning out during the operation of fuel assemblies with the standard and increased mass of ^{235}U in fuel elements. The received results have allowed to estimate the change of characteristics of energy release distributions and burning out in the investigated assemblies in the course of irradiation.

REFERENCES:

1. А.А. Цыканов, В.Г. Дворецкий, Ю.Ю. Косвинцев и др. Материаловедческие иссле-дования отработавшего топлива ИЯР СМ в обоснование концепции модернизации активной зоны. Сб. докладов на VII Российской конференции по реакторному материаловедению, 8-12 сентября 2003 г., Димитровград.

2. Е.А. Гомин, М.И. Гуревич, Л.В.Майоров, С.В. Марин. Описание применения и инструкция для пользователя программой MCURFFI расчета методом Монте-Карло нейтронно-физических характеристик ядерных реакторов. Препринт ИАЭ-5837/5. Москва, 1994.

3. А.Г. Калашников, В.М. Декусар. Об эффективной модификации метода переменных направлений. Вопросы атомной науки и техники. Сер. Физика и техника ядерных реакторов. 1985, вып. 5.

PRODUCTION CONDITIONS ANALYSIS OF COGENERATION UNITS BASED ON GAS ENGINE AND GAS TURBINE

Khisamutdinov N., Ptáček M.

Supervisor: Toman P., Associate Professor

Brno University of Technology, Faculty of Electrical engineering and Communication, Department of Electrical Power Engineering, Technicka 8, 616 00 Brno, Czech Republic, www.feec.vutbr.cz/UEEN

Email: xkhisa00@stud.feec.vutbr.cz, xptace10@stud.feec.vutbr.cz

ABSTRACT

This article describes the basic factors influencing the selection of cogeneration plants based on Gas-Turbine-Based Cogeneration Plant (GTCP) and Gas-Engine-Based Cogeneration Plant (GECP). The main reasons of Gas Turbine(GT) usage were defined. Also the paper involves classification of GECP and GTCP and gives recommendations for CHP unit selection in a modern market conditions.

Keywords: Cogeneration, Gas Engine, Gas Turbine, Combined Heat and Power (CHP) unit.

1 INTRODUCTION

Decentralized complex heat and power sources are becoming more and more popular, since they could be installed both on already acting heating boiler plants and on new constructed heat sources.

One of the possible solutions of that problem is installation of local heat and power systems with gas turbine units or gas powered electrical generators which run on natural gas, propane, or another type of a gas fuel with minimal methane number equal to 35.

2 REASONS FOR CHP UNITS APPLICATION

The construction of a decentralized power station might be caused by one of the following reasons: 1) Heat or power supply costs are comparable to the expanses for decentralized power station construction (new building); 2) There are problems with region power nets or with price for extra energy (power extension); 3) Power availability and quality is critical in terms of technical process stability or technology violation; 4) Charges for the following atmospheric gas emissions are comparable to costs of facility for electrical stations (oil producing companies); 5) Cheap or free gas could be used as a fuel for power stations (producing and transport fuel companies); 6) Possible electric power rate rising; 7) It is possible to use profitable biogas (agricultural companies, disposal works and private organizations).

3 GAS-ENGINE-BASED COGENERATION PLANT

Currently power stations based on gas engine (power rate 100kW – 9MW) are the most common source of constant energy for housing sector, industrial companies, coal-milling and oil organizations. Gas powered engines with power less then 20MW have higher efficiency (up to 47,3%) and 2-3 times longer operation life span compared to gas turbines. Besides they are less affected by a high air temperature and can operate with fractional loads [1].

Combustion engines acting on gas fuel can be divided into four groups:

1) *Dual – fuel diesel.* During exploitation the consumption of oil-fuel could be varied from 100% to 10-15%. The rest part of a fuel is nature gas mixed with air at the entry to the engine. At that, initiation of fuel combustion is the result of the temperature rising or it is caused by a constant ignition source.

2) *Dual – fuel gas reciprocating engines.* The main fuel for them is gas, but a small portion of a liquid fuel ("pilot fuel") is injected into a cylinder or commonly into a special pre-ignition chamber for combustion initiation of an air-gas mixture.

3) *Gas engine,* is working only on a gas fuel, without the pilot fuel usage. The factors that distinguish them are low compression rate and generally less economical efficiency.

4) *Tri-fuel technology* - It can be run either on natural gas or on light fuel oil (LFO) or on heavy fuel oil (HFO). The engine can smoothly switch between fuels during engine operation and is designed to give the same output regardless of the fuel. The engine operates on the lean-burn principle. Lean combustion enables high compression ratio which increases engine efficiency (up to 47,3) and reduces peak temperatures, and therefore also reduces NOx emissions.

4 GAS-TURBINE-BASED COGENERATION PLANT

Nowadays exist three basic types of GT:

The first and the second type GT - **a**eroderivative GT are more uprated and don't have a considerable unite weight (kg/kW), easy to service, less demanding for infrastructure, but at the same time have a shorter operation life span. The power rate of such plants is varied from 2,5MW to 20MW.

The third type - *Heavy-duty GT* prevail when the power rate is more then 50MW.

Steam injected gas turbine (STIG) has become a technological novelty in the sphere of improved

GT efficiency. This is a Combined Cycle Power Plant where steam from a recovery boiler is supplied to an air-gas channel of GT as an additional working medium for a mechanical energy increasing.

The STIG plan is characterized by the maximum capacity gain (70%), increased electrical efficiency up to 42.8% with maximum loads, emissions reduction (CO and NOx) without additional expenses and cut down relative capital investments

Table. 1 Production conditions analysis

№	Parameter	Dimension	GECP	GTCP
	Process conditions			
1	Electrical power	[MW]	1,05– 22,4	1,2 – 375 (570)*
2	Ratio of heat to electrical energy	-	from 0.5:1 to 1:1	from 2:1 to 1,5:1
3	Overload capacity	[kW]	110%	110%
4	Power-control band	[%]	50 - 100	20 – 100
5	Heat rate	[MW]	1,3 - 24	2,33 - 570
6	Net efficiency	[%]	38,1 – 47,3	24,3 – 40 (60)*
7	Combustion efficiency	[%]	75 - 94	70 - 90
8	Fuel Input (Hu=48744 kJ/kg)	[Nm3/kW*hr]	0,276 - 0,251	0,474 – 0,618
9	Unit oil consumption	[g/kW*hr]	0,3 – 0,5	0,04 - 2
10	Emission NOx	[ppm]	121,7 - 244,5	24,3 – 25
11	Number of starts	-	unlimited	200 - 450 per year
	Design factors and mass and dimensions parameters			
12	Specified life / overhaul life	10^3*machine hour	100/45-72 – 400/96	100/50-25 - 250/50-25
13	Unit weight of CHP units	[kg/kW]	16,83 – 18,93	8,31-1,17
14	Net weight	[T]	17,67 - 424	9,98 - 440
15	Use factor of CHP unit	[%]	65,5 – 70	68,5 – 90
	Economic effectiveness criterion			
16	Cost per unit (or capital investment)	[eur/kW]	650 - 1400	1500-200
17	Pay-back period (operation period 8000 hr)	at an annual rate	2-7	4-10(25)*
18	Profitability index, PI	-	generally more than 1	generally more than 1

5 CONCLUSION

The aim of the research work is the comparative analysis of GECP and GTCP characteristics and the following recommendations for the specific power plan selection. There are 5 groups of cogeneration unites to be pointed out according to the electrical power output:1) micro-CHP – up to 200kW; 2) mini-CHP – up to 700kW; 3) small-CHP – up to 1,5MW; 4) average-CHP – up to 50MW; 5) big-CHP – above 50MW. Concerning the fact that CECP and CTCP are limited by the following power rates 10kW - 22,4MW and 1,2MW-265MW respectively, the CHP plans of average and big class will be compared. Main criterions assessment such as technological, constructive and economical parameters is shown in table 1.

According to the data from table, the following can be concluded:
1. The GECP is distinct in high efficiency, which remains stable at temperature from -30ºC to +30ºC. Moreover, generally it consumes less fuel; has an unlimited number of starts and less cost per unit, what ensure reduction of a payoff period and financial risks.
2. Conversely, GTCP is more ecologically friendly and don't need an additional cleaning equipment to be applied. Besides, it consumes

much less lubrication and has 10 times less coefficient of metal consumption. Moreover GTCP generates more heat energy, what makes it possible to use combined cycle plant, and thus make up losses in energy generation efficiency with driving efficiency to more than 60%.

Having made a decision to purchase a cogeneration unit, an investor must know the answers for the following questions:
1. To define the operating conditions of a cogeneration unit.
- Climate service environment of the plant. The temperature of outside air for GTCP must be from -30 ºC to +10 ºC, and for GECP is between -30ºC and +30ºC;
- In terms of the geographical position, the altitude of GECP location must not exceed 300 and for GTCP - 2000 meters above the see level respectively;
- GT is advisable to utilize in main, continuous and load control operating mode, because of the limited starts number of a turbine machine;
- Definition of planed operation hours in a year at the nominal power rate;
2. Chose single-, dual- or tri-fuel technology and define a fuel cost for cogeneration unites;

3. The availability of service centers from cogeneration unites producers;

4. When choosing a concrete model among plants with the same power rate, it is necessary to compare: electrical and full efficiency, fuel utilization coefficient, the specified life or overhaul life, the capital repair costs, dependence of plan efficiency on load changing and environment, the plant configuration, as some differences may exist in plants configuration with the same price. It is necessary to look through different plans utilization review.

REFERENCES

[1] Barclay, Frederick J. - Combined Power and Process - An Exergy Approach (Revised Edition). John Wiley & Sons, 1998, 41p. ISBN 978-1-86058-129-8.

[2] Davison J., Freund P., Smith A. - Handbook of Electric Power Calculations (3rd Edition). McGraw-Hill, 2001, 28p. ISBN 978-0-07-136298-6

METHODS OF EXPERIMENTAL DEFINITION

OF HEAT LOSSES IN HEAT PIPES

Orlova L.V.

Scientific advisor:: Polovnikov V.Yu., Ph.D.Academic advisor: Nekrasova-Becker, T.M.

Tomsk polytechnic university, 634050, Russia, Tomsk, 30 Lenin Ave.

E-mail: orllove@rambler.ru

Introduction

The Russian Federation is characterized by the highest level of centralized heat supply (up to 80 %). more than 250 thousand kilometers of thermal networks (in two-unit calculation) with pipes from 57 to 1400 mm in diameter are laid on its territory [1]. The lengthof the main pipelines with the diameter of conditional pass 600 - 1400 mm makes 26 thousand km [1].

The most widespread type of heat pipe slining is underground which makes about 90 % of the total length ; and the main way of a lining is putting pipes in ferro-concrete channels. The Primary type of the insulation materials used for channel linings are the products of the mineral cotton wool [1].

The Reliability and accuracy of the definition of transport losses in centralized heat supply networks are extremely important. The urgency to investigate the thermal conditions of systems of transportation of heat, is caused by following factors [2]:

• The increase of requirements to the efficiency of heating;

• The increasing competition from the alternative, decentralized ways of heat supply;

• The necessity of the instrument account of heat consumption and the heat-carrier by the consumers;

• The Necessity to diagnose technical condition of heat pipes and to conduct the work to increase the reliability of a heating system .

It is possible to define the following principal causes leading to the increase of heat loss:

The use of heat pipes with the humidified thermal isolation;

The operation of heat pipes in the context of moral and physical ageing of thermal isolation.

There are several methods of experimental calculation of transport heat losses in a heating network [2]. They include:

The identification of technical heat-carrier parameters in the beginning and the end of a heat pipe unit;

Direct or indirect measurement of a linear heat flux density from an external surface of a heat pipe.

The purpose of the present work is to analyze the methods of experimental definition of heat losses at heat-carrier transportation, as well as determining their advantages and disadvantages.

DEFINITION MASS HEAT-CARRIER PARAMETERS IN THE BEGINNING AND IN THE END OF A HEAT CONDUCTOR SITE

Heat losses into the environment in the course of heat-carrier movement in a pipe in the absence of phase changes make:

$$\Delta q = \rho C_{\mathrm{p}} G \Delta T ,$$

Where Δq - heat losses at heat-carrier cooling, W; ρ - heat-carrier density, kg/m^3; C_{p} - heat capacity of the heat-carrier at constant pressure, J / (kgK); G - the volume expense of the heat-carrier, m3/with; ΔT – the temperature decrease of the heat-carrier in a heat pipe , K .

To define the temperature change of the heat-carrier with comprehensible accuracy it is necessary to conduct measurements on a piece

of a heat pipe which is enough long [2]. Expected heat losses Δq are approximately equal to product $q_L \cdot L$ where q_L - a linear heat flux density in environment, (Vt/m), L-length of a site of a heat conductor, m. So, the necessary length L can be defined as [2]:

$$L = \frac{q}{q_L} = 1.2 \cdot 10^3 \frac{G\Delta T}{q_L} \quad , (1)$$

Where expense G is measured in m3/h.

At an absolute measuring error ΔT, usually equal to 0.1 ^{0}C, and a demanded relative error Δq, equal to 0.1, the temperature decrease ΔT should make 1 ^{0}C. Then in (1) at G=100 m3/ch and q_L=100 (Vt/m) (a standard heat flux density for a two-unit heat pipe with diameter of pipes d=150 mm) the necessary length heating main will make 1.2 km.

Thus, to define the transport heat losses at cooling of the heat-carrier the measurements of big pieces of a heat pipe should be taken without taps or with disconnected taps. The Reduction of the demanded length of a heat conductor can be reached only at decrease in the expense of the heat-carrier.

The important positive feature of this measurement method of the heat-carrier temperature drop is the possibility of direct experimental definition of heat losses by the whole construction of a heat pipe .

MEASUREMENT OF A LINEAR HEAT FLUX DENSITY FROM A HEAT PIPE

heat losses from the pipe are equal to a total thermal stream through the mesh covering the sources of heat. For a stationary temperature field the linear heat flux density does not depend on a contour choice.

The Possibility of definition of heat losses from underground pipes by conducting the surface measurements is explained in fig. 1 where the ground cut of perpendicularly axis of an underground heat pipe and the schedule of surface temperature change are shown schematically [2]. For a stationary temperature field the linear heat flux density (heat losses) from the underground source of heat (q_L, Vt/m) for a homogeneous surface of a ground is equal [2]:

$$q_L = \int_{-\infty}^{+\infty} q(x)dx = \int_{-\infty}^{+\infty} \alpha(T(x) - T_{â})dx =$$

$$= \int_{-\infty}^{\infty} \alpha(T(x) - T(\infty))dx = \alpha M \quad , (2)$$

Where x - co-ordinate, m (fig. 1); $T(x)$ - surface temperature in point x,K; $T(\infty)$ - surface temperature at a great distance from the source of heat, K; T_{B} - free air temperature, K; $q(x)$ - a heat flux density from the ground surface (Vt/m). Difference $T(x) - T(\infty)$ is referred to as temperature contrast in point x; M - integral of temperature contrasts; α - effective coefficient of heat exchange between the ground surface and

the air which is equal to the sum of the coefficient of a convective heat dissipation and the coefficients of linear approximation of a heat dissipation radiation and evaporation.
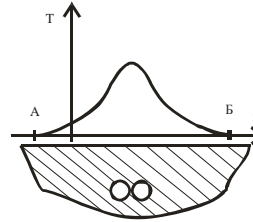
Fig. 1 - the Scheme of a ground cut perpendicular to the axis of an underground heat pipe and the schedule of the surface temperature change

For a non-stationary temperature field the superfluous heat flux density $q_L(\tau)$ at the moment of time τ is defined using the formula [2],

$$q_L(\tau) = \int_{-\infty}^{+\infty} \left[q(x,\tau) - q(\infty,\tau) \right] dx =$$

$$= \int_{-\infty}^{+\infty} \alpha(\tau) \left[T(x,\tau) - T(\infty,\tau) \right] dx = \alpha(\tau) M(\tau) \quad . (3)$$

The superfluous linear heat flux density from the surface (3), as well as for any mesh (isotherm) covering the linear source of heat, changes in due course and varies for different contours and does not equal to heat losses from the source of heat during any moment of time τ.

The basic restrictions and limitations of this method are listed below:

Strong dependence of registered temperature contrasts and a heat flux density on the ground surface on meteorological factors and heat exchange conditions on a surface;

Large error caused by the discrepancy in thermal and physical characteristics of the parameters.

The important advantages of the described method are:

Its application in a real mode of operation of thermal networks without switching-off of the consumers;

The possibility to Use at various times during the cold season and take repeated measurements;

The Possibility toinspect the wholethermal network to define heat losses in any part of the heating system network ;

The high efficiency caused by the small cost of inspection and the fact that no preparatory work is needed in a heating system.

CONCLUSIONS

The discussed lacks, as well as the increasing urgency and the practical importance of authentic and reliable definition of actual heat losses, define the need to improve the existing

technologies of definition of heat losses in heat pipes and construct the new ones.

THE LITERATURE

1. Buhin V. E. Preliminary isolated pipelines for centralized heat supply systems//Power system. - 2002. - № 4. - P. 24 - 29.

2. Shishkin A.V.definition of heat losses in centralized heat supply networks//Power system. - 2003. - № 9. - P. 68 - 74.

PRODUCT DISTRIBUTION FROM WOODY BIOMASS BY FIXED-BED PYROLYSIS PROCESS

M. Polsongkram, G.V. Kuznetsov

Faculty of Heat and Power Engineering, Tomsk Polytechnic University

Polsongkrammm@gmail.com

Abstract: Conversion of woody biomass to usable energy forms has gained much interest recently due to increase in energy cost as well as greater pressure on the environment by the use of fossil fuel. This paper presents quantitative understanding of the thermal decomposition behavior of woody biomass for which laboratory scale batch reactor is employed. Effect of temperature on the yields, composition and rate of formation of products for four different woody biomass materials has been studied. Char, liquid and total gas in relation to temperature for different samples is presented and compared. The percentage volatile matter in the char decreased with an increase in temperature, while there was an increase in the percentage fixed carbon. On the whole, the four investigated woods resemble in their pyrolysis behavior and their yield of pyrolysate, pyrolysis liquids and gas.

Keywords: *Pyrolysis, woody biomass, thermal decomposition.*

1. Introduction

Since the oil crisis in the early 1970s, awareness to fast depleting fossil fuel resources and need to reduce green house gas and other emission, has triggered search for alternative renewable energy source. Wood is a type of biomass that considered one of the most important renewable energy sources. It derives from forestry product or agricultural fast growing tree that abundantly available in the world and can be substituted for fossil fuel source. It can be used for energy production in several ways from old direct burning to modern gasification and pyrolysis. In developing counties, especially the use of woody biomass is of high interest, since these countries have economies largely base on agriculture and forestry [1].

Pyrolysis is the thermal decomposition of complex organic matter to simple molecules. It is the first stage in any thermal treatment of biomass in which the absence of Oxygen with a temperature ranging between 200 to 700 ^{o}C [2]. Main products of pyrolysis are char, liquid and gas. The char can be used as feed stock for gasifier, combustion applications and used as active carbon. The liquid obtained not only can be used as fuel for direct combustion by upgrading or added to petroleum products but also can be used for agricultural activities such as improves soil quality, eliminates pests and controls plant growth[3]. The gas obtained can be directly used for combustion. The amount and nature of end products of pyrolysis will depend on the operating temperature, the heating rate, particle size and the composition of the biomass feed stock.

In this study, four types of woody biomass; Jatropha Curcas Linn, Acacia auriculaeformis, Eucalyptus camaldulensis and Pine wood were chosen as the renewable energy source and they have been pyrolyzed under different conditions in a fixed - bed reactor. The aim of this study is to investigate the influence of the pyrolysis temperature in order to provide preliminary data for further investigation.

2. Raw material

The following are the experimental procedures implemented for this study: The three woody biomass samples were collected from Nongkhai province, Thailand and another is Pine wood that was collected from local sawmill in Tomsk region, Russia. The woody biomass samples were cut into small pieces and sun-dried to reduce the moisture content. Their size was 1-5 mm and less than 0.5 mm in thickness. Prior to the experiments, the samples were oven dried for 3 hours at 110 °C. The proximate analysis of the woody biomass samples are presented in Table 1.

Sample	Jatropha Curcas Linn.	Acacia auriculaeformis	Eucalyptus camaldulensis	Pine wood
MC	11.48	9.89	13.00	13.76
VM	84.39	81.43	78.53	79.41
FC	12.37	17.36	19.10	19.11
Ash	3.23	1.20	2.37	1.47

3. Experimental setup

The experimental setup fabricated for fixed-bed pyrolysis unit is shown in Fig.1. The setup consists of a reactor, condenser and liquid collector, helium source. The size of reactor was 40 mm in diameter and 145 mm in length constructed of stainless steel with the temperature controller. It was heated externally by electric heater. The helium gas was supplied to maintain the inert atmosphere in the reactor also to drive the pyrolyzed vapour product to the condenser and liquid collector. The maximum loading capacity of reactor vessel was 20 g of sample woody biomass. The condenser was fabricated in form of helical coiled tube, water at 10°C is used as coolant. The experiments were performed at different reactor temperatures ranging from 250-600 °C at a constant heating rate of 50 °C/min. The retention time was fixed for 3 hours in order to allow the sample to go to through a complete pyrolysis process. Run were taken for different temperature and raw materials selected. The liquid product was collected at the liquid collector point. The yields of the different products obtained were determined by weighing the solid residue (char) and liquid collected and gas evolution by difference. Yields are expressed as a percent by weight of the raw materials as a function of the end-operating temperature.
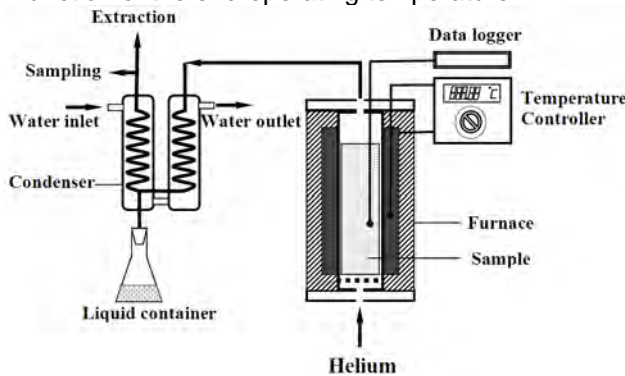
Fig.1 Experimental Setup

4. Results and Discussions

Figure 2 shows the products of distribution of char, liquid and gas in relation to temperature for different samples. At the lowest pyrolysis temperature of 250 °C, decomposition was significant as char was the major product. The char yield decreased rapidly with an increase in pyrolysis temperature for all species. The higher yield of carbonized material at 250 °C may be resulting limited thermal decomposition of extractives and hemi-cellulose in wood at temperatures between 190-270 °C. Cellulose is thermally degraded at temperatures between 270-400 °C and lignin start at 200 °C and continues till 700 °C [2]. The lignin is main sources of char yield in biomass fed under conventional pyrolysis conditions while the cellulose and hemi-cellulose are main sources of volatiles matter. In the present study, the char yield was reduced as the pyrolysis temperature was increased from 61.5-80 wt% at 250 °C to 24-28 wt% at 600 °C.
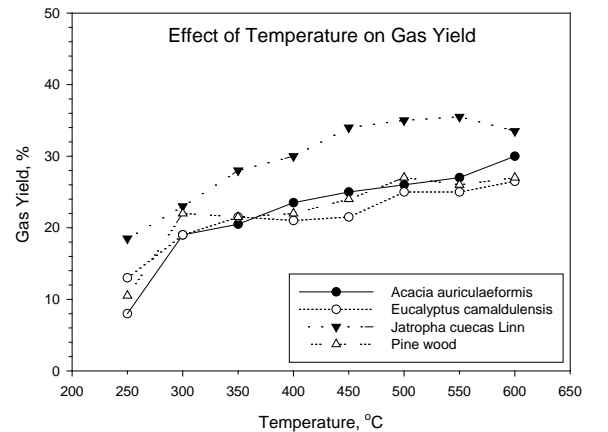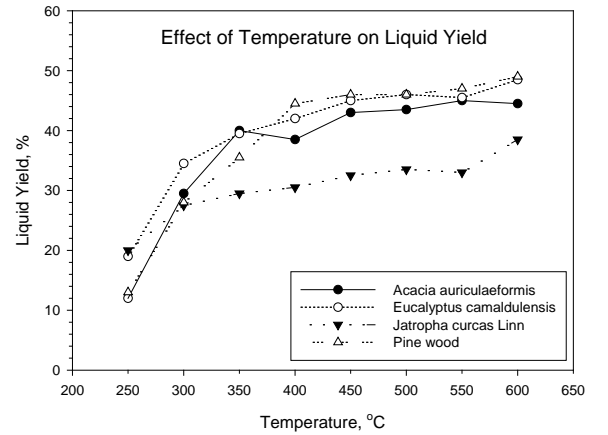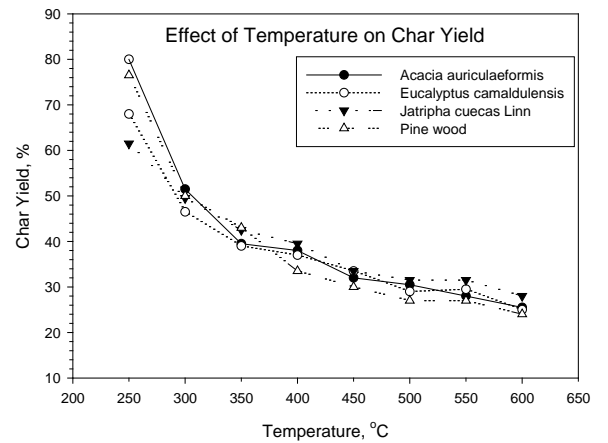
Fig.2 Effect of Temperature on product yield for different biomass

This decrease in the char yield with increasing temperature could be either due to greater primary decomposition of the wood at the higher temperatures or to secondary decomposition of char residue. As the temperature was increased the amount of condensed liquid yield increased until it reached nearly stable at 400-450 ^{o}C to a maximum value in the range of 30.5-46 wt% of total biomass fed. Below about 400 ^{o}C, decrease in liquid yields was observed resulting incomplete pyrolysis. Gas yield was obtained at the range 8-18.5wt% of biomass fed at the lowest pyrolysis temperature of 250 ^{o}C and it was increased till it reached a maximum value in the range of 26.5-33.5 wt% of biomass fed at the highest pyrolysis temperature of 600 ^{o}C for all species. The variation of these three properties with the end-pyrolysis temperature can be deduced from Fig. 3. Char formation processes simultaneously with an intensive development of the volatile products. The percentage volatile matter in char decreased with an increase in temperature, while there was an in crease in the percentage fixed carbon.
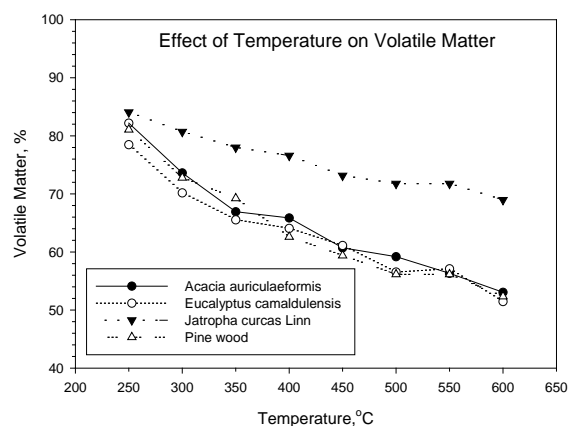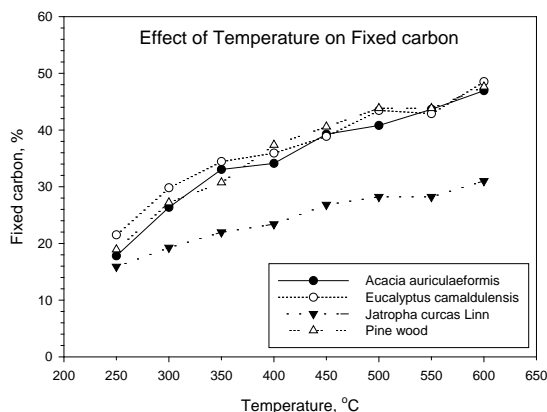
Fig.3 Effect of Temperature on composition of char from different biomass

5. Conclusion

It shows that for the above time-temperature history, decomposition of the wood is first observed at about 180 ^{o}C and becomes rapid from 250 ^{o}C onwards. Weight loss increases with temperature. Most of the devolatilisation takes place between 250 and 450 ^{o}C. Beyond 450 ^{o}C, the rate of decomposition becomes gradually stable.

References

1. P.McKendry,Bioresour.Technol. 83 (2002) 37.
2. S.Saravana Sampath, B.V.Babu, [online] available: http://discovery.bits-pilani.ac.in/~bvbabu/PyrSB_CC_2005.pdf
3.FFTC Practical Technology, Rural life PT2005-25[online] available: http://www.agnet.org/library/pt/2005025/

CALCULATION METHODS
OF HEAT LOSS IN THERMAL PIPES

Rodina L. Y.

Scientific advisor : Polovnikov V. Y. ., PhD

Academic advisor: Nekrasova-Becker T.M.

Tomsk Polytechnic University , 634050, Russia, Tomsk, 30 Lenin Ave.

E-mail: rodina_lubov@sibmail.com

INTRODUCTION

Determination of heat losses in heat pipes is an integral part of work in analyzing the effectiveness and improving the systems of heat transportation.

Improvement in current use and development of new technologies to determine the heat loss in heating pipes is an urgent task in the development of theoretical bases for creating energy-efficient heat transportation systems.

The basic calculation method to determine heat loss in heating pipes [1] is the determination of thermophysical characteristics, the temperature fields and thermal designs of heat resistance.

The aim of this work is the analysis of the present calculation methods to determine heat

losses when transporting the heat carrier, as well as identifying its strengths and weaknesses.

METHODS FOR CALCULATING HEAT LOSS

Heat loss can be calculated based on the thermophysical parameters of heat transfer (thermal resistance), but not measured at different operating conditions of a heating pipeline. Thus, a kind of alternative way of determining heat losses is realized.

Calculation of the temperature field of linear plots of heat and various reinforcing elements can be made for models of any complexity with the existing powerful software package. Thermophysical characteristics required for these calculations can be defined by empirical and theoretical laws or measured at different times in the laboratory or field conditions.

The method of estimation of heat losses using the values of thermal resistance is known for a long time [2]. Heat loss from the uninsulated pipe can be calculated using the formula::

$$q = \left(T_{av} - T_{air} \right) / R_g \ ,$$

where *Tav* - average annual temperature of heat carrier in the return pipe, K; *Tair* - the annual average ambient air temperature, K; *Rgr* - thermal resistance of the soil, K / W, determined from the expression:

$$R_{gr} = \left[\ln(4h / d_{eq}) \right] / 2\pi\lambda_{gr} \ ,$$

deq here – external diameter of the equivalent diameter of the heating system pipe, defined by the equation:

$$d_{eq} = \sum d_j L_j / \sum L_j \ ,$$

Lj and *dj* - the length and diameter of the sections of underground pipelines, m; *λgr* - thermal conductivity of soil, W / (m · K); *h* - depth of the axis of heating pipe , m .

Also, heat loss can be determined on the basis of the results (temperature fields) of mathematical modeling.

At present, the work with mathematical models is based on the use of numerical methods for solving differential equations with the help of computers [3].

For the approximate (numerical) solutions of boundary problems of thermal conductivity the finite difference method is widely used, allowing to solve complex equations of mathematical physics [3].

Typically, the number of unknown values in the obtained by approximation system of algebraic equations is large, but its solution is easier in terms of mathematical difficulty than the analytic solution of the initial value problem.

The main disadvantage of this method is to use a large number of thermal and geometric parameters, whose determination errors result in some calculation errors overall . This complication of the model, on the one hand, brings it to the real situation, but, on the other hand, may lead to an increase in error.

In practice, the analytical part of the method is most widely used. However, to use it successfully it should be supplemented with the experimental base with thermophysical characteristics.

The examples of application of this method in difficult conditions include the results of calculating the temperature field of underground two-unit heat pipes in the frozen soil, underground gas and oil pipelines in frozen ground [4], as well as evaluating the heat loss in the quarter closed networks of hot water heating systems for four-tubes laying [5].

The study of heat transfer processes in the construction of transportation systems are based on heat conduction equation for the various designs of heat.

In paper [6] the problem of unsteady temperature field of heating pipeline, working in one of the typical part-time modes - flooding the channel - is solved. This took into account the changing values of the effective thermophysical properties of thermal insulation when saturated with moisture, changes in heat loss in time and the presence of heat transfer from the peripheral coordinate. As a result of problem solving, it was determined that the heat loss of heating pipe in flooding condition is significantly higher than the norm values, and the main factor influencing the growth of heat loss is the increase of the effective thermal conductivity of the moisture saturated isolation.

The main disadvantage of this technique is the introduction of not quite correct physical model of heat transfer processes in the designs of heating pipe and the ambiguity of the solutions obtained in the absence of reliable information about the actual state of heating pipes.

ADVANTAGES AND DISADVANTAGES OF EXISTING METHODS FOR DETERMINING HEAT LOSS

All considered methods used in practice, characterized by the method of calculating heat loss, require research in stationary conditions. This situation is dictated by two main reasons.

First, this should be performed in order to to eliminate the need for a functional description of the initial and boundary conditions for the energy equation, heat internal properties of soil, isolation, and heating pipe, leading to a sharp increase in calculation errors.

Secondly, it makes sense to characterize the heat-shielding properties of the design of heating pipes and heat losses themselves only for stationary conditions. When determining the heat losses in underground pipes using the parameters of coolant or heat flow directly on the surface of the insulating layer the main

advantage is a significant weakening effect of external weather conditions on the results of the calculations. The relatively short-period (up to daily) fluctuations in temperature and heat transfer conditions on the ground surface (the speed of the environment (wind), solar heating, precipitation, evaporation or condensation, etc.) sharply decrease in amplitude with the increase in depth due to large thermal inertia of the soil.

CONCLUSION

All Reported limitations, as well as the increasing relevance and practical importance of accurate and reliable determination of the actual heat losses cause the need to improve existing technologies to determine the heat loss of heating pipes, and to develop the new ones.

With a reasonable accuracy of the results, the methods to analyze the extent of heat loss on the basis of mathematical modeling, does not require expensive hardware, performing any field work and other activities described above. When developing mathematical models of heat transfer in the designs of heat the impact of various factors influencing the intensification of heat losses during transport of the coolant can be recorded and analyzed, such as changing the

environment conditions , the presence of phase transitions, and others .

LITERATURE
1. Shishkin A. V. Determination of heat losses in the networks of district heating / Thermal. - 2003. - № 9. – p. 68 - 74.
2. Shubin Y. P., Satunovsky S. A. Piping insulation. M. - L.: Stroiizdat, 1941. - 100 pp.
3. Samarskiy A. A., Gulin, A. N. Numerical methods of mathematical physics. Moscow: Scientific World, 2000. - 316 pp.
4. Bakhmat G. V. Transport and storage of oil and gas in the examples and problems. - SPb.: Nedra, 1999. - 543 pp.
5. Zinger N. M., Burd A. L. Assessment of heat losses in hot water supply systems estates / Thermal. - 1977. - № 12. - 53 - 59.
6. Kuznetsov G. V., Polovnikov V. Y. Heat loss of trunk pipelines in full or partial flooding / / Proceedings of the universities. Problems of energy. - 2006. - № 3-4. - S. 3-12

PROSPECT OF BUILDING GEOTHERMAL THERMAL POWER PLANT (GPP) IN TOMSK REGION

Sinyakov I.V., Sinetskiy E.A.
Scientific advisor: Loginov V.S., ph.d., professor
Language advisor: Nekrasova-Becker T.M.
Tomsk Polytechnic University, 634050, Russia, Tomsk, 30 Lenin Ave.
E-mail: sinetskiyevgeniy@mail.ru

The use of alternative clean energy sources can significantly improve the economic and environmental characteristics of thermal energy. Along with the search and development of traditional sources (gas, oil), a promising direction in Tomsk region is to use the energy stored in the geothermal springs.

A characteristic feature of Siberian regions is very low population density in the vast areas, which are poorly developed in the industrial terms. Energy provision for the settlements, industrial and other facilities in such circumstances can only be done through the establishment of decentralized areas. The most common sources of energy in these areas today are diesel power station (DES), which mostly have outdated and worn-out equipment with low efficiency. Equipment on most of them is operated in violation of the rules of technical operation, which causes an increase in unit cost of fuel for heat energy. As a result the harmful

emission of 1 t.s.f. are higher than that of TPP in 1,5-3 times, which greatly affects the ecological situation in the region.

The main production assets of the fuel and energy complex (TEK) of Tomsk region are approaching the critical level in terms of their technical condition and exploitation age. About 20% of installed capacity has served its regulatory lifetime, which causes the increased accidents hazard, reduced fuel and energy efficiency. As a result the energy losses during its delivery to the consumers make up 20-25% of the released energy [1].

The use of alternative clean energy sources can significantly improve the environmental and economic characteristics of the production of thermal energy. Significant reserves in energy saving in the region are associated with the use of energy potential of geothermal water-based geothermal power plants.

The authors in the present work have attempted to comprehensively address the outlined problems by examining the renewable energy sources of Tomsk region and the prospects of building geothermal power plants on their basis. The method can be applied to any territorial district of Tomsk region, which has previously drilled oil exploration wells, and in this sense, the work may be of interest to a wide range of professionals working in the field of renewable energy.

In any settlement of Tomsk region there are underground thermal waters which possess various capacities. For example, in Tomsk and its enclose areas - Akademgorodok, Petrochemical Plant, Kuzovlevo there are thermal waters at the depth of 1,5-3 km, as well as in areas Asino, Teguldet, Zyryanovsk, Pervomajskoe, Bely Yar, Bakchar, Podgornoe. And for those hard to reach settlements, as Bely Yar, Katayga, Stepanovka, Nazino, Inkino, Bakchar and, to some extent, Narym, Parabel, Kargasok, Kolpashevo, Togur, Kanga and Pudino the use of thermal waters is vital, and, perhaps, is the only way to solve the energy and economic crises. In many of these communities previously drilled oil exploration wells have survived in good technical condition, whose recovery at 1-3 horizons of different depths and types of thermal waters does not present any technical difficulty is no. Moreover, in the case of their involvement in economic turnover, taking into account the drilling costs of about 50-60% in the total capital cost for the resettlement of thermal water pipes, this significantly reduces the cost of energy and the amount of initial capital investments [2].

Russia already has the experience in development and construction of GeoPP and geothermal power plants. Five GeoPP are successfully operated in Kamchatka and the Kuril Islands, the most powerful of which (Mutnovskaya, 50 MW) provides up to 30% of all electricity consumed in Kamchatka. Geothermal power plants are operated in Kamchatka, the Kuril Islands, in Dagestan, the Stavropol and Krasnodar Krai. Up to 30 million m^3 of geothermal water at the temperature of 80-110 °C is produced annually for their purposes. The greatest amount of geothermal water is used in Krasnodar region, where there are 12 geothermal fields with 79 wells drilled with the coolant temperature at the mouth of 75-110°C and the thermal capacity of 5 MW [3].

A special and very promising geothermally deviant, natural climatic and infrastructure situation has the central part of the region, including Kolpashevo, r.c. Bely Yar, Podgornoye, Parabel and Kargasok, villages Chazhemto, Inkino, Narym, Big Mane, Nazino, Lukashkin Yar, and possibly Napas near which there is a great number of previously drilled (and now dormant) deep oil exploration wells, that once had produced thermal water with the output temperature of 48-66°C. The wells Parabelsky 3-P, Kolpashevsky 5-P, Beloyarsk 1-P and Chazhemtovskaya 1-B still produce thermal water at the temperature of 47-60°C (since 1958-1986). With intensive specialized pumping selection of thermal waters, even from existing exploratory wells of small diameter the water at the temperature of 70-75°C can be extracted, which is enough to generate electricity in special heat exchangers mikroGeoPP (2-3 MW) with a low boiling (freon (and other) energy. In fact on the basis of existing wells (s.Chazhemto, r.c. Parabel and Bely Yar) mikroGeoPP can be used at present, as it is done in many other countries. Unfortunately, there is no experience of such an integrated use of thermal waters in Tomsk region, and it must be accumulated or, in extreme cases, borrowed in Stavropol and Krasnodar, as it was mentioned above .

Among the identified settlements Chazhemto takes a unique natural and climatic, geographical, hydro-geothermal position. This situation allows it to become a powerful Heat power center on a regional and even federal scale. More than 10 deep oil exploration wells are drilled here, allowing to output large amounts of heat to the surface, which is already enough to generate a significant amount of electricity and heat. Considering the discussed possibilities geothermal power plants can be installed in this region.

Villages Inkino, Nazino, Napas, Lukashkin Yar are the - areas densely populated by the selkup and other northern ethnic groups and therefore increasing the comfort of their residence is under special scrutiny of the government. In this regard, the establishment of autonomous thermal power centers on the basis of existing deep wells in these villages would significantly improve the housing and communal and social comfort there. Given the fact that there are seven deep oil exploration wells near village Nazino, it is already possible to create a set of Heat power (with GPP) of average power on their basis. Near village Inkino there are five oil exploration wells drilled, which suggests that the construction of geothermal power plant is also possible here. For villages Nappas and Lukashkin Yar which have one deep well each it would be more appropriate to create an autonomous center with the use of geothermal mikroGeoPP.

Thus, there are all necessary geological, climatic, socio-economic, scientific and methodological, technological, experimental, practical and even thermal water intake conditions of a quick and very effective

involvement of deep geothermal resources in the economy of Tomsk region. Unfortunately, local authorities and business structures are not psychologically ready yet to seriously consider geothermal resources as a real alternative source of heat.

References:

1. Sinetskiy E.A., Sorokin S.I. Prospects of application a heat pump installations for the needs of centralized (Thermal Power Plant) and decentralized heating (cottage construction) in Tomsk Region / All-Russia competition of scientific bachelor works in "Thermal Power Engineering" / Collection of works of the winners. - Tomsk: Tomsk Polytechnic University press, 2009. - p. 114 - 128.

2. Danchenko, A.M., Zadde G.O., Zemtsov A.A. and etc. An inventory of opportunities / B.V. Lukutin (ed.). - Tomsk: NTL press, 2002 .- 280p.

3. Butuzov V.A., Tomarov, G.V. Geothermal heating system using solar energy and heat pumps / Thermal Engineering, 2008, № 9. p.39-43

THE IMPROVEMENT OF HEAT DISTRIBUTION SCHEMES OF THERMAL POWER PLANTS USING THE HEAT PUMPS OF THE CONSUMER

Sorokin S.I.

Supervisor: Gubin V.E. Language adviser: Novokshonova K.I.

Tomsk Polytechnic University, 634050, Russia, Tomsk, Lenina 30

Mail: Sorokin.si@mail.ru

The effectiveness of the turbine is influenced by many factors. First of all, let's consider the effect of the temperature feedback on the performance of the network water turbine.

In the operating regime of the heat-extraction turbines according to the schedule developing by the thermal power is largely dependent on the temperature of the inverse power of water. The high temperature of the feedback network water coming to the power plant leads to the pressure increase in the regulated heat-extraction selection. It results that the pressure regulator gives the command to open the control valve which is situated before the high pressure cylinder. And it in its turn leads to unloading of the turbine. The temperature of the feedback network water is an uncontrollable parameter and is determined by the operating regime of the whole heating system.

The experience of the investigation of such great objects of Tomsk region, as AO Tomskenergo, Belovskaya city power plant, as well as the Krasnoyarsk city power plant-2 and Novocheboksarskiy heat-and-power plant show that the increased temperature of the feedback network water in comparison with a temperature chart. Analyzing the implementation of automatic control system heat consumption at central heat points, and sum up the situation with the increased temperature of network feedback water could be worse.

This work will be devoted to the development of heat schemes improving ways of thermal power plants.

The increase of the temperature of the feedback network (t_{fw}) water leads to the increase of the saturation temperature in the heater and as the result, to the shift of the pressure of heat-extraction selections and non-regime work of the part of the turbine which is situated between the heat- extraction selections and affects the efficiency of the entire turbine. According to the authors opinion the most perspective variants of improvement of schemes of the heat distribution of TPP with the using heat pump units of the consumer are presented (Fig. 3.1, 3.2, 3.3). Then the most promising variants of improving schemes of the heat deliver, according to the author of this work, options for improving patterns of heat from thermal power plant with heat pump units (HPU), the consumer [1].

Using HPU on the line feedback networks directly from the consumer may give the possibility to receive more heat energy in the quantities listed on fig.3.4. This will be followed by the decrease of temperature feedback network water.
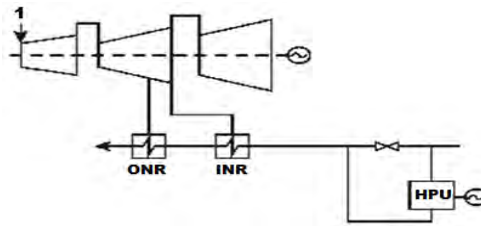
Fig.3.1. HPU and low-temperature heat

As for the next model, with the use of HPU it would be sufficient to illustrate the scheme of improving systems of heat, which enables the generation of electric energy in the implementation of additional heating network water (Figure 3.2). This scheme was proposed as the alternative. It is considered as the alternative of the proposed variants with the bottom turbines.
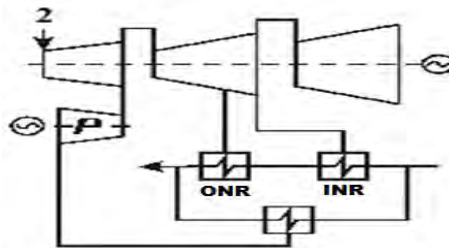
Fig.3.2. Connecting to industrial selection pressure turbine
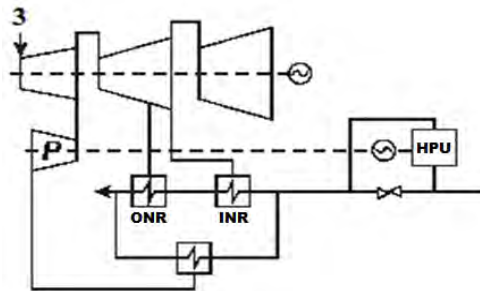
Fig.3.3. HPU and pressure turbine at an industrial selection

The scheme which is shown in fig.3.3. combines the advantages of 1 and 2 options. For the schemes 3.1, 3.2, 3.3 the evaluation of the efficiency was performed (for example, turbine PT-135/165-130/15).

The results are shown in Table 3.1.

Table 3.1. The evaluation of the effectiveness of the schemes

№	The Expected effect
1	The additional heat energy generation up to 40 MW at HPU and the temperature reduction of the feedback network water increase the electrical power for 5-20 MW at b_{sp} = 200 g/kW·h depending on the feedback network water temperature .
2	The additional heat energy generation to 130 MW, the steam before the bleeding generates an electrical power up to 35 MW in the high pressure part with b_{sp} = 200 g/kW·h and in the pressure turbine up to 24 MW with bud= 150 g/kW·h
3	The additional heat energy generation in the industrial bleeding up to 130 MW and in HPU up to 40 MW, steam before bleeding produces an electrical power up to 35 MW with b_{sp} = 200 g/kW·h and in the pressure turbine up to 24 MW with b_{sp} = 150 g/kWh and also the reduction of the feedback network water temperature , which will increase the electrical power for 5-20 MW

Fig.3.4. Number of additional quantities of heat from HPU when used as a source feedback line network (subject to over-t OS)
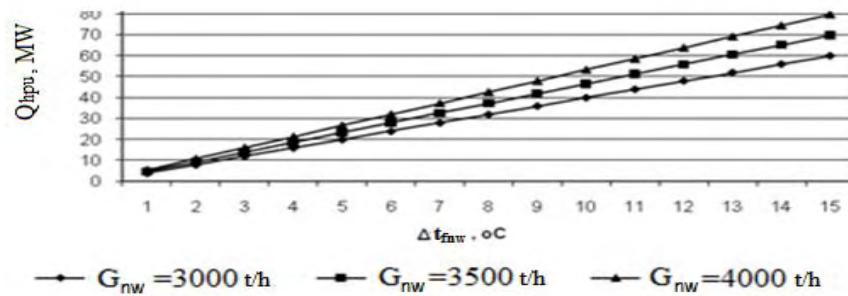
The given list of schemes is not completed and should be formed for a specific system "the thermal power station - the heat transport system - the set of heat consumers.

The process of energy efficient technologies implementation is extremely capital intensive, so in many cases, energy saving of the energy consumers in Russia should be considered along with the problem of updating facilities for energy producers. In other words, the problem of the current and future energy supply must be solved taking into consideration the agreement of the interests of producers and consumers of energy. It is necessary to organize properly the direction and volume of investment flows, if the development of the economic system the manufacturer – the consumer of energy is stable.

References:

1. Sinetsky E.A., Sorokin S.I. Prospects for the use of heat pump installations for the needs of centralized (CHP) and decentralized heating (cottage construction) in Tomsk Region / All-Russia competition of scientific works bachelors in "Thermal" Collection of works of the winners. - Tomsk: Publishing Tomsk Polytechnic University, 2009. - S. 114 - 128.

2. Shpil'rain E.E. Ability to use a heat pump at TPP / Thermal, 2003, №7. с.54-56.

ENERGY EFFICIENCY CONCEPT

Вахнер М.В.

Научный руководитель: Шеремет М.А., преподаватель; Новокшонова К.И., преподаватель

Томский политехнический университет, 634050, Россия, г. Томск, пр. Ленина, 30

E-mail: vahkner@sibmail.com

Abstract

This article focuses on the "Energy Efficiency Concept". The article depicts the value of renewable energy sources and ways of the efficiency increase. The aim of this work is the identification of the policies of the support and development of the implementation of technologies and management approaches which we can for society.

1. Introduction

Policymakers, commercial enterprises, scientists have focused their attention over the past few years on the issue of energy. Energy efficiency increased when an energy conversion device, such as a household appliance, automobile engine, or steam turbine, undergoes a technical change that enables it to provide the same service (lighting, heating, motor drive) while using less energy. The energy-saving result of the efficiency improvement is often called "energy conservation."

2. Energy Efficiency

The energy efficiency of buildings can be improved through the use of certain materials such as attic insulation, components such as insulated windows, and design aspects such as solar orientation and shade tree landscaping. Further, the energy efficiency of communities and cities can be improved through architectural design, transportation system design, and land use planning. Thus, energy efficiency involves all aspects of energy production, distribution, and end-use [1].

Energy efficiency is often viewed as a resource option like coal, oil, or natural gas. In contrast to supply options, however, the downward pressure on energy prices created by energy efficiency comes from demand reductions instead of increased supply. As a result, energy efficiency can reduce resource use and

environmental impacts [2]. Most of the recent effort has been directed toward new and better sources of energy, such as nuclear energy, renewable energy sources. But all the proposed sources have potential constraints and uncertainties. Nuclear energy carries with it worries about safe operation, long-term waste storage, and possible nuclear proliferation. Renewable energy sources have own constraints and uncertainties. Today's cost of energy generation from renewable sources is too expensive for widespread deployment.

3. Wind Power Technology

A good starting point in addressing energy efficiency is to examine wind future. The U.S. Department of Energy reports that wind is experiencing the strongest growth among the renewable energy sources with the falling generation cost. The wind power cost has dropped to 5 cents per kWh, and the DOE projections suggest that further reduction to about 2 cents is possible by 2010 with favorable financing. The American Wind Energy Association forecasts that the five top-growth markets for wind energy through 2005 will be the U.S.A., India, China, Germany, and Spain, with capacity additions of between 1,275 and 2,730 MW projected in each country. The renewable power sources are clean, abundant, and do not need to be imported. However, they must be economical on their own merit. The new developments are meeting this challenge on the both fronts, the initial capital cost and the cost per unit of electricity generated.

TABLE 1. Wind Power Technology, Past, Present and Future

Technology Status	1980	1997	After 2000
Cost per kWh	$0.35–$0.40	$0.05–$0.07	<$0.04
Capital cost per kW	$2,000–3,000	$500–800	<$500
Operating life	5–7 years	20 years	30 years
Capacity factor (average)	15 percent	25–30 percent	>30 percent
Availability	50–65 percent	95 percent	>95 percent
Size range	50–150 kW	300–1000 kW	500–2,000 kW

Since the early 1980s, wind technology capital costs have declined by 80 percent, operation and maintenance costs have dropped by 80 percent and availability factor of grid-connected plants has risen to 95 percent (Table1). For the wind plans at present, the capital cost has dropped below $800 per kW and the electricity cost to about 6 cents per kWh. The goal of current research programs is to bring the wind power cost below 4 cents per kWh by the year 2000. This is highly competitive with the cost of conventional power plant technologies. According

to the National Renewable Energy Laboratory, several research partners are negotiating with U.S. electrical utilities to install additional 4,200 MW of wind capacity at a capital investment of about $2 billion throughout the nation during the next several years. This amounts to the capital cost of $476 per kW, which is comparable with the conventional power plant costs. According to the Electric Power Research Institute, the continuing technology developments and production economy would make the wind the least-cost energy within a decade.

The industry experts make this forecast based on the following ongoing research programs:

• more efficient airfoil and blade design and manufacturing.

• better understanding on the structure and foundation loads under turbulence, operating fatigue loads and their effect on life.

• computer prototyping by accurate system modeling and simulation.

• integrated electrical generators and power electronics to eliminate the mechanical gearbox.

• efficient low cost energy storage at large scale.

• better wind speed characterization, particularly within a large wind farm.

Successful design, development, and demonstration based on the results of these research programs are expected to increase the share of wind power in the U.S.A. from a fraction of 1 percent to more than 10 percent over the next two decades.

The economy of scale is expected to continue in contributing to the declining prices. Future wind plants will undoubtedly be larger than those installed in the past, and the cost per square meter of the blade swept area decline with size [3].

Pursing energy efficiency depends not only on having available technology but also on economic of efficiency versus other options. The table 2 compares the cost of electricity generation from conventional and renewable technologies with the cost of saving electricity by amortizing the increased capital cost of a more efficient new building over its lifetime[4].

TABLE 2. Electricity power costs

Conventional technology	Cents/kW-hour
Nuclear	4-7
Gas (combined cycle)	4-6
Coal (with and without carbon capture)	4-8
Renewable technology	
Wind	3-8
Biomass	4-9
Small hydroelectric	5-10
Solar thermal electric	12-18
Solar photovoltaic	20-80
Efficiency of consumption	
Advanced building	0-6

Note that the listed costs of generation do not include transmission and distribution costs. Also the cost for fossil fuels does not include cost for carbon abatement. Today's costs for many renewable technologies receiving the most attention are much higher than the cost of the efficiency. A recent report reaches a similar conclusion.

Several organization have established ambitious goals for efficiency levels of future buildings. The American Institutes of Architect has goal of achieving, by the year 2012, a minimum 50% from the current level of consumption of fossil fuel used to construct and operate new and renovated buildings. They also would promote further reduction of remaining fossil-fuel consumption by 10% or more in each of the following five years [5]. Other groups called for substantial energy reduction, with some advocating that new construction within the next few decade approach zero net energy – the point at which on-site renewable energy production over the years competences for all primary energy consumed the same period.

The purpose of federal efficiency goals is to lead by example in saving energy, reducing costs, and helping transform markets for new equipment. The Energy Strategy shall:

1.   ensure a secure, reliable and quality energy supply;

2.   promote a long-term balance in energy sector development taking into account the fluctuations in energy consumption;

3.   maximize the use of energy resources available;

4.   promote the use of renewable energy resources;

5.   ensure the efficient use of energy;

6.   protect energy consumers;

7.   protect the environment in the performance of energy activities;

8.   promote investment in the energy sector;

9.   promote competition in the energy sector based on the principles of nondiscrimination and transparency.

References:

1.   Energy Efficiency in the built environment – Leon R. Glicksman – Physics Today, July 2008

2.   Energy Efficiency: Budget, Oil Conservation, and Electricity Conservation Issues -Updated December 1, 2004 - Fred Sissine- Resources, Science, and Industry Division-Congressional Research Service - The Library of Congress.

3.   Mukund R. Patel – Wind and Solar Power system, 1999

4.   Leon R. Glicksman, HVAC&R Res 13,2007

5.   American Institutes of Architect, position statement on sustainable architect practice, available athttp://www.aia.org/SiteObjects/files/HPB_position_statement.pdf

DESIGN AND TECHNOLOGY OF ART PROCESSING OF MATERIALS

THE USE OF ARTIFICIAL INTELLIGENCE
WHILE CREATING COMPUTER PAINTING

Butsilina M., Berchuk D.

Scientific supervisor: Pichugova I.L., senior teacher

Tomsk Polytechnic University, 30, Lenin Avenue, Tomsk, 634050, Russia

E-mail: maranova08@mail.ru

Nowadays rapid development of innovative technologies, particularly the development of artificial intelligence (AI), has resulted in the appearance of new directions in the arts by applying robots. For example, Japanese company Toyota created a musical robotic quartet, but music is just one of the directions in the arts. The Victoria and Albert Museum has been collecting pieces of art in the style of 'computer art' since 1960s and at present its collection contains over 350 items. These works were created by computers with the help of humans or by robots with AI (Fig. 1-5). Moreover, a robotic portraitist has been created. It takes a photo and reproduces the image immediately on the paper with the help of the brush. Some time ago a device capable of defining the thickness of the brush and the colour of the paint to draw a picture was created (Fig. 6-8). All the present computer masterpieces can be related to abstract art, where pictures do not possess peculiar picturesqueness, but only graphic features. However, it is possible to make these computer works more picturesque.

But to start with, let us talk about technical features of AI and find out those points where AI can surpass the human being.

1. Robots can work round the clock (except the cases of technical failure or damage) and due to customization. The artist is not capable of working 24 hours a day without stopping due to his physical structure. To create an artwork the human artist needs inspiration, some muse, appropriate perception of the world, feelings, emotions, creative environment, etc. These are factors which a real masterpiece depends on.

2. The reaction of AI to the represented object is immediate while the human needs some time to concentrate on the composition.

3. Taking all the above into consideration, the speed of creating pictures by AI will be very high.

4. The pictures of the humanoid can be duplicated. The human artist will never be able to paint even two absolutely identical pictures because of the reasons mentioned in the first point.

Now let us consider the potentialities of using AI while creating computer painting. While creating pictures artists use a certain set of rules with the result of a composition ideally built.

Painting techniques and its colouring depend on the following things:

1. the remoteness of the objects and their arrangement;

2. forms and textures of the objects

3. light source direction;

4. the foreground and background of the picture.

All these criteria and rules can be applied with the help of AI. For example, the remoteness of the objects and their arrangement can be recognized by means of computer vision. Then, with the help of fuzzy logic algorithms the robot can do the arrangement of objects in the picture in the optimum way, according to its knowledge base.

Forms and textures of the objects can also be recognized by means of computer vision. But the way of reproducing the objects in a picture can be chosen with the help of an expert system. The human only needs to create a perfect expert system.

At present light source and direction can be recognized with pinpoint accuracy. The robot is able to skillfully reproduce light in the picture with the help of rigid algorithm for light reproduction.

The foreground and background of the picture can be recognized by means of computer vision and reproduced in the picture with precision.

Thus, the separate AI elements are able to carry out tasks executed by the artist while creating a painting. However, as you can see, the robot does not possess creativity. It will be capable to draw from nature or by using its knowledge base. To draw paintings like the human artist, it is necessary to create a comprehensive artificial intelligence system instead of using its separate elements.

The human artist has an innate sense of harmony (in colouring, composition overloading), he has the understanding of aesthetics, objects performed in the composition (in colours, forms, textures). It is necessary to adopt this perception and understanding in AI. On the other hand, one should not create some standard so that computer painting can acquire new directions which are different from human mind. Otherwise, the robot with AI will never create a masterpiece. If we want to compete with AI in painting, we must provide it with opportunities. In future artificial neural networks can be taught the

criteria of the correctness of applying painting techniques. They probably will be able to draw faster and much better than the human artist. However, it can cause the standardization of computer art. In terms of technical skills these paintings can be arranged absolutely correctly, but they will never be recognized as a masterpiece because masterpieces are considered by human wish.

Every person has his own understanding what a masterpiece is. Some people appreciate paintings of abstract art and cubism and it is precisely AI that will serve as a source of satisfaction and pleasure for them. For those people who appreciate masterpieces of the Renaissance, Baroque or Rococo style, the human artist will definitely take over the leadership. Such results were achieved according to the survey of schoolchildren's, students' and professor's attitudes to the problem. The survey revealed that:

- in primary school – 19% are in favour of AI, 81% are in favour of human artists
- in secondary school – 15% are in favour of AI, 85% are in favour of human artists
- in university (students of the Computer Science and Engineering Faculty, Tomsk Polytechnic University) – 3% are in favour of AI, 97% are in favour of human artists

Having analysed the survey results, it is possible to draw the following conclusion: schoolchildren believe that computers and robots will outstrip humans one day. But students of Computer Science and Engineering Faculty feel some doubts that AI has the best of the arts. The professor of the Computer Science and Engineering Faculty (The Computer Technology Department) supposes that AI has a 10% chance of winning recognition and love of all the viewers. In March-April 2010 a number of conferences devoted to the development of AI in the arts will take place in London. What new aspects will they illuminate? We can only guess.
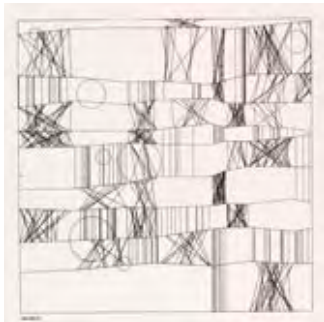
Figure 1 – The picture 1 by AI

Figure 2 – The picture 2 by AI
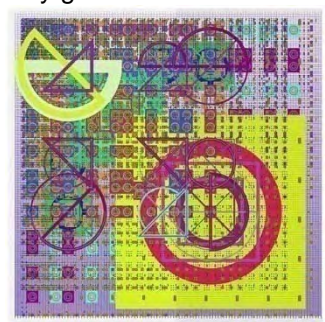
Figure 3 – The picture 3 by AI

Figure 4 – The picture 4 by AI

Figure 5 – The picture 5 by AI

Figure 6 – The Portraitist Robot

Figure 7 – The plotter with brush

Figure 8 – The holder of brush by plotter

PROBLEMS OF COMPSITION ARRANGEMENT AND SELECTION
OF PERSPECTIVE ANGLE IN PHOTO DESIGN

A. Kozlova, M.S. Kukhta

Tomsk Polytechnic University, 30 Lenin Avenue, Tomsk, 634050, Russia

E-mail: misery@sibmail.com

New century. New technologies. New life style. My research deals with photo design, because professional photography is getting more and more popular this days, especially among people of new generation. The purpose of this work is to consider and to analyze the basic principles of composition arrangement in photo frame. Besides this, the research touches upon the influence of perspective angle selection on the visual characteristics of the imaging object.

The firs photographers appeared on the streets and squares of Paris. This happened thanks to two inventors and their long laborious experiments, which eventually led to the discovery of photographing technology.

French inventors Nicéphore Niépce and Louis Daguerre worked with silver compounds based on a fact that silver and chalk mixture darkens when exposed to light. Niépce made the first permanent photograph from nature with a camera obscura in 1826. However, because his photographs took so long to expose (8 hours), he sought to find a new process. In 1839 Daguerre took the first ever photo of a person while taking a daguerreotype of a Paris street and pedestrian stopped for a shoe shine, long enough to be captured by the long exposure (several minutes). Finally, France agreed to pay Daguerre a pension for his formula, in exchange for his promise to announce his discovery to the world as the gift of France, which he did in 1839.

After that event painting monopoly in imaging of people and nature came to end. So most of portrait-painters changed their palettes and brushes for cameras obscura. So this newly-made photographers and set up a basement of professional photography. [1]

Thus, let's appeal to the fundamental theory of photo design. Composition is one of the most important points to know if dealing with photo art.

Composition (from lat. "Composito") — is a connection of several separate elements as a whole, in one definite creation. Composition is not able to play an independent role, because it's only a way to express the author's idea. It's necessary to arrange a composition in a special correct way to reach the best visual results. So here are 8 significant rules of compositional arrangement:

1. **Crossing (diagonal) lines** – the main idea if this rule is to make eye to follow the desirable direction (lines). Zero point of these lines should locate in one of the angles of the frame. Left upper angle is considering as a best starting point, because the majority of people are starting to look at the picture exactly from this point. (see fig. 1a as an example) It's possible to use other variants of line locations, but anyway it should be comprehensible and clear organized. (see fig. 1b)
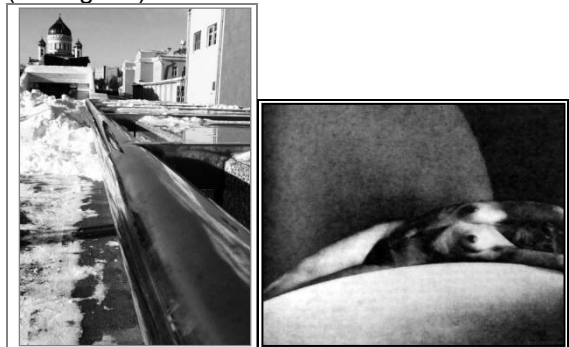
Fig. 1 a,b Crossing (diagonal) lines
a) left upper angle start point. A.Kozlova Moscow 2010
b) alternative start point
Frantisek Drtikol "Akt" 1929 [3]

2. **"One third" rule** – this rule follows from the "golden section" system. The sense of the rule is that the best compositional effect can be reached by dividing a frame in special proportions, which are combinations of any two numbers from the Fibonacci sequence: 1, 2, 3, 5, 8, 13, 21, 34, 55, 89… so if to simplify, one of the most popular and easiest proportion is the first one 1:2 or the "one third rule". That means that the picture should be mentally divided into three parts. The upper one third part can be filled with sky for example, and the rest two thirds can be filled with ground, that's how it works. (see fig.2a) This rule is valid for any-direction division, whatever vertical or horizontal or inclined. (on fig. 2b see the example of diagonal division)

Fig. 2 a,b One third rule
a) Kozlova A., Moscow 2010
b) Vienna, 2009

3. **Emphasizing of object by sharpness** – to use this rule, it's necessary to set up the camera lance on the shallow depth of sharpness. So the open diaphragm makes it possible to highlight the main object with sharpness and to blur all the rest. (fig. 3a,b)

4. **Emphasizing of object by contrast**- when people are looking through the pictures, their eyes are usually focusing on the most contrast parts of the frame, so this property of man's eye can be used to attract an attention to the definite parts of the picture. (fig. 4 a,b)

Fig. 3 a,b Emphasizing of the object by sharpness
a) Still life example
b) Magdalena Robinsonova, 1962 [3]

Fig.4 Emphasizing of object by contrast
a) Slava Stochl «Pesaci» [3]
b) A. Kozlova, Vienna 2010

5. **Framing of object** – framing effect is also useful to call an extra attention to the major object. (fig. 5a,b) Important point is to choose the suitable frame, it should be dark or neutral color, and should not detract an attention from the framed view. Windows, arches, fences or even tree brunches can act as a frame.

fig. 5 a,b Framing of object [3]
a) Milada Einhornova, 1962
b) Milada Einhornova, 1955

6. **Emphasizing of object by light** – the idea of this method is to light up the main object and to darken the rest area of the picture. See the example on fig. 6a,b.
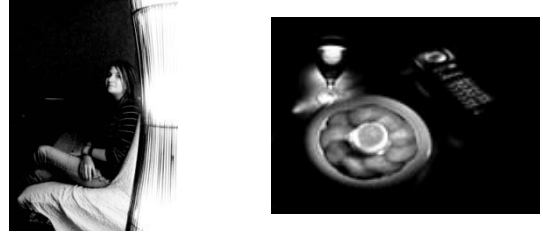
Fig. 6a,b Emphasizing of object by light
a, b) portrait and still life examples

7. **Usage of lines** – lines have a great influence on spectator's emotional perception of photo creation. For example curve lines are calming, polygonal lines are irritating, vertical lines are making picture more fundamental, horizontal lines are giving calmness and serenity, diagonal lines – dynamics and speed. All this lines can work for photographer's needs if he wants to express some feelings on his pictures.

8. **Tonality of pictures** – Photographer is able to show his mood or spirit by tonality as well. Dark tones - shadows, black color are usually associating with night, seems mysterious. Light tones – white color and light-gray hues are associating with sunlight and cheerful mood. [4]

Next important step of photo design is a choice of shooting point and perspective angle.

The process of choosing a shooting point is a creative method of frame compositional arrangement. Positions of the shooting point can be different. For example if to put camera in front of the object, the composition will be central-organized; if to shoot from the side – the composition will be diagonal-organized. This type of composition organization shows three-dimensional shape and a spatial position of object, emphasizing dynamic movements in photo frame. Horizon line and proportions of vertical dimensions of objects can be determined by selection of height position of camera. In case of the upper shooting point - objects are locating against a background (earth surface) and its vertical dimensions seem reduced. In case of lower shooting point – front objects seem bigger. This visual effect can be used to show the significance of the photographed object, even if its real dimensions are rather small.

Selection of perspective angle is a further step in photo design.

Perspective angle – is a position of the imaging object, characterized by the strong shortening of the parts which are in a big distance from the camera.

fig. 7 Two perspective angles of stairs in Paris passage "Vivienne".
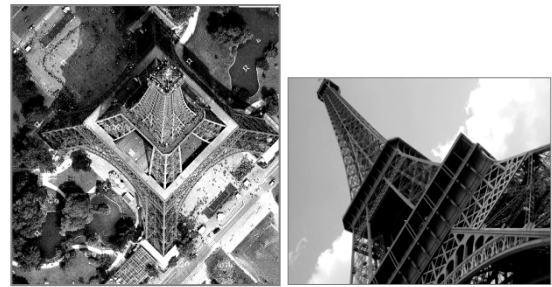
fig.8 Upper and lower perspective angles of Eiffel Tower

Variations of perspective angles allow to reach interesting unusual phenomenon on the picture, such as intense convergence of the vertical perspective lines, sizeable shortening of this lines, decreasing of upper part's scale of object, relative to the lower parts (lower perspective angle) and inversely (upper perspective angle). As a result usual ordinary imaging subjects like buildings, bridges, people, animals or whatever are getting totally different appearance, with unnatural proportions and giving absolutely unexpected impression, which always attracts attention.(See fig. 7,8)[5]

In conclusion I want to pay attention to the fact, that a good photo of high quality is not just a random pressing on camera button, it's a laborious task, result of precise analysis of different factors, work on composition and so on. That's why professional photographer can be treated as a true artist. And of course only common rule's knowledge is not enough to create a photo-masterpiece. Photographer should also apply his gut intuitive feeling, put his heart and soul into a frame, to express his impressions and experience from the imaging object to the audience.

References:

1.Stigneev V., Baskakov A., Klod L. Photo art of Russia. History, development, contemporary condition.– M.: Planet ,1990. – 400 p. with ill.
2. J. Wade Technique of landscape photography: translation from eng. – M.:Mir, 1989. – 200 p, with ill.
3. Daniela Mrazkova, Vladimir Remes. Cesty ceskoslovenske fotografie, Praha: Mlada fronta, 1989. – 360 p. with ill.
4. www.photoline.ru
5. www.fotoman.name

SPECIAL DESIGN OF LED-LAMPS USING HEAVY DUTY DIODES

Vera A. Poddubnaya, Daria A. Pischulina, Maria S. Kuchta

Tomsk Polytechnic University, 30, Lenin Avenue, Tomsk, 634050, Russia

E-mail: verapoddubnaja@rambler.ru

The purpose of this article is highlight the issue of new methods of lighting. They are distinguished by high productivity and firmly holding their positions in the world of lighting pushing traditional technologies involving electric and halogen lamps. It is a light-emitting diodes. This article develops the theme of design features of fixtures with using of super-power LEDs.

The instances of such technologies can be Luminus SST-90 of the serie PhlatLight ® and Luxeon K2 (Fig. 1). One can experience the benefits of several innovative approaches in the field of chip technology-packaging and thermal management regimes. These advances allow creating projects with a high luminous efficiency and high brightness. Photonic lattice technology allows you to create an effective surface emission, which is achieved by a small variation of brightness levels within the entire surface of the diode crystal [1], [2].
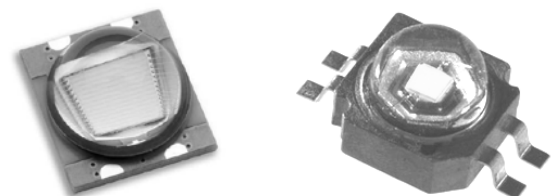
Fig. 1 LEDs Luminus SST-90 and Luxeon K2

One should notice that due to the above electromechanical properties of a new generation of LEDs, design of lighting, which is based on their using, has several features that affect the design.

It must be taken into account that workflow LEDs with such a powerful light flux (about 2250 lumens) is accompanied by a huge amount of heat due to dissipation of power. The design of the diode is provided an electrically insulated heat sink. In this regard, the case, the surface on which you will be mounting LEDs shall be manufactured from a material with a high thermal conductivity, and also have a large amount to prevent overheating diodes.

Another condition for effective work of super-diode is the stabilization of the current. High-brightness LEDs depending on type demand from the DC power supply from 300 to 700 mA, to ensure the desired brightness and color of the glow. For this there are available special modules, so-called LED Drivers. Their work is that when the input voltage and external loads changes , the control scheme is a correction from the difference between the control signal and reference signal via feedback that regulates the pulse width of the supply voltage, increasing or decreasing it. As a result, we obtain a stable output voltage, stable current (i.e. the corresponding constant voltage or current). In connection with this need in the construction of the lamp should be the place for the stabilizers [3]. If the LED driver is mounted with a group of LEDs, it must stand with a high temperature environment and the temperature of 80 ° C shouldn't be perceived as very high [4]. Moreover, recent developments make it possible to place a system current stabilization in the body size, less than a matchbox. There is a choice of hull shape depending on the design of the lamp (Fig. 2). A number of modules is determined by the stabilization of the ratio: the number of LED * power of a single LED / supply (driver) power [3].
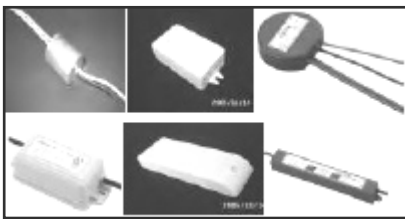
Fig.2 Options of LED drivers

One should also note that powerful light output of the used LEDs involves ultra-high brightness, not comfortable for human vision. Consequently, there is ergonomically advantageous to dress these elements in the system plafond. Material of plafond may be chosen depending on the purpose and destination of the product.

Besides, studying the issue of new methods of illumination, thus, led to design own version of lighting products. Was a task - to simulate the type of street lamp for bicycle lanes and pedestrian sidewalks. The result was the design of a street lamp "Night Light".

Thus, here one should consider tha frame structure. The frame structure is composed of 6 elements (Fig. 3). This base, cover with the base-mounted LEDs, 3 shaped plates, which are painted plafonds for LEDs, the metal canopy and metal piles supporting it. Base, canopy and piles are made of structural steel and are galvanized to prevent corrosion. The base contains the basic system of electric power, stabilization the current and energy supply for lighting in the lower part, buried in the ground, the openings for wires and connection of the entire system of fixtures. Piles are welded to the cap and the cover of base. The cover is made of zinc, a plate of 40 mm thick and attached to the base of the bolts, in order to carry out maintenance and repair the electric scheme. The surface of the cover is equipped with 3 rectangular grooves in which the planned installation of LEDs. Therefore, the material was selected based on the highest heat. Of all construction materials, zinc has the highest thermal conductivity, which is equal to 0,110 kW / m$*^{\circ}C$. In this way, expected to prevent overheating of LEDs because the part is quite heavy. Three shaped plate made of plexiglass by laser cutting. The plates are installed in the grooves on the cover. Each plate is fastened with 4 screws, 2 on each side. In plates there are carved holes for each LED. The system lights "Night Light" assumed a light-sensitive switch, which will apply to the current facility at nightfall. (Fig. 4)
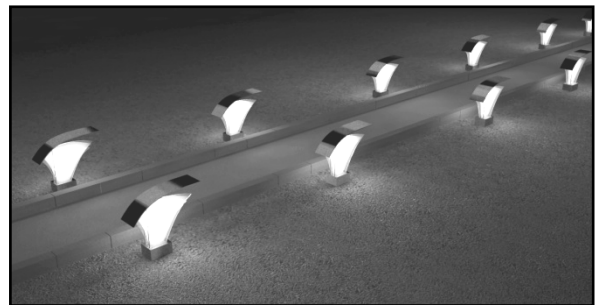
Fig. 3 lamp at super-diode "Night Light"

Fig. 4 System of lighting street lamps "Night Light"

Work on the design of lighting by using super-light-emitting diodes requires an integrated approach. But among the advantages of such technologies: high efficiency, energy efficiency and reliability, as well as a wide range of operating temperatures. In addition, the most compelling argument for transition to LEDs from other light sources is their lifetime, reaching 100 thousand hours, which can are enclosed in 10 years of continuous operation. In addition to the above is to emphasize their small size and resistance to vibration. The minimum lifetime of LEDs is 50 000 hours, gave impetus to abandon the conventional electric lamps, whose service does not exceed 1000 hours, and halogen lamps with a lifetime of about 2000 hours. That means that the LEDs operate without replacement of 25 to 50 times longer than lights with a filament bulbs, as applied to the same content requires a large staff to replace them, not to mention the need for their delivery to the installation site [4].

In conclusion it should be noted that at the moment there is already a number of engineering and electrical engineering solutions that make use of LEDs is gaining momentum. The using of these technologies will minimize the number and size of light sources. Therefore, designers should pay attention to new opportunities for lighting technology and design of exhibition spaces.

REFRENCES:

1.   http://www.ebvnews.ru
2.   http://eicom.ru/
3.   http://www.radiodetali.com "Manual power supplies (drivers) LEDs "
4.   http://led.contrel.ru

Section XII

NANOMATERIALS, NANOTECHNOLOGIES AND NEW ENERGETICS

WAVE ENERGY POTENTIAL

Gusakov N.N., Korsak V.V.

Supervisor: Ermakova Ya. V.; Advisor: Chertkov U.B.

Tomsk polytechnic university, 634050 Tomsk, Lenin Avenue 30

E-mail: lavisionary@gmail.com

RESOURCE POTENTIAL

Ocean waves represent a form of renewable energy created by wind currents passing over open water. Capturing the energy of ocean waves in offshore locations has been demonstrated as technically workable.

Because wind is generated by uneven solar heating, wave energy can be considered a concentrated form of solar energy. Incoming solar radiation levels that are near 100 W/m2 are transferred into waves with power levels that can exceed 1,000 kW/m of wave crest length. The transfer of solar energy to waves is greatest in areas with the strongest wind currents, near the equator with persistent trade winds, and in high altitudes because of polar storms.

Estimates of the worldwide economically recoverable wave energy resource are in the range of 140 to 750 TWh/yr for existing wave-capturing technologies that have become fully mature. With projected long-term technical improvements, this could be increased by a factor of 2 to 3. The fraction of the total wave power that is economically recoverable in U.S. offshore regions has not been estimated, but is significant even if only a smal fraction of the 2,100 TWh/yr available is captured. WEC (wave energy conversion) devices have the greatest potential for applications at islands such as Hawaii because of the combination of the relatively high ratio of available shoreline per unit energy requirement, availability of greater unit wave energies due to trade winds, and the relatively high costs of other local energy sources.

RESOURCE UTILIZATION TECHNOLOGIES

Terminators

Terminator devices extend perpendicular to the direction of wave travel and capture or reflect the power of the wave. These devices are typically installed onshore or nearshore; however, floating versions have been designed for offshore applications. The oscillating water column (OWC) is a form of terminator in which water enters through a subsurface opening into a chamber with air trapped above it. The wave action causes the captured water column to move up and down like a piston to force the air though an opening connected to a turbine. A full-scale, 500-kW, prototype OWC is undergoing testing offshore at Port Kembla in Australia, and a further project is under development for Rhode Island. In an Electric Power Research Institute (EPRI)-cosponsored study a design, performance, and cost assessment was conducted for an

Energetech commercial-scale OWC with a 1,000-kW rated capacity, sited 22 km from the California shore. With the wave conditions at this site

(20 kW/m average annual), the estimated annual energy produced was 1,973 MWh/yr. For a scaled-up commercial system with multiple units producing 300,000 MWh/yr, the estimated cost of electricity would be on the order of $0.10/kWh. Another floating OWC is the "Mighty Whale" offshore floating prototype, which has been under development at the Japan Marine Science and Technology Center since 1987

Attenuators

Attenuators are long multisegment floating structures oriented parallel to the direction of the wave travel. The differing heights of waves along the length of the device causes flexing where the segments connect, and this flexing is connected to hydraulic pumps or other converters.

The McCabe wave pump has three pontoons linearly hinged together and pointed parallel to the wave direction. The center pontoon is attached to a submerged damper plate, which causes it to remain still relative to fore and aft pontoons. Hydraulic pumps attached between the center and end pontoons are activated as the waves force the end pontoons up and down. The pressurized hydraulic fluid can be used to drive a motor generator or to pressurize water for desalinization.

A similar concept is used by the Pelamis, which has four long floating cylindrical pontoons connected by three hinged joints . Flexing at the hinged joints due to wave action drives hydraulic pumps built into the joints.

Point Absorbers

Point absorbers have a small horizontal dimension compared with the vertical dimension and utilize the rise and fall of the wave height at a single point for WEC. One such device is the PowerBuoy. The construction involves a floating structure with one component relatively immobile, and a second component with movement driven by wave motion (a floating buoy inside a fixed cylinder). The relative motion is used to drive electromechanical or hydraulic energy converters. A commercial-scale PowerBuoy system is planned for the northern coast of Spain, with an initial wave park (multiple units) at a 1.25-MW rating.

The AquaBuOY is a point absorber that is the third generation of two Swedish designs that utilize the wave energy to pressurize a fluid that is then used to drive a turbine generator. The vertical movement of the buoy drives a broad, neutrally buoyant disk acting as a water piston contained in a long tube beneath the buoy. The water piston motion in turn elongates and relaxes a hose containing seawater, and the change in hose volume acts as a pump to pressurize the seawater.

The AquaBuOY design has been tested using a full-scale prototype, and a 1-MW pilot offshore demonstration power plant is being developed offshore at Makah Bay, Washington.

Overtopping Devices

Overtopping devices have reservoirs that are filled by impinging waves to levels above the average surrounding ocean. The released reservoir water is used to drive hydro turbines or other conversion devices. Overtopping devices have been designed and tested for both onshore and floating offshore applications. The offshore devices include the Wave Dragon, that is 11-MW project .

ENVIRONMENTENTAL CONSIDERATIONS

Conversion of wave energy to electrical or other usable forms of energy is generally anticipated to have limited environmental impacts. However, as with any emerging technology, the nature and extent of environmental considerations remain uncertain. The impacts that would potentially occur are also very site specific, depending on physical and ecological factors that vary considerably for potential ocean sites.

Visual appearance and noise are device-specific, with considerable variability in visible freeboard height and noise generation above and below the water surface. Offshore devices would require navigation hazard warning devices such as lights, sound signals, radar reflectors, and contrasting day marker painting. The air being drawn in and expelled in OWC devices is likely to be the largest source of above-water noise. Some underwater noise would occur from devices with turbines, hydraulic pumps, and other moving parts.

Reduction in wave height from wave energy converters could be a consideration in some settings; however, the impact on wave characteristics would generally only be observed 1 to 2 km away from the WEC device in the direction of the wave travel. It is estimated that with current projections, a large wave energy facility with a maximum density of devices would cause the reduction in waves to be on the order of 10 to 15%, and this impact would rapidly dissipate within a few kilometers, but leave a slight lessening of waves in the overall vicinity. Little information is available on the impact on sediment transport or on biological communities from a reduction in wave height offshore.

Marine habitat could be impacted positively or negatively depending on the nature of additional submerged surfaces, above-water platforms, and changes in the seafloor. Artificial above-water surfaces could provide habitat for seals and sea lions or nesting areas for birds. Underwater surfaces of WEC devices would provide substrates for various biological systems, which could be a positive or negative complement to existing natural habitats. With some WEC devices, it may be necessary to control the growth of marine organisms on some surfaces.

Toxic releases may be of concern related to leaks or accidental spills of liquids used in systems with working hydraulic fluids. Any impacts could be minimized through the selection of nontoxic fluids and careful monitoring, with adequate spill response plans and secondary containment design features.

Installation and decommissioning. Disturbances from securing the devices to the ocean floor and installation of cables may have negative impacts on marine habitats. Potential decommissioning impacts are primarily related to disturbing marine habitats that have adapted to the presence of the wave energy structures.

ECONOMIC CONSIDERATIONS

Cost estimates of energy produced by WECs are dependent on many physical factors, such as system design, wave energy power, water depth, distance from shore, and ocean floor characteristics. Economic factors, such as

219

assumptions on discount rate, cost reductions from a maturing technology, and tax incentives, are also critical. A detailed evaluation of potential wave energy development in the U.S. coastal areas has been conducted, taking into account variability in these factors .

The resulting cost estimate of electricity from the first commercial-scale facilities in the California, Hawaii, Oregon, and Massachusetts offshoreregions with relatively high wave energy was in the range of $0.09 to $0.11/kWh, after tax incentives.

These facilities are very capital intensive, and these costs currently have a high degree of uncertainty. For example, capital investment cost estimates for the applications noted above range from $4,000 to $15,000/kW, suggesting that significant breakthroughs in capital cost would be needed to make this technology cost competitive.

REFERENCES

1. AquaEnergy Group, Ltd., 2006, "AquaBuOY Wave Energy Converter." Available at www.aquaenergygroup.com.

2. Archimedes Wave Swing, 2006, "ArchimedesWave Swing Website." Available at www.waveswing.com.

3. Bedard, R., et al., 2005, *Final Summary Report, Project Definition Study, Offshore Wave Power Feasibility Demonstration Project*, EPRI Global WP 009 –US Rev 1, Jan. 14, 2005.

4. Christensen, L., 2006, e-mail from Christensen (Wave Dragon ApS, Copenhagen, Denmark) to L. Habegger (Argonne National Laboratory, Argonne, Ill.), June 22.

5. Department of the Navy, 2003, *Environmental Assessment, Proposed Wave Energy Technology Project, Marine Corps Base Hawaii, Kaneohe Bay, Hawaii*, Jan.

Section XIII

ROUND TABLE
«TECHNIC PHILOSOPHY»

TSIT: STIMULUS OR FETTERS OF INNOVATION ACTIVITY

Stepanov K.A.

Tomsk State University

E-mail:elena.stepanowa2010@yandex.ru

It's typical for Russian society to ignore domestic discover and inventions with subsequent borrowing from the West like a certain know-how. Theory of solution of invention tasks which was made in 1960s from USSR has the same fate.

Today TSIT is international civic organization which is directed to make effective technologies of creativity as integral part of world culture. TSIT is effectively used by such firms like Samsung, Hewlett Packard, Dior, Procter & Gamble, Intel, LG Electronics, Philips, Boeing and many other famous companies. Private consulting companies are developing actively using TSIT in different countries: the USA, Germany, Japan, Southern Korea, Italy, France and so on. Economical effect from inventions, which were made by TSIT, constitutes several hundreds of millions dollars a year.

Henrico Saulovich Altshuller, TSIT's author thought that solution of tasks which are tough insoluble can be found by using certain algorithms, and one can exchange experience with other researchers. With the help of analyses of 40 thousands of patents and inventions he found out 40 main and 10 additional principles of resolution of technical contradictions: turn harm into benefit; principle of crushing; principle of concentration; reception of the wrong way and so on.

But theory of solution of invention tasks is not the panacea and has its supporters and opponents. Then we will try to compare arguments of supporters and opponents of TSIT for its detailed analyses.

Theoretical basis of TSIT is proclaimed with dialectical laws of development of technical systems which don't depend on will of engineers and inventors. Their competent adoption is permitted to solve task and create new technical systems. One of these laws is the *law of uneven development part of system:* elements of technical system (TS) are developing unevenly. It leads to contradictions' appearance. Any invention is exposing and overcoming contradictions which are available in technical systems. For example, on evacuation of factory during Patriotic War in 1941 heavy press must be lower into pit of foundation. Contradiction is necessary to use crane so that lower press and impossible to use crane because we don't have it. Other important law is the *law of striving for ideal*. Ideal system is a system which doesn't exist (that is, expenses for its manufacture and exploitation don't exist; we don't have to use expensive materials and so on), but all function of system are carried out without control. All technical systems strive for increase degree of ideal. For example in task for press instead crane we can use ordinary ice. Press is moved on ice then after time lapse ice will melt and lower press into pit. It is ideal solution: we didn't use press but its function is carrying out.

Significant part of TSIT is dedicated to analyze and use resource. In task about lowering press we used a few resources: water is substance which is available in large quantity; drop in temperature is also resource; and time is a resource which is permitted us to wait until press is lowered into pit.

Law of transition to oversystem is often used in theory. Any technical system (for example, sailing vessel) is reaching for define its development's stage, is going to oversystem – unite with another system. One of effective way of transition to oversystem is transition on development's line "mono-bi-poly". Another system is added to monosystem, which creates new function and forms of bisystem. For example, two different sails can be used instead of one sail. If we know this development's line, next step is plain: it is many different sails – such sailing vessel uses air streams much effective.

Opponents think that majority of laws which were formulated in TSIT aren't laws. They should be named tendencies of technology's development, moreover they are much incomplete. For that case, well-constructed methodology of tasks' solution which was founded on development's law doesn't exist. And formulated laws were used on the whole as systematic basis to given examples of inventions.

Different models are used in TSIT (like in chemistry, physics, math and many other sciences) for presentation of primary invention task. Process of intention task's solution can be presented in the form of plan: description of real situation or task is converted into task's model then (using certain methods) into model of task's solution then into real solution.

Instrument's varieties which are used in TSIT are united into system in algorithm of solution of invention tasks (ASIT). ASIT is quiet difficult instrument with many mechanisms, rules, prompts, information fond and so on.

TSIT's opponents say that ASIT like any algorithm fetter creative thought, and ASIT's improvement didn't go on way of created inexactness' removing but on lone of algorithm's complicating.

We will try to give only general presentation of ASIT's work on actual example.

In 1949 all-union competition on freezing mountain-rescuer's outfit was declared. Conditions: outfit must protect human for two hours by external temperature 100 degrees of C and relative humidity 100% moreover outfit's weight mustn't be exceed 8-10 kilogram. Task was considered to be principally unsolving. Even using the most powerful freezing substance outfit's weight was more than 20 kg. 28-30 weight can be loaded on a human, but mountain-rescuer had respiratory device (12 kg) and instruments (7 kg).

Insoluble contradiction was kept in task: freezing outfit's weight mustn't be more than 8-10, but if we used ice or liquefied gases, outfit's weigh will turn out more than 20 kg. If we create heavy (20 kg) freezing outfit, it will be able to cool of mountain-rescuer, but it wouldn't let him to organize necessary works because of great weight. If we create light (less than 10 kg) freezing outfit, mountain-rescuer will be able to organize necessary works, but necessary temperature can't be created.

Ideal system is that things which are in primary technical system must provide cooling and rescuer's breathing itself, at the same time save equipment's lightness.

Analysis of the resource show that oxygen apparatus can be used. In accordance with law of transition to oversystem, we can go to bi-system, and united respiratory device and freezing outfit. Guide of physical effects show that liquid oxygen can be used for in this situation. At first it can be used for cooling and then secondary for breathing.

Solution is really ideal: freezing outfit doesn't exist, and respiratory device as one execute function of cooling.

Modern algorithm of solution of invention tasks consist of 9 parts, every part means realization of several consecutive steps. Is it fetters? Really, without computers and further improvement of algorithm it can be a long monotonous process. But if thinking process stopped, "dead-end situation" arose in invention activity, "insoluble" contradiction appeared, creative quest can be stimulate by prompts from TSIT.

On the given stage of development the theory of solution of invention tasks can be both stimulus and fetters for innovation activity.

Table of Contents

Section I: Power engineering

Section II: Instrument making

Section III: Technology, equipment and machine-building production automation

Section IV: Electro mechanics

Section V: The use of modern technical and information means in health services

Section VI: Material science

Section VII: Informatics and control in engineering systems

Section VIII: Modern physical methods in science, engineering and medicine

Section IX: Quality management control

Section X: Heat and power engineering

Section XI: Design and technology of art processing of Materials

Section XII: Nanomaterials, nanotechnologies and new energetics

Section XIII: Round table «Technic philosophy»

16th International Scientific and Practical Conference of Students, Post-graduates and Young Scientists

MODERN TECHNIQUE AND TECHNOLOGIES MTT' 2010

April 12−16, 2010, Tomsk, Russia

Система менеджмента качества
Томского политехнического университета сертифицирована
NATIONAL QUALITY ASSURANCE по стандарту ISO 9001:2000
. 634050, г. Томск, пр. Ленина, 30.